SYNTHESIS OF NOVEL BIOMASS-DERIVED DIOL AND EPOXIDE MONOMERS FOR COATINGS APPLICATIONS

A Dissertation
Submitted to the Graduate Faculty
of the
North Dakota State University
of Agriculture and Applied Science

By

Catherine Annette Sutton

In Partial Fulfillment of the Requirements
for the Degree of
DOCTOR OF PHILOSOPHY

Major Program:
Chemistry

June 2022

Fargo, North Dakota

North Dakota State University
Graduate School

Title

Synthesis of Novel Biomass-derived Diol and Epoxide Monomers for Coatings Applications

By

Catherine Sutton

The Supervisory Committee certifies that this ***disquisition*** complies with North Dakota State University's regulations and meets the accepted standards for the degree of

DOCTOR OF PHILOSOPHY

SUPERVISORY COMMITTEE:

Mukund Sibi
Chair

Gregory Cook

Kenton R. Rodgers

Glenn Dorsam

Approved:

July 10, 2022
Date

Gregory Cook
Department Chair

ABSTRACT

There are few monomers or precursors in the polymer industry that are more ubiquitous than bisphenol A (BPA). According to the CDC, about 5-6 billion pounds of BPA are produced worldwide annually. For the synthesis of coatings and polymeric materials, BPA is polymerized directly as a diol into polycarbonates or, to a lesser extent, glycidated into an epoxy monomer or resin. For coatings applications, BPA epoxy resins are utilized in protecting metal cans from acidic foods and beverages to heavy machinery like farm equipment from weather-related corrosion.

In part, this popularity has led to scrutiny of the popular monomer from a few different perspectives. Since BPA is petroleum-derived, there is an effort to find a renewably sourced alternative from a sustainability perspective. Additionally, the structural similarity of BPA and the hormone estradiol make BPA an endocrine disruptor. This combined with its widespread applications, means BPA could be a larger issue than previously understood.

To meet that challenge, many researchers, Sibi group included, have turned to biomass-derived “building-block” chemicals. Biomass feedstocks contain unique structures not easily obtained from petroleum sources. While avoiding detrimental structure-activity relationships associated with BPA, the newly synthesized compound would need to retain or mimic the structure-property relationships of BPA-containing polymers for coatings applications.

The cellulosic monomer, 2,5-furandicarboxylic acid (FDCA), with exciting similarities to and some improvements upon petroleum-derived terephthalic acid was known, and its oxidative family of furans was being explored at the start of this project. A collection of furan diols was synthesized from 5-hydroxymethylfurfural (HMF), 2, 5-diformylfuran (DFF) and FDCA were synthesized by alkylation with various alkyl groups resulting in mono-, di-, and tetraalkylated diols, respectively. Depending on the alkyl group, certain materials properties were anticipated from these furanic diols.

The diols were screened for estrogenic, androgenic, anti-thyroid activity via CALUX assays. The cytotoxicity of the diols was also determined via cell death studies. From those results, few low molecular weight furan diols do not exhibit any observable activity as endocrine disruptors or an observable cytotoxicity. Subsequently, a selection of furanic diols were glycidated for use in epoxy coating synthesis.

ACKNOWLEDGMENTS

First and foremost, I would like to thank my advisor, Dr. Mukund Sibi, for allowing me to join his lab. Not only was I able to research exactly the type of chemistry I had hoped to learn more about, but I had a knowledgeable advisor who is one of the most dedicated scientists I have ever met. I feel supremely lucky to have researched in the Sibi group, and I have grown as a chemist from my time as his student.

Next, I must acknowledge my committee members, Dr. Gregory Cook, Dr. Kenton Rodgers and Dr. Glenn Dorsam. Truly I am grateful for your questions and suggestions on my research and the way I communicate science.

To all the Sibi group members I have worked with or next to over the years - thank you for all of the serious chemistry conversations as well as for the jokes and laughter.

Lastly, this work would not have been possible but for the financial support of Akzo Nobel and the Nation Science Foundation through the North Dakota Established Program to Stimulate Competitive Research (ND-EPSCoR) through the Center for sustainable Materials Science (CSMS). Thank you.

DEDICATION

I would like to dedicate this to my family and friends, but I must single out two amazing women. Thank you to my mother, Shauna Dawson Sutton for her incredible, unwavering love and support. Thank you to my aunt, Lynda Sutton, who indulged me in conversations of science, art, and history as a child. I would not be who I am, or where I am, without you both.

TABLE OF CONTENTS

LIST OF TABLES

LIST OF FIGURES

LIST OF SCHEMES

LIST OF ABBREVIATIONS

^{1}H NMR	Proton Nuclear Magnetic Resonance
^{13}C NMR	Carbon Nuclear Magnetic Resonance
$CDCl_3$	Deuterated Chloroform
FT-IR	Fourier-Transform Infrared Spectroscopy
HRMS	High Resolution Mass Spectrometry
Hz	Hertz
MHz	Megahertz
NMR	Nuclear Magnetic Resonance
TLC	Thin Layer Chromatography

LIST OF SYMBOLS

°C ..... Degree Celsius

δ ..... Chemical Shift in Parts-Per-Million

J ..... Coupling Constant, Hz (NMR)

R ..... Alkyl Group

T_g ..... Glass Transition Temperature

LIST OF APPENDIX FIGURES

1. INTRODUCTION TO FURANS FROM CELLULOSIC BIOMASS

1.1. Cellulosic biomass

1.1.1. Cellulose

The driver of this thesis work was the 12 principles of green chemistry. Encompassing all 12 principles of green chemistry was preferred, and performed, when possible, three of the principles were the main focus of this dissertation: # 3- Less hazardous synthesis, # 4- Design benign chemicals and # 7- Use of Renewable Feedstocks. Principle #7 was the true foundation of all work presented, and so requires a deeper understanding and context to the motivation of the research featured in later chapters. Concern surrounding finding and utilizing renewable and sustainable chemical sourcing through biobased feedstocks in the 2010s was the landscape in which furan monomers emerged. There are several types of biomass with varying bioavailability, but the three main types of biomass are oil seeds, lignin and cellulose. Of these three, cellulosic biomass has risen in popularity in the field of coatings and materials related science due to a unique set of furans developed from it.

The abundance of cellulose makes it a prime target for biobased materials; cellulose is a natural polymer found in nearly all plants. It is exclusively made up of glucose monomers with β 1,4 linkages, forming microfibrils that support lignin in the plant cell wall.[1-2] Although it does not contain a diversity of unique monomer units within its polymer chain like lignin, it is easier to depolymerize and is therefore considered by some a more useful biomass feedstock. Like lignin, cellulose is difficult to chemically alter but this is due to its strong H-bonding interactions within its polymer matrix. A field of research is dedicated to understanding cellulose to exploit it, but it remains somewhat elusive.[3-4] Instead, many chemists turn to the depolymerization of cellulose to utilize it as a feedstock for biobased materials. Enthusiasm towards the utilization of cellulose as a feedstock began after the 2004 report by the US Department of Energy on the top value-added biobased chemicals of the time.[5]

Furanic compounds have been proposed for use as pharmaceuticals, fuels, surfactants, monomers and more. The purpose of this thesis work was to explore furans as possible replacements to petroleum-derived monomers used in polymeric coatings, specifically for coatings in contact with food. Although lignin-derived monomers contain benzenoid features making them the most similar in structure to traditional petroleum derived monomers, cellulosic furans became surprise trailblazers for biobased

replacements of petroleum-derived monomers. Despite the structural differences, the proposed furanic replacement of commonplace monomer terephthalic acid with biobased 2, 5-furandicarboxylic acid (FDCA) proved to be comparable in terms of physicochemical properties, but FDCA was shown to outperform its petroleum-based counterpart.

Much like a snowball rolling downhill, research into FDCA began slowly and then increased in speed as it has grown over the past nearly 20 years. Shortly after the 2004 report, Alessandro Gandini's research group published the first polymerization of poly(ethylene furanoate) (PEF), a potential alternative to poly(ethylene terephthalate) (PET).[6]

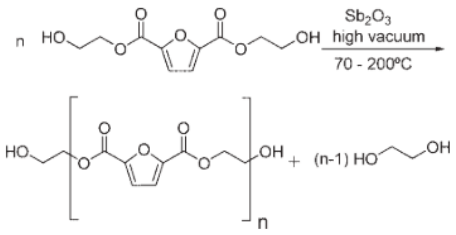

Scheme 1.1. The first reported synthesis of poly(ethylene furanoate).[6]

Gandini's group had published on the chemistry and polymerization of numerous furans for about a decade before their research on FDCA polyester synthesis was published.[7-11] In their 2009 article, they report their synthesis of PEF and mark it as a potential alternative to the petroleum-derived PET. This was interesting information in sustainable polymer synthesis, but it was the subsequent viscoelastic properties of FDCA polymers that garnered the broader enthusiasm of polymer materials scientists, chemists, and engineers.

Although the structure of benzene and furan differ, there were a few shared characteristics that made furans a viable alternative to benzene-containing petrochemicals. Huckle's rules for aromaticity state that in order to be aromatic, a compound must be conjugated, cyclic, planar, and have $4n+2$ π electrons. Benzene rings fit this description exactly, but furans, and other similar heterocycles, are not planar to the same degree as benzene rings. Furthermore, heteroaromatic rings have polarized rings, making the sharing of electrons, and the current of electrons in the ring, slightly unequal. The level of aromatic character of the heteroaromatics differs from benzene as a result.

Heteroaromatic rings, such as furans, have the ability to perform reactions that benzene rings cannot under the same conditions. More importantly for materials science, the difference in structure implies difference physical characteristic possibilities. This was confirmed in the study comparing polymer properties of the standard poly(ethylene terephthalate) (PET) to biobased poly(ethylene furanoate) (PEF).

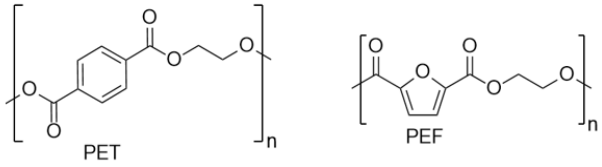

Figure 1.1. Representative structures of PET and PEF.

In 2014 a duo of articles was published by Burgess et al., detailing the initial findings followed by a deeper analysis into the cause of the surprising oxygen barrier properties. They found PEF to have ~11x reduction in oxygen permeability at 35 °C, while showing only minor deviation in key characteristics from PET, like density, glass transition temperature and melting temperature.[12] For the ease of processability, so-called “drop-in replacements” like PEF must behave as similar to the material they are replacing as possible. Retaining key physical properties, such as glass transition temperature can avoid expensive purchasing of new industrial processing equipment and the time-consuming process of a mammoth industry homogeneously learning completely new techniques to handle biobased materials.

Further study gave evidence to the theory that the unique oxygen barrier qualities of PEF were due to its lower polymer chain mobility compared to that of PET. In effect, oxygen was not as soluble in amorphous PEF as in PET, noted by its lower permeation ability in the biobased polymer. In addition, the higher energy barrier to ring rotation of the furan due to its polar nature and semi-planarity was considered to be another contributing factor to the improved oxygen barrier ability of PEF compared to PET.[12-13] Later work demonstrated that slight increase in glass transition temperature of furans compared to analogous benzene-containing monomers was due to their increased ability to participate in H-bonds.[14]

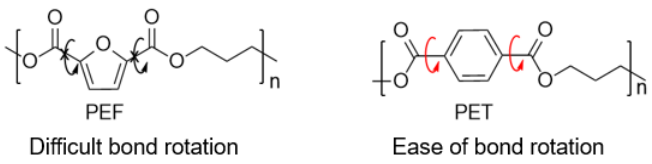

Figure 1.2. Bond rotation of PEF and PET, redrawn from Burgess et al.[13]

The work by Burgess et al. set forth a new wave of interest in research into cellulose-derived furans, particularly FDCA, not simply for its potential as a sustainable alternative to petrochemical analogues, but for beneficial materials properties. This added a potential cost-savings appeal; if the oxygen barrier to perishable foods could be drastically improved it would mean fewer expired foodstuffs being discarded by grocery stores at a loss to the manufacturing company. Furthermore, it could also aid in corrosion resistance in performance coatings for automobiles and architecture. The idea of a potential financial improvement piqued the interest of more academic and industrial researchers, noted by the reference to the improved oxygen barrier ability of PEF to PET in future journal articles.

Another article of 2014 published by Thiyagarajan et al established that PEF synthesized from 2, 5-FDCA, as opposed to 2,4-FDCA and 3,4-FDCA, was the most similar to PET in terms of materials properties like glass transition temperature, and crystallinity.[15] Such properties are important to avoid costly changes in polymer processing machinery and methods. All of the FDCA's were biobased, but the cellulosic 2,5-FDCA was arguably the most straightforward biobased option compared to the hemicellulosic-derived 2, 4 & 3, 4 isomers.

1.1.2. FDCA: A useful biobased monomer

The synthesis of FDCA can be grouped into two main reaction types: oxidation of 5-hydroxymethylfurfural (HMF) from cellulosic biomass, and carboxylation of 2-furoic acid/esters from hemicellulosic biomass. A standard method of synthesizing FDCA from HMF was to oxidize the later with KMnO4.16 The highlight of this method was that it utilized a typical oxidizing agent and methods used in a chemistry lab, and the reaction could be conducted on a mole scale. An example of FDCA synthesis from hemicellulosic starting material was published by Dick et al. in 2017. This reaction was arguably "greener", since it employed a catalytic synthesis route and the main reagent other than furoic acid was CO_2.[17]

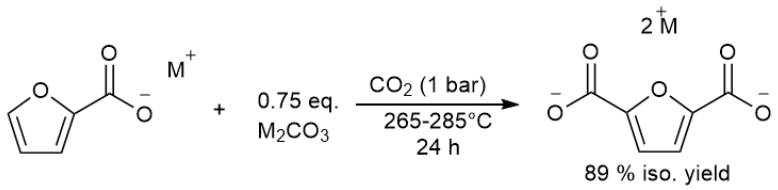

Figure 1.3. Furoic acid carboxylation redrawn from Dick et al.[17]

Not only did this method potentially reduce waste, but it was also run on a mole scale. This was not the only notable FDCA synthesis of the last five years. Although the following may not have all had scalable synthetic methods described in their publications, they were noteworthy in their method or in their yields.

Sourced from furoic acid, Zhang et al. demonstrated a method of FDCA in a bromination of the 5-position, followed by a Pd-catalyzed carbonylation at the same position. Wang et al. published a biocatalytic oxidation of HMF into FDCA by whole-cell biocatalysis. By co-expressing HMF/furfural oxidoreductase and vanillin dehydrogenase in E. Coli, they could produce FDCA on a gram scale.[18] In 2018, Ji et al. used microwaves, rather than thermal means, to oxidize HMF into FDCA in an “ultrafast method”. In combination with H_2O_2, they prepared Au/TiO_2 catalyst to selectively oxidize HMF to FDCA in 99.5 % yield (by HPLC) with a 30 minute reaction time.[19]

Improved synthetic methods continue to be explored in academia, while it can also be purchased from companies such as AVA Biochem. The ability to purchase FDCA can facilitate the exploration of FDCA derivatives and polymerizations, particularly in labs that do not focus on traditional organic chemistry methods as well as those without specialty equipment.

In 2014, Burgess et al. published two research articles on PEF. Both presented surprising, yet exciting, information featuring the advantages of PEF over PET.[12-13] First, they found that PEF has a comparable polymer density, glass transition temperature, melting temperature and decomposition temperature. This was an extremely important finding.

PEF showed a ~11x improvement oxygen barrier properties. This could have an outstanding impact in food packaging to avoid spoiling of food (a cost savings) but could also aid in corrosion resistance in performance coatings for automobiles and architecture. FDCA became a desirable commodity following this work, and research relating to FDCA synthesis and its use flooded the field of biomass-derived

chemistry and polymer science.[20-21] Some chemists turned their attention to other related furans, namely the FDCA precursor 5-(hydroxymethyl)furfural (HMF).[22]

1.1.3. HMF: Synthetic antecedent to FDCA

The standard route for obtaining useful 2, 5 -furanic monomers has been through the foundational compound, 5-hydroxymethyl furfural (HMF). HMF has proven to be a stable intermediate from which a multitude of foundational monomers have emerged, thus it has become a platform chemical and thus a target for synthetic optimizations and further derivatization.

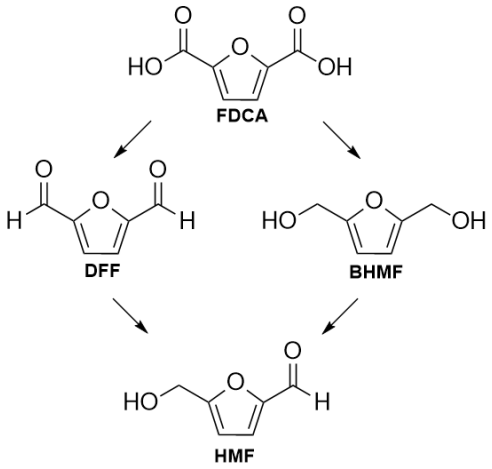

Figure 1.4. Oxidation products of HMF.

Early publications on the synthesis of HMF and its derivatives in the 2000s tended to be sub-gram scale reactions that required formation and use of catalytic systems not available in the typical synthetic organic chemistry lab. This was a bottleneck in terms of gram-scale synthetic methods of HMF and its derivatives were, particularly in the 2000s, especially difficult to find in the literature. The seminal work by Binder et al. published in 2009 provided one of the earliest examples of HMF synthesis from fructose, a cheap and readily available starting material, on a gram scale.[22] Not only can HMF be synthesized from the acid-catalyzed dehydration of fructose, but it can be produced, albeit in lower yields, from raw biomass. They explored not only HMF synthesis from fructose starting material, but also glucose and even cellulose. The DMA solvent-LiCl salt (10 %) system with a catalytic amount of either H_2SO_4 or

CuCl. Other additives and only DMA were also used. The highest yield (determined by HPLC) of HMF was 93 % from fructose, 80 % from glucose and 54 % from cellulose.

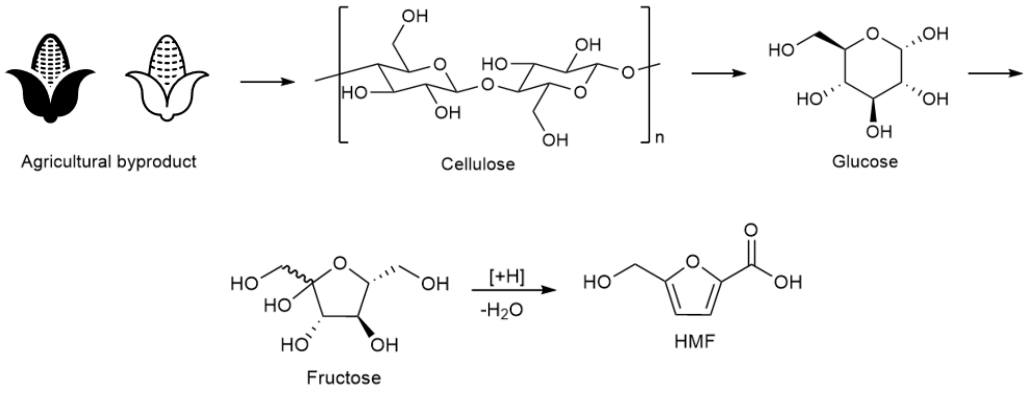

Scheme 1.2. Generalized transformation of biomass to HMF.

In 2017, a synthesis was reported by Wang et al. featuring the conversion of corncob acid hydrolysis residues (CAHR), a lignocellulosic byproduct, into HMF. By using $AlCl_3$ in combination with HCl. They obtained 30 % yield of HMF from CAHR and 54 % yield from glucose. Another route to HMF synthesis was examined by Nishimura et al.[23] Furfural was hydroxymethylated over Amberlyst-15 with aqueous formaldehyde. They tested their method both in batch reactions and in-flow resulting in 43 % yield with 57 % selectivity, measured via HPLC.

Like FDCA, HMF can now be purchased both in and outside the USA, making it more available for larger scale derivatizations.

1.1.4. BHMF: Diol of HMF

The reduction product of HMF, 2, 5-bis(hydroxymethyl)furan is like FDCA in that it can be directly used in polymerizations as a monomer, however it has gained popularity from its functionalization. BHMF has the benefit of containing two readily alterable hydroxymethyl groups, which have been diglycidated, bis-aminated, di(meth)acrylated, and so on.[20, 24-25]

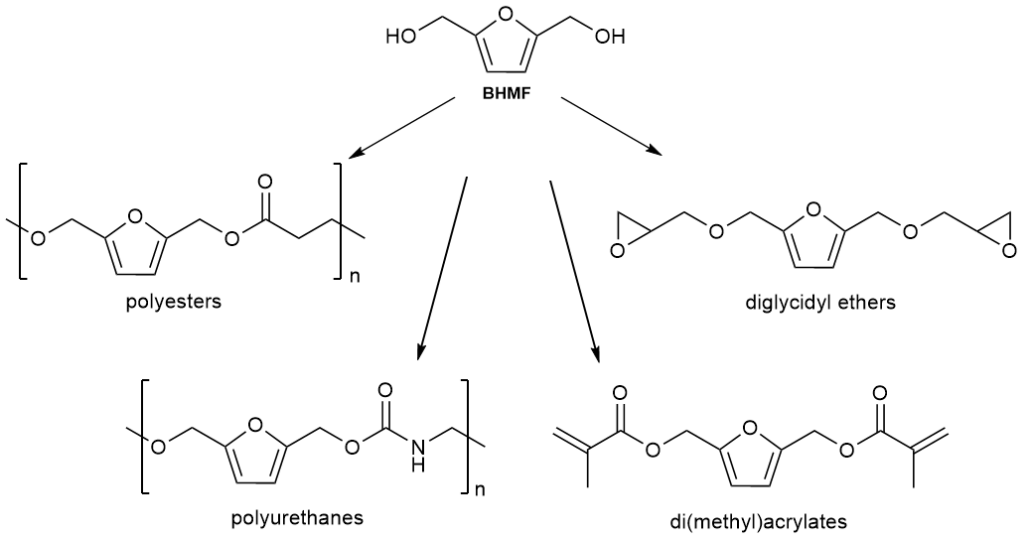

Figure 1.5. BHMF as a platform monomer.

Similar to FDCA, BHMF could be formed from HMF using typical reagents in the organic chemistry lab, in this case $NaBH_4$. Reduction of HMF via $NaBH_4$ was also a reaction that could be scaled up to tens of grams per reaction, with a crystallization purification. In the last five years, some interesting research has evolved into catalytic methods for BHMF synthesis.

In 2020, An updated version of the standard reduction mentioned was optimized by running the $NaBH_4$ reduction of HMF in deep eutectic solvents (DES), which is considered to be a green solvent. DES allowed for high concentration (40 wt % HMF) conversion of HMF to provide "~80 %" isolated yield of BHMF.[26] A selective reduction of HMF into BHMF was reported by Zhang et al. Their hydrothermal nickel catalysts supported on carbon produced 88 % yield of BHMF with a 94 % selectivity.[27] An electrocatalytic method of BHMF and FDCA formation from fructose was published by Liu et al. Without isolation, HMF was synthesized via microwave irradiation facilitated by HCl. It then underwent electrocatalytic conversion and which selectively be tuned to form FDCA or BHMF.[28]

New synthetic methods for BHMF formation demonstrates the continued interest in furan diol structure. As interest in replacing petroleum-based monomers other than terephthalic acid increases, the need for fine-tuned properties from biobased sources increasing. Detailed in the next four chapters, novel furan diols from cellulosic biomass were explored as possible alternatives to bisphenol A (BPA), a

monomer ubiquitous in coatings for innumerable applications. The dynamic nature of those furan diols was tested by functionalizing them in to epoxy monomers. Details on the synthesis and other findings are described herein, as well as future directions.

1.2. References

1. Alberts, B. J., A.; Lewis, J., *Molecular Biology of the Cell. .* 4th ed. ed.; Garland Science: New York, 2002.

2. Zhang, X.; Yang, W.; Blasiak, W., Modeling Study of Woody Biomass: Interactions of Cellulose, Hemicellulose, and Lignin. *Energy & Fuels* **2011,** *25* (10), 4786-4795.10.1021/ef201097d.

3. Onwukamike, K. N.; Grelier, S.; Grau, E.; Cramail, H.; Meier, M. A. R., Critical Review on Sustainable Homogeneous Cellulose Modification: Why Renewability Is Not Enough. *ACS Sustain. Chem. Eng.* **2019,** *7* (2), 1826-1840.10.1021/acssuschemeng.8b04990.

4. Rose, M.; Palkovits, R., Cellulose-Based Sustainable Polymers: State of the Art and Future Trends. *Macromolecular Rapid Communications* **2011,** *32* (17), 1299-1311.10.1002/marc.201100230.

5. Top value added chemicals from biomass Volume I: Results of screening for potential candidates from sugars and synthesis gas. agency, E. p., Ed. Pacific northwest national laboratory and the National renewable energy laboratory: 2004; Vol. 1, pp 1-76.

6. Gandini, A.; Silvestre, A. J. D.; Neto, C. P.; Sousa, A. F.; Gomes, M., The furan counterpart of poly(ethylene terephthalate): An alternative material based on renewable resources. *Journal of Polymer Science Part A: Polymer Chemistry* **2009,** *47* (1), 295-298.https://doi.org/10.1002/pola.23130.

7. Mitiakoudis, A.; Gandini, A., Synthesis and characterization of furanic polyamides. *Macromolecules* **1991,** *24* (4), 830-835.10.1021/ma00004a003.

8. Belgacem, M. N.; Quillerou, J.; Gandini, A., Urethanes and polyurethanes bearing furan moieties—3. Synthesis, characterization and comparative kinetics of the formation of diurethanes. *European Polymer Journal* **1993,** *29* (9), 1217-1224.https://doi.org/10.1016/0014-3057(93)90151-5.

9. Boufi, S.; Belgacem, M. N.; Quillerou, J.; Gandini, A., Urethanes and polyurethanes bearing furan moieties. 4. Synthesis, kinetics and characterization of linear polymers. *Macromolecules* **1993,** *26* (25), 6706-6717.10.1021/ma00077a003.

10. Choura, M.; Belgacem, N. M.; Gandini, A., Acid-Catalyzed Polycondensation of Furfuryl Alcohol: Mechanisms of Chromophore Formation and Cross-Linking. *Macromolecules* **1996,** *29* (11), 3839-3850.10.1021/ma951522f.

11. Gandini, A.; Belgacem, M. N., Furans in polymer chemistry. *Progress in Polymer Science* **1997,** *22* (6), 1203-1379.https://doi.org/10.1016/S0079-6700(97)00004-X.

12. Burgess, S. K.; Karvan, O.; Johnson, J. R.; Kriegel, R. M.; Koros, W. J., Oxygen sorption and transport in amorphous poly(ethylene furanoate). *Polymer* **2014,** *55* (18), 4748-4756.https://doi.org/10.1016/j.polymer.2014.07.041.

13. Burgess, S. K.; Leisen, J. E.; Kraftschik, B. E.; Mubarak, C. R.; Kriegel, R. M.; Koros, W. J., Chain Mobility, Thermal, and Mechanical Properties of Poly(ethylene furanoate) Compared to Poly(ethylene terephthalate). *Macromolecules* **2014,** *47* (4), 1383-1391.10.1021/ma5000199.

14. Liu, Y.; Zhao, J.; Peng, Y.; Luo, J.; Cao, L.; Liu, X., Comparative Study on the Properties of Epoxy Derived from Aromatic and Heteroaromatic Compounds: The Role of Hydrogen Bonding. *Industrial & Engineering Chemistry Research* **2020,** *59* (5), 1914-1924.10.1021/acs.iecr.9b05904.

15. Thiyagarajan, S.; Vogelzang, W.; J. I. Knoop, R.; Frissen, A. E.; van Haveren, J.; van Es, D. S., Biobased furandicarboxylic acids (FDCAs): effects of isomeric substitution on polyester synthesis and properties. *Green Chemistry* **2014,** *16* (4), 1957-1966.10.1039/C3GC42184H.

16. Serum, E. M. Exploitation of Biomass for Applications in Sustainable Materials Science. Ph.D., North Dakota State University, Ann Arbor, 2019.

17. Dick, G. R.; Frankhouser, A. D.; Banerjee, A.; Kanan, M. W., A scalable carboxylation route to furan-2,5-dicarboxylic acid. *Green Chemistry* **2017,** *19* (13), 2966-2972.10.1039/C7GC01059A.

18. Wang, X.; Zhang, X.-Y.; Zong, M.-H.; Li, N., Sacrificial Substrate-Free Whole-Cell Biocatalysis for the Synthesis of 2,5-Furandicarboxylic Acid by Engineered Escherichia coli. *ACS Sustain. Chem. Eng.* **2020,** *8* (11), 4341-4345.10.1021/acssuschemeng.0c00058.

19. Ji, T.; Liu, C.; Lu, X.; Zhu, J., Coupled Chemical and Thermal Drivers in Microwaves toward Ultrafast HMF Oxidation to FDCA. *ACS Sustain. Chem. Eng.* **2018,** *6* (9), 11493-11501.10.1021/acssuschemeng.8b01630.

20. Hu, F.; La Scala, J. J.; Sadler, J. M.; Palmese, G. R., Synthesis and Characterization of Thermosetting Furan-Based Epoxy Systems. *Macromolecules* **2014,** *47* (10), 3332-3342.10.1021/ma500687t.

21. Deng, J.; Liu, X.; Li, C.; Jiang, Y.; Zhu, J., Synthesis and properties of a bio-based epoxy resin from 2,5-furandicarboxylic acid (FDCA). *RSC Advances* **2015,** *5* (21), 15930-15939.10.1039/C5RA00242G.

22. Binder, J. B.; Raines, R. T., Simple Chemical Transformation of Lignocellulosic Biomass into Furans for Fuels and Chemicals. *Journal of the American Chemical Society* **2009,** *131* (5), 1979-1985.10.1021/ja808537j.

23. Nishimura, S.; Shibata, A.; Ebitani, K., Direct Hydroxymethylation of Furaldehydes with Aqueous Formaldehyde over a Reusable Sulfuric Functionalized Resin Catalyst. *ACS Omega* **2018,** *3* (6), 5988-5993.10.1021/acsomega.8b00120.

24. Wu, J.; Qian, Y.; Sutton, C. A.; La Scala, J. J.; Webster, D. C.; Sibi, M. P., Bio-Based Furanic Di(meth)acrylates as Reactive Diluents for UV Curable Coatings: Synthesis and Coating Evaluation. *ACS Sustain. Chem. Eng.* **2021,** *9* (46), 15537-15544.10.1021/acssuschemeng.1c05588.

25. Cho, J. K.; Lee, J.-S.; Jeong, J.; Kim, B.; Kim, B.; Kim, S.; Shin, S.; Kim, H.-J.; Lee, S.-H., Synthesis of carbohydrate biomass-based furanic compounds bearing epoxide end group(s) and evaluation of their feasibility as adhesives. *Journal of Adhesion Science and Technology* **2013,** *27* (18-19), 2127-2138.10.1080/01694243.2012.697700.

26. Wang, T.; Wei, J.; Liu, H.; Feng, Y.; Tang, X.; Zeng, X.; Sun, Y.; Lei, T.; Lin, L., Synthesis of renewable monomer 2, 5-bishydroxymethylfuran from highly concentrated 5-hydroxymethylfurfural in deep eutectic solvents. *Journal of Industrial and Engineering Chemistry* **2020,** *81*, 93-98.https://doi.org/10.1016/j.jiec.2019.08.057.

27. Zhang, Z.; Liu, C.; Liu, D.; Shang, Y.; Yin, X.; Zhang, P.; Mamba, B. B.; Kuvarega, A. T.; Gui, J., Hydrothermal carbon-supported Ni catalysts for selective hydrogenation of 5-hydroxymethylfurfural toward tunable products. *Journal of Materials Science* **2020,** *55* (29), 14179-14196.10.1007/s10853-020-05052-0.

28. Liu, X.; Leong, D. C. Y.; Sun, Y., The production of valuable biopolymer precursors from fructose. *Green Chemistry* **2020,** *22* (19), 6531-6539.10.1039/D0GC02315A.

2. INTRODUCTION TO FURANIC DIOLS FOR POLYMER SYNTHESIS

2.1. Bisphenols and the search for biomass replacements

2.1.1. The BPA controversy

This dissertation was initiated, in part, as a response to consumer concern over the presence of bisphenol A (BPA) in food and beverage containers. Concern arose in the 1990s when a study by researchers at Stanford University discovered that BPA can leach out of polymer materials in small amounts.[1] This prompted a number of studies from academia and third-party testing facilities via the government to determine the circumstances in which BPA leaching occurs and the dangers associated. Academics largely published work suggesting BPA in food and beverage containers is harmful to human and environmental health. Third-party research funded by the government, and research by chemical companies, suggests the average amount of BPA that humans are exposed to is too low to be of concern. The conflicting data seems to be due to inconsistent testing methods between these main data sources.

The estromimetic behavior of BPA was first noticed in the 1930s by E. Charles Dodds.2 Dodds was searching for estrogen-like compounds with an augmented ability to elicit estrus in rats. BPA was found to be active, but with ~10x weaker activity than estradiol, and weaker still compared to a similar compound in Dodds' studies, diethylstilbestrol (DES) (Figure 2.1). 3 Although it failed to become pharmaceutical like DES, BPA became undeniably popular when utilized as a monomer in the preparation of polymeric coatings and materials industries in the 1950s.

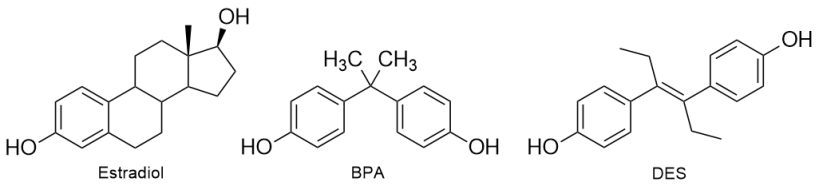

Figure 2.1. Estradiol, BPA, and DES.

The diol functionality of BPA can react directly in polymerization (e.g.: polycarbonates) or be altered before polymerization (e.g.: epoxy resins). Epoxy resins and polycarbonates have a vast presence in adhesives, food and beverage containers, thermal paper, flooring, and more.[4-6] BPA has a strong

presence in everyday products, but since BPA is used for non-pharmaceutical purposes, its hazards were evaluated in terms of acute toxicity, not possible carcinogenic behavior.[7] Due to the high volume at which it is used with respect to exposure to workers, the carcinogenic potential of BPA was investigated by the National Cancer Institute (NCI) beginning in 1977. The NCI's research would become the benchmark for understanding health hazards of BPA and a source of contention.

Critics of the study focused on the lack of research on transplacental effects with the knowledge that a sister compound of BPA, DES, had to be removed from the pharmaceutical market as it caused rare vaginal cancers in daughters born to women who took the drug.[8] The drug effected not only mothers and daughters, but grandchildren.[9] Critics also challenged the NCI's assumption that, like non-hormone toxic chemicals, BPA would act monotonically, in other words, a dose-dependent fashion. Based on this assumption, the NCI did not study low-dose effects of BPA even though it is suspected that low-doses are the problem. Low doses of hormones do not necessarily follow the behavior of the same chemical at higher doses.[10] The NCI did suggest that it was possible BPA influenced the formation of cancers of the hematopoietic system, but not statistically significant enough to call the diol 'carcinogenic'.[11] The confusing conclusions by the NCI, along with the revelation that several of the laboratories contracted by the NCI had "poor quality-control measures, and poor pathology practices… [which] they concluded, could have affected the outcome of any research" would later be pointed out as reasons to reconsider the NCI results on BPA carcinogenicity.[7, 12] The report was published without reassessment by the NCI or the overseeing agency it was passed to in the middle of the study, the National Toxicology Program (NTP). This report was the foundation the Environmental Protection Agency and the Food and Drug Administration worked from to create rules on safe BPA exposure limits. These limits and the effect of BPA in general went unchallenged until an accidental observation in 1993.

The Feldman group, an endocrinology research group at Stanford University observed what was thought to be evidence of endogenous estrogen from yeast activating estrogen-responsive breast cancer cells. What it actually was, was BPA which had leached out of their polycarbonate flasks used in their lab.[1] This observation caused Feldman group, and later other academic researchers, to question the amount to which humans and the environment are exposed to BPA.

Several studies followed the findings at Stanford University in the next decade, but a controversial trend developed. The methods used to evaluate the hormone activity of BPA and the conclusions made upon that research tended to depend on the source. Academia tended to test for low-dose effects and generally agreed that BPA is an endocrine disruptor while evaluations by the chemical industry concluded that BPA was safe at the higher doses they tested. The lack of low-dose testing by the chemical industry was heavily criticized, but the FDA's ruling on the safety of BPA remained in place.

2.1.2. Low-dose effects

The National Toxicology Program (NTP) defines low-dose effects as any biological change observed at a level of typical human exposure, or, effects "at doses lower than those typically used in standard testing protocols". [13] Parrott et al. adds that "low doses of endocrine disrupting chemicals may not follow a monotonic dose-response relationship".[14]

Critics of the "low-dose hypothesis" point out a lack of cohesion in literature on low-dose effect quantitative methods concerning BPA. They have demanded that proponents of the low-dose effect define an exact number below which nonmonotonic dose-response relationships are established for BPA.[15] Critics also assert that there is no, or not enough, strong evidence of low-dose effects of BPA.[16-17] The back-and-forth between proponents of low-dose effects of BPA and their critics continue to the present time. Ultimately, it obscures a clear understanding of what action to take: Replace it, limit it, or let it remain in industry and consumer products as it is?

The push to replace BPA was revitalized once consumers became aware of potential health effects of BPA, and the controversy surrounding it. [18] This negative attention on BPA from the public caused manufacturers to swiftly remove BPA from baby bottles, water bottles and other food & beverage containers. How were they able to introduce an alternative so quickly?

2.1.3. Industry alternatives to BPA

"BPA-free" food and beverage containers, from a consumer's perspective, have the same physical character as their BPA-containing predecessors. Considering the structure of the two most common BPA replacements, this was not surprising.

The structure of a molecule dictates its behavior, whether it is chemical reactivity, biological activity, or physical properties in polymeric materials. Bisphenol F (BPF) and Bisphenol S (BPS) are two

of the many bisphenols in the monomer toolbox for polymer and materials scientists to use (Figure 2.2).[4, 19] The similarity of BPF and BPS to BPA is ideal in terms of mimicking BPA's materials properties. Unfortunately, they share potential health pitfalls with BPA, too.[19-21]

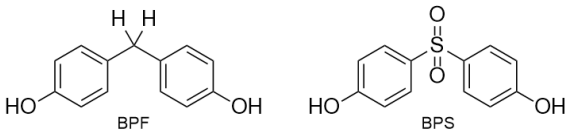

Figure 2.2. BPF and BPS.

Finding real alternatives to bisphenols for food and beverage applications is a great opportunity to try and improve upon some of its drawbacks while, ideally, retaining its merits. To do that, we need to understand some of the mechanism of BPA's biological activity, and to pinpoint the facets of BPA's structure that make it useful for coatings applications.

2.1.4. Structure-activity relationships of BPA

In 2012, Delfosse et al. published XRD and *in silico* predictions for the interactions of estradiol, BPA, and two other bisphenols in the estrogen receptor, ERα.[22] For the scope and purpose of this work, the interactions of BPA in the ligand binding domain of the transcriptional activation factor (AF-2) of ERα can be simplified to two aspects:

1. Van der Waals interactions between the ligand (BPA) and the ligand-binding domain (LBD) and
2. The distance of the ROH groups of the bisphenols compared to estradiol.

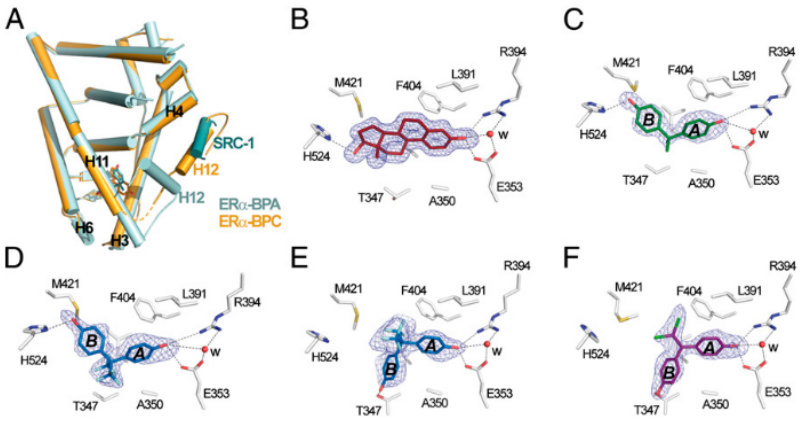

Fig. 3. Two different binding modes of bisphenols. (*A*) The whole structure of the ERα Y537S LBD in complex with SRC-1 NR2 and BPA (cyan) superimposed on that of WT ERα LBD bound to BPC (orange). The orange dashed line denotes residues not visible in the electron density map. (*B–F*) Interaction networks of E_2 (*B*), BPA (*C*), BPAF (*D* and *E*), and BPC (*F*) with LBP residues in ERα. Oxygen, nitrogen, sulfur, fluorine, and chlorine atoms are colored in red, blue, yellow, cyan, and green, respectively. Hydrogen bonds are indicated by black dashed lines. For clarity, not all protein–ligand interactions are depicted. The blue electron density represents a F_o-F_c simulated annealing omit map contoured at 3σ.

Figure 2.3. Structure-activity relationships of bisphenols in estrogen receptors from V. Delfosse et al.[22]

Although BPA can be oriented in such a way that the distance and angle of its hydroxyls are similarly displaced to the alcohols of estradiol, BPA and other bisphenols lack the same amount of hydrophobic character as the native ligand. The mostly aromatic character of bisphenols results in the inability of BPA to participate in an interaction between it and a key ligand binding domain (LBD) residue, leucine 525 (L525) (Figure 2.4).[22]

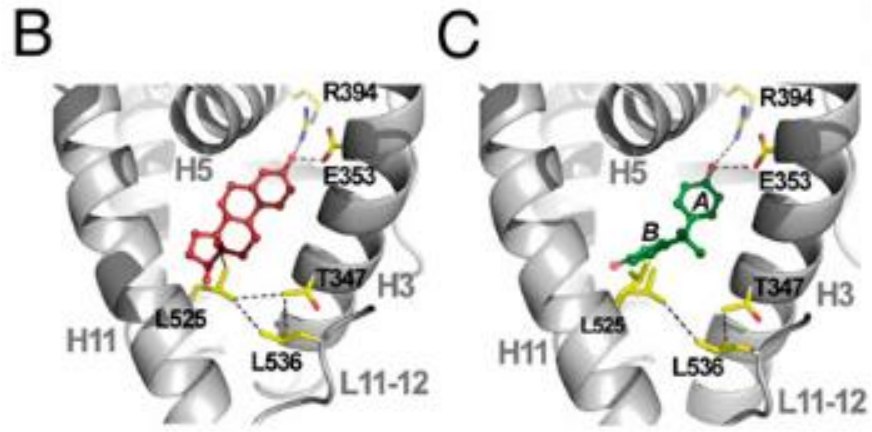

Figure 2.4. B) Estradiol in ERα; C) BPA in ERα. Taken from V. Delfosse et al.[22]

Without this key interaction, a network of other residues cannot interact with BPA as well as it does with estradiol, likely resulting in the well-known lower AF-2 activation ability of BPA compared to the native ligand. In addition to a lack of van der Waals interactions, it is worth considering that if BPA and

other bisphenols had a shorter distance between alcohols, bisphenols might have had lower binding affinity to AF-2.

2.1.5. Structure-property relationships of BPA in polymer applications

"The critical properties of most coatings films relate to their ability to withstand use without damage. The range of potential mechanical damage is large." [4]

Traditionally, polymer and materials science has been a field populated by engineers with a smattering of chemists. In this work, discussion of monomers was primarily from a fundamental chemistry perspective, rather than those engineers might use. The properties BPA provides to coatings has been attributed to one of its three main components (Figure 2.5):

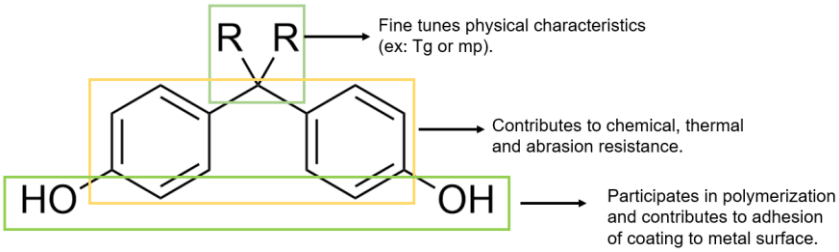

Figure 2.5. A breakdown of the three main components of BPA by functional group.

The purpose of a coating is to protect a surface and if a coating has poor adhesion, either inherently or under stress, it cannot perform its main objective. It is important then to understand what makes a polymer adhere to a surface. The focus here will be metal surfaces, like those in food containers. Whether as a free alcohol able to participate in H-bonding, or as an ether within the polymer chain, the oxygens/alcohols are the main contributors to adhesion of the polymer coating to a metal surface.[23]

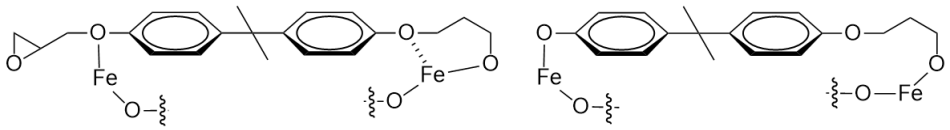

Figure 2.6. Adhesion mechanism of epoxy resin on iron oxide. Redrawn from M. Nakazawa et al.[23]

Although there are likely some π-Metal (M) interactions at the coating-metal interface, its contribution to adhesion is dwarfed by H-bonding and Oxygen-Metal interactions.[24] The phenyl ring's strength is in the van der Waals π-π interactions with other phenyl groups within the amorphous polymer matrix.[25] This type of interaction is what makes bisphenols ubiquitous in materials science. The strength of π-π interactions improve chemical and thermal resistance since they can be more difficult to 'interrupt' than, for example, London dispersion forces of long aliphatic chains, or poor interactions between sterically hindered molecules. At the same time, these interactions are not so strong that any bisphenol-containing polymer is too brittle to form useful coatings.

Lastly, the bisphenol bridging groups affect polymer properties, namely crystallinity of the polymer by increasing or decreasing the number and quality of favorable intermolecular interactions within the polymer matrix. This effect can be observed by comparing the melting points of BPA (158-159 °C), BPF (162-164 °C) and BPS (245-250 °C) (melting points obtained from Sigma-Aldrich Supelco chemicals). The bridge between phenols can disrupt favorable interactions between bisphenols (BPA vs BPF), and they can enhance them through stronger forces (BPS), depending on the desired outcome.

2.1.6. The biomass plan

With insight into which structural aspects should and should not be emulated, we had a reasonable range of structures to consider as BPA alternatives. In general, it is important to avoid a diol structure when the alcohols can span, and remain stiffly in one conformation, in the ERα AF-2. Additionally, it is important to avoid a large, nonpolar core as it plays an integral role in ERα activation. Alongside the "don'ts", certain characteristics are required to ensure that new diols can withstand the mechanical stresses of BPA's food and beverage coatings applications. The molecule must be a diol, it must have an aromatic core (not a pendant group) to retain a desirable thermal, chemical and abrasion resistance. The new foundational diol monomer would need to be derivatizable to suit different applications, just as is seen with the bridging groups of bisphenols.

In the Sibi group and as a part of the Center for Sustainable Materials Science (CSMS), we wanted the molecules to be derived from a renewable and, ideally, sustainable resource. The best biobased feedstock to source a BPA replacement is lignocellulosic in origin. Lignocellulose provides a multitude of aromatic structures, both benzylic and furanic. Such aromatic structures can provide the most

similar materials properties like good metal adhesion and thermal resistance when compared to aliphatic biobased structures. After careful consideration, furans became the aromatic core of choice due to their unique aromatic structure and chemistry.

2.1.7. Lignin-based monomers

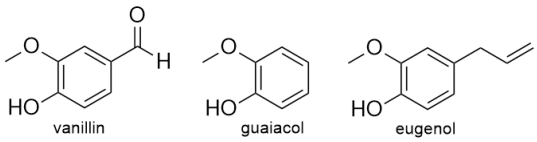

Figure 2.7. Structures of selected lignins.

Vanillin, guaiacol, and eugenol are some of the popular biobased options for BPA replacements. A 'pro' of using these compounds is that they could be purchased in bulk at the time this project began (~2015). Typically, in literature these phenols would be bridged to create a diol, forming a structure not unlike the petroleum-derived bisphenols being replaced. The goal of such research is solely focused on what it could do, which was to address the issue of finding a renewably sourced alternative to a petroleum-based compound.[26] Investigators in this field did not consider potential health concerns of their biobased bisphenols, evident in the synthesis of DES-like monomers.[27] Lignin derived compounds like vanillin, guaiacol, and eugenol might be better suited as a biobased Novolac, not as a BPA alternative.[28]

2.1.8. Cellulosic monomers

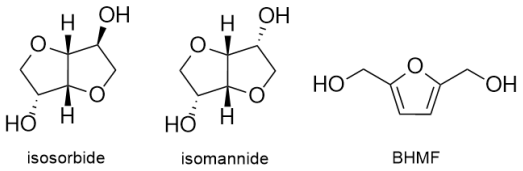

Figure 2.8. Isosorbide, isomannide and 2,5- Bis(hydroxymethyl)furan (BHMF) structures.

Cellulosic biomass is the source of two potential bisphenol alternatives explored in literature: isohexides and furans. Isohexides sought as BPA replacements are more often directed towards applications as polyurethane foams and adhesives, rather than coatings.[29] This is likely due to their significantly lower Tg than bisphenols; bisphenol A epoxies have a melting point starting at 65 °C, while isohexides range from -55 °C to +52 °C.[29-30] Most literature examples alter the properties of isohexide

polymers with an aromatic comonomer, such as furans or bisphenols.[31] Even with hydrophobic comonomers, isohexides are well-known for their degradation properties; they swell and degrade in the presence of water.[32] Of course, for single-use plastics, this may be a very fortunate property to have, but for performance coatings that prize durability, isosorbide-containing polymers should not be considered.

Alternatively, furans, as described in chapter 1, have been successfully employed as monomers since the polymer industry boom post-WWII. Furfural and other mono-functional furans were discounted for the same reasons as the mono-alcohol lignins. Furthermore, the synthesis and purification of discrete bridged furan dimers synthesized from mono-functional furans in the style of bisphenols is not facile.[33] Difunctional furans (2 & 5 positions) were a rising star in the 2010s wave of biomass-derived alternatives for petroleum-based chemicals.[34] There was already literature indicating the promise of furan diols, and we could see the potential for more by other furans in the 5-hydroxymethyl furfural (HMF) family. The furan diol 2, 5-bis(hydroxymethyl)furan (BHMF) became our starting point to determine if furan diols could be potential BPA substitutes according to our requirements.[35]

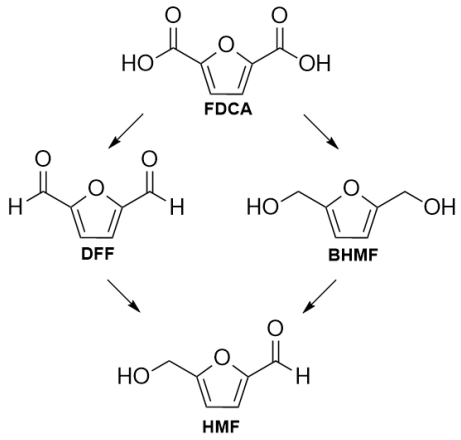

Figure 2.9. HMF-derived family of compounds.

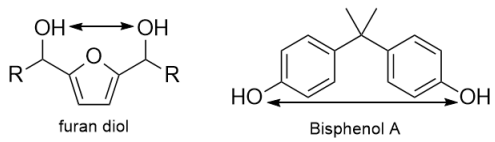

Figure 2.10. Visualization of the distance between furan diols vs BPs diols.

The shorter distance between the furanic alcohols than bisphenols would not theoretically have as strong of an activity in the ERα as BPA. Also, furans have a heteroaromatic core which is more polarizable (polar) and less aromatic than benzene. The polar character of the furan ring could evade key nonpolar interactions which cannot be avoided with BPA and estradiol within AF-2 of ERα. Additionally, the oxygen within the furan ring could have stronger interactions with a metal surface for improved adhesion. Alternatively, the polarity of the ring could cause issues with moisture retention from the atmosphere or aqueous workup of the polymerization, leading to corrosion resistance issues. Stronger H-bonding type interactions between the ring and remaining alcohols could cause coatings to be brittle.

The tuning of physical properties could still be obtained, but not via methylene bridge. 'R' groups could be added to the furan at the 2 or 2 & 5 positions of the furan in the diol synthesis from 5-hydroxymethylfurfural (HMF) or 2,5-diformyl furan (DFF), respectively. As a bonus, developing furans meant that we could explore recyclability with self-healing polymers made possible by the reversable Diels-Alder reaction. [36-37]

Considering the pros and cons, developing 2,5-substituted furans as BPA replacements was an advantageous start towards our goal of novel biobased diols without endocrine-disrupting activity.[38] Before moving forward, it is important to address why we did not simply use 2,5-bishydroxymethyl furan (BHMF) instead of synthesizing new furanic diols.

2.1.9. Why not further develop BHMF coatings?

BHMF is a great starting point for 2, 5-furan diols in terms of understanding its foundational materials properties, however, just as there are many types of bisphenols and each with their own niche, we wanted to do the same with furans. Varied R groups would alter the mechanical properties and toughness of subsequent coatings, potentially for a plethora of applications, just as BPA and other diols in polymer synthesis.

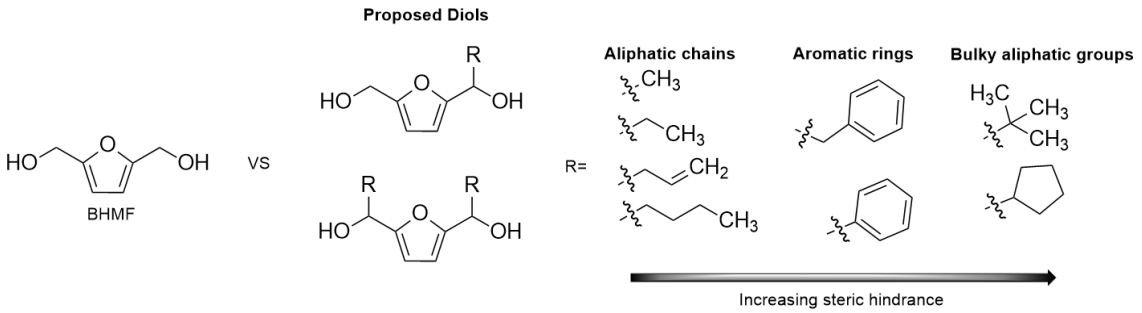

Figure 2.11. Proposed diols compared to BHMF.

One improvement anticipated, was that, based on the R group, the HMF and DFF-based diols would be liquid, rather than solids like BHMF (mp = 74-77 °C). That BHMF is a solid is a mild barrier to its potential adoption in industry, as it leads to increasing solvent content in polymer synthesis and coatings formulations, a blow to limiting waste. It could also lead to production complications. To form coatings from BHMF directly, such as would be the case for polycarbonate synthesis, it would need to be dissolved in an organic solvent to be able to polymerize with its crosslinker. The evaporation of that solvent could cause problems like bubbling of the coating making an accurate measurement of adhesion difficult to obtain. Solvent evaporation is also unnecessarily wasteful and would extend coating curing time, slowing production. It was anticipated that the addition of an aliphatic chain could produce liquid furan diols which would greatly simplify the application of the coating reaction components.

In addition to ease of use, the addition of different hydrocarbon R groups were anticipated to alter final materials properties, particularly the stacking and entangling of polymer chains. Allyl groups were added for possible post-polymerization crosslinking/modifications via Diels-Alder reaction.[39] Phenyl and benzyl groups were considered for their π-stacking ability, the influence behind chemical and thermal resistance. Lastly, the effect of steric hindrance was to be studied by adding progressively longer, then bulkier, aliphatic groups. Aliphatic groups, particularly the cyclopentyl groups, could add elements of hydrophobicity allowing for corrosion resistance of metals.

2.1.10. Literature methods of furan diol synthesis

Two types of transformations were considered to synthesize the proposed furanic biobased monomer: A) Alkylation of cellulose-derived furans (ex: HMF and DFF); B) Acylation of hemicellulose-derived furans (ex: furfural).

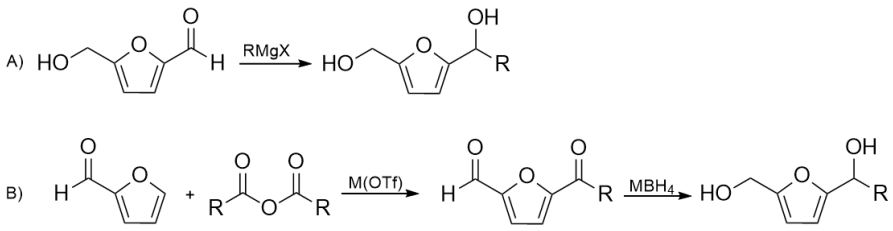

Scheme 2.1. A) Alkylation of cellulosic furan; B) Acylation of hemicellulosic furan.

The exact procedures could not be found in literature, but the alkylation of furanic carbonyl groups was not expected to be arduous, since the furan ring is not directly involved in the reaction mechanism. Concern for furan ring-opening as a side-product as well as the formation of the colored impurity common to furans in general was the only source of some hesitation for any furanic transformation. In some cases, the chemistry of the furan ring has been oversimplified in the biomass-derived chemical community as being the same in reactivity as benzene since they are both aromatic molecules. Something that cannot be stressed enough is that due to the polarizability of the heteroaromatic ring, the cycle is more vulnerable to conditions like Bronsted and Lewis acids, as well as strong bases, than benzene rings. Such conditions would cause furan ring-opening or color impurity formation. While this may seem to be a fault of furans, it could be seen as more of a learning curve to its use, and an opportunity to explore furan chemistry. Unlike benzene-based compounds, furanic compounds do not require as harsh of conditions for the same transformations. This could mean milder reaction conditions, and in turn, potentially safer working conditions for researchers.

Three organometallic reagents were possible starting points for the alkylation method, each with a different level of nucleophilic behavior: the Grignard reagent (RMgX), organolithium reagents (n-Butyl lithium), and organocadmium reagents (R_2Cd). The Grignard reaction is very well-known and reliable, and the reagent can be synthesized inhouse or purchased. However, if the Grignard reagent was not nucleophilic enough, an organolithium reagent could be used. If the Grignard reagent was too nucleophilic and caused excessive color impurity formation, an organocadmium reagent could be used. However, this is not a viable alternative since cadmium compounds are very toxic.

The Grignard reagent was tested first and provided good to excellent yields (>80 %). It had a quick reaction time (1 h) and the color impurity formation could be mitigated. In the end, other types of organometallic reagents were not needed for the proof-of-concept synthesis of furanic diols. Still, there were some disadvantages to the alkylation method of furan diol synthesis, primarily concerning the amount of waste created from the Grignard reaction at larger scale (0.1 mol). Acylations of monosubstituted furans is described in some literature in the 1930s, but the reactions are more complex with the formation of char and other side products with which to contend. This catalytic method could lower waste formation, but it would take more time to develop. Elaboration of the chemistry and methods for catalytic acylation of monosubstituted furans is described in the following chapter.

2.2. Results and discussion

2.2.1. Discussion of synthesis results

One of the things that helped the Sibi group biomass team the most was that we could scale-up HMF and 2,5-diformylfuran (DFF) synthesis. The mole-scale DFF synthesis was something our group had access to that other biomass researchers did not, through the work by E. Serum.[40]

No synthetic method was found in literature searches for any of the furans we planned to synthesize via alkylation, and BHMF is the product of HMF reduction via $NaBH_4$. Performing an alkylation on furan aldehydes with a stoichiometric reagent was necessary as a proof-of-concept venture; it might not be the "green" option, but it would help to determine whether the desired diols could be synthesized and remain stable enough to undergo subsequent alterations and polymerization. A concern that the proof-of-concept reactions could dispel was that the furans might ring-open from the harsh reaction conditions, another was that polymerization could occur. These matters were considered when choosing an alkylation method for novel furan diol synthesis.

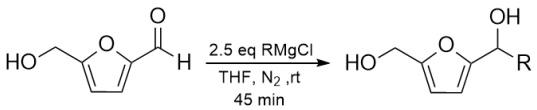

Scheme 2.2: Initial conditions for Grignard reaction-led synthesis of furan diols.

The Grignard reaction was chosen for its simplicity and ease of access; it could be purchased or synthesized the reagents. The reaction of the Grignard reagent-led alkylation of furanic aldehydes was quick and had a straightforward quenching and aqueous workup. Further, the yields were generally good to excellent (Table 2.1 & 2.2).

The yields for HMF-based diols ranged from good to excellent. The lowest yielding reaction was that for the synthesis of **1a,** the HMF-based methyl diol at 77 %, with the cyclopentyl version following after at 78 % yield. Based on TLC monitoring and ^{1}H NMR, there was no remaining starting material to account for the yield, so it did not seem to be a matter of poor conversion. Rather, it is suspected that it is more to do with the higher solubility of the HMF-based methyl diol due to it likely being the least hydrophobic of the diols from a lower hydrocarbon to hydroxy ratio than the other diols. It is suspected that in the aqueous workup, some of the desired product was solubilize in the brine wash.

The HMF-based cyclopentyl diol does not have the same issue of poor hydrophobicity due to its higher hydrocarbon content. It is possibly however, that the steric hindrance of the bulky R group does cause some issues. The crude product spectra show not just the desired material, but also minute amounts of several side-products. It could be that the steric hindrance allows for a slightly slower reaction rate, allowing the opportunity for alternate reaction pathways to be utilized, like oligomerization and elimination reactions. The same could be said for fellow sterically hindered R group products like the benzyl-containing compound **1h**.

The HMF-based diol series produced the only stable solid, that of the alkylation via phenyl group (**1g**). The pi-stacking between the furans and the phenyl rings was strong enough that it could form a solid product with a melting point of 95° C. As a result, this diol had the shortest workup following quenching; it did not require extended periods of time and care drying under nitrogen flow or HiVac, it simply needed to be allowed to freeze (4 C) after solvent removal via rotovap. The resulting solid could be crushed, and residual solvent removed briefly under HiVac. Unfortunately, the same could not be said of the DFF-based version, because it could not be worked up without turning into a highly viscous, dark resin.

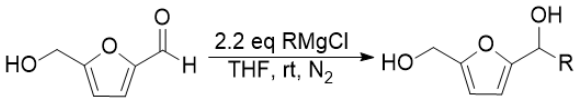

Table 2.1. HMF -based diols 8 mmol scale results.[41]

Entry	R group	Iso. Yield (%)
1A	methyl	77
1B	ethyl	91
1C	Allyl	88
1D	n-butyl	94
1E	t-butyl	95
1F	c-pentyl	78
1G*	Phenyl	87
1H	benzyl	80

*solid (mp = 95.0 °C, 87.4 °C onset).
All diols are liquids, unless otherwise noted.

It is likely possible that the DFF-based phenyl diol could be obtained, but it would require such care being kept under constant nitrogen and possibly out of light and away from temperatures above 20 °C that it did not make sense for it to be pursued for bulk monomer synthesis. It was by far the most difficult of the diols to work with, and since it could not be worked up without resinification, it was not considered for a time-costly optimization study. Attempts were made to analyze the product from this reaction, but the resin was not fully soluble in NMR solvents and, frankly, any attempt to analyze it by HRMS would have resulted in a mess inside the instrument due to the resin's generally stickiness and lack of solubility.

Other than the discontinued pursuit of a DFF-based phenyl diol, the overall trend observed in Table 2.1 in terms of the diols with higher hydrocarbon content being more hydrophobic thus allowing for higher isolated yield mirrored those for the DFF-based diols (Table 2.2). The isolated yields were, at worst, 80 %.

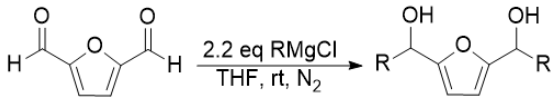

Table 2.2. DFF-based diols 8 mmol scale results.[41]

Entry	R group	Iso. Yield (%)
2A	methyl	98
2B	ethyl	95
2C	allyl	90
2D	n-butyl	94
2E	t-butyl	95
2F	c-pentyl	80
2G	benzyl	83

All DFF-based diols are liquids.

Last but not least was the alkylation of the ester 2,5-furandicarboxylic acid (FDCA-Me) to produce a tetramethyl diol. The isolated yield was in the range expected of “mirrored”-type furan diols like DFF-based diols. It is a solid, yet unlike the compound **1g** , it is not stable, degrading into a yellow semisolid. Not surprisingly, it did require an extended reaction time of 16 hours, which was to be expected due to steric hindrance of reacting two methyl groups to the same carbon.

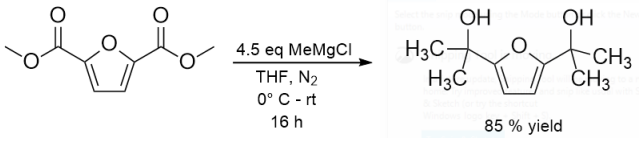

Scheme 2.3. Alkylation of the methyl ester of FDCA.

Still, the criticism of the slightly lower yields observed is perhaps an over-analysis; the yields are roughly in the same range overall and that range was beyond acceptable compared to anticipated low (30 %) yields. The synthetic path to the results of the of Tables 2.1 & 2.2 was relatively unobscured. It was the workup and the handling those diols in the above tables that took time to understand. The methods and their impetus are described.

2.2.2. Evaluation of synthesized furan diols by CALUX assays

CALUX results were provided by BioDetection Systems. CALUX is an acronym for chemically activated luciferase gene expression.[42] A sample of each novel furan diol and BHMF were compared to BPA and estradiol for activation of estrogen, androgen, anti-androgenic and thyroid activity. Cytotoxicity was also measured. The favorable interaction of a molecule in a particular receptor activates the luciferase reporter gene. The bioluminescent light emitted by the gene is then quantitatively analyzed by a luminometer. The value shown is the concentration at which a response was observed and recorded. The higher the value, the higher the concentration needed to activate that the specific receptor (Tables 2.6-2.9). It was very encouraging to observe that some of the diols, marked "NA" synthesized indicated no hormone activity, from what was tested, and no cytotoxicity. It was initially surprising that the furans with more aliphatic character (1C, 1D, 2B, 2C) could interact favorably with the hormone receptors, albeit much higher concentrations of the substrates were needed to do so compared to BPA (Table 2.6-2.9).

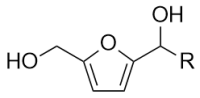

Table 2.3. Endocrine activity of asymmetric furanic diols vs BPA (μM)

Entry	ER-α-CALUX	AR CALUX	Anti-AR CALUX	Anti-TRβ-CALUX
BPA	0.075	ND	0.013	27
BHMF	NA	NA	NA	NA
5a	NA	NA	NA	NA
5b	NA	NA	NA	NA
5c	410	NA	78	300
5d	710	NA	120	360
5e	NA	NA	49	NA
5f	62	NA	40	110
5g	9.65	NA	NA	NA
5h	53	NA	50	71

When considering that aliphatic groups can trigger further favorable interactions with the polar groups of a molecule, it is not so surprising.22 Still, it was thought that the nonpolar character between the alcohols was more of an issue than nonpolar character distantly associated with the alcohol groups.

Preliminary predictions on what type of furan diol could avoid the endocrine-disruption pitfalls of BPA were partly confirmed through the CALUX assay results. The shorter aliphatic chains (1A, 1B, 2A, 3), particularly when there were fewer of them (HMF rather than DFF), the very sterically hindered R groups (1E, 2E), along with the closer proximity of the alcohol groups, compared to those of BPA, proved to be difficult for some hormone receptors to interact with in this preliminary study.

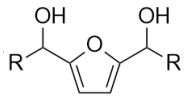

Table 2.4. Endocrine activity of DFF-based furanic diols vs BPA (μM)

Entry	ER-α-CALUX[b]	AR CALUX[b]	Anti-AR CALUX[c]	Anti-TRβ-CALUX[c]
BPA	0.075	ND	0.013	27
6a	NA	NA	340	NA
6b	630	NA	180	NA
6c	226	NA	46.9	NA
6d	28.2	NA	8.1	NA
6f	180	NA	43	NA
6e	NA	NA	3	NA
6g	34	NA	22	41
8	NA	NA	30	34

In tables 2.6 and 2.7, all values are in μM concentrations. ERα and AR CALUX values are bPC10; the concentration of chemical at which its response equals 10 % of the max. response of the reference standard. The anti-AR and anti-TRβ values are cPC80; the concentration of chemical at which its response equals 80 % of the max. response of the reference standard.

Unfortunately, BPA was not included in the cytotoxicity testing, making the ability for comparison difficult (Table 2.8-2.9). However, the cytotoxicity assays followed the trends of the assays for endocrine

disruption. The diols showing high activity in ERα and anti-AR CALUX assays have an observed response in the cytotoxicity assay.

Table 2.5: PC_{80} values of Cytotox CALUX study of HMF-based diols in mM.

Entry	Cytotox CALUX
1a	NA
1b	NA
1c	1.6
1d	1.9
1e	0.96
1f	0.83
1g	0.279
1h	0.34

Table 2.6: PC_{80} values of Cytotox CALUX study of DFF-based diols in mM.

Entry	Cytotox CALUX
2a	NA
2b	5.1
2c	0.0852
2d	0.785
2f	0.92
2e	0.33
2g	0.19
3	0.19

Comparing the cytotoxicity results between the mono and di-alkylated product lines, the diols with lower hydrocarbon content did not show detectable toxicity to cells, namely 1a-b and 2a. It is encouraging that the cytotoxicity assay results are in harmony with the endocrine-disrupter assay results. Although these are preliminary results, they indicate that, for the purpose of avoiding certain human and environmental health concerns, the compounds 1a-b and 2a should be pursued of all the diols synthesized.

From a chemistry standpoint, however, the materials properties were to be investigated in a scope larger than those three key furan diols. Following the success of HMF, DFF and FDCA-based diol formation, a plan to modify the diols into diglycidyl ethers was put into action. A few of those furan

diglycidyl ether reactions were then scaleup and given to our collaborators in the Coatings and Polymeric Materials Department to polymerize the monomers and analyzed their coatings properties.

2.3. Experimental

2.3.1. Furan diol workup and handling

Initially, in an attempt to be "green" by limiting solvent waste, the first Grignard reactions tested were run in just enough solvent to dissolve the substrate. Grignard reagent was added to the solution in concentrated form (1-3.4 M in ether) as purchased, turning the reaction a deep amber color. The amber color would persist into the final product unless the product was passed through a silica plug. Unfortunately, the diols themselves are sensitive to silica, which is acidic, and polymerize onto silica columns eluting trace amounts of desired product. The amber product can be run through a quick silica plug, but it will only lessen the amber color, not completely remove it. The color, a suspected conjugated oligomer or polymer of the furans, is common to furan chemistry. It typically is formed in response to harsh conditions such as high heat in the presence of oxygen, strong acid, or strong base. The amber color, as far as is known at the time this is written, is not known, or presumed to be a single compound but has also not been characterized. It can be said that it is a potent pigment; it is in such low concentrations that it is only slightly noticeable in ^{1}H NMR and often not at all in ^{13}C NMR. It should be noted that the amber color was more of an aesthetic issue than a chemistry one; it would not be as marketable to have brown coatings or other plastics than clear and colorless ones.

Through subsequent method optimizations the color was improved from deep, opaque amber to translucent yellow, the molar equivalence of Grignard reagent was decreased from 2.5 eq. to 2.2 eq (or 2.1 eq on 0.1 mol scale) and reaction time was extended to 1 hour for full conversion.

Scale-up (0.1 mol) of this was as nearly as straightforward as the small-scale reactions (8 mmol), but certainly took more time in the setup, reaction time, workup and drying of the resulting oil. The reaction needed to be in an ice bath for the addition of the substrate to the Grignard reagent solution to control the exotherm. Scale-up also meant extra washing with brine was needed to remove the magnesium salts that would otherwise remain suspended in the oil and only become observable after cooling in a freezer (4° C). The other issue with larger quantities of product was the drying process. A full drying or removal of solvent should be done within a day or two of the diol being used in further reactions,

not for storage. If the diols are stored in concentrated form past about a week, the oil becomes a resin and cannot be used in any of our further reactions. It was not clear if this resin was the product of ring-opened furans from the proximity of intermolecular alcohol protons, elimination reactions of the alcohols, another unknown reaction, or a mixture of all three. Attempts to analyze via NMR and HRMS provided "forests" of peaks. Some IR spectra showed alcohol stretching, but others did not.

2.3.2. Synthesis of HMF-based and DFF-based diols via Grignard reaction

A reaction vessel containing solution of purchased Grignard reagent (2.2 eq, diluted from 1.0 -3.4 M to a 0.5 M solution in inhibitor-free drysolv THF) was flushed with N2 and kept under positive N2 pressure. A solution of substrate (HMF and DFF dissolved to form a 0.2 M solution dissolved to form a 0.1 M solution in inhibitor-free drysolv THF) was added dropwise via syringe into the dry 50 mL round bottom flask reaction vessel. The reaction was monitored by TLC, until the reaction was complete (1h). To quench the reaction, 6 mL of 0.1 M trisodium citrate (aq) was added via syringe. The reaction mixture was filtered through filter paper, then the THF was removed in vacuo. The resulting oil was then diluted with ethyl acetate (40 mL) and washed with brine (3 x 10 mL) in a 60 mL separatory funnel. The organic layer was dried over sodium sulfate, then filtered and solvent removed in vacuo. Final drying on small and large scale by placing the oil under HiVac while stirring, occasionally sparging with inert gas. Warming the substrate in water or oil bath at 30° C completed the process faster without negative effects. The products were consistently pale-yellow viscous oils with yields ranging 77-98 %.

2.3.3. Synthesis of FDCA ester-based tertiary diol

A reaction vessel containing solution of purchased Grignard reagent (13.5 mmol, diluted from 1.0 -3.4 M to a 0.5 M solution in inhibitor-free drysolv THF) was flushed with N2 and kept under positive N2 pressure. A solution of substrate (3 mmol, dissolved to form a 0.1 M solution in inhibitor-free drysolv THF) was added dropwise via syringe into the dry 50 mL round bottom flask reaction vessel. The reaction was monitored by TLC, until the reaction was complete (1-2 h). To quench the reaction, 6 mL of 0.1 M trisodium citrate (aq) was added via syringe. The reaction mixture was filtered through filter paper, then the THF was removed in vacuo. The resulting oil was then diluted with ethyl acetate (40 mL) and washed with brine (3 x 10 mL) in a 60 mL separatory funnel. The organic layer was dried over sodium sulfate, then filtered, and solvent removed in vacuo to obtain the diol product 3 in 85% yield. The solid diol was

not stable and underwent dehydration readily, observable by 1H NMR. However, the compound could be stored in a freezer without decomposition if stored diluted in a solvent like ethyl acetate. Its shelf life, when stored properly, is about a week.

2.4. HMF-based diol spectral data

2.4.1. Sample preparation for instrumental analysis and notes

All NMR samples were, unless noted otherwise, neat samples dissolved in deuterated solvent. The standard deuterated solvent was $CDCl_3$, but some other solvents and solvent combinations were used in at least one instance, which is noted in the title for the spectrum. Masses ranging from 12-20 mg of the furan diols were diluted with 0.75 mL of deuterated solvent, no matter the solvent.

All IR spectra samples were neat, unless otherwise noted.

HRMS samples were prepared by diluting the furan substrates in UPLC-grade methanol.

2.4.2. Written spectral data

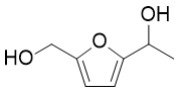

Compound 1a: ^{1}H (400 MHz, $CDCl_3$) δ 6.16 (dd, *J* = 18.2, 3.1 Hz, 2H), 4.81 (dd, *J* = 6.3, 4.2 Hz, 1H), 4.51 (d, *J* = 4.9 Hz, 2H), 3.35 (d, *J* = 10.9 Hz, 2H), 1.50 (d, *J* = 6.6 Hz, 3H).; ^{13}C (101 MHz, $CDCl_3$) δ 157.5, 153.3, 108.2, 105.8, 63.3, 57.1, 21.0. FTIR (neat) cm^{-1} 3316, 2979, 2932, 1635, 1557, 1369, 1320,1239, 1187, 1072. HRMS calculated for $C_7H_{10}O_3Na$: 165.0528; Found: 165.0537.

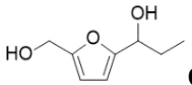

Compound 1b: ^{1}H (400 MHz, $CDCl_3$) δ 6.17 (d, *J* = 3.2 Hz, 1H), 6.13 (d, *J* = 2.8 Hz, 1H), 4.50 (s, 3H), 3.46 (s, 1H), 3.29 (s, 1H), 1.94 – 1.75 (m, 2H), 0.93 (t, *J* = 7.4 Hz, 3H); ^{13}C (101 MHz, $CDCl_3$) δ 156.5, 153.3, 108.7, 106.5, 69.0, 57.0, 28.3, 10.0. FTIR (neat) cm^{-1} 3304, 2965, 2933, 2876, 1556, 1378, 1318, 1242, 1183, 960. HRMS calculated for $C_8H_{12}O_3Na$: 179.0684; Found: 179.0730.

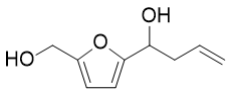

Compound 1c: ^{1}H (400 MHz, $CDCl_3$) δ 6.26 – 6.22 (m, 2H), 5.84 (ddt, *J* = 17.2, 10.2, 7.1 Hz, 1H), 5.24 – 5.17 (m, 2H), 4.76 (t, *J* = 7.4, 5.7 Hz, 1H), 4.61 (s, 2H), 2.67 – 2.63 (m, 2H), 1.92 (s, 2H); ^{13}C (101 MHz, $CDCl_3$) 156.0, 153.4, 133.6, 118.6, 108.4, 106.8, 66.9, 57.4, 39.9. FTIR (neat) cm^{-1} 3315, 2955, 2931, 2861, 1724, 1559, 1457, 1377, 1243, 1182. HRMS calculated for $C_9H_{12}O_3Na$: 191.0684; Found: 191.0721.

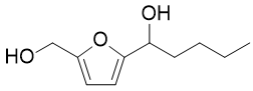

Compound 1d: ^{1}H (400 MHz, $CDCl_3$) δ 6.23 (d, *J* = 3.2 Hz, 1H), 6.18 (d, *J* = 3.2 Hz, 1H), 4.65 (t, *J* = 6.9 Hz, 1H), 4.58 (s, 2H), 2.30 (s, 2H), 1.86 (h, *J* = 7.3 Hz, 2H), 1.48 – 1.27 (m, 4H), 0.93 (t, *J* = 7.0 Hz, 3H).; ^{13}C (101 MHz, $CDCl_3$) δ 156.9, 153.3, 108.3, 106.5, 67.8, 57.4, 35.1, 27.7, 22.4, 14.0. FTIR (neat) cm^{-1} 3396, 2955, 2870, 1723, 1552, 1479, 1464, 1394, 1364, 1197. HRMS calculated for $C_{10}H_{16}O_3Na$: 207.0997; Found: 207.0997

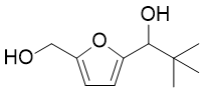

Compound 1e: ^{1}H (400 MHz, $CDCl_3$) δ 6.19 (d, *J* = 3.1 Hz, 1H), 6.15 (d, *J* = 3.1 Hz, 1H), 4.53 (s, 2H), 4.37 (d, *J* = 8.6 Hz, 1H), 2.85 (s, 1H), 2.74 (s, 1H), 2.37 (q, *J* = 8.1 Hz, 1H), 1.90 – 1.84 (m, 1H), 1.66-1.47 (m, 6H), 1.25 – 1.18 (m, 1H); ^{13}C (101 MHz, $CDCl_3$) δ 156.7,153.2, 108.2, 106.9, 71.8, 57.3, 44.4, 29.2, 25.5. FTIR (neat) cm^{-1} 3327, 2949, 2867, 1704, 1559, 1449, 1362, 1311, 1885, 931. HRMS calculated for $C_{10}H_{16}O_3Na$: 207.0997; Found: 207.0982.

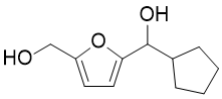

Compound 1f: ^{1}H (400 MHz, $CDCl_3$) δ 6.19 (d, *J* = 3.2 Hz, 1H), 6.16 (d, *J* = 3.2 Hz, 1H), 5.80 (td, *J* = 17.2, 7.0 Hz, 1H), 5.18 – 5.11 (m, 2H), 4.67 (t, *J* = 6.5 Hz, 1H), 4.51 (s, 2H), 3.26 (s, 1H), 3.20 (s, 1H), 2.59 (t, *J* = 7.2 Hz, 2H); ^{13}C (101 MHz, $CDCl_3$) δ156.0, 153.4, 133.8, 118.3, 108.3, 106.8, 66.9, 57.2, 39.8. FTIR (neat) cm^{-1} 3320, 2923, 1641, 1557, 1416, 1316, 1182, 916, 860, 793. HRMS calculated for $C_{11}H_{16}O_3$ Na: 219.0997; Found: 219.0999.

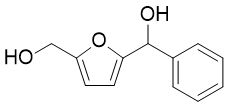

Compound 1g: ^{1}H NMR (400 MHz, DMSO-d6) δ 7.41 (d, *J* = 4 Hz, 2H), 7.37 – 7.33 (m, 2H), 7.29 – 7.25 (m, 1H), 6.18 (d, *J* = 3.1 Hz, 1H), 6.04 (d, *J* = 3.1 Hz, 1H), 5.96 (d, *J* = 5.0 Hz, 1H), 5.66 (d, *J* = 5.0 Hz, 1H), 5.15 (t, *J* = 5.7 Hz, 1H), 4.33 (d, *J* = 5.7 Hz, 2H); ^{13}C NMR (101 MHz, DMSO-d6) δ 157.1, 155.1, 143.1, 128.4, 127.6, 127.0, 107.8, 107.3, 68.9, 56.1. FTIR (neat) cm^{-1} 3242, 2881, 1601, 1555, 1491, 1452, 1291, 1263, 1193, 1008. HRMS calculated for $C_{12}H_{12}O_3Na$: 227.0684; Found: 227.0686.

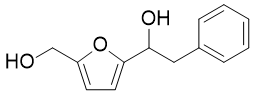

Compound 1h: ^{1}H NMR (400 MHz, $CDCl_3$) δ 7.31 – 7.17 (m, 5H), 6.17 (d, *J* = 3.1 Hz, 1H), 6.12 (d, *J* = 3.1 Hz, 1H), 4.84 (dd, *J* = 7.9, 5.9 Hz, 1H), 4.51 (s, 2H), 3.31 (s, 1H), 3.13 (qd, *J* = 13.7, 6.9 Hz, 2H), 2.76 (s, 1H); ^{13}C NMR (101 MHz, $CDCl_3$) δ 155.7, 153.4, 137.5, 129.4, 128.4, 126.6, 108.4, 107.1, 68.6, 57.2, 42.0. FTIR (neat) cm^{-1} 3379, 3027, 2922, 1702, 1602, 1495, 1453, 1416, 1360, 1221. HRMS calculated for $C_{13}H_{14}O_3Na$: 241.0841; Found: 241.0839.

DFF-based Diols

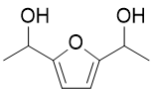

Compound 2a: ^{1}H (400 MHz, $CDCl_3$) δ 6.17 (s, 2H), 4.87 (q, *J* = 7.8, 6.9 Hz, 2H), 2.29 (s, 2H), 1.55 (d, *J* = 6.6 Hz, 6H); ^{13}C (101 MHz, $CDCl_3$) δ 156.9, 105.6, 63.5, 21.0. FTIR (neat) cm^{-1} 3391, 2980, 2934, 1764, 1702, 1446, 1370, 1302, 1238, 1192. HRMS calculated for $C_8H_{12}O_3Na$: 179.0684; Found: 179.0713.

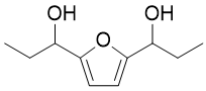

Compound 2b: ^{1}H (400 MHz, $CDCl_3$) δ 6.13 (s, 2H), 4.51 (t, *J* = 6.8 Hz, 2H), 2.94 (s, 2H), 1.86 – 1.79 (h, 7.2 Hz, 4H), 0.93 (t, *J* = 7.4 Hz, 6H); ^{13}C (101 MHz, $CDCl_3$) δ 195.9, 106.3, 69.0, 28.4, 9.9. FTIR (neat) cm^{-1} 3316, 2964, 2934, 2876, 1557, 1456, 1377, 1315, 1187, 1094. HRMS calculated for $C_{10}H_{16}O_3Na$: 207.0997; Found: 207.1007.

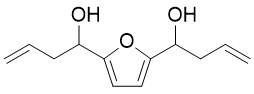

Compound 2c: ^{1}H (400 MHz, $CDCl_3$) δ 6.22 (s, 2H), 5.90 – 5.76 (m, 2H), 5.26 – 5.12 (m, 4H), 4.75 (t, *J* = 6.0 Hz, 2H), 2.64 (hept, *J* = 7.9, 7.3 Hz, 4H), 2.12 (s, 2H); ^{13}C (101 MHz, $CDCl_3$) δ 155.5, 133.6, 118.6, 106.7, 66.9, 40.0. FTIR (neat) cm^{-1} 3337, 2955, 2930, 2860, 1725, 1557, 1457, 1376, 1242, 1104. HRMS calculated for $C_{12}H_{16}O_3Na$: 231.0997; Found: 231.1004.

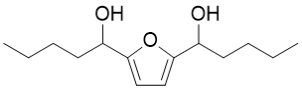

Compound 2d: ^{1}H NMR (400 MHz, $CDCl_3$) δ6.18 (d, *J* = 1.3 Hz, 2H), 4.66 (t, *J* = 7.5 Hz, 2H), 2.02 (s, 2H), 1.89 – 1.83 (m, 4H), 1.48 - 1.30 (dqt, *J* = 20.5, 14.2, 6.9 Hz, 8H), 0.93 (t, *J* = 7.0 Hz, 6H); ^{13}C NMR (101 MHz, $CDCl_3$) δ 156.2, 106.3, 67.8, 35.1, 27.7, 22.4, 14.0. FTIR (neat) cm^{-1}3309, 3076, 2914, 1640, 1431, 1310, 1186, 859, 794, 643. HRMS calculated for $C_{14}H_{24}O_3Na$: 263.1623; Found: 263.1639.

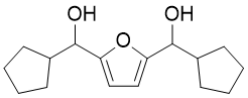

Compound 2e: ^{1}H (400 MHz, $CDCl_3$) δ 6.18 (d, *J* = 2.7 Hz, 2H), 4.42 (t, *J* = 6.7 Hz, 2H), 2.45-2.36 (m, 2H), 1.94 (s, 2H), 1.91 – 1.68 (m, 2H), 1.65-1.49 (m, 12H), 1.32 – 1.16 (m, 2H); ^{13}C (101 MHz, $CDCl_3$) δ 155.9, 106.8, 72.0, 44.6, 29.1, 25.6. FTIR (neat) cm^{-1} 3332, 2951, 2867, 1710, 1650, 1450, 1187, 1011, 794, 622. HRMS calculated for $C_{16}H_{24}O_3Na$: 287.1623; Found: 287.1623.

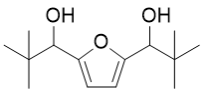

Compound 2f: ^{1}H (400 MHz, $CDCl_3$) δ 6.19 (d, *J* = 4.7 Hz, 2H), 4.36 (d, *J* = 6.1 Hz, 2H), 1.97 (s, 2H), 0.98 (s, 18H); ^{13}C (101 MHz, $CDCl_3$) δ 154.7, 107.5, 76.4, 35.7, 25.8. FTIR (neat) cm^{-1} 3429, 3101, 2956, 2871, 1561, 1513, 1413, 1365, 1241, 1189. HRMS calculated for $C_{14}H_{24}O_3Na$: 263.1623; Found: 263.1628.

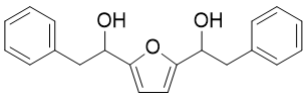

Compound 2g: ^{1}H NMR (400 MHz, $CDCl_3$) δ7.39 – 7.20 (m, 10H), 6.15 (d, *J* = 3.1 Hz, 2H), 4.91 (ddd, *J* = 8.0, 5.6, 3.8 Hz, 2H), 3.20 – 3.10 (s, 4H), 1.91 (s, 2H); ^{13}C NMR (101 MHz, $CDCl_3$) δ 155.2, 137.3, 129.4, 128.5, 126.7, 107.1, 68.7, 42.1. FTIR (neat) cm^{-1} 3346, 2955, 2905, 2869, 1682, 1557, 1479, 1462, 1389, 1365. HRMS calculated for $C_{20}H_{20}O_3Na$: 331.1310; Found: 331.1311.

FDCA-based Diol

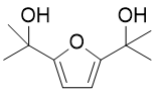

Compound 3: ^{1}H (400 MHz, $CDCl_3$) δ 6.09 (s, 2 H), 2.49 (s, 2 H), 1.58 (s, 12 H); ^{13}C (101 MHz, $CDCl_3$) δ 159.0, 104.0, 68.7, 28.5. FTIR (neat) cm^{-1} 3362, 2979, 2900, 1375, 1267, 1164, 1115, 1022, 959, 840. HRMS calculated for $C_{10}H_{16}O_3Na$: 207.0997; Found: 207.0994.

2.5. References

1. Krishnan, A. V.; Stathis, P.; Permuth, S. F.; Tokes, L.; Feldman, D., Bisphenol-A: an estrogenic substance is released from polycarbonate flasks during autoclaving. *Endocrinology* **1993,** *132* (6), 2279-2286.10.1210/endo.132.6.8504731.

2. Dodds, E. C.; Lawson, W., Synthetic strogenic Agents without the Phenanthrene Nucleus. *Nature* **1936,** *137* (3476), 996-996.10.1038/137996a0.

3. Dodds, E. C.; Lawson, W.; Noble, R. L., BIOLOGICAL EFFECTS OF THE SYNTHETIC ŒSTROGENIC SUBSTANCE 4 : 4'-DIHYDROXY-α : β-DIETHYLSTILBENE. *The Lancet* **1938,** *231* (5990), 1389-1391.https://doi.org/10.1016/S0140-6736(00)89468-4.

4. Wicks, Z. W. J., Frank N.; Pappas, S. Peter; Wicks, Douglas A. , Organic Coatings. Third Edition ed.; John Wiley & Sons, Inc.: Hoboken , New Jersey, 2007.

5. Karrer, C.; de Boer, W.; Delmaar, C.; Cai, Y.; Crépet, A.; Hungerbühler, K.; von Goetz, N., Linking Probabilistic Exposure and Pharmacokinetic Modeling To Assess the Cumulative Risk from the Bisphenols BPA, BPS, BPF, and BPAF for Europeans. *Environmental Science & Technology* **2019,** *53* (15), 9181-9191.10.1021/acs.est.9b01749.

6. Michałowicz, J., Bisphenol A – Sources, toxicity and biotransformation. *Environmental Toxicology and Pharmacology* **2014,** *37* (2), 738-758.https://doi.org/10.1016/j.etap.2014.02.003.

7. Vogel, S. A., The politics of plastics: the making and unmaking of bisphenol a "safety". *Am J Public Health* **2009,** *99 Suppl 3* (Suppl 3), S559-S566.10.2105/AJPH.2008.159228.

8. Herbst, A. L.; Ulfelder, H.; Poskanzer, D. C., Adenocarcinoma of the Vagina. *New England Journal of Medicine* **1971,** *284* (16), 878-881.10.1056/NEJM197104222841604.

9. Zamora-León, P., Are the Effects of DES Over? A Tragic Lesson from the Past. *International Journal of Environmental Research and Public Health* **2021,** *18* (19).10.3390/ijerph181910309.

10. Vandenberg, L. N.; Colborn, T.; Hayes, T. B.; Heindel, J. J.; Jacobs, D. R., Jr.; Lee, D.-H.; Shioda, T.; Soto, A. M.; vom Saal, F. S.; Welshons, W. V.; Zoeller, R. T.; Myers, J. P., Hormones and endocrine-disrupting chemicals: low-dose effects and nonmonotonic dose responses. *Endocr Rev* **2012,** *33* (3), 378-455.10.1210/er.2011-1050.

11. Carcinogenesis Bioassay of Bisphenol A (CAS No. 80-05-7) in F344 Rats and B6C3F1 Mice (Feed Study). *National Toxicology Program technical report series* **1982,** *215*, 1-116

12. Bernstein, P. A. *Report to the Honorable Henry Waxman, House of Representatives, Enclosure III, " NCI has not adequately Monitored Tractor-Jitco's Bioassay Responsibilities."*; Washington, DC., 1979;

13. Melnick, R.; Lucier, G.; Wolfe, M.; Hall, R.; Stancel, G.; Prins, G.; Gallo, M.; Reuhl, K.; Ho, S.-M.; Brown, T.; Moore, J.; Leakey, J.; Haseman, J.; Kohn, M., Summary of the National Toxicology Program's report of the endocrine disruptors low-dose peer review. *Environmental Health Perspectives* **2002,** *110* (4), 427-431.10.1289/ehp.02110427.

14. Parrott, J. L.; Bjerregaard, P.; Brugger, K. E.; Gray Jr, L. E.; Iguchi, T.; Kadlec, S. M.; Weltje, L.; Wheeler, J. R., Uncertainties in biological responses that influence hazard and risk approaches to the regulation of endocrine active substances. *Integrated Environmental Assessment and Management* **2017,** *13* (2), 293-301.https://doi.org/10.1002/ieam.1866.

15. Council, A. C. Low Dose Hypothesis. https://www.endocrinescience.org/glossary/low-dose-hypothesis/ (accessed 12/06/2021).

16. Rhomberg, L. R.; Goodman, J. E., Low-dose effects and nonmonotonic dose–responses of endocrine disrupting chemicals: Has the case been made? *Regulatory Toxicology and Pharmacology* **2012,** *64* (1), 130-133.https://doi.org/10.1016/j.yrtph.2012.06.015.

17. Kamrin, M. A., The “Low Dose” Hypothesis: Validity and Implications for Human Risk. *International Journal of Toxicology* **2007,** *26* (1), 13-23.10.1080/10915810601117968.

18. Layton, L., Industry-funded studies on plastic chemical questioned. *The Washington Post* 2008.

19. Chen, D.; Kannan, K.; Tan, H.; Zheng, Z.; Feng, Y.-L.; Wu, Y.; Widelka, M., Bisphenol Analogues Other Than BPA: Environmental Occurrence, Human Exposure, and Toxicity—A Review. *Environmental Science & Technology* **2016,** *50* (11), 5438-5453.10.1021/acs.est.5b05387.

20. Ponting, D. J.; Ortega, M. A.; Niklasson, I. B.; Karlsson, I.; Seifert, T.; Stéen, J.; Luthman, K.; Karlberg, A.-T., Development of New Epoxy Resin Monomers – A Delicate Balance between Skin Allergy and Polymerization Properties. *Chem. Res. Toxicol.* **2019,** *32* (1), 57-66.10.1021/acs.chemrestox.8b00169.

21. Mao, J.; Jain, A.; Denslow, N. D.; Nouri, M.-Z.; Chen, S.; Wang, T.; Zhu, N.; Koh, J.; Sarma, S. J.; Sumner, B. W.; Lei, Z.; Sumner, L. W.; Bivens, N. J.; Roberts, R. M.; Tuteja, G.; Rosenfeld, C. S., Bisphenol A and bisphenol S disruptions of the mouse placenta and potential effects on the placenta–brain axis. *Proceedings of the National Academy of Sciences* **2020,** *117* (9), 4642.10.1073/pnas.1919563117.

22. Delfosse, V.; Grimaldi, M.; Pons, J.-L.; Boulahtouf, A.; le Maire, A.; Cavailles, V.; Labesse, G.; Bourguet, W.; Balaguer, P., Structural and mechanistic insights into bisphenols action provide guidelines for risk assessment and discovery of bisphenol A substitutes. *Proceedings of the National Academy of Sciences* **2012,** *109* (37), 14930.10.1073/pnas.1203574109.

23. Nakazawa, M., Mechanism of Adhesion of Epoxy Resin to Steel Surface. *Nippon Steel Technical Report* **1994,** *63*, 16-22

24. Kotb, Y.; Cagnard, A.; Houston, K. R.; Khan, S. A.; Hsiao, L. C.; Velev, O. D., What makes epoxy-phenolic coatings on metals ubiquitous: Surface energetics and molecular adhesion characteristics. *J Colloid Interface Sci* **2021,** *608* (Pt 1), 634-643.10.1016/j.jcis.2021.09.091.

25. Tu, J.; Tucker, S. J.; Christensen, S.; Sayed, A. R.; Jarrett, W. L.; Wiggins, J. S., Phenylene Ring Motions in Isomeric Glassy Epoxy Networks and Their Contributions to Thermal and Mechanical Properties. *Macromolecules* **2015,** *48* (6), 1748-1758.10.1021/ma5022506.

26. Nicastro, K. H.; Kloxin, C. J.; Epps, T. H., Potential Lignin-Derived Alternatives to Bisphenol A in Diamine-Hardened Epoxy Resins. *ACS Sustain. Chem. Eng.* **2018,** *6* (11), 14812-14819.10.1021/acssuschemeng.8b03340.

27. Zago, E.; Dubreucq, E.; Lecomte, J.; Villeneuve, P.; Fine, F.; Fulcrand, H.; Aouf, C., Synthesis of bio-based epoxy monomers from natural allyl- and vinyl phenols and the estimation of their affinity to the estrogen receptor α by molecular docking. *New Journal of Chemistry* **2016,** *40* (9), 7701-7710.10.1039/C6NJ00782A.

28. Yang, G.; Rohde, B. J.; Tesefay, H.; Robertson, M. L., Biorenewable Epoxy Resins Derived from Plant-Based Phenolic Acids. *ACS Sustain. Chem. Eng.* **2016,** *4* (12), 6524-6533.10.1021/acssuschemeng.6b01343.

29. Kieber, R. J.; Silver, S. A.; Kennemur, J. G., Stereochemical effects on the mechanical and viscoelastic properties of renewable polyurethanes derived from isohexides and hydroxymethylfurfural. *Polymer Chemistry* **2017,** *8* (33), 4822-4829.10.1039/C7PY00949F.

30. Lillie, L. M.; Tolman, W. B.; Reineke, T. M., Structure/property relationships in copolymers comprising renewable isosorbide, glucarodilactone, and 2,5-bis(hydroxymethyl)furan subunits. *Polymer Chemistry* **2017,** *8* (24), 3746-3754.10.1039/C7PY00575J.

31. Noordover, B. A. J.; Duchateau, R.; van Benthem, R. A. T. M.; Ming, W.; Koning, C. E., Enhancing the Functionality of Biobased Polyester Coating Resins through Modification with Citric Acid. *Biomacromolecules* **2007,** *8* (12), 3860-3870.10.1021/bm700775e.

32. Hong, J.; Radojčić, D.; Ionescu, M.; Petrović, Z. S.; Eastwood, E., Advanced materials from corn: isosorbide-based epoxy resins. *Polymer Chemistry* **2014,** *5* (18), 5360-5368.10.1039/C4PY00514G.

33. Grieger, K. D. Synthesis and Applications of Dialdehydes. M.S., North Dakota State University, Ann Arbor, 2018.

34. Gandini, A.; Lacerda, T. M.; Carvalho, A. J. F.; Trovatti, E., Progress of Polymers from Renewable Resources: Furans, Vegetable Oils, and Polysaccharides. *Chem. Rev.* **2016,** *116* (3), 1637-1669.10.1021/acs.chemrev.5b00264.

35. Hu, F.; La Scala, J. J.; Sadler, J. M.; Palmese, G. R., Synthesis and Characterization of Thermosetting Furan-Based Epoxy Systems. *Macromolecules* **2014,** *47* (10), 3332-3342.10.1021/ma500687t.

36. Dolci, E.; Michaud, G.; Simon, F.; Boutevin, B.; Fouquay, S.; Caillol, S., Remendable thermosetting polymers for isocyanate-free adhesives: a preliminary study. *Polymer Chemistry* **2015,** *6* (45), 7851-7861.10.1039/C5PY01213A.

37. Zeng, C.; Seino, H.; Ren, J.; Hatanaka, K.; Yoshie, N., Bio-Based Furan Polymers with Self-Healing Ability. *Macromolecules* **2013,** *46* (5), 1794-1802.10.1021/ma3023603.

38. Ventura, S. M., P.; Coelho, J.; Sintra, T.; Coutinho, J.; Afonso, C. , Evaluating the toxicity of biomass derived platform chemicals. *Green Chemistry* **2016,** *18*, 4733-4742.10.1039/c6gc01211f.

39. Mou, Z.; Chen, E. Y. X., Polyesters and Poly(ester-urethane)s from Biobased Difuranic Polyols. *ACS Sustain. Chem. Eng.* **2016,** *4* (12), 7118-7129.10.1021/acssuschemeng.6b02007.

40. Serum, E. M. Exploitation of Biomass for Applications in Sustainable Materials Science. Ph.D., North Dakota State University, Ann Arbor, 2019.

41. Sutton, C. A.; Polykarpov, A.; Jan van den Berg, K.; Yahkind, A.; Lea, L. J.; Webster, D. C.; Sibi, M. P., Novel Biobased Furanic Diols as Potential Alternatives to BPA: Synthesis and Endocrine Activity Screening. *ACS Sustain. Chem. Eng.* **2020,** *8* (51), 18824-18829.10.1021/acssuschemeng.0c08207.

42. Windal, I.; Denison, M. S.; Birnbaum, L. S.; Van Wouwe, N.; Baeyens, W.; Goeyens, L., Chemically Activated Luciferase Gene Expression (CALUX) Cell Bioassay Analysis for the Estimation of Dioxin-Like Activity: Critical Parameters of the CALUX Procedure that Impact Assay Results. *Environmental Science & Technology* **2005,** *39* (19), 7357-7364.10.1021/es0504993.

3. ACYLATION OF FURANS DERIVED FROM HEMICELLULOSE

3.1. The necessity of a greener synthesis

The Grignard reaction is a robust method in most situations, including the synthesis of furan diols. It promoted a reliable, scalable 1-hour reaction with moderate to high yields (+75%) and only trace to zero observable side-product formation, making further purification via column unnecessary. Upon scaling up the reaction, however, issues in terms of sustainability and green chemistry principles became undeniable, namely the following: super stoichiometric quantities of Grignard reagent for the HMF-based diols' synthesis leading to excessive magnesium salt waste, excessive solvent in the reaction itself to avoid side-product formation as well as solvent used in the reaction workup to remove magnesium salts. Even though the process of running pyrophoric reactions on small scale is not difficult (~8 mmol or less), repeatedly running larger scale reactions became cumbersome and time consuming. Furthermore, potential industry partners were interested in the novel furan diols, but not the Grignard-mediated process of synthesis. This was an important aspect to consider; it may not matter how much better than BPA the furan diols are if they require large changes in production infrastructure, they will never be of interest to industry. We needed a more practical synthesis utilizing common reagents, rather than specialty reagents to make the process more marketable.

All of these considerations led to a prospective alternative: acylation of furans followed by reduction via common reagents, like $NaBH_4$, to produce the novel furan diols. Planning began with an idealized outline with monosubstituted furans sourced from hemicellulose as the prime feedstock.

3.1.1. An idealized method

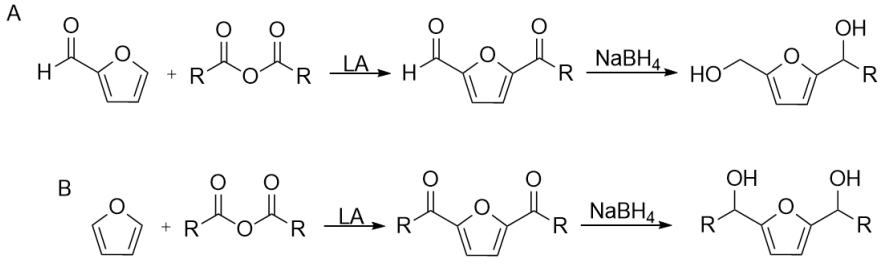

Scheme 3.1. Lewis Acid (LA) Acylation reaction schemes for formerly A) HMF-based and B) DFF-based diols.

An ideal synthesis would be catalytic, avoid super stoichiometric amounts of reagents, and allow for concentrated reaction. The workup would be straight-forward and have no side-product to remove via column. It would, ideally, be all of this and the starting material would still be sourced from biomass.

In order to avoid specialty reagents, such as Grignard reagents, a Friedel-Crafts-type reaction was envisioned. This type of reaction would use a readily available catalyst and common acylation agents like anhydrides or acid chlorides. The furans available to provide the aromatic core of the diols would need to be either monofunctional at the 2-position or unfunctionalized to be acylated. Luckily, there is an available feedstock to source such furans, and it has been in use for polymeric materials for decades.

3.1.2. Furfural: fruit of hemicellulosic biomass

The synthesis of furfural, as a byproduct of formic acid synthesis was first published in 1832 by chemist Johann Wolfgang Dobereiner, and it would be about 100 years before it would be industrially produced.[1] Finding themselves with an excess of oat hulls and left-over 8 x 12' pressure cookers abandoned from a prior project the Quaker oats company decided, as any chemist at the time would, to digest the oat hulls in the abandoned pressure cookers with sulfuric acid. Brownlee and Miner describe a process of digesting raw biomass.[2] Since then, newer methods have grown from academia and industry aimed at improving issues of the original method. The targets include improving the low yield (50 %), long reaction time, and environmental issues from acidic waste handling by running dilute acid and continuous flow systems, allowing them to avoid side-product formation thus improving yield while lowering the amount of acidic waste.[3]

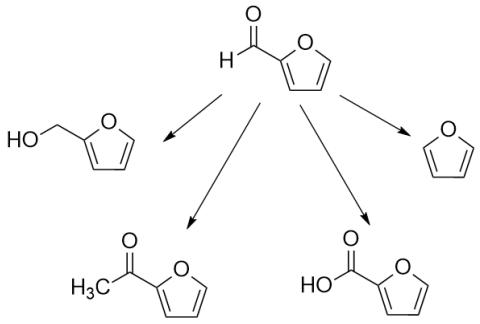

Figure 3.1. Furfural derivative tree.

Hemicellulose is second to cellulose in abundance and, as hinted, hemicellulose is to furfural as cellulose is to HMF. Furfural can be produced from one of two starting points: directly from the hemicellulose found in biomass or from its monosaccharide component, xylose (Scheme 3.1).

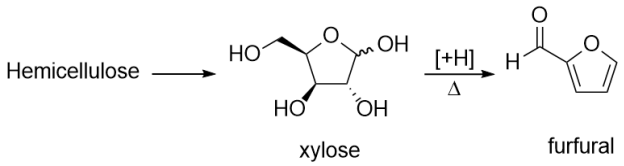

Scheme 3.2. Sugars in hemicellulose (vs cellulose) Rough scheme of how furfural is produced.

A 2019 review by Yiping Luo et al. summarizes contemporary academic examples of furfural synthesis starting from raw hemicellulosic biomass (xylan) and purified xylose.[4] The synthesis of furfural from raw lignocellulosic biomass is by acid processing and from distillation of the crude product. The intermediate of that reaction, xylose, can be purified away from oligomers, other sugars, and char formed from the initial acid processing. Then, the 'clean' xylose can in turn be acid processed, providing a cleaner product, but at the price of technically being two reaction steps, or 'two-pot' reaction, from raw lignocellulosic biomass to final product instead of a single reaction. Both methods have been explored in academia and industry.[3, 5-6]

3.1.3. Searching for evidence of 2,5-acylations of furans

In the early 1930's, a series of papers were published called "Super-Aromatic Properties of Furan" by Henry Gilman and N. O. Calloway. Each article in the series has a set of reactions as its focus and the second article focuses on the Friedel-Crafts reaction performed on furans.[7] This article would end up containing key information showing how furans could be twice acylated at the 2 and 5 positions of the ring. It was not until a piece of more recent Russian was translated that we found another useful example of such an acylation of furans.[8] The lack of evidence of 2,5-acylation of furans meant that either 1) such products could not be formed by the methods available or 2) the product was not of general interest, and so it had not been investigated in depth. Determining which was the answer was an issue that plagued this project from start to finish.

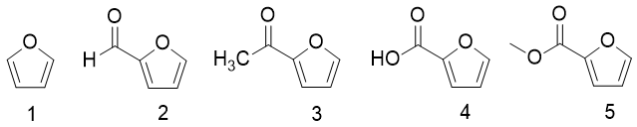

Figure 3.2. Furan and monofunctional furan structures.

The 1933 Gilman paper provided evidence that the acylations of 2-acyl furans was possible, though not the most selective reaction. Unlike alkylations, which could be performed on 2-acyl furans (like **3** and **5** in Figure 3.3), only methyl-2-furoate (**5**) could be acylated. Gilman and Calloway obtained a 30 % yield by using $FeCl_3$ or $SnCl_2$ as a Lewis acid catalyst in the reaction of the furoic ester. The classic Friedel-Crafts reagent $AlCl_3$ did not facilitate any product formation.[7]

If the Gilman paper was unknown, the next few papers would have made it seem as if 2,5-acylation of furans was impossible. The lack of any description of over-acylation when the desired product was a 2-acyl furan, and the avoidance of any words on char and oligomerization was puzzling.[9-16] Sometimes this seems to be due to furans not being the of the study for these papers; the focus was either on their new catalyst or the furan reaction was tacked onto a long list of substituted benzenoid molecules to show the range of their new method. Another issue may have been that the catalysts used on furans were too acidic, causing reactions which were "uncontrollable, giving polymeric material".[17] It was not until the mid-1980s and again in the mid-1990s to the present day that furans were once again a focus for acylations.

One such paper was published in 1985 by Fayed et al. Although it did not feature a diacylation of furans, it did describe "polymerization of furan" products- *char* formation in the presence of phosphoric acid. In fact, they included the char formation towards the yield of a few of their "acylated" products.[18] This is an odd choice, but it does not seem like they were the only researchers to provide that unusual arithmetic in their publications. The Fayed paper also mentioned that their reactions did not run to completion, resulting in a mixture of the desired product and the starting material. In addition, they purported that the presence of triflic acid (HOTf) could push the equilibrium reaction forward to more product formation.

Several subsequent papers were published showcasing the ability of various metal triflates to mediate Friedel-Crafts acylations, but they did not feature furans.[19-21] At least, not until the 2001 Indium triflate mediated monoacylation of furan by Chapman et al.[12] The papers of the early 2000s, again, would only describe their catalytic method. They did not take the opportunity to describe how selective their catalytic methods were by providing clean, single product reactions with acid-sensitive furans; instead, there was no mention of a lack of polymerization or char formation, and no mention of any difficulties working with furans. Despite the general concern over the shortage of details in the literature, a fruitful method was developed from the available literature examples.

3.2. Method development

Our synthetic starting point was a method from Sarvari et al. where they claim a 94 % isolated yield via the method shown in Scheme 3.2. Imagining how simple it would be if, in terms of waste reduction and sustainability, this solvent-free catalytic reaction would successfully form diacyl furans, we decided it would be a good, hopeful place to start. We were mistaken.

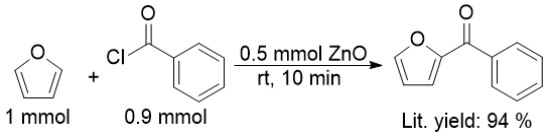

Scheme 3.3. Redrawn from Sarvari et al. (2004).[15]

Although the reference boasts a 94 % isolated yield, the actual testing of that method in our labs made it seem they performed the same arithmetic as the Chapman paper described. This method was tested in our lab once, twice, several times with slight alterations all in an attempt to obtain any organic soluble product. At least from our labs, the acylation could not be performed in the way claimed in the reference paper.

Several more methods were attempted, forming not the desired product to any degree, but instead we observed either no reactivity in the system, or polymerization and char formation.[22] The catalysts implemented never seemed to be the right reactive "fit" for the furans tested (furan, furfural, 2-acetyl furan). At a certain point, the question was no longer, "Can we form this product in a desirable

green catalytic method", but "Can we form this perform this transformation at all". Mercifully, the answer was a "yes", but it was a long road to that achievement. To avoid lamenting all the methods tested, a few key reactions will be featured, starting with the method providing the first successful 5-acylation of a 2-substituted furan for this thesis work (Scheme 3.3).

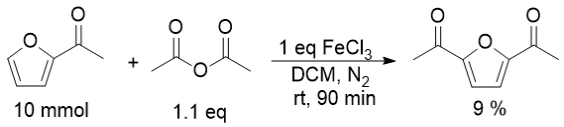

Scheme 3.4. First successful acylation in Sibi group labs.

Stepping away from the "ideal green synthesis", the first successful acylation of 2-acetyl furan in Sibi group labs transpired via a stoichiometric system, rather than a catalytic one. Monoacylation of furan was obtained from the synthesis shown in the 2002 publication by Kobayashi et al., but the acylation could not be forced, at this point, to provide the 2,5 diacyl product. Instead, it needed to be seen that it was even possible for a 2-acyl furan to be acylated at the 5-position.

The first evidence of such a transformation being possible was via a simple, updated Friedel-Crafts acylation using a stoichiometric amount of FeCl3.23 Acylation of 2-acetyl furan to form 2,5- diacetyl furan was, finally, made possible. Although the low isolated yield and low conversion left a lot to be desired, this reaction was a positive indication that the previous furans and mediators of prior Friedel-Crafts acylations run were mismatched in terms of reactivity. A rough attempt was made at finding a trend in order to predict what 2-substituted furans would provide higher conversion and higher yield based on 1H and 13C NMR chemical shifts (Figure 3.4).

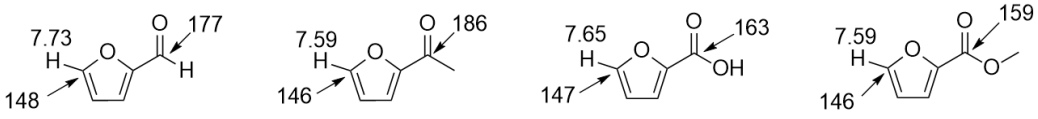

Figure 3.3. NMR shifts of specific protons and carbons of selected furans.

Acylation attempts of furfural resulted in quick and exothermic reactions with organic and aqueous insoluble char, or possibly a polyfurfuryl alcohol-like substance, as the product. Acylation of 2-acetyl furan was incomplete, but some product did form with little to no char formation when $FeCl_3$ acted as acylation facilitator.

The reaction results and the chemical shifts together were used to aid in clarifying which was more important – the deshielding of the selected proton for ease of removal to be replaced by an acetyl group, the electrophilicity of the carbonyl carbon at the 2-position leaving it more or less prone to nucleophilic attack, resulting in homopolymerization, or lowering the furan's susceptibility to a ring-opening mechanism by attaching a less electron-donating carbonyl group. Some indication of reactivity could also be obtained from looking at resonance structures of each furan above, but NMR shifts provided a more quantifiable value.

3.3. Results and discussion

3.3.1. Initial success with $FeCl_3$

Each compound shown in Figure 3.4 was to be compared in terms of reactivity at the bench and see if there was a correlation to the NMR. Unfortunately, 2-furoic acid was not readily soluble in organic solvents, so the next-best furan to try to acylate was methyl-2-furoate. Methyl-2-furoate would serve as a useful comparison to 2-acetyl furan since they share proton and carbon shifts at the 5-position but differ at the 2-position's furanic carbonyl carbon.

At the bench, methyl-2-furoate worked amazingly in comparison to all prior attempts on other furans. The yield was still low at 24 %, but it was a marked improvement from the 9 % for acetylation of 2-acetyl furan (Table 3.1). Furthermore, it was very encouraging that the only side product was a trace amount of color impurity, likely from a minute amount of oligomerization of the furan. This result suggested that the carbonyl at the 2-position is a major necessary stabilizing force on the furan ring, since char formation, which would indicate a possible ring-opening polymerization, was not observed.

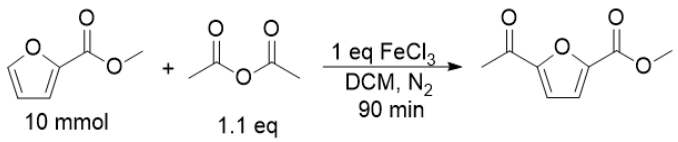

Table 3.1. $FeCl_3$ - mediated acylation of methyl-2-furoate.

Entry	Temp (° C)	Conv. (%)	Isolated Yield (%)
1	rt	45	24
2	40	66	51
3*	40	57	49
4	60	55	53

*4 hour reaction. Conversion calculated by reclaimed starting material.

Something that persisted, even in the subsequent bismuth triflate-catalyzed acylations, was the lack of full conversion of the acylations. Suggestions for avoiding this issue are discussed in chapter 5.

Taking what was learned from the reaction in Table 3.1, the 2002 Kobayashi catalytic system was attempted with methyl-2-furoate as the substrate.[14] To success! The results are described in the next section, as well as the reduction method of 5-acetyl-2-methyl furoate.

3.3.2. Metal selection for triflate catalysts

The initial selection of metals in the metal triflate catalysts used for methyl-2-furoate acylation was based on literature. The first choice which we observed to acylate furan was not scandium, as featured in Kobayashi group publications, but bismuth. One of the routes attempted to an alternative furan diol synthesis was that of scheme 3.5.

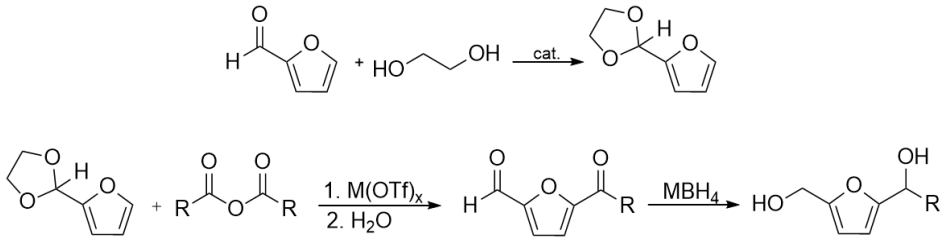

Scheme 3.5. Ideal furan dioxolane route to novel furan diols.

In the presence of water, bismuth triflate is known to deprotect aldehydes protected with a dioxolane group. This would be ideal; a one-pot acylation followed by deprotection, meaning one less aqueous workup step. Unfortunately, the ideal was not reality. A protection step and deprotection step in addition to the acylation, which was 7 % yield at best, then finishing with a reduction step to achieve the desired diol was not ideal, so this method was eventually abandoned. Yet, from the time working on this method, it was observed that bismuth triflate did not cause excessive char formation. It was a rather positive sign for the future, such that when a catalytic alternative to the stoichiometric $FeCl_3$ -- mediated acylation of methyl-2-furoate was needed, bismuth triflate was the first choice. And it worked!

Other metal triflates were scouted for any acylation activity in the optimal conditions found for bismuth triflate. They were sourced partly due to their use in benzene acylations in literature, and partly due to availability and ease of use.[14, 19, 21] Ease of use and scalability were particularly important as some triflates, like gallium triflate, are hygroscopic but deactivated by water, and therefore could not be considered for this project.[24] Still, that left several other possibilities, and a few of them were tested, as seen in Table 3.2. Interestingly, the other metals (Sm, Yb, La) were not capable of performing the desired transformation, but this may simply be a case of a HOMO-LUMO mismatch; some of these metals show markedly better results for more aromatic heterocycles like thiophene and pyrrole.[14]

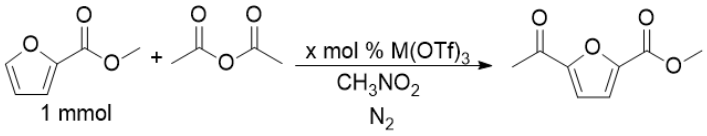

Table 3.2. Metal triflate acylation of methyl-2-furoate.

Entry	Temp (° C)	Time (h)	$M(OTf)_3$	% cat	Isolated Yield (%)
1	rt	72 h	Bi	5	NR
2	40	10 h	Bi	5	27
3	50	72 h	Bi	5	48
4	50	72 h	Yb	5	5
5	50	4 h	Sm	10	NR

That begs the question, why does bismuth triflate perform the acylation of monoacyl-furan so well, by comparison? Bismuth is unique.[25-26] Although it sits next to toxic metals in the periodic table, it is considered to be a comparatively non-toxic and even "eco-friendly" metal.[25] Bismuth has a lone pair of electrons, and although some sources comment that it is a weak Lewis base, when it is bound to strong electron withdrawing groups, like triflate (trifluroacetone), it behaves like a Lewis acid. Hard-soft acid-base theory could provide some insight to the observed behavior of bismuth (and iron) compared to other metal triflates tested for furan acylation. While the other metals (Sc, Y, Yb, etc) are hard acids, bismuth is a considered a borderline acid.[27]

To continue this project, one aspect to probe would be to explore other intermediate and soft acid triflates, as well as bismuth catalysts substituted with something other than trifluoroacetone in order to alter its activity.

By comparison, the reduction reactions were exceptionally straightforward and high yielding. There was some concern that the ester of the starting material might not reduce with the milder $NaBH_4$ and would require a stronger reducing agent like $LiBH_4$. That the ester is only a methyl ester, rather than a more stable longer chain ester, encouraged the attempt at reduction with $NaBH_4$. It was predicted that the methanol solvent would over-solubilize the reducing agent $NaBH_4$, causing it to react with any moisture present rather than the starting material. Considering the increase in yield, albeit for the partly reduced species “A”, this may have been the case.

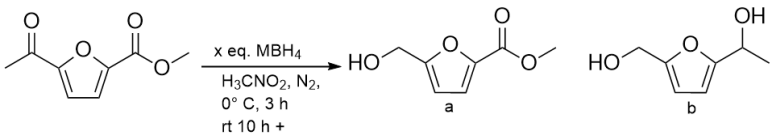

Table 3.3. Screening reductions of 5-acetyl-2-methylfuroate on 1 mmol scale (isolated yields).

Entry	Solvent	Reducing agents (molar eq)	A (yield %)	B (yield %)
1[28]	MeOH	$NaBH_4$ (1 eq)	51	0
2[28]	EtOH	$NaBH_4$ (1 eq)	75	0
3	THF*	$NaBH_4$ / $NaBH(OAc)_3$ (4 eq/ 0.2 eq)	62	0
4	THF	$NaBH_4$ (1 eq), LiBr (1 eq)	NR	NR
5*[29]	THF	$LiBH_4$ (1 eq)	0	86

* 0.247 mmol. See comments for tables above

This project, the acylation of the 5-position of 2-acyl furans, is by no means complete. Even so, it is a good foundation for further research into this deceptively challenging transformation.

3.4. Alternative diol synthesis experimental

A note: All furans should be vacuum distilled before use to avoid color impurity carryover into final products and as a preventative measure when surveying new reaction methods.

3.4.1. Acylation of methyl furoate via $Bi(OTf)_3$

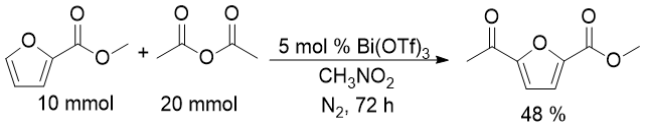

In a 25 mL beaker methyl-2-furoate (1.26 g, 10 mmol) was diluted with nitromethane (15 mL). A 25 mL two-necked round bottom flask was charged with a stir bar and $Bi(OTf)_3$ (328.1 mg, 0.5 mmol), then flushed with N_2. Then acetic anhydride (2.0 g, 20 mmol) was added to the reaction vessel via syringe. The mixture was stirred at room temperature until $Bi(OTf)_3$ dissolved completely. The reaction vessel was then lowered into the oil bath (50 °C). The dilute methyl-2-furoate was added dropwise via syringe over 1-2 minutes. The reaction was kept under N_2 for the duration of the reaction (72 h).

Workup: The reaction mixture was diluted in ethyl acetate (80 mL). The organic solvent was washed with $NaHCO_3$ (20 mL x 3) in a 125 mL separatory funnel. The organic layer was then dried over Na_2SO_4. The solvent was removed *in vacuo*. The crude mixture was crystallized out of 3-5 mL of ethyl acetate in a freezer. After it crystallized, the dark solvent was removed, and the solid product was washed with a minute amount of cold ethyl acetate. The solid was then dried under high vacuum. Yield: 0.81 g (48 %).

3.4.2. Reduction of 5-acetyl-2-methylfuroate

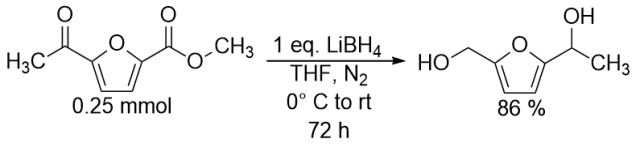

To a 10 mL single-necked rbf charged with a stir bar, 3 mL of drysolv THF was added, followed by $LiBH_4$ (0.123 mL of 2 M in THF soln.). The vessel was flushed with N_2 and remained under positive N_2 pressure via balloon. The vessel was then placed in an ice bath and stirred for ~1 minute before a

solution of 5-acetyl-2-methylfuroate (41.5 mg, 0.247 mmol) in 1 mL drysolv THF via syringe over 15 seconds. The reaction stirred in the ice bath which was allowed to reach room temperature. The reaction was monitored via TLC for completion until the 72 h, at which point the reaction was found to have consumed all starting material. The only product was the diol "b" from Table #. The reaction was quenched with an aqueous saturated solution of NH_4Cl (1 mL), then stirred at room temperature for 5 minutes. The crude mixture was diluted further with 10 mL diethyl ether, transferred to a 25 mL separatory funnel by decanting off of the salts formed in the quenching. The organic solution was then washed with brine (3 mL x 2) and DI H_2O (2 mL x 1). The washed organic layer was dried over Na_2SO_4. The bulk of the solvent was removed *in vacuo*, residual solvent removed under high vacuum. Yield 30.2 mg (86 %).

3.5. Acylation spectral data

3.5.1. Sample preparation

All NMR samples were, unless noted otherwise, neat samples dissolved in deuterated solvent. The standard deuterated solvent was $CDCl_3$, but some other solvents and solvent combinations were used in at least one instance, which is noted in the title for the spectrum. Masses ranging from 12-16 mg of the furan diols were diluted with 0.75 mL of deuterated solvent, no matter the solvent.

All IR spectra samples were neat, unless otherwise noted.

3.5.2. Written spectral data for 5-acetyl-2-methylfuroate

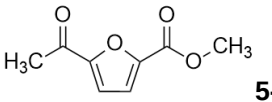

5-acetyl-2-methylfuroate. ^{1}H NMR (400 MHz, Chloroform-*d*) δ 7.24 (d, *J* = 3.7 Hz, 1H), 7.21 (d, *J* = 3.7 Hz, 1H), 3.95 (s, 3H), 2.58 (s, 3H). ^{13}C NMR (101 MHz, $CDCl_3$) δ 187.5, 158.6, 154.2, 146.2, 118.8, 116.6, 52.4, 26.4. FTIR (neat) cm^{-1} 3104, 3071, 2962, 1714, 1671, 1576, 1431.

3.6. References

1. Döbereiner, J. W., Ueber die medicinische und chemische Anwendung und die vortheilhafte Darstellung der Ameisensäure. *Ann. Phar.* **1832,** *3* (2), 141-146.https://doi.org/10.1002/jlac.18320030206.

2. Brownlee, H. J.; Miner, C. S., Industrial Development of Furfural. *Industrial & Engineering Chemistry* **1948,** *40* (2), 201-204.10.1021/ie50458a005.

3. Dashtban, M.; Gilbert, A.; Fatehi, P., Production of furfural: overview and challenges. *J. Sci. Technol. Forest Prod. Process* **2012,** *2* (4), 44-53

4. Luo, Y.; Li, Z.; Li, X.; Liu, X.; Fan, J.; Clark, J. H.; Hu, C., The production of furfural directly from hemicellulose in lignocellulosic biomass: A review. *Catal. Today* **2019,** *319*, 14-24.https://doi.org/10.1016/j.cattod.2018.06.042.

5. Mariscal, R.; Maireles-Torres, P.; Ojeda, M.; Sádaba, I.; López Granados, M., Furfural: a renewable and versatile platform molecule for the synthesis of chemicals and fuels. *Energy & Environmental Science* **2016,** *9* (4), 1144-1189.10.1039/C5EE02666K.

6. Li, X.; Jia, P.; Wang, T., Furfural: A Promising Platform Compound for Sustainable Production of C4 and C5 Chemicals. *ACS Catal.* **2016,** *6* (11), 7621-7640.10.1021/acscatal.6b01838.

7. Gilman, H.; Calloway, N. O., Super-Aromatic Properties of Furan. II. The Friedel—Crafts Reaction. *Journal of the American Chemical Society* **1933,** *55* (10), 4197-4205.10.1021/ja01337a053.

8. Khusnutdinov, R. I.; Baiguzina, A. R.; Mukminov, R. R.; Dzhemilev, U. M., New procedure for synthesis alkyl esters of 5-acetyl-2-furan-carboxylic acid alkyl ester. *Russian Journal of Applied Chemistry* **2009,** *82* (2), 340-342.10.1134/S1070427209020335.

9. Hartough, H. D.; Kosak, A. I., Acylation Studies in the Thiophene and Furan Series. II. Zinc Chloride Catalyst. *Journal of the American Chemical Society* **1947,** *69* (5), 1012-1013.10.1021/ja01197a010.

10. Robinson, G. C., Directive Effects in Acylation of Methyl Furan-2-carboxylate. *The Journal of Organic Chemistry* **1966,** *31* (12), 4252-4252.10.1021/jo01350a514.

11. Feringa, B. H., R.;Rikers, R.; Brandsma, L., Dimethylation of Furans and Thiophenes. One-Pot Procedures for Furan-2,5-and Thiophene-2,5-dicarboxylic acid. *Heterocycles communications* **1988**, 316-318

12. Chapman, C. J.; Frost, C. G.; Hartley, J. P.; Whittle, A. J., Efficient aromatic and heteroatom acylations using catalytic indium complexes with lithium perchlorate. *Tetrahedron Letters* **2001,** *42* (5), 773-775.https://doi.org/10.1016/S0040-4039(00)02122-5.

13. Fürstner, A.; Voigtländer, D.; Schrader, W.; Giebel, D.; Reetz, M. T., A “Hard/Soft” Mismatch Enables Catalytic Friedel−Crafts Acylations. *Organic Letters* **2001,** *3* (3), 417-420.10.1021/ol0069251.

14. Komoto, I.; Matsuo, J.-i.; Kobayashi, S., Catalytic Friedel–Crafts Acylation of Heteroaromatics. *Topics in Catalysis* **2002,** *19* (1), 43-47.10.1023/A:1013829215544.

15. Sarvari, M. H.; Sharghi, H., Reactions on a Solid Surface. A Simple, Economical and Efficient Friedel−Crafts Acylation Reaction over Zinc Oxide (ZnO) as a New Catalyst. *The Journal of Organic Chemistry* **2004,** *69* (20), 6953-6956.10.1021/jo0494477.

16. Fang, Y.; Du, X.; Jiang, Y.; Du, Z.; Pan, P.; Cheng, X.; Wang, H., Thermal-Driven Self-Healing and Recyclable Waterborne Polyurethane Films Based on Reversible Covalent Interaction. *ACS Sustain. Chem. Eng.* **2018,** *6* (11), 14490-14500.10.1021/acssuschemeng.8b03151.

17. Mazur, Y.; Karger, M. H., Mixed sulfonic-carboxylic anhydrides. III. Reactions with aromatic ethers and aromatic hydrocarbons. *The Journal of Organic Chemistry* **1971,** *36* (4), 540-544.10.1021/jo00803a011.

18. Fayed, S.; Delmas, M.; Gaset, A., Acylation of furan by variously functionalized carboxylic acids in the presence of phosphonic ionexchange resins used as catalysts. *Journal of Molecular Catalysis* **1985,** *29* (1), 19-31.https://doi.org/10.1016/0304-5102(85)85127-0.

19. Hachiya, I.; Moriwaki, M.; Kobayashi, S., Catalytic Friedel-Crafts acylation reactions using hafnium triflate as a catalyst in lithium perchlorate-nitromethane. *Tetrahedron Letters* **1995,** *36* (3), 409-412.https://doi.org/10.1016/0040-4039(94)02221-V.

20. Kawada, A.; Mitamura, S.; Kobayashi, S., Ln(OTf)3–LiClO4 as reusable catalyst system for Friedel–Crafts acylation. *Chem. Commun.* **1996,** (2), 183-184.10.1039/CC9960000183.

21. Kawada, A.; Mitamura, S.; Matsuo, J.-i.; Tsuchiya, T.; Kobayashi, S., Friedel-Crafts Reactions Catalyzed by Rare Earth Metal Trifluoromethanesulfonates. *Bull. Chem. Soc. Jpn.* **2000,** *73* (10), 2325-2333.10.1246/bcsj.73.2325.

22. Wang, J.-G.; Liu, X.-Q.; Zhu, J., From Furan to High Quality Bio-based Poly(ethylene furandicarboxylate). *Chinese Journal of Polymer Science* **2018,** *36* (6), 720-727.10.1007/s10118-018-2092-0.

23. Miles, W. H.; Nutaitis, C. F.; Anderton, C. A., Iron(III) Chloride as a Lewis Acid in the Friedel-Crafts Acylation Reaction. *Journal of Chemical Education* **1996,** *73* (3), 272.10.1021/ed073p272.

24. Prakash, S. G. K. Y., Ping; Torok, Bela; Bucsi, Imre; Tanaka, Mutsuo; Olah, George. , Gallium (III) trifluoromethanesulfonate: a water-tolerant, reusable Lewis acid catalyst for Friedel-Crafts reactions. *Catal. Lett.* **2003,** *85*, 1-6

25. Desmurs, J. R.; Labrouillère, M.; Le Roux, C.; Gaspard, H.; Laporterie, A.; Dubac, J., Surprising catalytic activity of bismuth (III) triflate in the Friedel-Crafts acylation reaction. *Tetrahedron Letters* **1997,** *38* (51), 8871-8874.https://doi.org/10.1016/S0040-4039(97)10401-4.

26. Gaspard-Iloughmane, H.; Le Roux, C., Bismuth(III) Triflate in Organic Synthesis. *European Journal of Organic Chemistry* **2004,** *2004* (12), 2517-2532.https://doi.org/10.1002/ejoc.200300754.

27. Ho, T.-L., Chemoselectivity of organometallic reactions: A hsab appraisal. *Tetrahedron* **1985,** *41* (1), 3-86.https://doi.org/10.1016/S0040-4020(01)83470-0.

28. Brown, H. C.; Mead, E. J.; Subba Rao, B. C., A Study of Solvents for Sodium Borohydride and the Effect of Solvent and the Metal Ion on Borohydride Reductions1. *Journal of the American Chemical Society* **1955,** *77* (23), 6209-6213.10.1021/ja01628a044.

29. Brown, H. C.; Narasimhan, S., New powerful catalysts for the reduction of esters by lithium borohydride. *The Journal of Organic Chemistry* **1982,** *47* (8), 1604-1606.10.1021/jo00347a057.

4. DIGLYCIDATION OF FURAN DIOLS

4.1. Background

To avoid completely restating the reasons behind the widespread use of BPA as a monomer foundation, this chapter will jump directly to what is most relevant- epoxide monomers and epoxy resins, and the general materials properties of epoxy polymers.

4.1.1. Epoxides in polymer synthesis

There are three flavors of oxiranes utilized for epoxy resin and polymer synthesis: ethers, esters and epoxidized alkenes with carbon rather than oxygen linkages in the main monomer backbone. Of the epoxies available, BPA epoxy resins are the most popular in industry for their high glass transition temperatures and high viscosity, making them easier to handle in processing than hydrogenated alternatives. Zeno Wicks states it well in the book *Organic Coatings*, "BPA epoxy resins perform especially well in coating applications in which excellent adhesion, electrical properties and corrosion resistance are required".[1] If we are trying to replace or at the very least subsidized BPA diglycidyl ether (BPADGE) use for coatings applications, we need to have an understanding of how it is formed and applied. Descriptions of BPA and its proposed mode of adhesion to metal substrates was previously described in Chapter 2. Instead, this chapter will start with what is most immediately relevant to the topic- the synthesis of epoxy monomers a.k.a diglycidyl ethers.

It should first be mentioned that there is a stark difference between the research produced in academia and industry, though they do relate. While academic papers published nearly exclusively feature monomer synthesis, in industry there is a strong tendency to avoid monomer use, opting for resins in their place. The main reason for this is processability, both in the formation and in the implementation of the resins. Health hazards, due to volatility and skin-permeability, are a close second reason why monomers are avoided in industry. How then, are these larger oligomers, or resins as they will be called from this point on, made? The fusion process (Scheme 4.1).

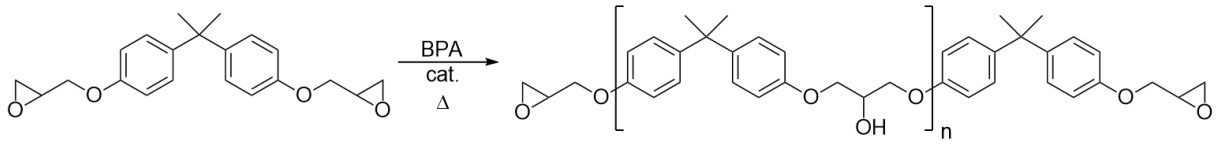

Scheme 4.1. Generalized fusion process of BADGE resin formation.

While monomer formation requires a super stoichiometric excess of epichlorohydrin, the fusion process is less wasteful in terms of residual epichlorohydrin (ECH), a toxic chemical with difficult handling and disposal. Although ECH is still administered in super stoichiometric quantities, less is added to the reaction overall. The reaction is relatively straightforward. A diglycidyl ether is combined with its diol precursor, a catalyst, such as tetrabutylammonium bromide (TBAB), and heat.[2-5] Depending on the ratios of diglycidyl ether to diol, a variety to high molecular weight resins can be synthesized, each with a certain set of applications.

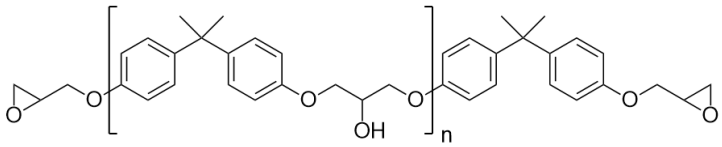

Figure 4.1. General BADGE resin structure.

In industry, the small molecule BADGE is not desirable for a few manageability reasons. When n= 1, the resin is a solid, requiring either high temperatures or solvent for processing.[1] A larger molecule (n> 1) lowers worker and environmental exposure, but because the ideal for coatings formation tends to be room temperature curing with no volatile organic compound (VOC) emission, the solid resins are problematic. The formation and analysis of an exact, single product is not necessarily important- the viscoelastic properties (materials properties) and ease of use are the top priorities. For example, the resin Epon 828 has an *n* of ~0.5, is a liquid, making it ubiquitous in coatings since a solvent is not required for its application. The higher molecular weight Epon 2002 has an *n* of ~2-4 and is a solid. It is not as prevalent as Epon 828, but it does have applications in powder coatings. These resins can be cross-

linked, creating coatings that have very good adhesion, cohesion and impact resistance in comparison to films and coatings from monomeric BADGEs.[1]

As an organic chemist, the synthesis, characterization, and application of a discreet monomer is important for the understanding of the chemistry of the structure and of its structure-activity relationships, but not as much concern is for its end use. This chapter, like previous chapters, takes a more traditional synthetic chemist's approach to materials science. For that reason, monomers, not resins, were the desired synthesis products. Based on the literature available at the start of this project, a ready conversion of the novel furanic diols into diglycidyl ethers was anticipated. [6-7] A few diglycidation methods were attempted, ultimately the Cho method was the most selective and highest yielding synthetic process. That method was further optimized, and the general method created is described.

4.1.2. Known furan epoxies

For more detail on the prior art, there were few examples of furanic diglycidation known at the start of this project (Figure 4.2). The literature featuring the above furan glycidyl ethers did a commendable job gathering initial viscoelastic properties to compare and contrast them to their phenylic counterparts. Some of the earliest mentioned of furanic glycidations is on the hemicellulosic furans, like furfuryl alcohol and furoic acid due to their ease of availability.[6, 8-10]

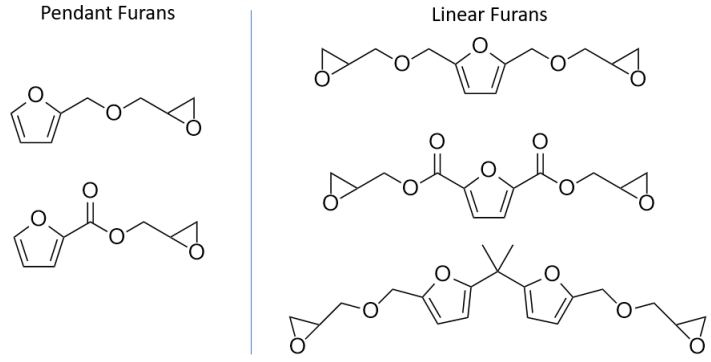

Figure 4.2. Pendant and linear furan diglycidyl ethers in literature.

Such compounds, due to their monofunctionally, acts as bulky pendant groups to a polymer backbone and can aid in crosslinking. It is because of this that their effect on the overall physical properties is not as influential as if they were within the linear polymer chain.

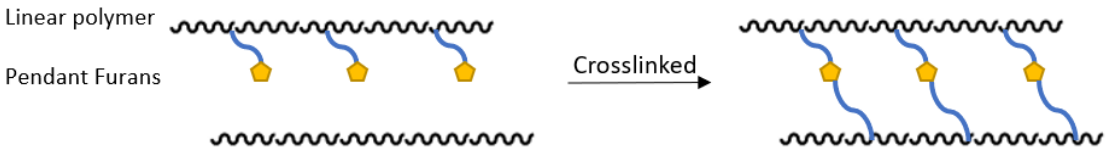

Figure 4.3. Illustration of pendant groups and crosslinked structure.

A better comparison to the proposed novel furan diglycidyl ethers featured in this work is the set of diglycidyl ethers shown in Figure 4.4.[6-7, 11] Although the diglycidyl ethers typically have to be synthesized in-house rather than purchased, the effort is worth it as they provide a better comparison on the effect a furan ring has on materials properties.

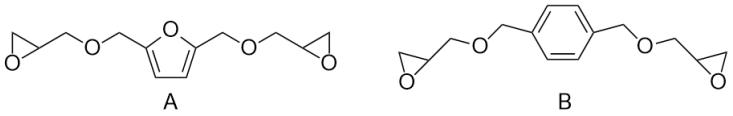

Figure 4.4. Furan vs phenyl diglycidyl ether comparison.

Although they were not the first to synthesize polymers from BHMF diglycidyl ether, Hu et al. laid the foundation for viscoelastic property comparison between furan and phenyl epoxies.[7] They found that qualities such as glass transition temperature (T_g), and overall stiffness of the materials were actually relatively higher than that of benzene – a positive result. This is not surprising, as both aromatic rings can participate in π stacking, but the furan has the added ability to H-bond. This suggests improved chemical and thermal resistance of the material. The only negative to these strong intermolecular interactions is that the materials tend to be, as Hu et al. say, an increased "stiffness". This is a delicate way to report the result. A better term for those furanic materials is *brittle* – the strong intermolecular forces are perfect until they, in reality, snap. A coating generally needs to be tough, but flexible, not brittle.

In 2017, Shen et al. probed how H-bonding affects polymer properties of coatings and materials, featuring furan-containing polymers.[12] In it, they compare the mechanical properties of the structures shown in Figure 4.4. Their findings were in line with those of Hu et al. but added mechanical analysis like crosslink density. The furan and benzene-derived diglycidyl ethers shared the same crosslink density. This information further shows how much of a role H-bonding plays when disparities between the two

epoxy monomers is observed in properties like T_g and storage modulus. Their research describes via IR that the comparatively higher T_g and stiffer mechanical properties of the furan is not caused by the higher energy required for furan ring rotation than benzene, but the H-bonding in which it participates. They followed up these results with a paper published in 2020 comparing FDCA and terephthalic acid diglycidyl ethers, providing further confirmation of their prior results.[13]

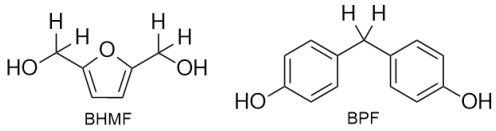

Figure 4.5. Comparing BHMF and bisphenol F (BPF) structures.

Employing BHMF diglycidyl ether as a monomer could be compared to bisphenol F (BPF). BPF, similar to BHMF, is unencumbered by alkyl groups (Figure 4.5). It also imparts brittleness to its materials if not mitigated by additives. What seems like a small alteration from BPF to BPA by the addition of two methyl groups is actually a great mediation of the properties of bisphenols. BPA-containing materials have good chemical and thermal stability due to their π-stacking interactions, but they are not stiff to the point of brittleness. This showcases how BHMF might also be altered to the benefit of its materials properties.

There are several examples in literature of how flexibility can be added to a polymer by the addition of monomers with pendant alkyl chains.[14-15] The furan diols synthesized in Chapter 2 of this thesis would be a great exploration into how the flexibility of coatings synthesized from furans could be improved from the results of the related BHMF diglycidyl ether. As a precaution, if materials comprised of the HMF-based diglycidyl ethers were too brittle for coatings applications, the doubling of alkyl groups from DFF-derived diglycidyl ethers was expected to be an improvement. Overall, the pendant R groups are expected to disrupt some of the intermolecular forces, namely H-bonding, thus providing coatings without major flexibility and adhesion issues resulting from brittleness.

4.1.3. Addressing UV-susceptibility of furans

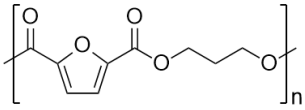

Figure 4.6. FDCA polyester example.

Recently, research was published exposing the susceptibility of FDCA-containing polyesters to degrade under UV light.[16] This is a major weatherability problem; how useful is a protective coating if it degrades considerably after being subjected to reasonable amounts of sunlight or indoor lights? Potentially, this is a major issue for the future of furanic polymers, but something to consider is that the conjugation of the furan with its 2,5 carbonyl groups may be the source of the problem. Similar issues were not reported for furans without an expanded conjugated system for UV-curing of furanic polymers.[6] Further research should be conducted to evaluate the sensitivity of furanic monomers to UV light to know for certain whether all furans have an inherent weatherability problem, or simply FDCA-based ones.

Thanks to literature examples, a suitable method of novel furan diglycidyl ether synthesis was found, and diglycidyl ethers of each furan diol synthesized in Chapter 2 was formed. Herein is a description of the results, optimizations of methods and a discussion of the project.

4.2. Results and discussion

For nearly every furan diol successfully synthesized in Chapter 2, there is an ensuing diglycidyl ether. All of the HMF-based furan diols produced diglycidyl ethers (Figure 4.7), meanwhile, just as occurred in the diol synthesis, the DFF-based diglycidyl ethers were more prone to degradation at a rate too quickly to be used for future polymer synthesis.

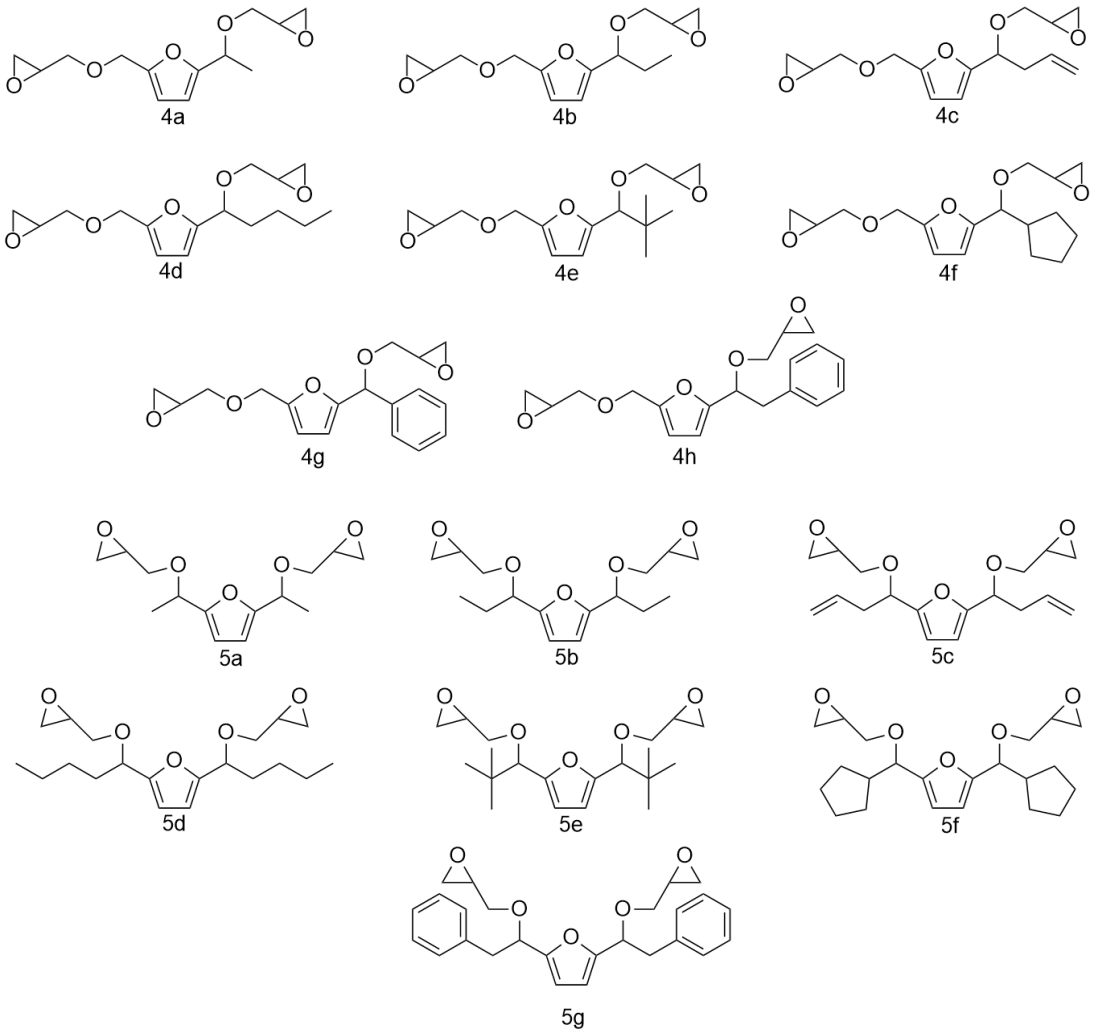

Figure 4.7. HMF (**4)** and DFF (**5**)-based diol diglycidation products.

The reactions featured ran to completion; all of the starting material was consumed, with a couple of exceptions where trace monoglycidation was observed for some of the bulkier R groups presented. Those bulky group-containing furan diglycidyl ethers were particularly acid sensitive; prolonged contact with the slightly acidic silica gel for column purification could slightly to *fully* degrade and/or polymerize those furan diglycidyl ethers. The silica pH was ~6.5-7.5. To avoid degradation and polymerization on the column, alumina was explored as an alternative because of its more neutral pH. Unfortunately, the furan diglycidyl ethers did not adsorb onto the alumina, making it more like a solid filtration than a separation. A possibility for the future would be to mix silica with varying amounts of alumina to see if a reaction on the

column can be avoided. It was because of this difficulty in separation without alteration of the desired product that compounds **4e**, **4h**, **5e**, and **5g** were not effectively column-purified; they were quickly passed through a plug of silica or half-height column to try to remove the ECH oligomer, leaving any other impurities behind in the final product. Therefore, the yields described in this work for those compounds mentioned above are for crude product.

Table 4.1. Asymmetric diglycidyl ethers derived from HMF.

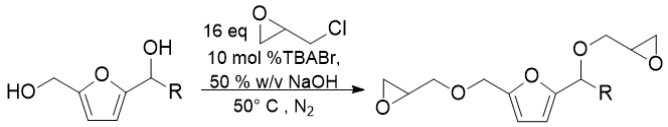

Entry	R	Rxn time (h)	Isolated Yield (%)
4a	Methyl	2	64
4b	Ethyl	2	73
4c	Allyl	2	74
4d	nButyl	2	72
4e*	tButyl	3	38*
4f	cPentyl	2	34
4g	Phenyl	2	61
4h	Benzyl	12	5

*Crude yield.

Reactions with short chains (entries 1-4 of both tables) and the lone phenyl R group in table 4.1 only took 2 hours, where the remaining furanic diols required from 4 to 6 hours for full diglycidation. This extended reaction time is likely due to the steric hindrance about the furylic carbon.

All products were column-purified via flash column to remove a highly polar colored impurity as well as oligomerized ECH. A note- if the crude mixture is on the column for too long, the desired compound polymerizes, quite exothermically, onto the column. Following that exotherm, no desired product will be obtained.

In the very first few glycidations, the solid diol **1g**, was dissolved to administer it to the biphasic reaction mixture. Melting of the solid was avoided since heating the diols causes some degradation

and/or polymerization forming more color impurity. This occurs in the presence of atmospheric oxygen and under inert gas.

Unlike BHMF, the phenyl-furanol could not be dissolved in water and was instead dissolved in THF. THF is miscible in ECH and water, which disrupts the separation of the organic and aqueous layer. Like in previous liquid furanic diol reactions, this substrate was consistently accompanied by a side product, but in a greater quantity. Upon purification and analysis, the impurity was revealed to be a known hexamer of ECH (Figure 4.9).[17]

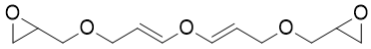

Figure 4.8. Epichlorohydrin (ECH)-derived side-product.

The formation of the hexamer of ECH has been shown in literature to be facilitated by increased contact of epichlorohydrin with NaOH.[17]

4.2.1. DFF-based diglycidyl ethers: High steric hindrance provides low yields

The yields are comparable, by R group, between the HMF and DFF-based furans. Generally, the low yields could partly be due to solubility issues in the aqueous workup. The poorest yields being from the most sterically hindered groups, benzyl, t-butyl and cyclopentyl R groups, although the phenyl-HMF-based diglycidyl ether achieved a fair 61 % yield. However, for those worst-yielding examples from each furan, the issue was side-product formation.

Table 4.2. Symmetric diglycidyl ethers derived from DFF.

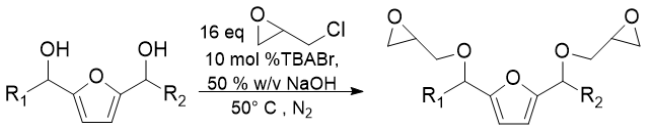

Entry	R	Rxn time (h)	Isolated Yield (%)
5a	Methyl	2	66
5b	Ethyl	2	78
5c	Allyl	2	74
5d	nButyl	2	55
5e*	tButyl	4	40*
5f	Benzyl	16	5

*crude yield.

Unfortunately, it was very difficult to discern what the cause of side-product formation was because the side-products themselves could not be explicitly described by spectral analysis. This is not to say that attempts were not made to determine the cause. The DFF-based cyclopentyl products (compound 5f) were column separated and analyzed, although the column separation seems to have caused some reaction or degradation of the products, as observed in changes of crude vs "purified" TLC. Still, three fraction sets were analyzed by NMR, IR and HRMS.

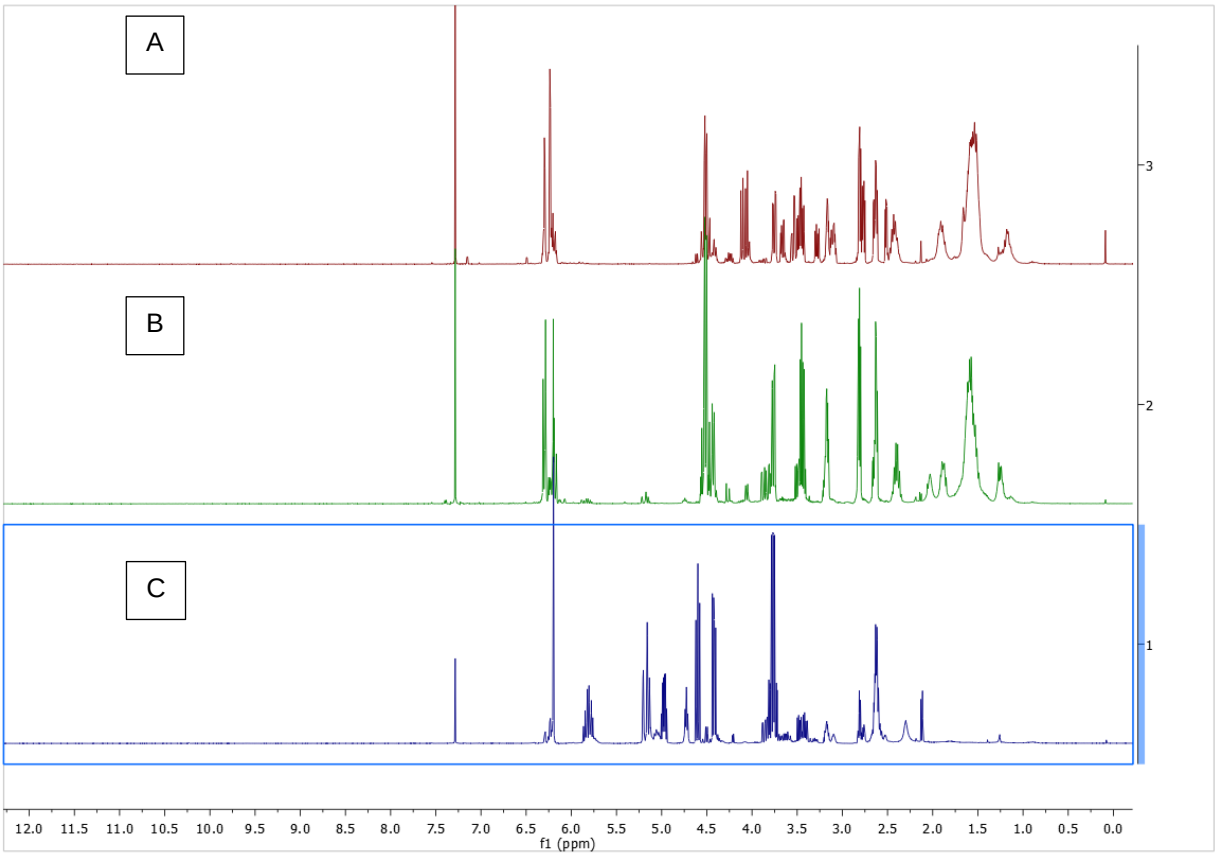

Figure 4.9. ^{1}H NMR of cPentylDFF-based DGE products (**5f**).

The results of the column-separated products were unexpected and seemed to be conflicting. The proton NMR for both fraction sets in Figure 4.10 shows a main product with at least one impurity. Spectra A and B feature chemical shifts with the anticipated peak splitting indicating a 2,5-subsituted furan, there is a glycidyl ether section, and lastly characteristic splitting for cyclopentyl groups. At first glance, spectrum B appears to be of a monoglycidyl ether, interpreted from the ROH group and the lack of duplicate splitting of peaks in the diglycidyl ether region making it appear sparse. The final fraction set, shown in spectrum C, reveals what appears to be an allyl group, a single furan peak and an alcohol group. Potentially, signs of an elimination reaction.

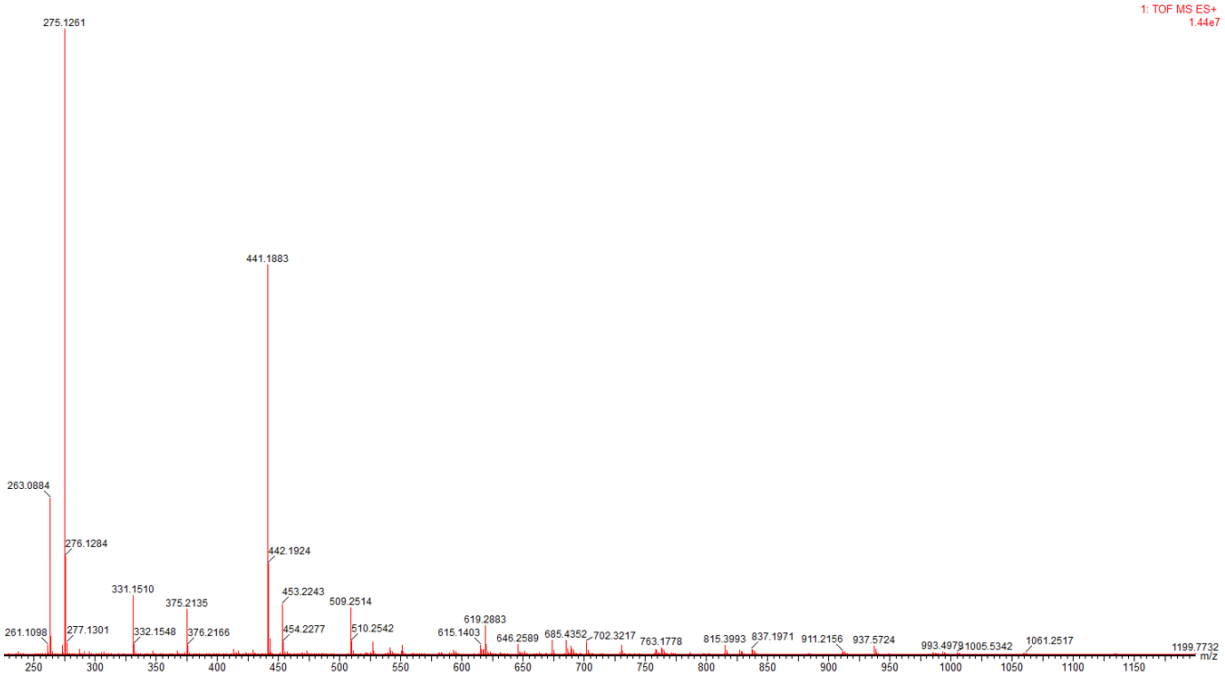

Figure 4.10. Mass spectrum via HRMS for products of **5f** synthesis fraction set "A".

The HRMS results did not confirm but conflicted with those predictions/expectations. The mass peak for compound **5f** (399.4127) was not present (Figure 4.11). The HRMS results correlating to spectrum B did not show evidence of any monoglycidation. Interestingly, a mass peak (331.1521) correlating to the cyclopentyl-HMF-based diglycidyl ether is present in the HRMS for both fraction sets.

Still, based on the NMR results, there appears to be 2, 5-substituted furans, cyclopentyl groups assumingly at the furylic positions and glycidyl ethers present. The higher masses could be from oligomers, and an elimination reaction could be occurring, but further analysis would be necessary to confirm that idea.

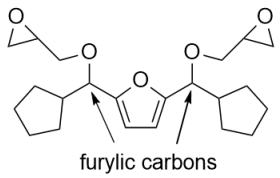

Figure 4.11. Furylic carbon positions.

The result of the reaction for **5f** synthesis was undesirable, but it did provide some insight into the trend of DFF-based diols with bulky R groups providing lower yields from attempted diglycidation than their HMF-based diol counterparts. In earlier chapters, and even at the start of this project, the side-products tended to be color impurities from conjugated oligomerized furans and ring-opened furans. These products do not seem to fall into either category exactly, though further experiments and analysis would be needed to determine what the products and their synthetic pathway are, if desired. The conclusion to all of this is that the sterically hindered symmetric furanic diols are prone to oligomerization and elimination reactions which do not fully negate or remove the functionality or aromaticity of the starting material.

4.2.2. Yield disparity between 4g and 4h synthesis

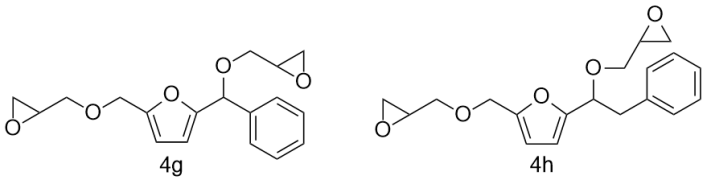

Figure 4.12. Structure comparison: **4g** vs **4h**.

The presence of a single methylene spacer between the furanic position and a benzene drastically lowers the furanic diglycidyl ether yield of **4g** from 61 % to that of 5 % in **4h**. This is likely due to steric hindrance blocking the alkoxide from attacking ECH.

The bulk in addition to the flexibility granted by the methylene linker leads to an increase ability for the benzene ring to obstruct the furan alkoxide's attack on ECH. While the pathway to glycidation is hindered, the competing route to color-forming oligomerization & degradation is still available. This was observed that the benzyl diols, both HMF and DFF-based, formed persistent bright yellow color in their synthesis and when in storage- a sign of oligomerization.

4.3. Experimental

4.3.1. Path to the final general glycidation procedure

My attempts at synthesizing diglycidyl ethers from novel furanic diols took two forms:

- Deprotonation and subsequent alkylation of HMF or DFF via n-Butyl Lithium and quenching of the resulting alkoxide with epichlorohydrin

- Deprotonation of a novel furanic diol with NaOH with subsequent reaction with epichlorohydrin
- Initial method for novel furan diol diglycidation
- Modifications on Hayashi method
- Modifications on ARL method
- Cho method
- Optimizations of the Cho method

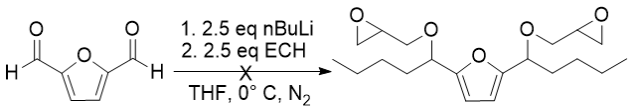

Scheme 4.2. nBuLi method

The result was several of products visualized by TLC using $KMnO_4$ stain from both the initial reaction of DFF and nBuLi and the subsequent "quenching" via the addition of epichlorohydrin. No diglycidated product was obtained. HRMS showed only the diol.

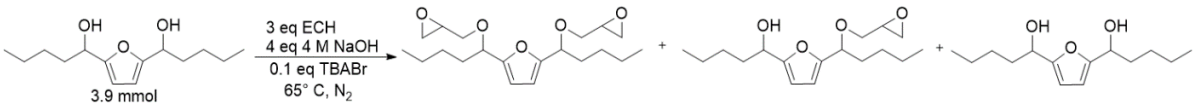

Scheme 4.3. Initial NaOH method

This reaction was designed without a literature reference. It was anticipated that NaOH should be able to deprotonate the furanic diols, that a quaternary salt would be necessary for phase transfer, and that the diols might be able to react with epichlorohydrin.

The reaction did produce the desired diglycidyl ether product, but it was joined by the monoglycidyl ether and unreacted diol, as observed by HRMS. This result was encouraging, but a better method was needed.

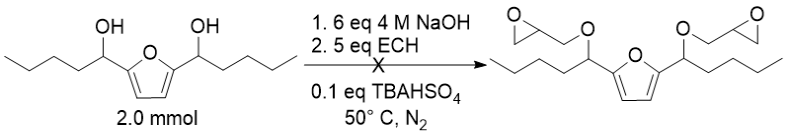

Scheme 4.4. Hayashi method[18]

In this method, the furanic diol reacted with NaOH without epichlorohydrin present, and then the epichlorohydrin was added. Upon workup of this reaction, no product could be obtained. This is not so surprising, as the reaction mixture went from a light yellow (original diol color), to deep orange, to colorless. Typically, if any of the furanic compounds go from having a color to colorless in the reaction mixture, it is a sign of ring-opening into, we suspect, aliphatic water-soluble molecules or oligomers.

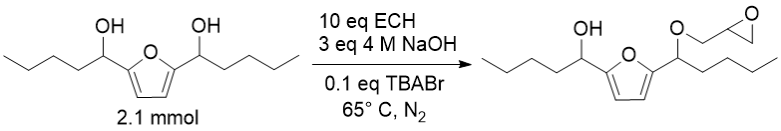

Scheme 4.5. Army Research Lab method[7]

In the literature, this method was used on bis(hydroxymethyl)furan. The crude reaction product was analyzed by HRMS. Instead of the desired diglycidyl ether, this reaction specifically formed the monodiglycidyl ether.

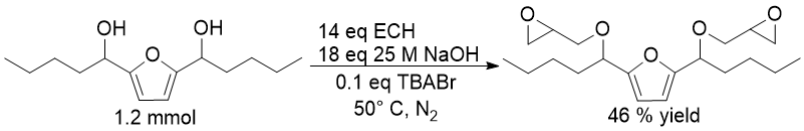

Scheme 4.6. Cho method[6]

In the literature, this method was used on bis(hydroxymethyl)furan. The crude reaction product was analyzed by HRMS. It formed diglycidyl ether which was worked up and collected. The key to this reaction was that the NaOH was in a 25 M aqueous solution (50 % w/w), whereas previous reactions were run at only 4 M NaOH aqueous solutions. The 25 M and 4 M aqueous NaOH solutions differed

greatly in viscosity. Whereas the 4 M NaOH solution was similar in viscosity to water, the 25 M NaOH solution was like a gel. This gel-like solution led to better separation of the aqueous and organic phases in the reaction mixture. It is suspected that this physical difference kept the furanic diol from having enough direct contact with NaOH to form side reactions (see scheme 3 method). Furthermore, an excessive amount of both epichlorohydrin (14 molar equivalents) and NaOH (18 molar equivalents) was used. This result was encouraging, and subsequent glycidation reactions were modifications of this method.

4.3.2. Final general glycidation procedure

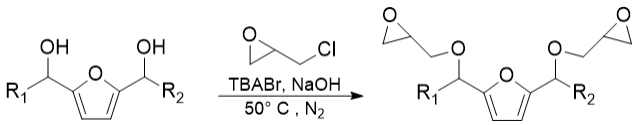

This method was used to complete tables 4.1 and 4.2. In a vial, furanic diol (5 mmol, 1 eq) was diluted with epichlorohydrin (4 mL) and set aside. A 50 mL two-necked round bottom flask was charged with a stir bar and NaOH (2 g, 10 eq). Water (2 mL) was added and the contents stirred until a clear solution formed. Tetrabutylammonium bromide (0.161 g, 10 mol %) and epichlorohydrin were added to the reaction vessel, which was then flushed with nitrogen. Total epichlorohydrin used was 16 mL (40 eq). While slowly stirring (~180-200 rpm) the furanic diol diluted in epichlorohydrin was then added dropwise over 2 minutes via syringe pump. Once additions of diol were complete, the vessel was placed in the oil bath (50° C) for 2 hours, but for a few compounds as long as 16 hours, depending on the steric hindrance caused by the R groups.

Once the reaction reached completion, observed via TLC, the hot reaction contents were poured over ice. The cooled contents were transferred to a 250 mL separatory funnel with ethyl acetate. Ethyl acetate was added (80 mL) and the organic layer was washed with brine (15 mL x 3). The organic layer was collected and dried over sodium sulfate. The solvent was removed *in vacuo*, and the resulting oil stored in a freezer (4 °C) until purified via column (gradient up to 2 Hexanes :1 Ethyl Acetate).

4.3.3. Side quest: Comparison of petroleum and biobased epichlorohydrin

Figure 4.13. Reaction A (biobased) and Reaction B (petroleum-derived) crude products.

There was concern as to the level of color present which would carry over to final products, as that color might be off-putting to consumers. A comparison of the diglycidation of methyl HMF-based diol was run with two different sources of ECH to determine if any improvement in color could be discerned. Glycidation results based on ECH source were compared: *Reaction A* using a biobased ECH sourced from Advanced Biochemical (Thailand) Co., Ltd. and *Reaction B* using a petroleum-derived ECH (Sigma-Aldrich). Reaction B is only very slightly deeper amber than Reaction A. Interestingly, the biobased ECH gave a slightly cleaner product observed via NMR (Figure 4.13). It seems like the petroleum-derived ECH may have impurities which facilitate an oligomeric impurity. In the end, however, once purified, both reactions had comparable yields, and color.

Based on this experiment biobased ECH was used for the screening of furanic compounds, and subsequently for the larger-scale monomer synthesis (0.1 mol and up).

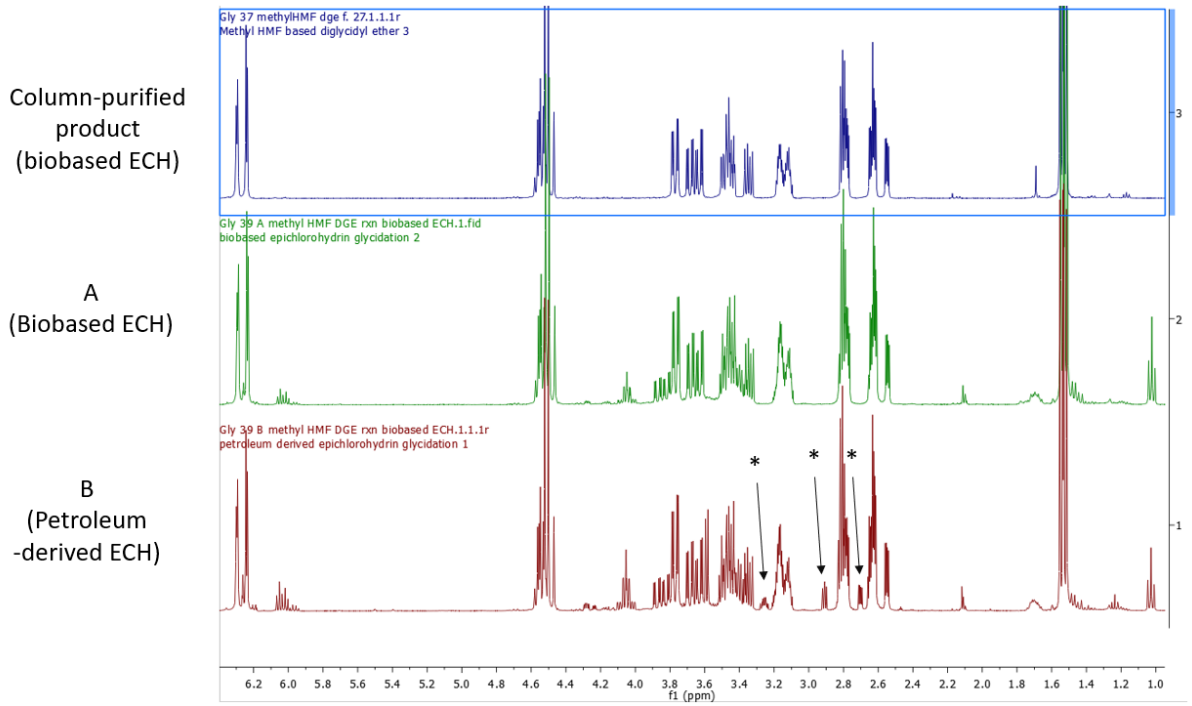

Figure 4.14. ^{1}H-NMR comparison.

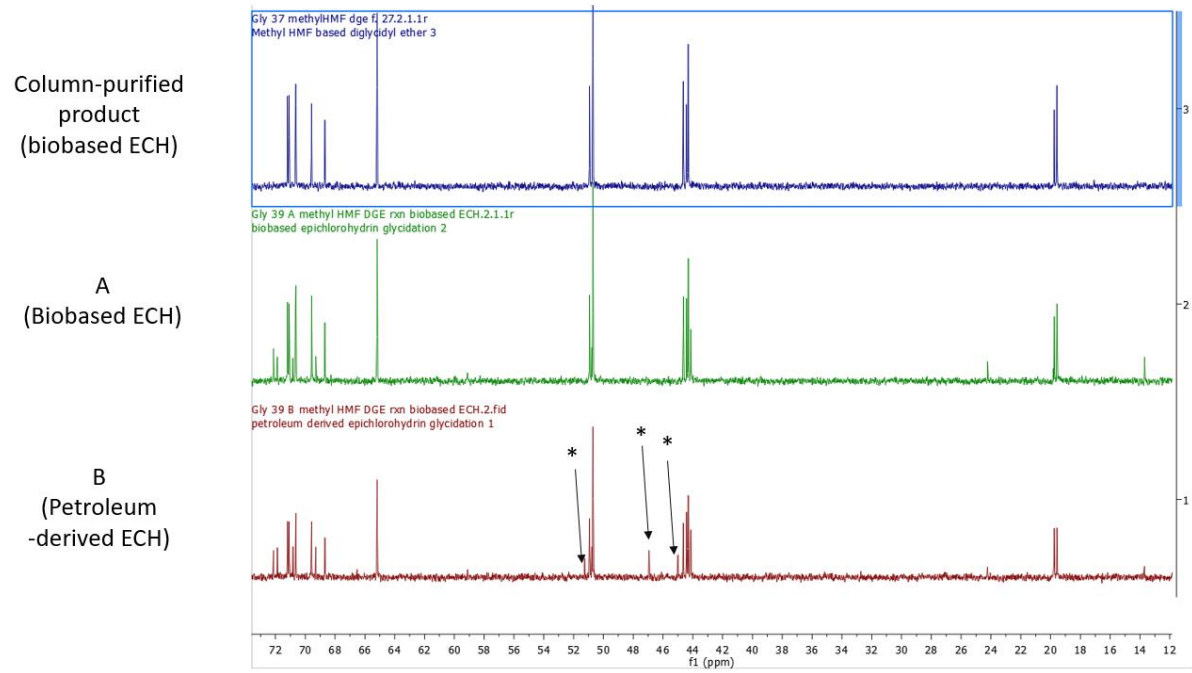

Figure 4.15. ^{13}C-NMR comparison.

4.4. Spectra

4.4.1. Sample preparation

All NMR samples were, unless noted otherwise, neat samples dissolved in deuterated solvent. The standard deuterated solvent was CDCl3, but some other solvents and solvent combinations were used in at least one instance, which is noted in the title for the spectrum. Masses ranging from 20-30 mg of the furan diols were diluted with 0.75 mL of deuterated solvent, no matter the solvent.

All IR spectra samples were neat, unless otherwise noted.

HRMS samples were prepared by diluting the furan substrates in UPLC-grade methanol.

4.4.2. Written spectral data: HMF-based DGEs

Written spectral data for the spectra of the combined enantiomers and diastereomers of each compound.

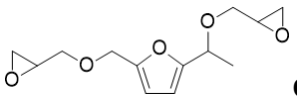

Compound 4a. ^{1}H NMR (400 MHz, Chloroform-*d*) δ 6.28 (d, *J* = 3.0 Hz, 1H), 6.23 (d, *J* = 3.2 Hz, 1H), 4.58 – 4.43 (m, 3H), 3.76 (dd, *J* = 12.3, 3.1 Hz, 1H), 3.65 (ddd, *J* = 20.7, 11.4, 3.3 Hz, 1H), 3.49 – 3.29 (m, 2H), 3.15 (dq, *J* = 6.0, 3.0 Hz, 1H), 3.10 (dq, *J* = 7.6, 3.9, 3.3 Hz, 1H), 2.81 – 2.74 (m, 2H), 2.64 – 2.51 (m, 2H), 1.52 (dd, *J* = 8.6, 6.6 Hz, 3H). ^{13}C NMR (101 MHz, $CDCl_3$) 155.7, 155.5, 151.1, 151.0, 110.1, 110.0, 107.9, 107.7, 71.1, 71.0, 70.6, 69.5, 68.6, 65.1, 50.9, 50.7, 44.6, 44.4, 44.2, 19.7, 19.5. FTIR (neat) cm^{-1}: 2987, 2868, 1444, 1253, 1084, 1014,853, 757. HRMS calculated for $C_{13}H_{18}O_5Na$: 277.1052; Found: 277.1049.

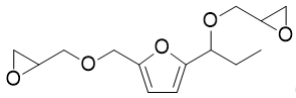

Compound 4b. ^{1}H NMR (400 MHz, Chloroform-d) δ 6.30 (dd, J = 3.1, 1.6 Hz, 1H), 6.25 (d, J = 3.1 Hz, 1H), 4.58 – 4.42 (m, 2H), 4.28 (dt, J = 13.6, 6.9 Hz, 1H), 3.91 – 3.56 (m, 2H), 3.54 – 3.28 (m, 2H), 3.22 – 3.07 (m, 2H), 2.79 (ddd, J = 13.6, 5.1, 4.2 Hz, 2H), 2.69 – 2.51 (m, 2H), 1.99 – 1.78 (m, 2H), 0.93 (td, J = 7.4, 4.6 Hz, 3H).^{13}C NMR (101 MHz, $CDCl_3$) δ 154.9, 151.2, 110.1, 108.5, 72.1, 70.6, 69.7, 68.9, 65.2, 50.7, 44.3, 27.2, 10.1. FTIR (neat) cm^{-1}: 2967, 2876, 1736, 1458, 1249, 1075, 853, 796. HRMS calculated for $C_{14}H_{20}O_5Na$: 291.1208; Found: 291.1205.

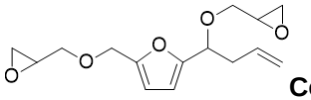

Compound 4c. ^{1}H NMR (400 MHz, Chloroform-*d*) δ 6.30 (dd, *J* = 3.2, 1.7 Hz, 1H), 6.25 (d, *J* = 3.2 Hz, 1H), 5.86 – 5.70 (m, 1H), 5.16 – 5.00 (m, 2H), 4.58 – 4.34 (m, 3H), 3.91 – 3.57 (m, 2H), 3.53 – 3.29 (m, 2H), 3.22 – 3.07 (m, 2H), 2.85 – 2.67 (m, 3H), 2.67 – 2.51 (m, 4H). ^{13}C NMR (101 MHz, $CDCl_3$) δ 154.3, 151.3, 133.9, 117.4, 110.1, 108.8, 75.3, 72.1, 70.6, 69.7, 68.9, 65.1, 50.7, 44.3, 38.5. FTIR (neat) cm^{-1}: 2998, 2920, 1642, 1253, 1080, 908, 846, 798. HRMS calculated for $C_{15}H_{20}O_5Na$: 303.1208; Found: 303.1205.

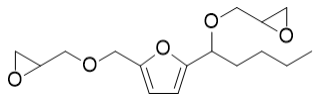

Compound 4d. ^{1}H NMR (400 MHz, Chloroform-*d*) δ 6.29 (dd, *J* = 3.2, 1.7 Hz, 1H), 6.23 (d, *J* = 3.2 Hz, 1H), 4.58 – 4.44 (m, 2H), 4.33 (dt, *J* = 14.3, 7.0 Hz, 1H), 3.80 – 3.24 (m, 4H), 3.23 – 3.06 (m, 2H), 2.85 – 2.48 (m, 4H), 2.00 – 1.75 (m, 2H), 1.48 – 1.18 (m, 4H), 0.90 (td, *J* = 7.1, 0.8 Hz, 3H).^{13}C NMR (101 MHz, $CDCl_3$) δ 155.1, 151.1, 110.1, 108.3, 75.7, 75.5, 70.6, 69.7, 68.9, 65.2, 50.7, 44.3, 33.8, 27.8, 22.5, 14.0. FTIR (neat) cm^{-1}: 2929, 2861, 1736, 1458, 1252, 1083, 847, 797. HRMS calculated for $C_{16}H_{24}O_5Na$: 319.1521; Found: 319.1507.

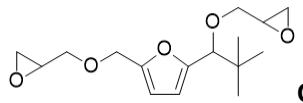

Compound 4e. ^{1}H NMR (400 MHz, Chloroform-*d*) δ 6.30 (d, *J* = 3.1 Hz, 1H), 6.19 (d, *J* = 3.2 Hz, 1H), 4.58 – 4.41 (m, 2H), 4.37 (s, 1H), 3.91 – 3.70 (m, 1H), 3.54 – 3.38 (m, 1H), 3.17 (dddtd, *J* = 11.4, 5.8, 4.2, 2.8, 1.4 Hz, 1H), 2.86 – 2.76 (m, 1H), 2.68 – 2.58 (m, 2H), 0.97 (s, 8H). ^{13}C NMR (101 MHz, $CDCl_3$) δ 156.3, 150.2, 110.2, 107.7, 77.4, 77.0, 76.7, 76.5, 76.5, 72.1, 71.9, 70.4, 70.3, 65.1, 50.8, 50.7, 50.7, 44.3, 44.2, 44.1, 35.7, 25.8. FTIR (neat) cm^{-1} 3462, 2954, 2905, 2868, 1736, 1479, 1241, 1073. HRMS calculated for $C_{16}H_{24}O_5Na$: 319.1521; Found: 319.1495.

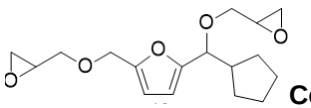

Compound 4f. ^{1}H NMR (400 MHz, Chloroform-*d*) δ 6.29 (t, *J* = 2.7 Hz, 1H), 6.23 (d, *J* = 3.1 Hz, 1H), 4.59 – 4.42 (m, 2H), 4.08 (dd, *J* = 20.1, 9.0 Hz, 1H), 3.92 – 3.22 (m, 4H),

3.20 – 3.04 (m, 2H), 2.84 – 2.49 (m, 4H), 2.43 (p, *J* = 8.2 Hz, 1H), 1.99 – 1.09 (m, 8H). ^{13}C NMR (101 MHz, $CDCl_3$) δ 155.0, 151.1, 110.0, 109.0, 108.7, 80.1, 79.8, 71.9, 70.5, 69.7, 68.9, 65.2, 51.1, 50.7, 44.7, 44.3, 43.7, 29.8, 29.0, 25.5. FTIR (neat) cm^{-1} 2951, 2866, 1736, 1452, 1243, 1077, 845, 797. HRMS calculated for $C_{17}H_{24}O_5Na$: 331.1521; Found: 331.1520.

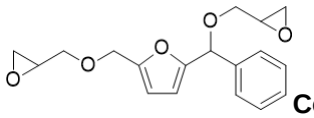

Compound 4g. ^{1}H NMR (400 MHz, Chloroform-*d*) δ 7.49 – 7.28 (m, 5H), 6.26 (d, *J* = 3.2 Hz, 1H), 6.08 (td, *J* = 6.3, 5.6, 3.3 Hz, 1H), 5.48 (d, *J* = 2.9 Hz, 1H), 4.57 – 4.39 (m, 2H), 3.82 – 3.69 (m, 2H), 3.66 – 3.35 (m, 3H), 3.25 – 3.08 (m, 1H), 2.84 – 2.46 (m, 4H). ^{13}C NMR (101 MHz, $CDCl_3$) δ 154.6, 151.7, 138.7, 128.4, 128.2, 127.3, 110.2, 109.4, 77.6, 72.1, 71.9, 70.6, 69.8, 69.6, 65.2, 50.8, 44.5, 44.3. FTIR (neat) cm^{-1} 2998, 2867, 1452, 1253, 1070,845, 796, 701. HRMS calculated for $C_{18}H_{20}O_5Na$: 339.1208; Found: 339.1205.

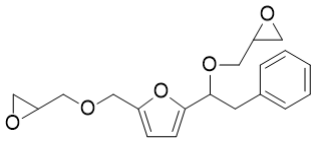

Compound 4h. ^{1}H NMR (400 MHz, Chloroform-*d*) δ 7.36 – 7.14 (m, 6H), 6.28 (t, *J* = 2.9 Hz, 1H), 6.19 (t, *J* = 3.2 Hz, 1H), 4.64 – 4.45 (m, 3H), 3.80 – 3.73 (m, 1H), 3.67 (ddd, *J* = 11.6, 3.2, 0.8 Hz, 1H), 3.55 (dd, *J* = 11.5, 3.4 Hz, 1H), 3.50 – 3.39 (m, 2H), 3.34 – 3.10 (m, 4H), 3.07 – 3.00 (m, 1H), 2.77 (dt, *J* = 38.7, 4.5 Hz, 2H), 2.64 (dtt, *J* = 3.5, 2.6, 1.6 Hz, 2H), 2.50 (ddd, *J* = 16.4, 5.1, 2.7 Hz, 1H). ^{13}C NMR (101 MHz, $CDCl_3$) δ 154.0, 153.8, 151.3, 151.3, 137.7, 129.4, 128.2, 126.4, 110.2, 110.2, 109.4, 109.1, 76.9, 76.5, 70.5, 69.7, 69.2, 65.1, 50.8, 50.7, 50.6, 44.5, 44.3, 44.2, 40.8. FTIR (neat) cm^{-1} 2999, 2923, 1739, 1076, 1496, 1251, 840, 729. HRMS calculated for $C_{19}H_{22}O_5Na$: 353.1365; Found: 353.1376.

4.4.3. Written spectral data: DFF-based DGEs

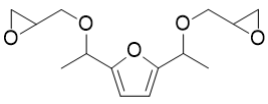

Compound 5a. ^{1}H NMR (400 MHz, Chloroform-*d*) δ 6.23 (d, *J* = 1.1 Hz, 1H), 4.55 (q, *J* = 6.5 Hz, 1H), 3. (m, 0H), 3.65 (ddd, *J* = 16.7, 11.4, 3.4 Hz, 1H), 3.53 – 3.31 (m, 1H), 3.22

– 3.06 (m, 1H), 2.85 – 2.74 (m, 1H), 2.67 – 2.52 (m, 1H), 1.54 (t, 3H). ^{13}C NMR (101 MHz, $CDCl_3$) δ 154.9, 107.7, 72.1, 71.1, 69.5, 68.7, 50.9, 44.5, 19.6. FTIR (neat) cm^{-1} : 2983, 2933, 1736, 1445, 1240, 1088, 853, 795. HRMS calculated for $C_{14}H_{20}O_5Na$: 291.1208; Found: 291.1212.

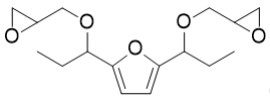

Compound 5b. ^{1}H NMR (400 MHz, Chloroform-*d*) δ 6.24 (t, *J* = 1.2 Hz, 1H), 4.27 (dt, *J* = 12.4, 7.0 Hz, 1H), 3.71 – 3.53 (m, 1H), 3.52 – 3.28 (m, 1H), 3.17 – 3.03 (m, 1H), 2.82 – 2.74 (m, 1H), 2.67 – 2.50 (m, 1H), 1.90 (dtt, *J* = 20.7, 13.7, 7.2 Hz, 2H), 0.91 (tt, *J* = 6.8, 3.3 Hz, 3H).^{13}C NMR (101 MHz, $CDCl_3$) δ 154.1, 108.3, 69.6, 68.8, 50.6, 44.7, 27.1, 10.0. FTIR (neat) cm^{-1} 2966, 2934, 2876, 1737, 1463, 1250, 1074, 792. HRMS calculated for $C_{16}H_{24}O_5Na$: 319.1521; Found: 319.1523.

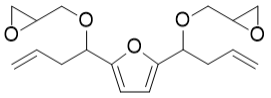

Compound 5c. ^{1}H NMR (400 MHz, Chloroform-*d*) δ 6.25 (q, *J* = 1.6 Hz, 1H), 5.76 (ddtt, *J* = 17.0, 10.1, 6.8, 3.3 Hz, 1H), 5.15 – 4.97 (m, 2H), 4.47 – 4.33 (m, 1H), 3.74 – 3.54 (m, 1H), 3.49 – 3.27 (m, 1H), 3.11 (qd, *J* = 6.3, 5.7, 3.9 Hz, 1H), 2.84 – 2.71 (m, 1H), 2.73 – 2.47 (m, 3H). ^{13}C NMR (101 MHz, $CDCl_3$) δ 153.5, 133.8, 117.4, 108.8, 75.0, 69.6, 68.8, 50.9, 44.3, 38.5. FTIR (neat) cm^{-1} 3075, 2999, 2920, 1745, 1642, 1082, 908. HRMS calculated for $C_{18}H_{24}O_5Na$: 343.1521; Found: 343.1521.

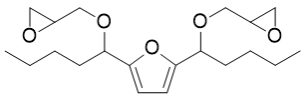

Compound 5d. ^{1}H NMR (400 MHz, Chloroform-*d*) δ 6.21 (t, *J* = 1.8 Hz, 1H), 4.31 (dt, *J* = 13.8, 7.0 Hz, 1H), 3.66 – 3.50 (m, 1H), 3.48 – 3.22 (m, 1H), 3.08 (tt, *J* = 7.8, 4.6 Hz, 1H), 2.78 – 2.71 (m, 1H), 2.66 – 2.45 (m, 1H), 1.97 – 1.71 (m, 2H), 1.43 – 1.12 (m, 4H), 0.87 (t, *J* = 7.1 Hz, 3H). ^{13}C NMR (101 MHz, $CDCl_3$) δ 154.1, 108.3, 75.6, 69.6, 68.8, 50.9, 44.3, 33.6, 27.7, 22.4, 14.0. FTIR (neat) cm^{-1} 2929, 2861, 1741, 1458, 1252, 1084, 847, 769. HRMS calculated for $C_{20}H_{32}O_5Na$: 375.2147; Found: 375.2163.

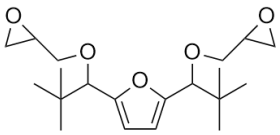

Compound 5e. ^{1}H NMR (400 MHz, $CDCl_3$) δ 6.19, 6.18, 4.36, 4.35, 3.90, 3.89, 3.87, 3.84, 3.81, 3.51, 3.48, 3.45, 3.44, 3.41, 3.28, 3.27, 3.25, 3.24, 3.21, 3.19, 3.18, 3.16, 2.93, 2.91, 2.90, 2.82, 2.72, 2.70, 2.66, 2.64, 2.62, 0.97. ^{13}C NMR (101 MHz, $CDCl_3$) δ 154.8, 107.5, 76.4, 72.1, 71.8, 70.8, 51.3, 50.7, 46.9, 45.8, 45.0, 44.1, 35.7, 25.8. FTIR (neat) cm^{-1} 3001, 1734, 1432, 1243, 1093, 926, 852, 722. HRMS calculated for $C_{20}H_{32}O_5Na$: 375.2147; Found: 375.2148.

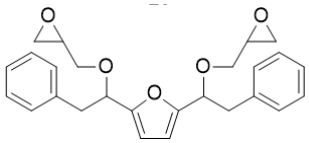

Compound 5g. ^{1}H NMR (400 MHz, Chloroform-*d*) δ 7.26 – 7.05 (m, 11H), 6.17 – 6.14 (m, 1H), 6.12 (t, *J* = 1.2 Hz, 1H), 4.62 – 4.49 (m, 1H), 4.23 (s, 1H), 4.10 (q, *J* = 5.5 Hz, 2H), 3.91 – 3.80 (m, 1H), 3.74 – 3.57 (m, 3H), 3.47 (ddd, *J* = 27.6, 11.6, 5.9 Hz, 2H), 3.32 – 2.99 (m, 2H), 2.83 (t, *J* = 5.2 Hz, 1H), 2.77 – 2.59 (m, 4H), 2.57 – 2.45 (m, 1H). ^{13}C NMR (101 MHz, $CDCl_3$) δ 153.2, 137.7, 129.4, 128.2, 126.4, 109.3, 76.4, 72.1, 69.6, 68.9, 65.3, 50.8, 46.0, 44.2, 40.7. FTIR (neat) cm^{-1} 3451, 2925, 1738, 1496, 1231, 1091, 909, 848. HRMS calculated for $C_{26}H_{28}O_5Na$: 443.1834; Found: 443.1830.

4.5. References

1. Wicks, Z. W. J., Frank N.; Pappas, S. Peter; Wicks, Douglas A. , Organic Coatings. Third Edition ed.; John Wiley & Sons, Inc.: Hoboken , New Jersey, 2007.

2. Hefner, R. M., Michael; Metral, Guillaume; Frey, Johann-Wilhelm; Hoevel, Bernd. Epoxy resin compositions. 8,937,145 B2, January 20, 2015, 2015.

3. Koenig, R. H., Guenter. Method for increasing the functionality of an epoxy resin. 4,722,990, 1988.

4. Bertram, J. W., Louis; Van I. W., Stuart. Latent catalysts for epoxy reactions. 4725652, 1988.

5. Marshall, C. Process for reacting a phenol with an epoxy compound. 3,978,027, 1976.

6. Cho, J. K.; Lee, J.-S.; Jeong, J.; Kim, B.; Kim, B.; Kim, S.; Shin, S.; Kim, H.-J.; Lee, S.-H., Synthesis of carbohydrate biomass-based furanic compounds bearing epoxide end group(s) and evaluation of their feasibility as adhesives. *Journal of Adhesion Science and Technology* **2013,** *27* (18-19), 2127-2138.10.1080/01694243.2012.697700.

7. Hu, F.; La Scala, J. J.; Sadler, J. M.; Palmese, G. R., Synthesis and Characterization of Thermosetting Furan-Based Epoxy Systems. *Macromolecules* **2014,** *47* (10), 3332-3342.10.1021/ma500687t.

8. Tian, Q.; Rong, M. Z.; Zhang, M. Q.; Yuan, Y. C., Optimization of thermal remendability of epoxy via blending. *Polymer* **2010,** *51* (8), 1779-1785.https://doi.org/10.1016/j.polymer.2010.02.004.

9. Peterson, A. M.; Jensen, R. E.; Palmese, G. R., Room-Temperature Healing of a Thermosetting Polymer Using the Diels−Alder Reaction. *ACS Appl. Mater. Interfaces* **2010,** *2* (4), 1141-1149.10.1021/am9009378.

10. Pratama, P. A.; Sharifi, M.; Peterson, A. M.; Palmese, G. R., Room Temperature Self-Healing Thermoset Based on the Diels–Alder Reaction. *ACS Appl. Mater. Interfaces* **2013,** *5* (23), 12425-12431.10.1021/am403459e.

11. Cho, J. G.; Kim, B. J.; Kim, S. Y.; Lee, D. H.; Lee, S. H.; Lee, J. S. Preparation of furan-based curable compounds derived from biomass for solvent-free curable compositions. KR1116450, 2012.

12. Shen, X.; Liu, X.; Dai, J.; Liu, Y.; Zhang, Y.; Zhu, J., How Does the Hydrogen Bonding Interaction Influence the Properties of Furan-Based Epoxy Resins. *Industrial & Engineering Chemistry Research* **2017,** *56* (38), 10929-10938.10.1021/acs.iecr.7b02901.

13. Liu, X.; Leong, D. C. Y.; Sun, Y., The production of valuable biopolymer precursors from fructose. *Green Chemistry* **2020,** *22* (19), 6531-6539.10.1039/D0GC02315A.

14. Nameer, S.; Larsen, D. B.; Duus, J. Ø.; Daugaard, A. E.; Johansson, M., Biobased Cationically Polymerizable Epoxy Thermosets from Furan and Fatty Acid Derivatives. *ACS Sustain. Chem. Eng.* **2018,** *6* (7), 9442-9450.10.1021/acssuschemeng.8b01817.

15. Cai, H.; Li, P.; Sui, G.; Yu, Y.; Li, G.; Yang, X.; Ryu, S., Curing kinetics study of epoxy resin/flexible amine toughness systems by dynamic and isothermal DSC. *Thermochimica Acta* **2008,** *473* (1), 101-105.https://doi.org/10.1016/j.tca.2008.04.012.

16. Maaskant, E.; van Es, D. S., Unexpected Susceptibility of Poly(ethylene furanoate) to UV Irradiation: A Warning Light for Furandicarboxylic Acid? *ACS Macro Lett.* **2021,** *10* (12), 1616-1621.10.1021/acsmacrolett.1c00676.

17. Yao, Y.; Li, Z.; Qiu, Y.; Bai, J.; Su, J.; Zhang, D.; Jiang, S., Unprecedented reactions: from epichlorohydrin to epoxyglycidyl substituted divinyl ether and its conversion into epoxyglycidyl propargyl ether. *Scientific Reports* **2015,** *5*, 14231.10.1038/srep14231

https://www.nature.com/articles/srep14231#supplementary-information.

18. Hayashi, Y.; Ogasawara, S., Time Economical Total Synthesis of (−)-Oseltamivir. *Organic Letters* **2016,** *18* (14), 3426-3429.10.1021/acs.orglett.6b01595.

5. FUTURE DIRECTIONS

5.1. Continuing the work

The purpose of this chapter is to address some of the lingering questions that were unanswered in this body of work.

5.1.1. Suggestions for diglycidyl ether purification

The main issue that was not resolved in the glycidations of novel furan diols, was their purification away from the persistent epichlorohydrin (ECH) oligomeric impurity.

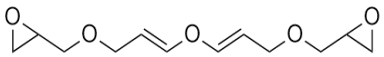

Figure 5.1. ECH (epichlorohydrin) oligomer.

Due to the ever-defiant formation of the ECH oligomer in the diglycidation process, column purification was required for each reaction shown. Column purification of the furan diglycidyl ethers away from color impurity and ECH oligomer was not necessarily facile, but not impossible. The diglycidyl ethers are not as acid sensitive as their diol precursors, but acid still seems to trigger polymerization.

Preventing ECH oligomerization was attempted by altering the synthesis. This was semi-successful on larger scale (~20 -30 g); by decreasing the volume of ECH and NaOH (50 % w/v aq.) and adding ECH-diluted furan dropwise to the reaction mixture, less ECH oligomer was formed. Purifications were also attempted, most notably vacuum distillation. Vacuum distillation seemed a real possibility for removal of the impurity, however its boiling point could never be achieved since the furan components of the crude mixture would routinely darken, indicating a different, furanic polymerization.

While it was frustrating that the problem of ECH oligomer was not solved in this project, there was the persistent idea that there must be a way to remove such an impurity, since it is something formed in any situation where NaOH and ECH are combined, and especially when heated. The question became, how the removal of the oligomer is removed in industry. An answer to that question came only after lab work was concluded for this thesis, but it is useful information for future furanic glycidations.

In industry, impurities form the diglycidation of epoxy monomers of BPA, which were not characterized but can be partly assumed to be ECH oligomer, are purified away from by cold (-20° C)

crystallization of the aromatic diglycidyl ether.[1] It is a procedure that could become difficult on larger scale without specialized equipment, but not as cumbersome as running a column on that same scale. It should also improve the isolated yields, which has been a *major* stopgap in supplying sufficient material for collaborative projects.

5.1.2. Suggestions for future furan acylations

There were many 'cons' and questions to be answered in the acylations of furans featured in chapter 3, namely, why the $FeCl_3$ and the $M(OTf)_3$ mediated acylations do not completely consume the starting material.

A few alterations to both methods were attempted to force the reaction to consume all starting material towards the desired product: increasing temperature, increasing reaction time, increasing the metal triflate catalyst to 1 molar equivalent from 1 mole %, and finally, doubling or tripling the amount of acetic anhydride. None of these alterations could force the reaction to proceed as desired.

What if there is an equilibrium issue at play? The Fayed et al. publication hints at the possibility that the there is an equilibrium issue stunting product formation, since the addition of trifluoroacetic acid was able to, minutely, force the reaction forward.[2] To add to this idea, a publication was found in 2021 on the acylation of 2-acetyl furan.[3] Although originally published in Russian in 2009, it must have been translated into English only recently. They report a 95 % isolated yield. The procedure of running the reaction in a hermetically sealed ampoule is not appealing for large-scale synthesis, but that they added 8 molar equivalents of the acylating agent (a carboxylic acid) to the system was intriguing (Scheme 5.1).

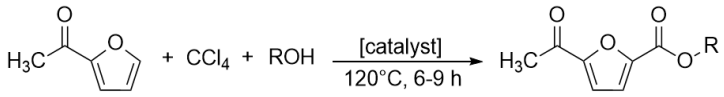

[cat.] - $Fe(C_5H_5)_2$, $Fe(acac)_3$, $FeBr_2$; R= Me, Et, *n*-Pr, *i*-Pr

Scheme 5.1. Acylation of 2-acetyl furan in an ampule, redrawn from Khusnutdinov et al.[3]

Perhaps more acid, or at least the *right* acid is the answer. Dalpozzo et al., in a review connecting the results of several publications, to describe the catalytic cycle of electrophilic aromatic substitution (EAS) via metal triflates improved upon with the addition of $LiClO_4$ as a co-catalyst (Scheme 5.2).[4]

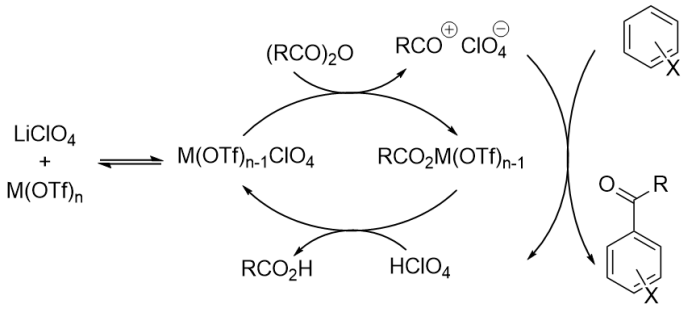

Scheme 5.2. Proposed mechanism for co-catalyst role in EAS, redrawn from Dalpozzo et al.[4]

Improved consumption of the acylating agent and increase in product formation were observed when $LiClO_4$ is added to metal triflate-catalyzed acylations. To move forward in the methods described in chapter 3, the use of $LiClO_4$ is suggested for improved results. It may give the acylation of 2-substituted furans the potential to become green alternative methods for the synthesis of novel furan diols.

Hopefully, these suggestions can be useful to the continued development of the novel furan diols synthesized in this dissertation.

5.2. References

1. Lastovica, J. E., jr. Method for purifying diglycidyl ether of BPA. US 3,142,688, 1964.

2. Fayed, S.; Delmas, M.; Gaset, A., Acylation of furan by variously functionalized carboxylic acids in the presence of phosphonic ionexchange resins used as catalysts. *Journal of Molecular Catalysis* **1985,** *29* (1), 19-31.https://doi.org/10.1016/0304-5102(85)85127-0.

3. Khusnutdinov, R. I.; Baiguzina, A. R.; Mukminov, R. R.; Dzhemilev, U. M., New procedure for synthesis alkyl esters of 5-acetyl-2-furan-carboxylic acid alkyl ester. *Russian Journal of Applied Chemistry* **2009,** *82* (2), 340-342.10.1134/S1070427209020335.

4. Dalpozzo, R.; Bartoli, G.; Sambri, L.; Melchiorre, P., Perchloric Acid and Its Salts: Very Powerful Catalysts in Organic Chemistry. *Chem. Rev.* **2010,** *110* (6), 3501-3551.10.1021/cr9003488.

APPENDIX A: SPECTRA FROM CHAPTER 2

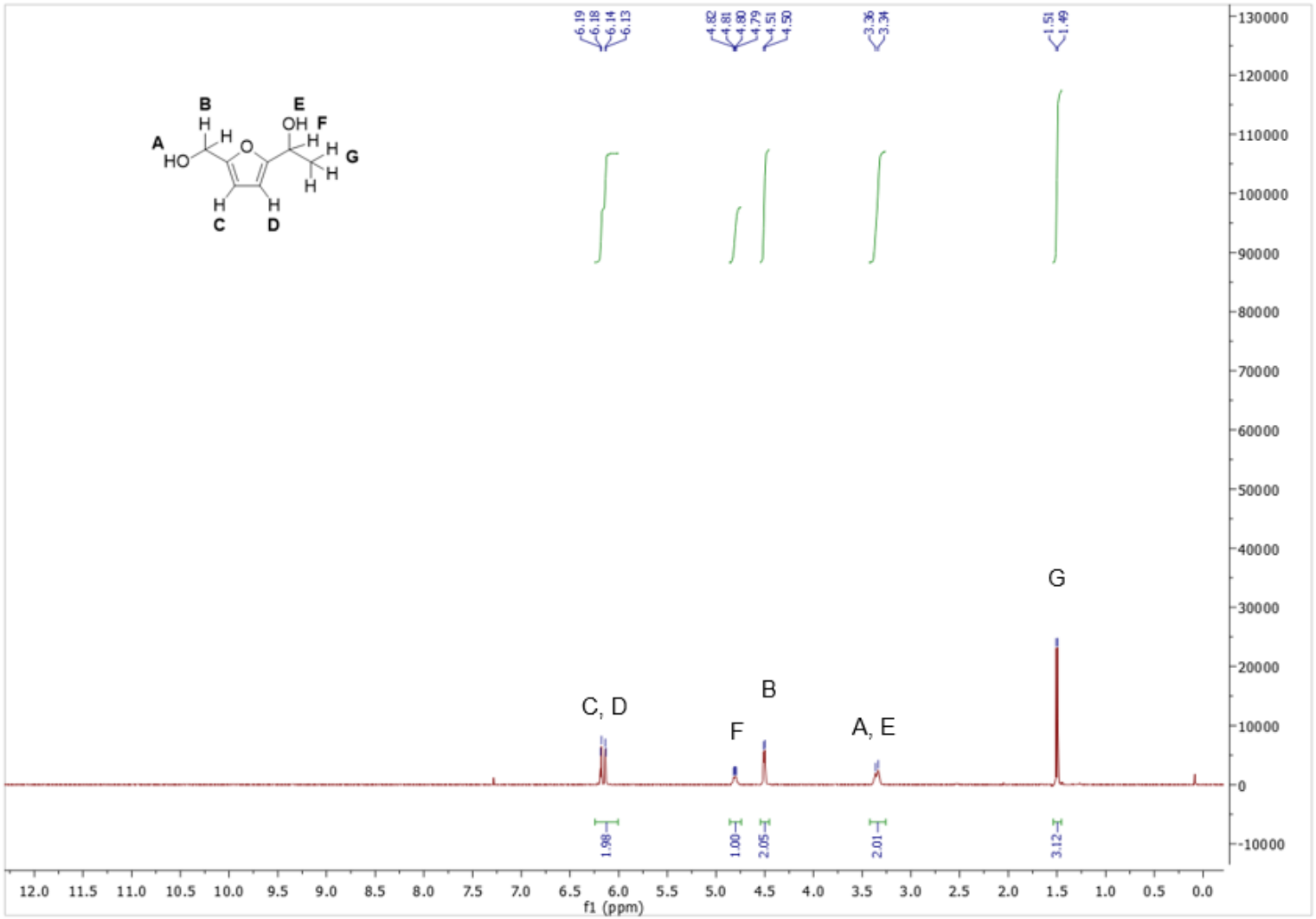

A1. ^{1}H NMR ($CDCl_3$) spectrum of Compound **1a**.

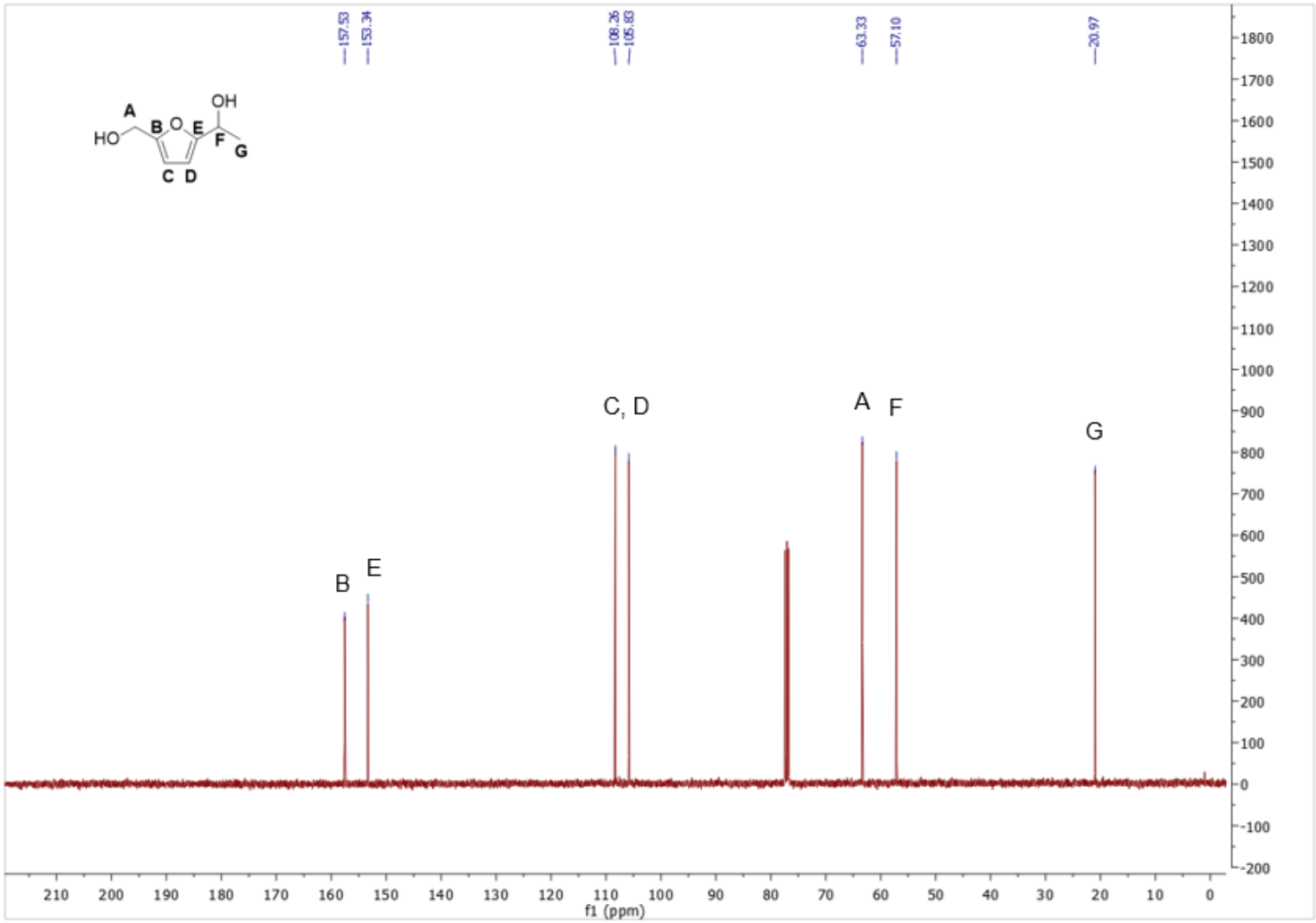

A2. ^{13}C NMR ($CDCl_3$) spectrum of Compound **1a**.

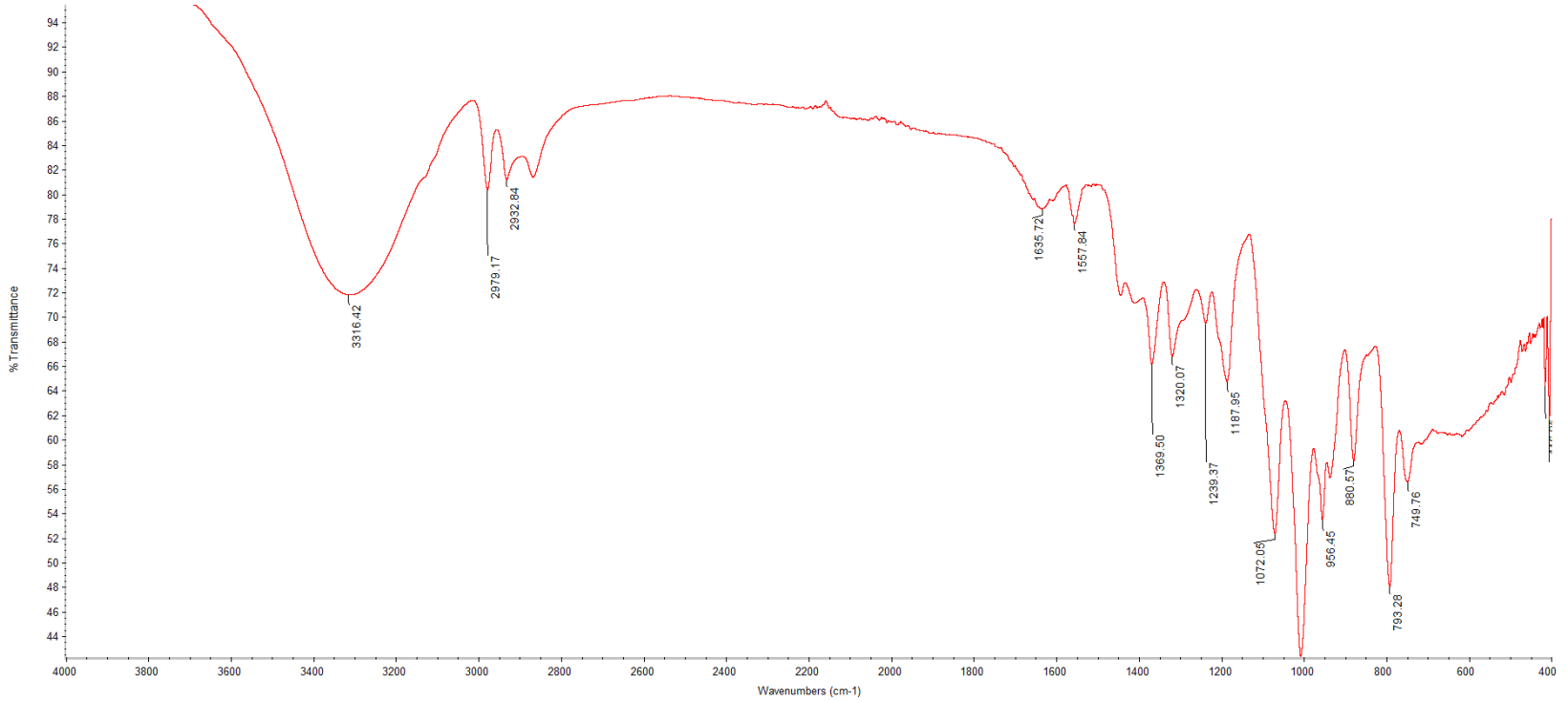

A3. FT-IR spectrum of Compound **1a**.

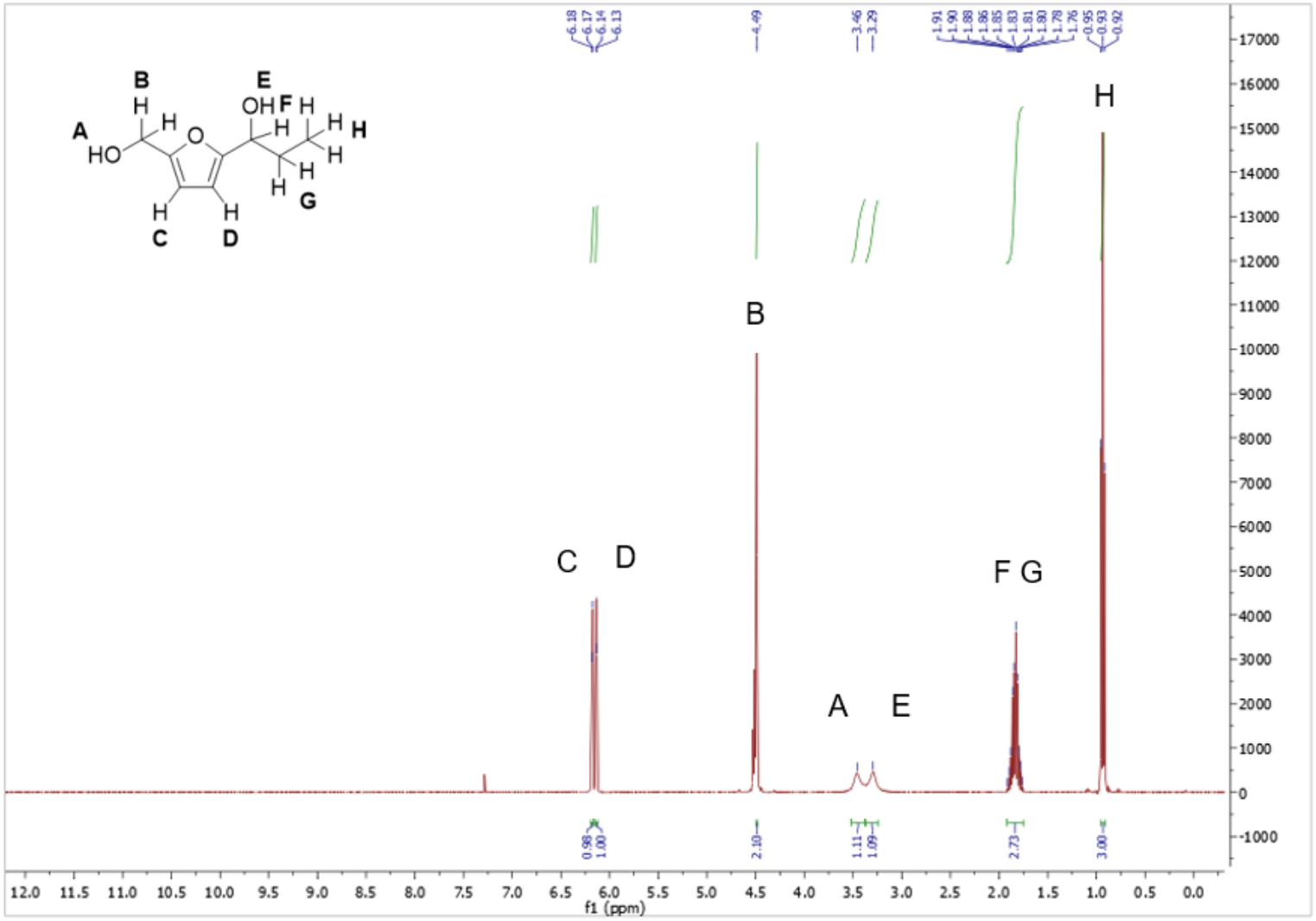

A4. ^{1}H NMR ($CDCl_3$) spectrum of Compound **1b**.

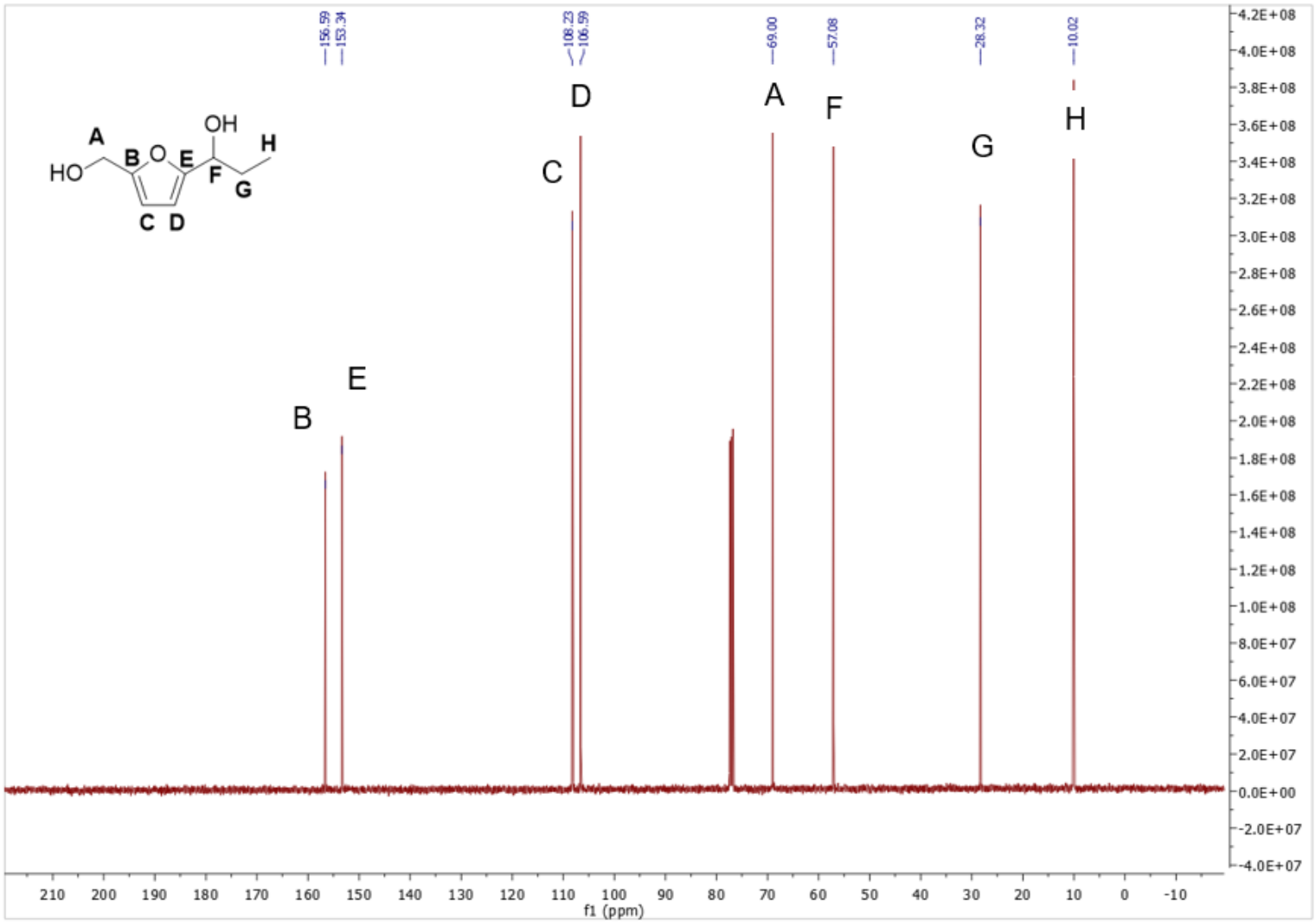

A5. ^{13}C NMR ($CDCl_3$) spectrum of Compound **1b**.

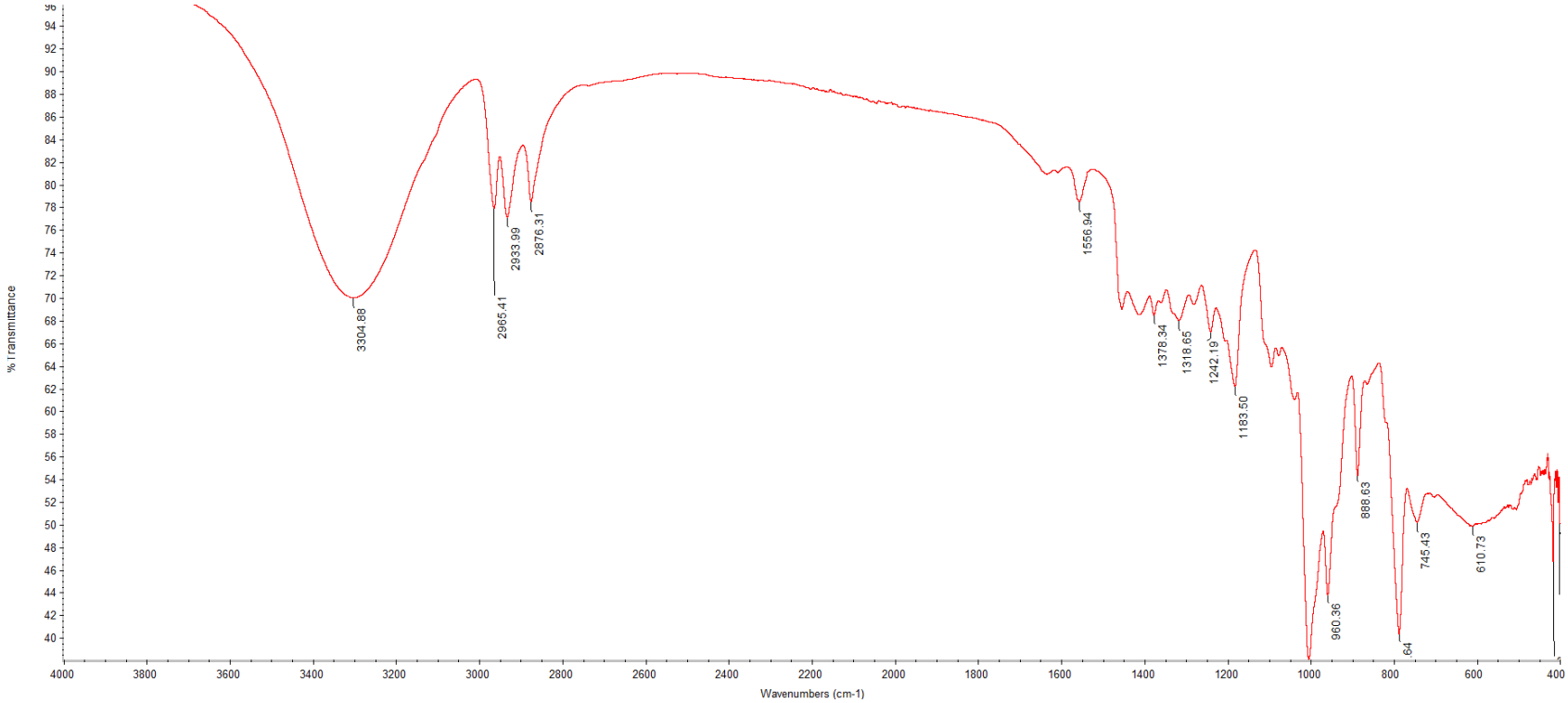

A6. FTIR spectrum of Compound **1b**.

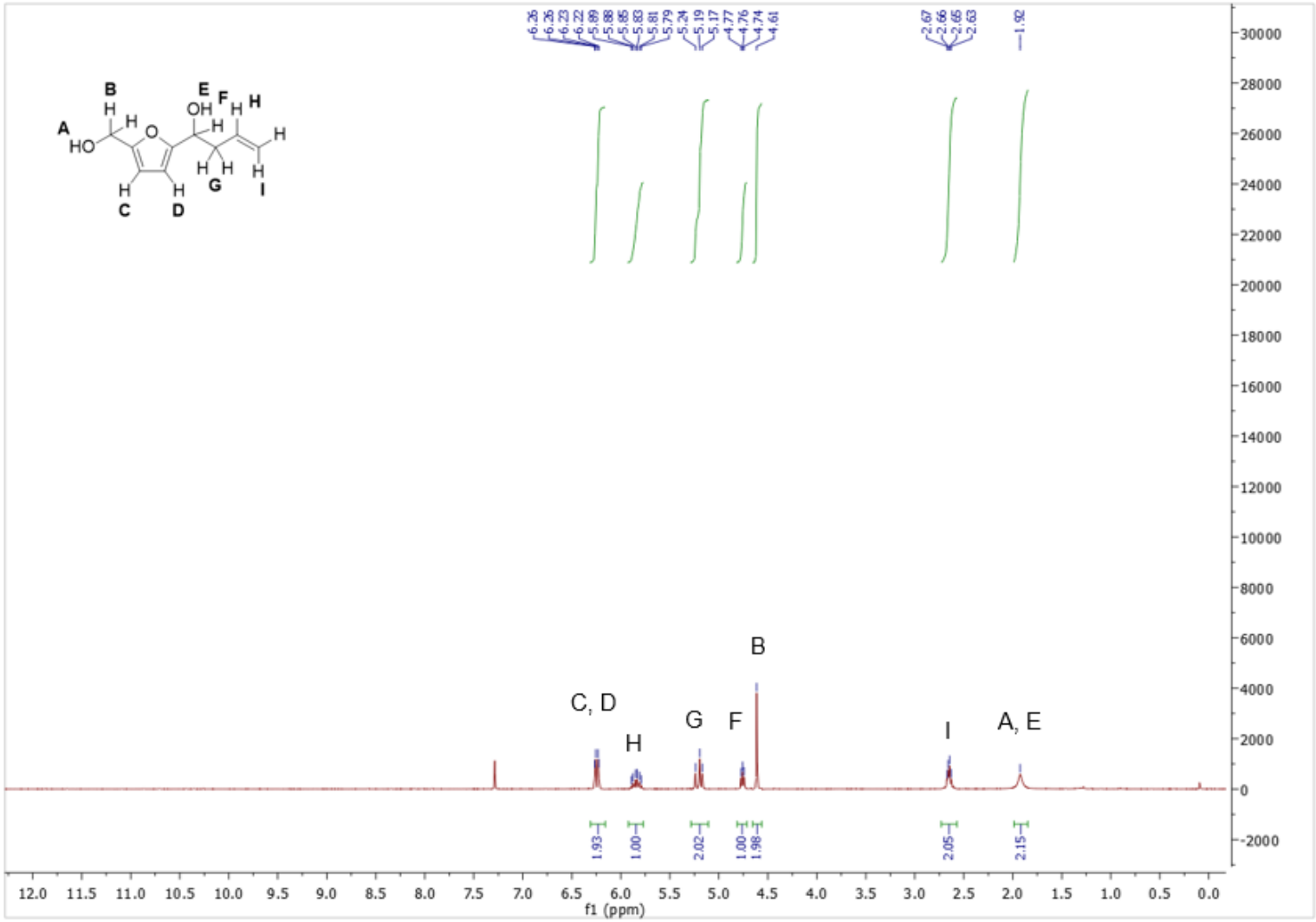

A7. ^{1}H NMR ($CDCl_3$) spectrum of Compound **1c**.

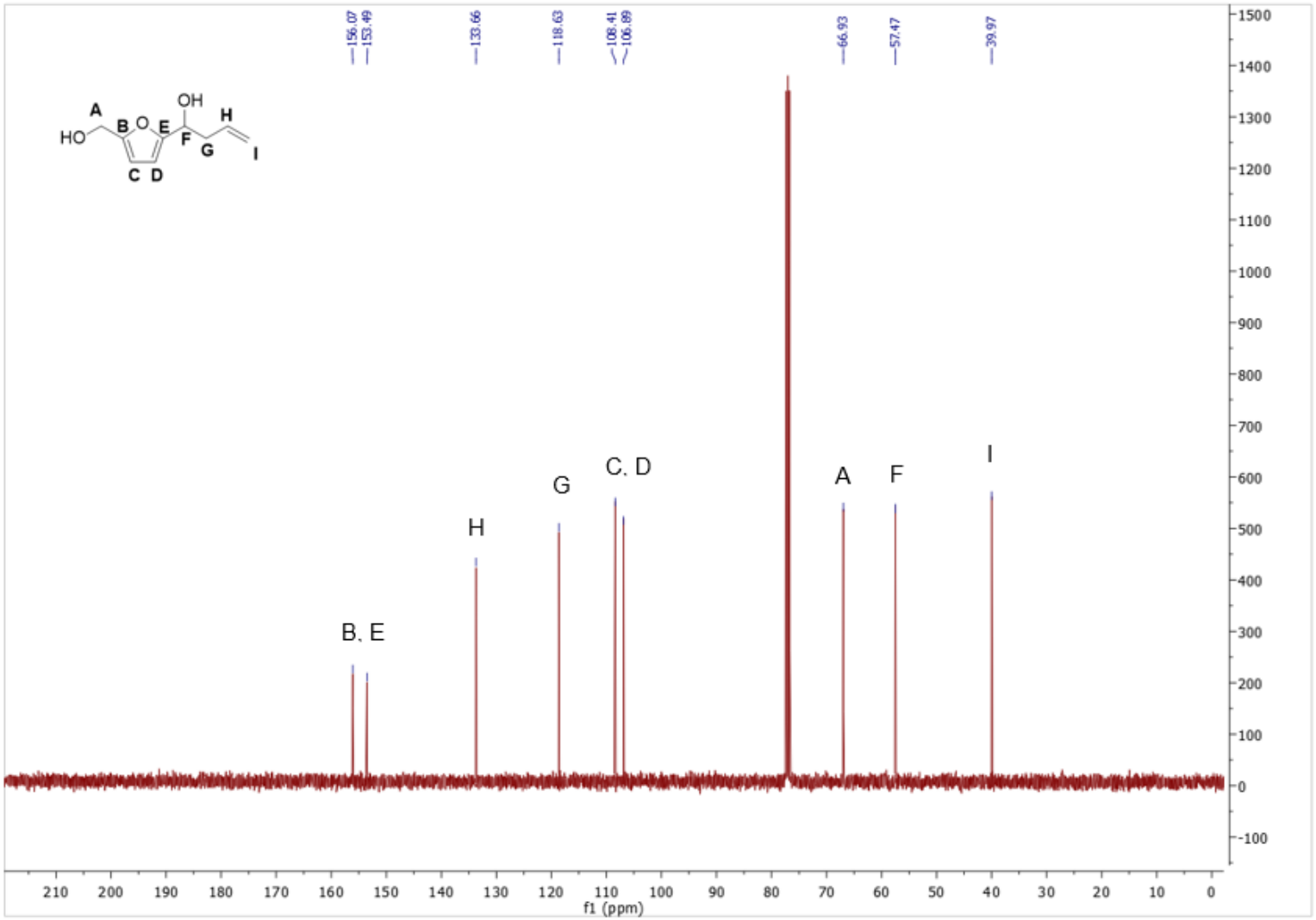

A8. ^{13}C NMR ($CDCl_3$) spectrum of Compound **1c**.

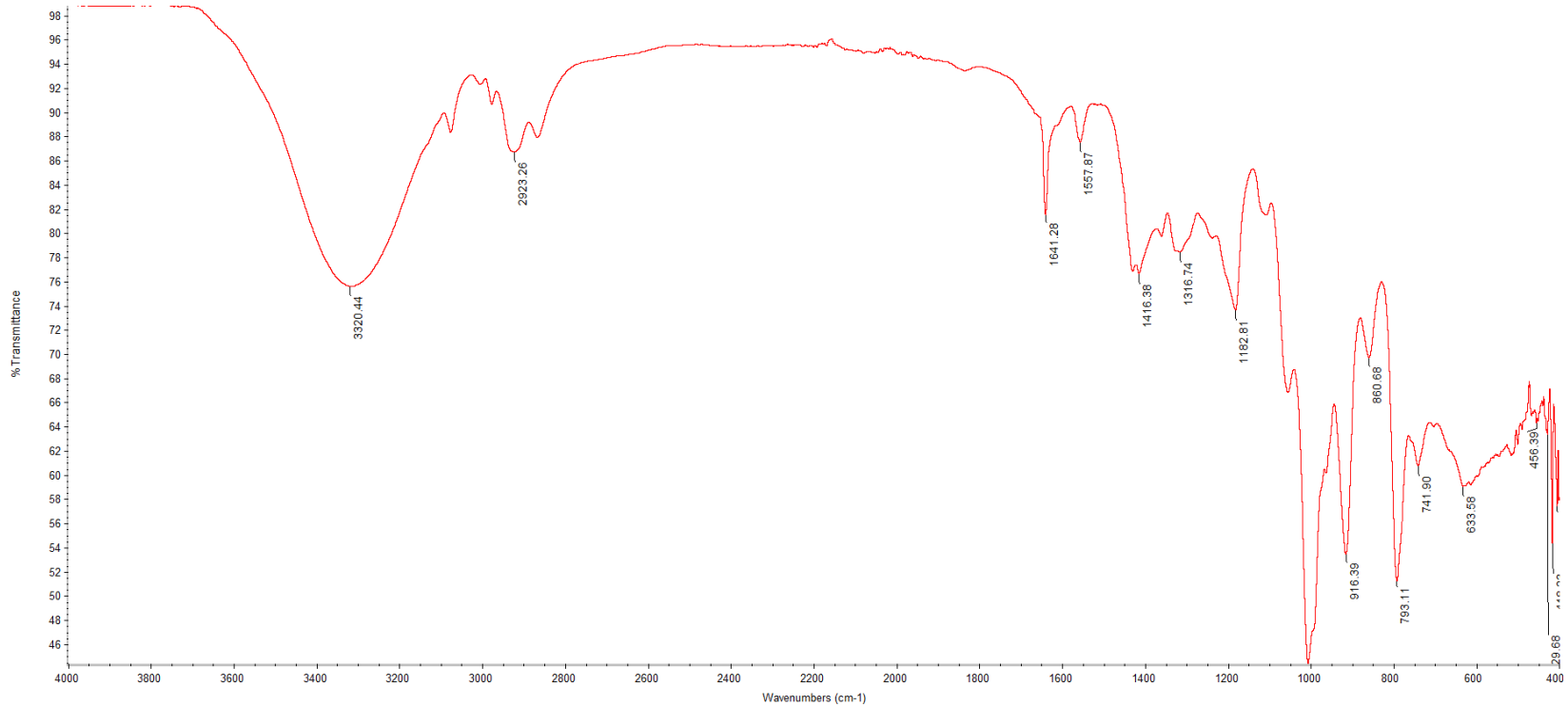

A9. FTIR spectrum of Compound **1c**.

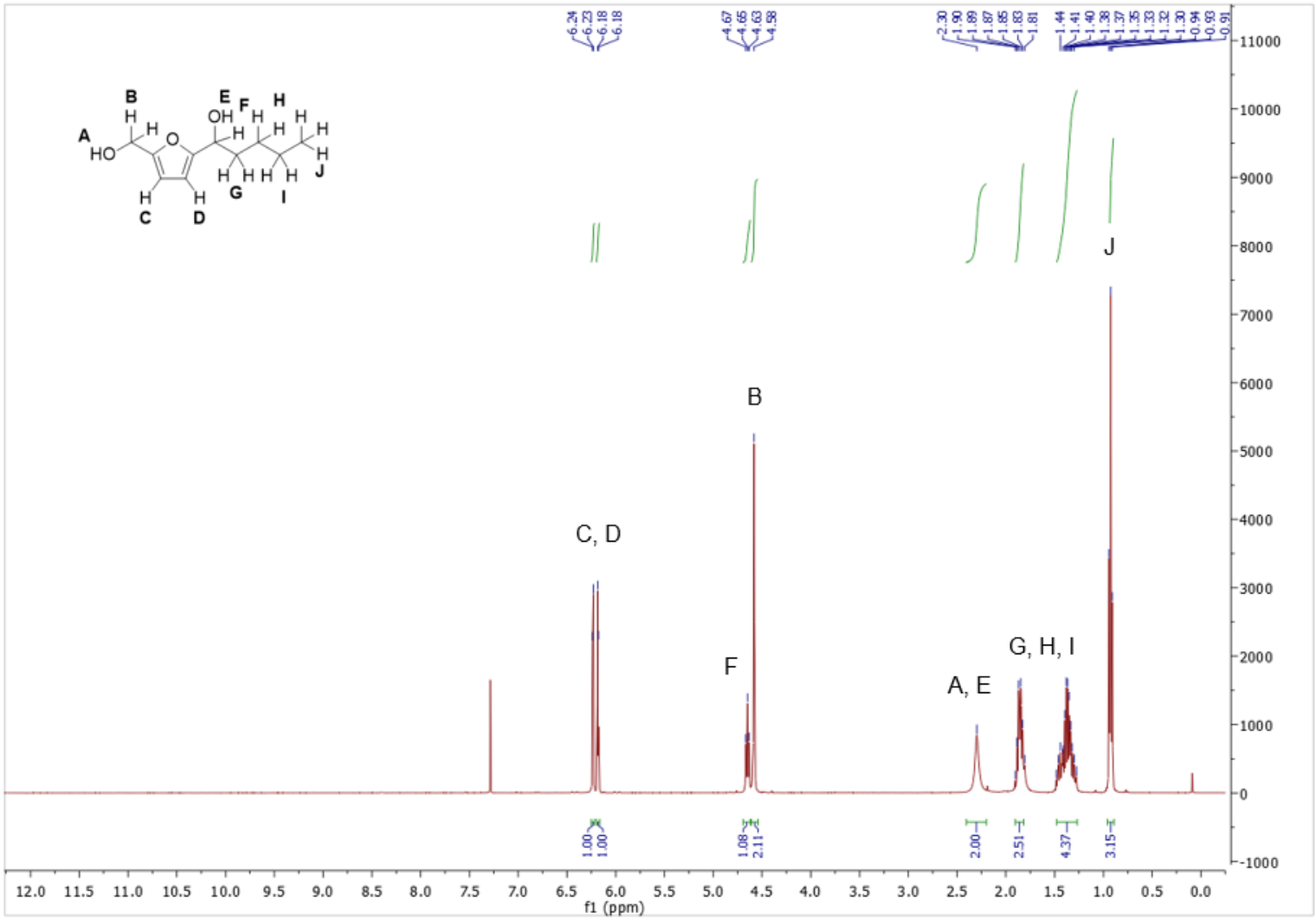

A10. ^{1}H NMR ($CDCl_3$) spectrum of Compound **1d**.

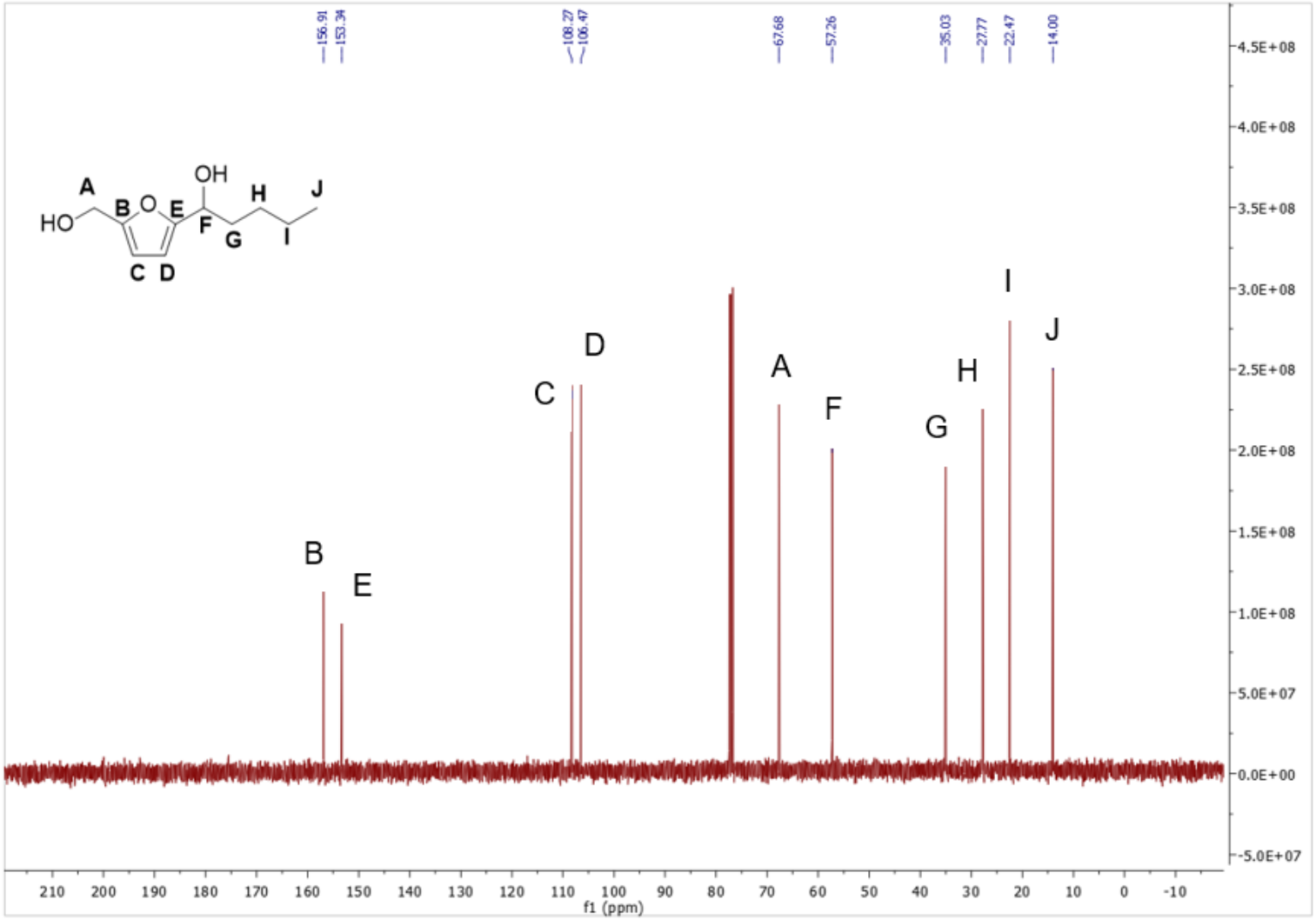

A11. ^{13}C NMR ($CDCl_3$) spectrum of Compound **1d**.

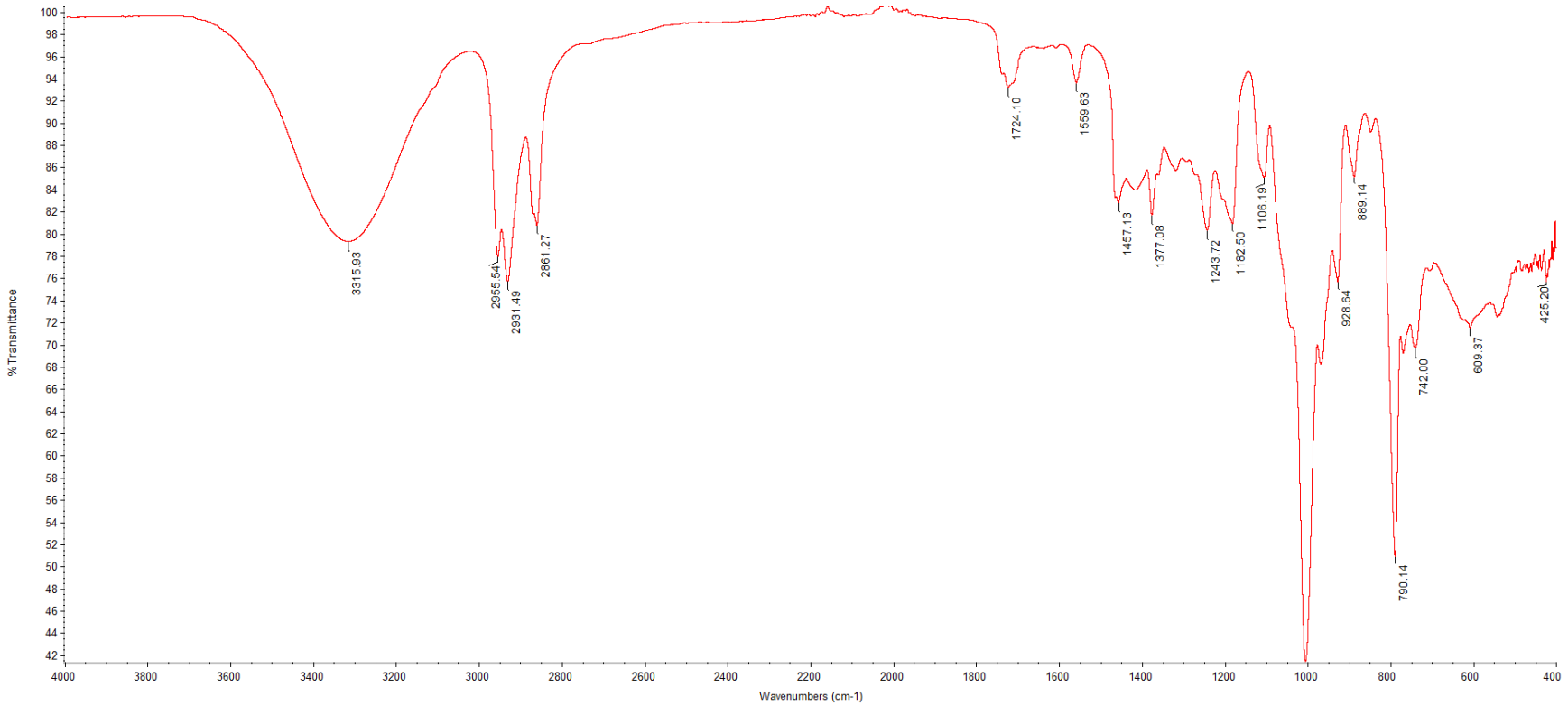

A12. FTIR spectrum of Compound **1d**.

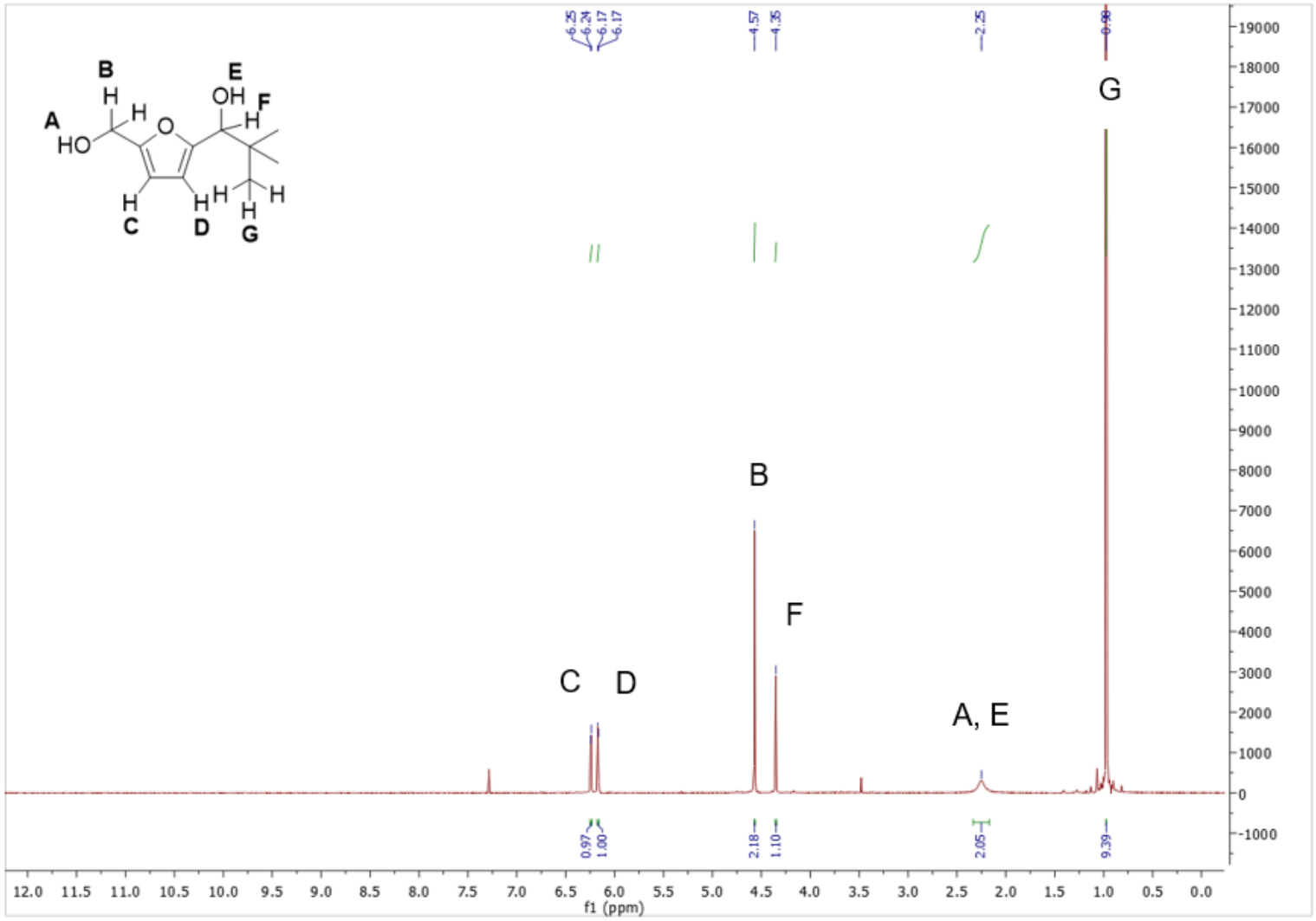

A13. ^{1}H NMR ($CDCl_3$) spectrum of Compound **1e**.

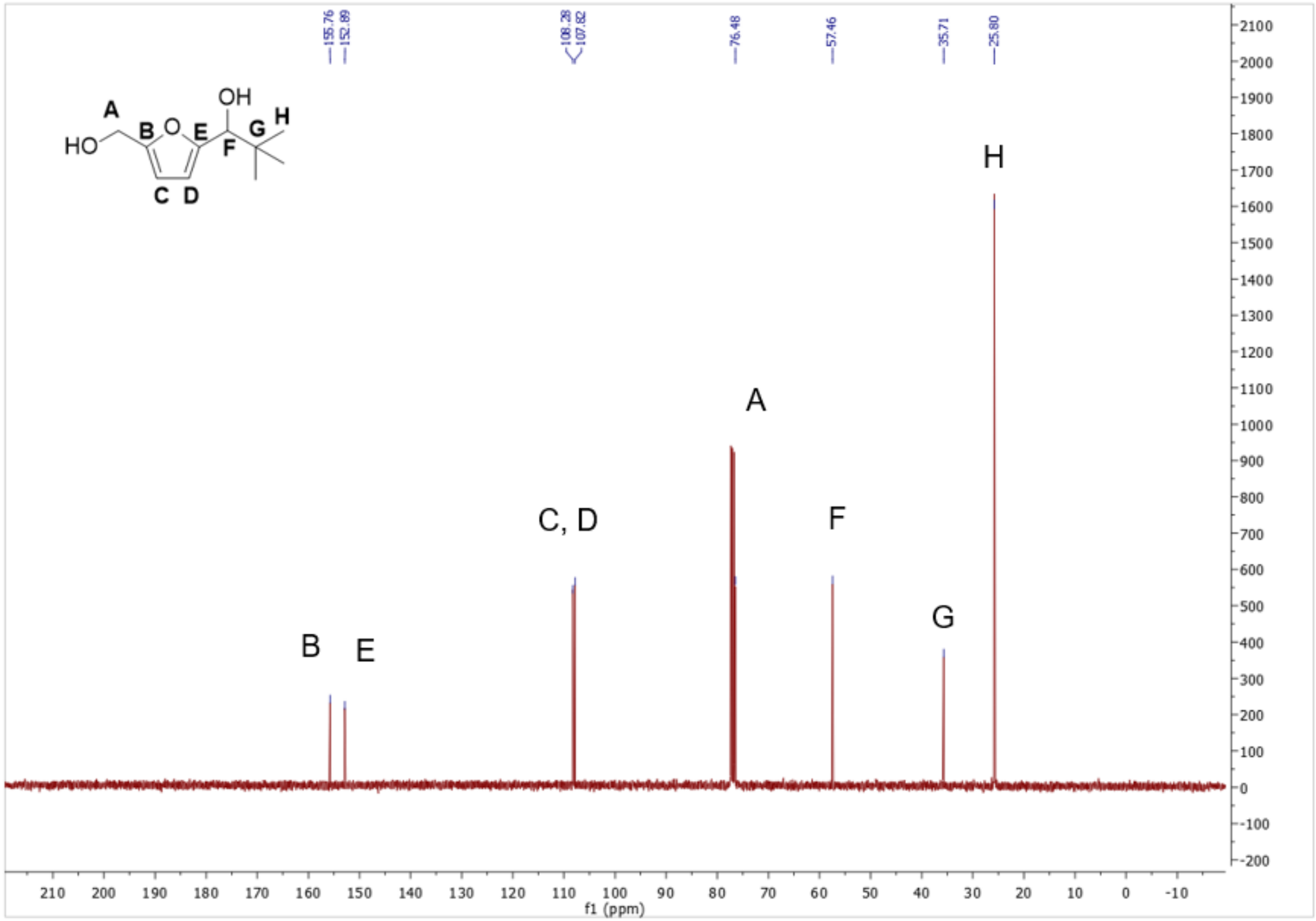

A14. ^{13}C NMR ($CDCl_3$) spectrum of Compound **1e**.

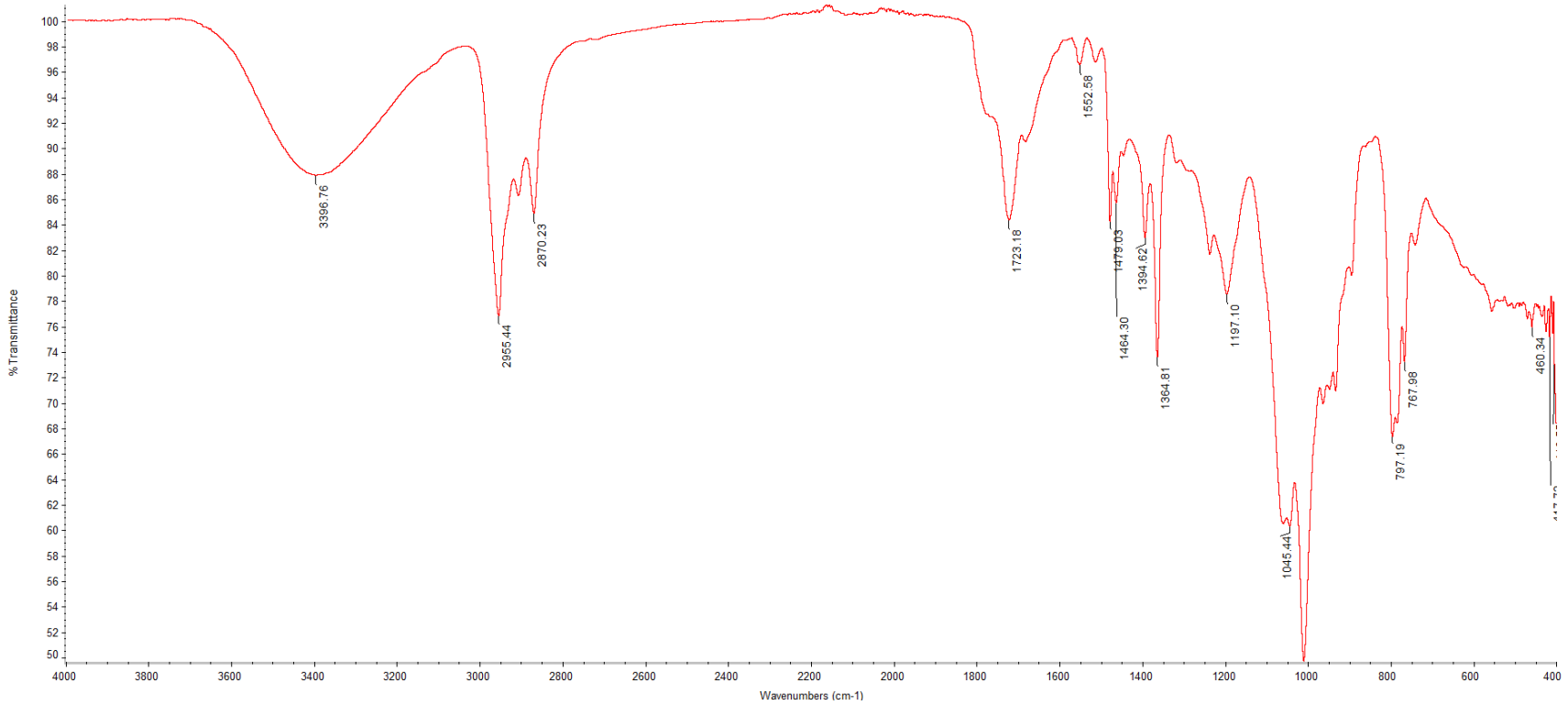

A15. ^{1}H NMR ($CDCl_3$) spectrum of Compound **1e**.

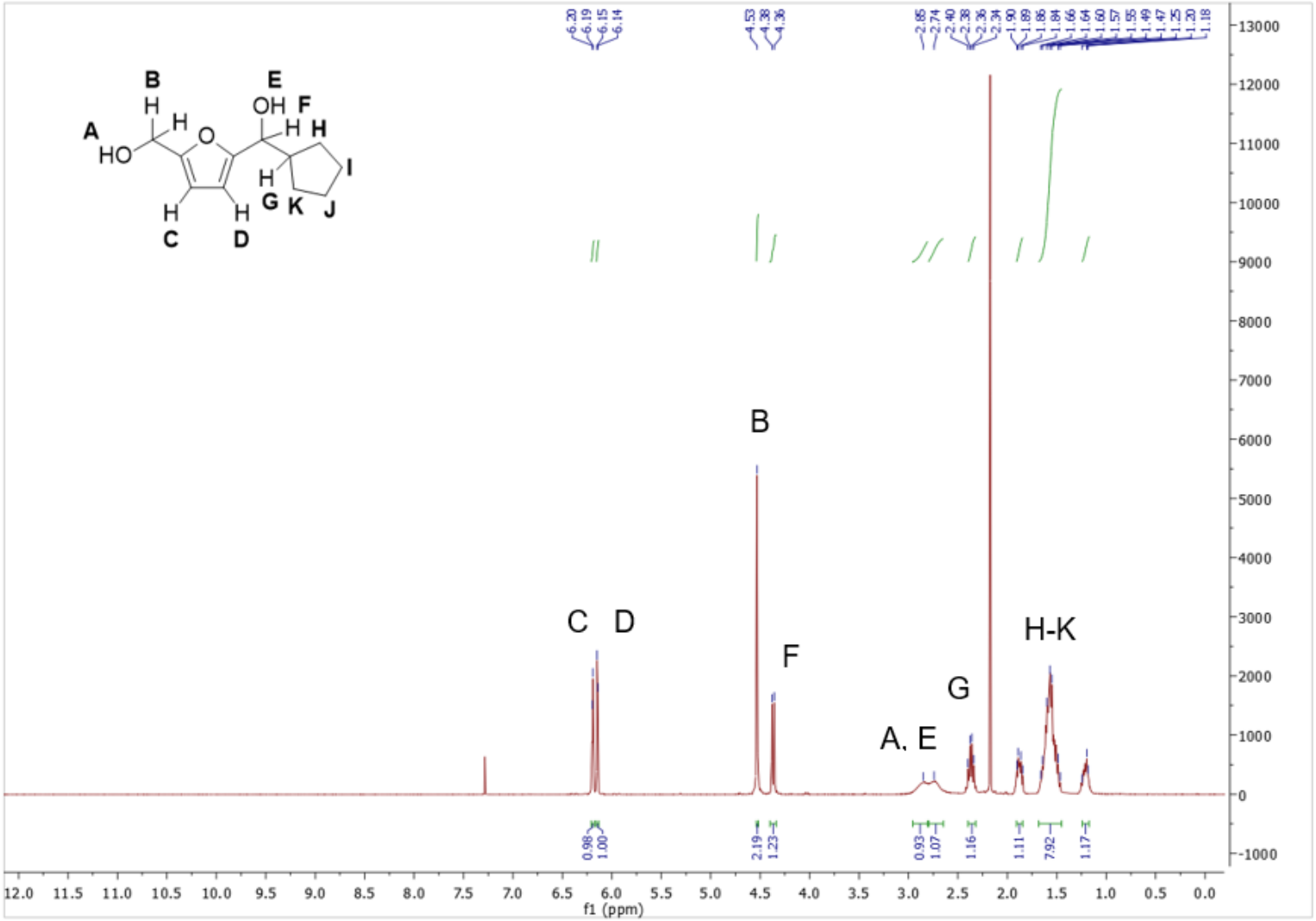

A16. ^{1}H NMR ($CDCl_3$) spectrum of Compound **1f**.

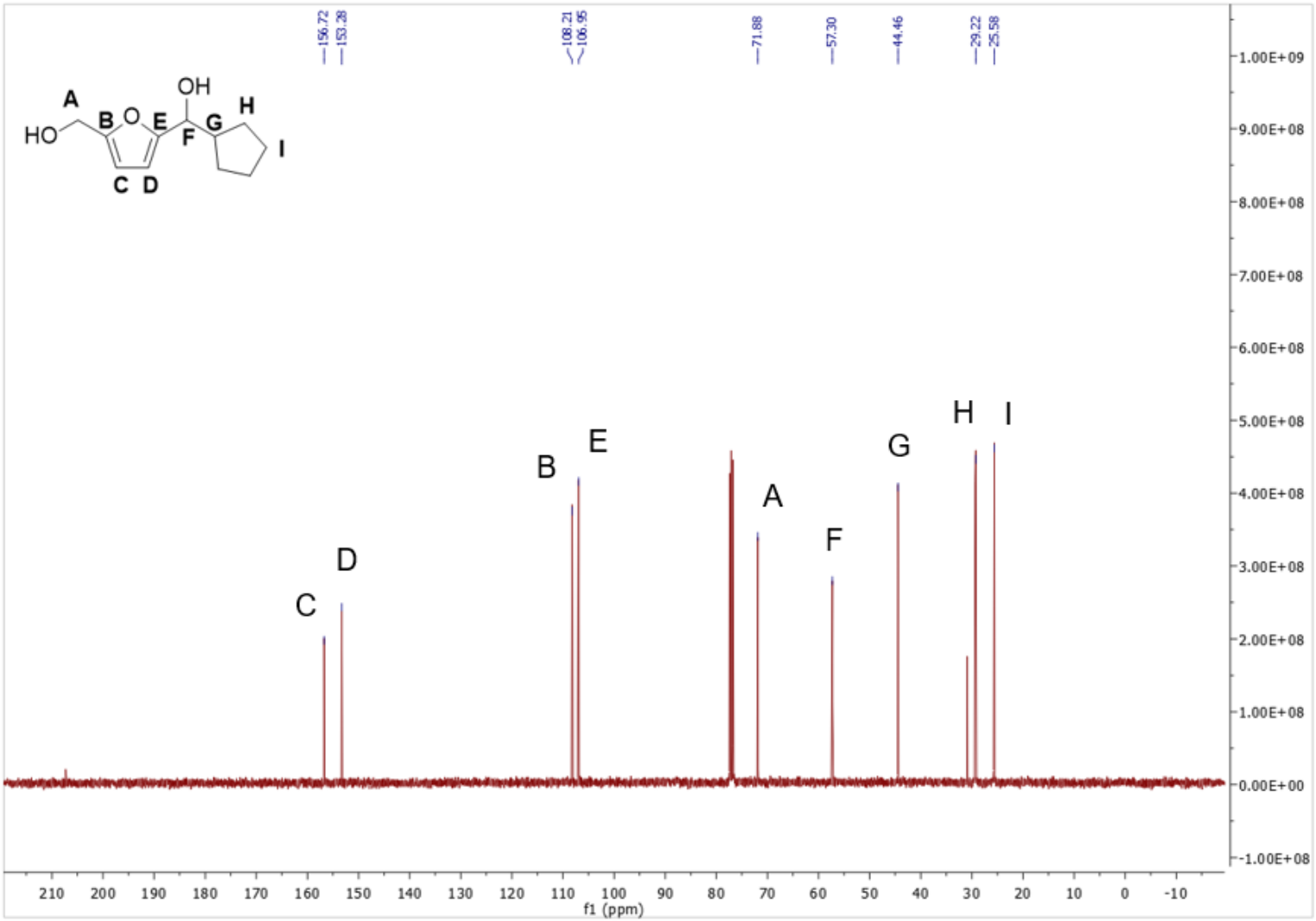

A17. ^{13}C NMR ($CDCl_3$) spectrum of Compound **1f**.

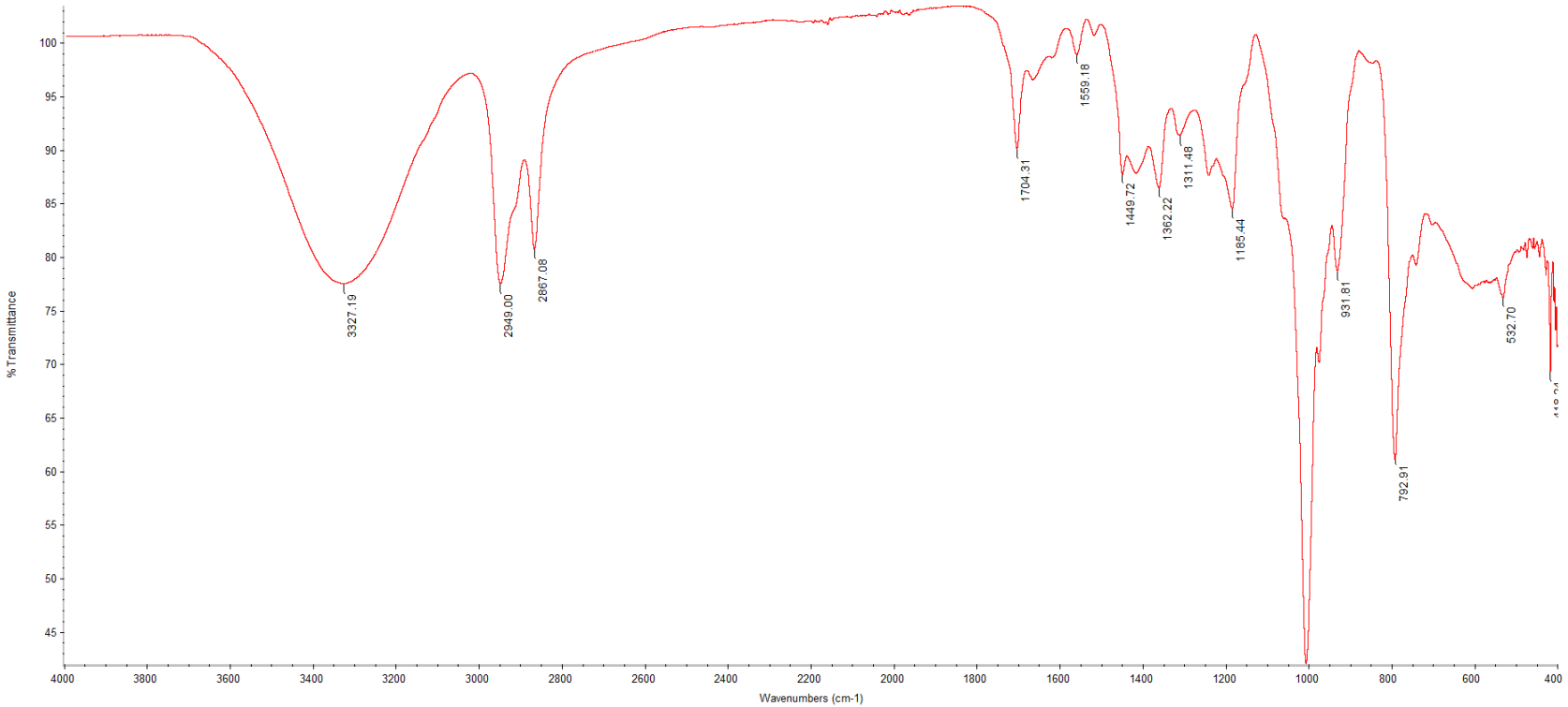

A18. FTIR spectrum of Compound **1f**.

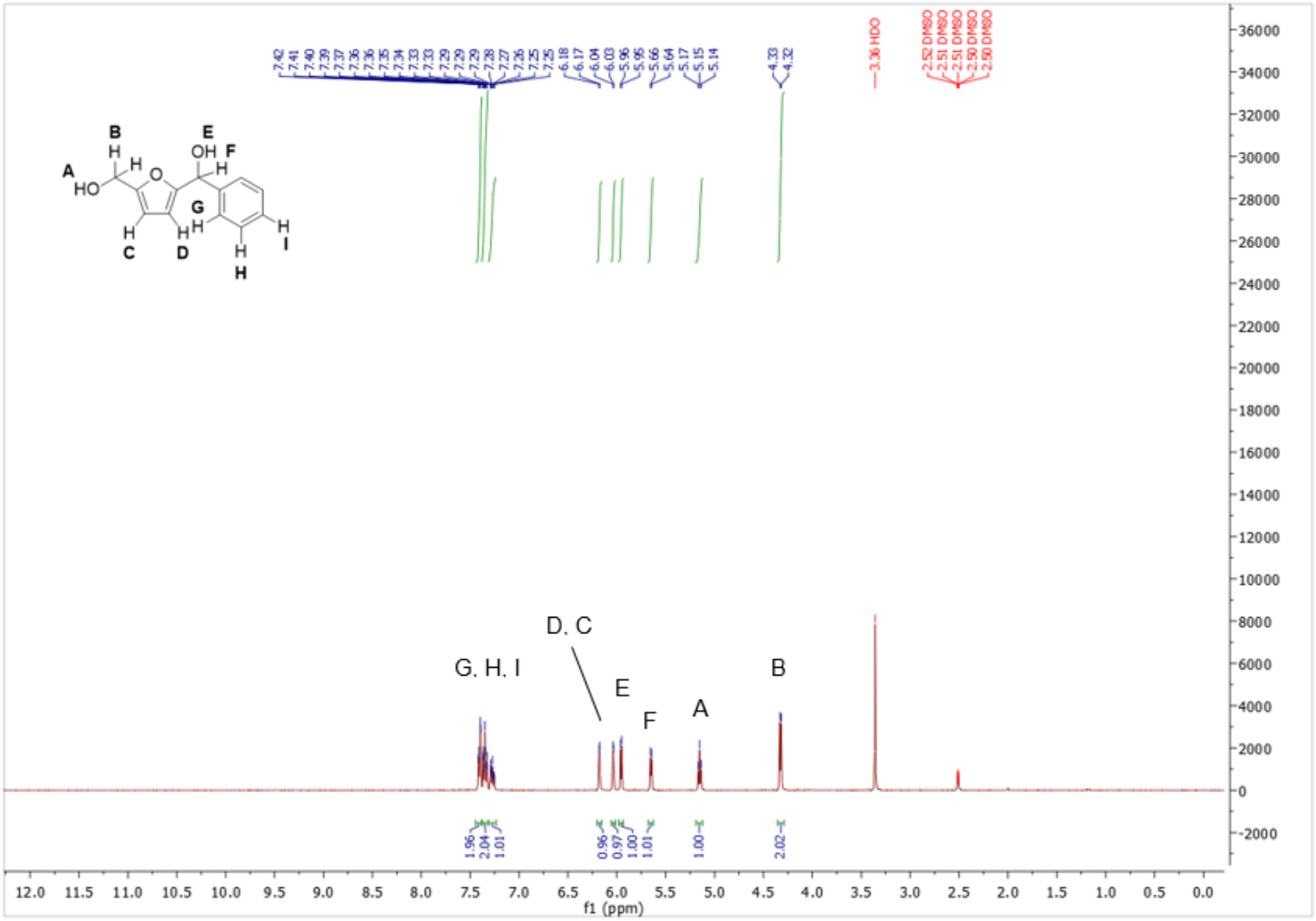

A19. 1H NMR (DMSO- d6) spectrum of Compound **1g**.

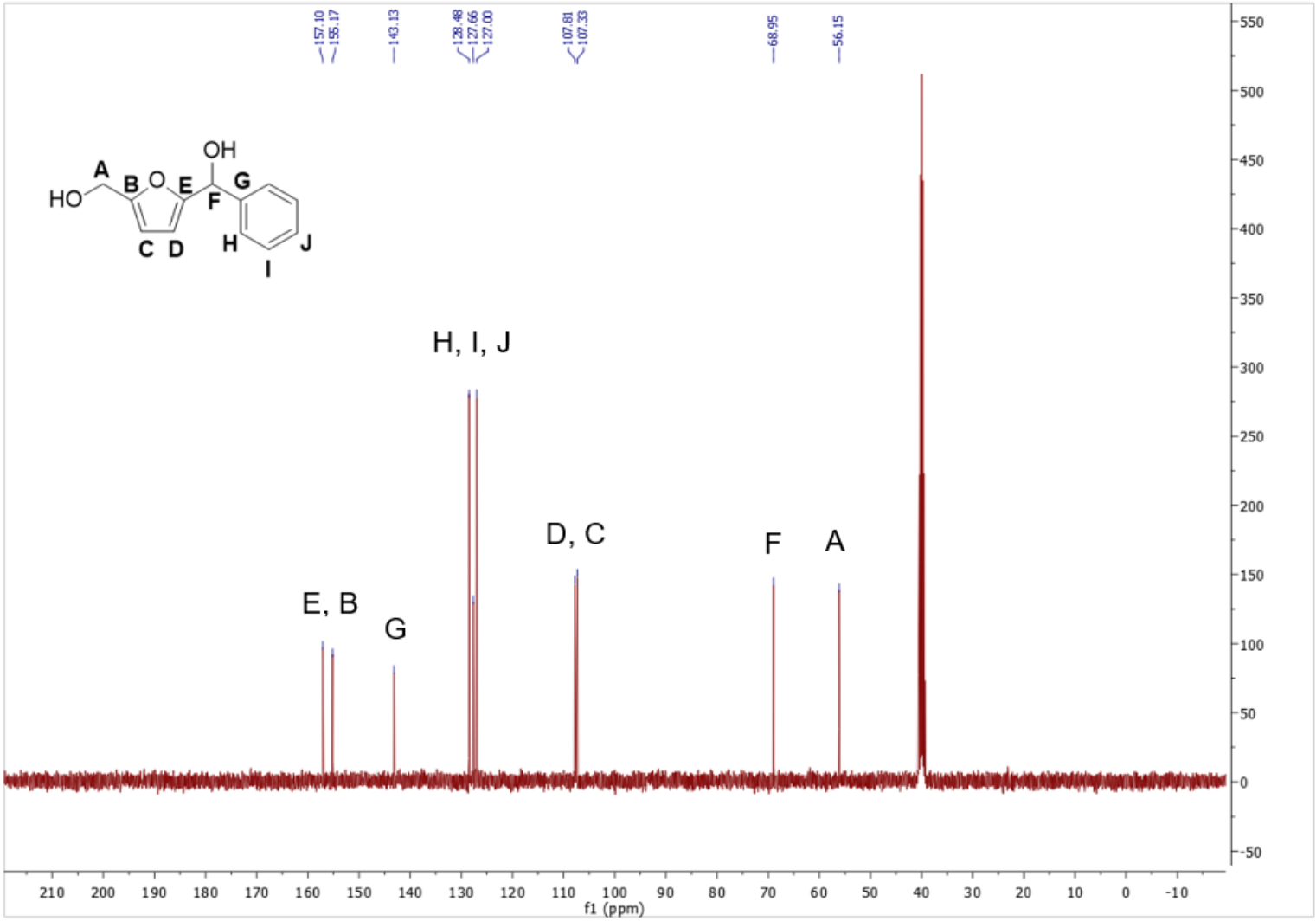

A20. ^{13}C NMR (DMSO-d_6) spectrum of Compound **1g**.

A21. FTIR spectrum of Compound **1g**.

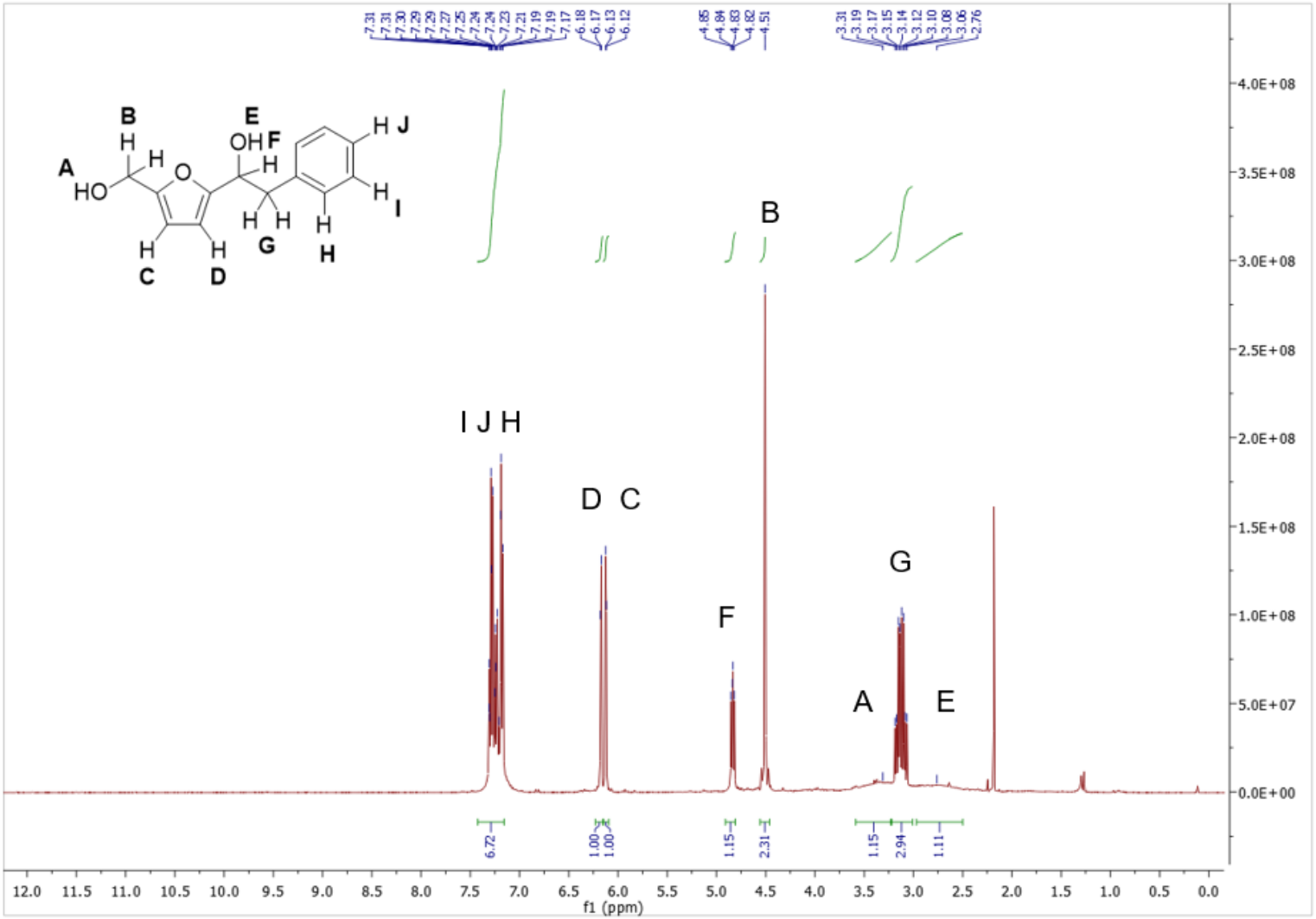

A22. ^{1}H NMR ($CDCl_3$) spectrum of Compound **1h**.

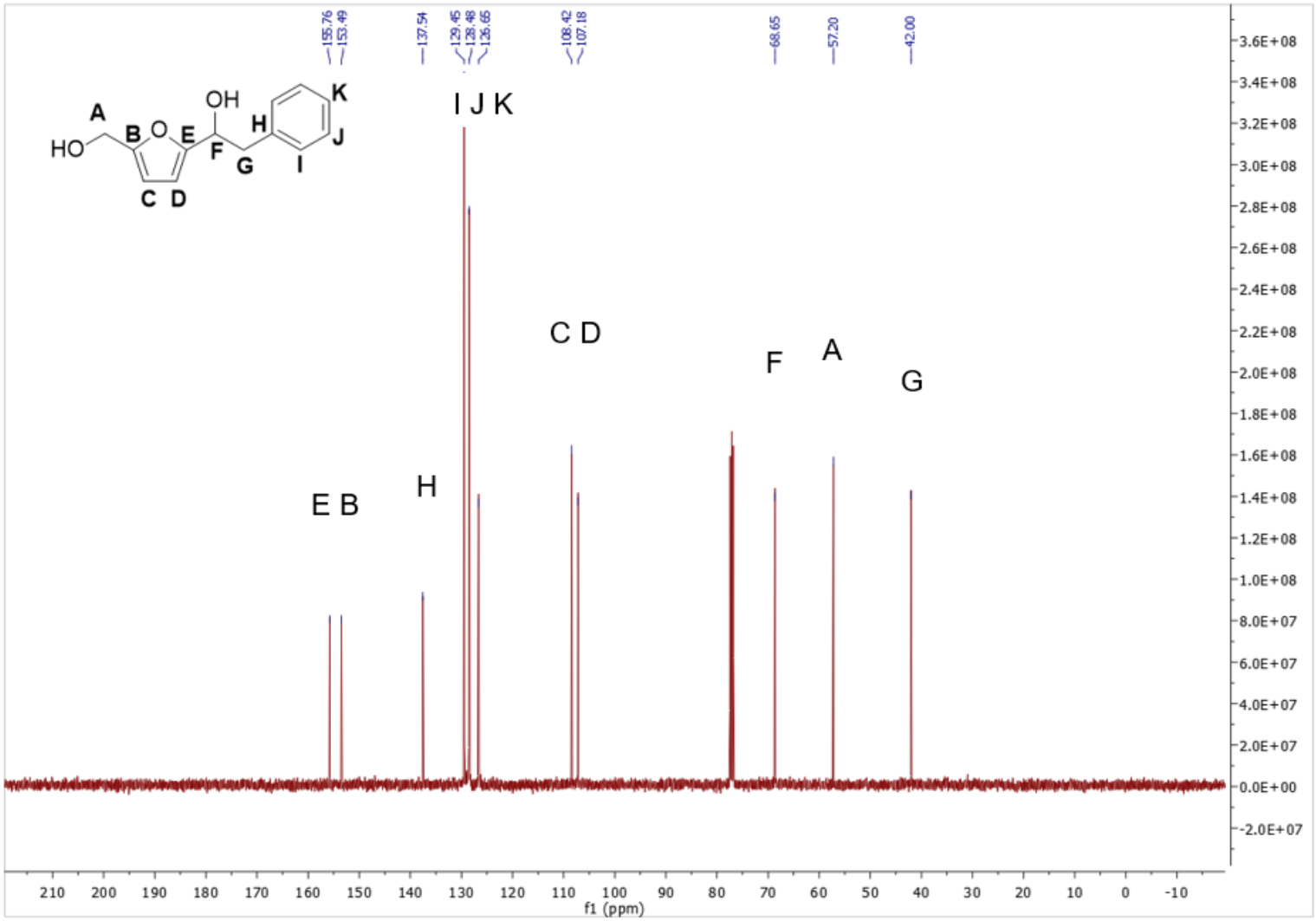

A23. ^{13}C NMR ($CDCl_3$) spectrum of Compound **1h**.

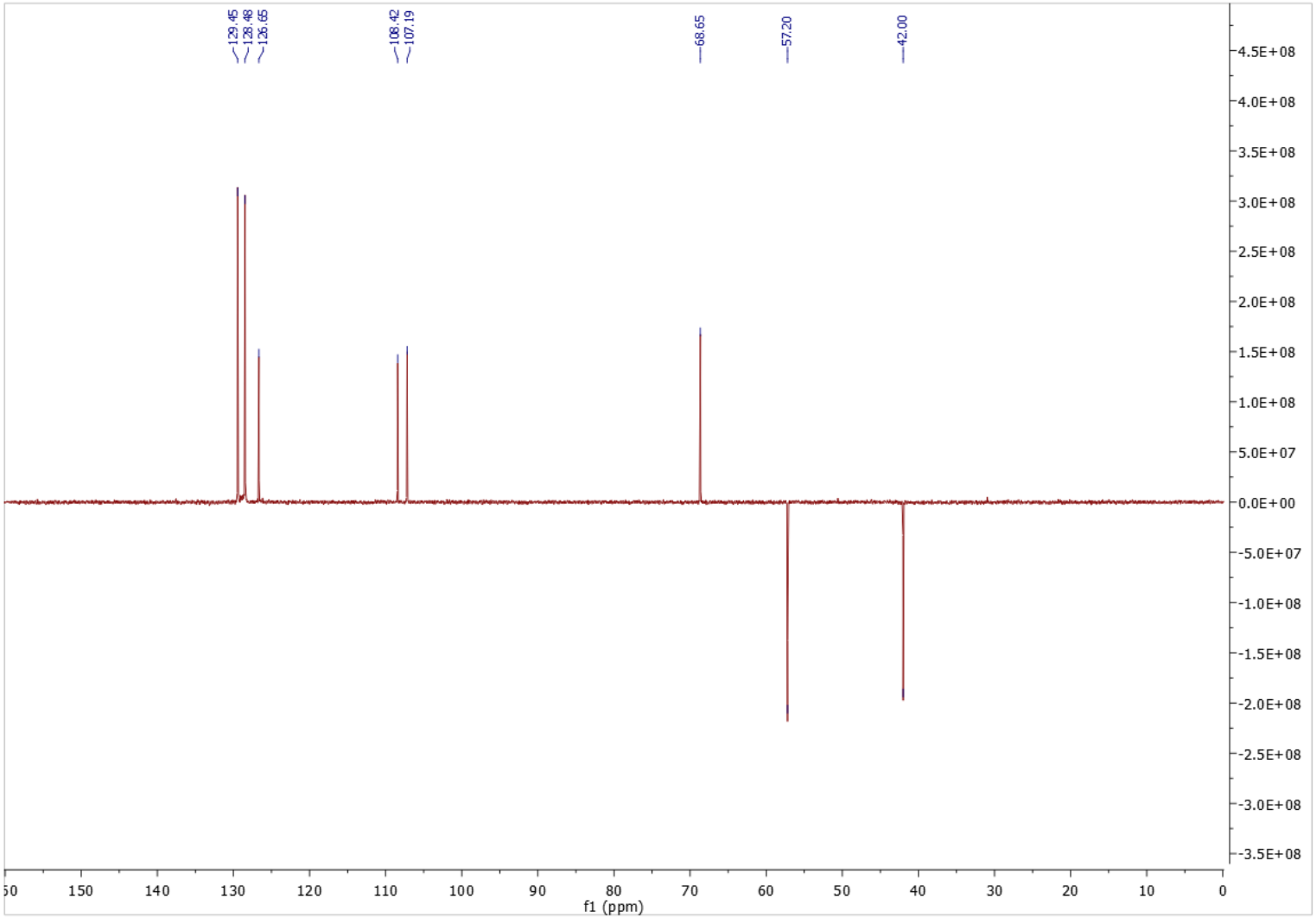

A24. ^{13}C-DEPT-135 NMR ($CDCl_3$) spectrum of Compound **1h**.

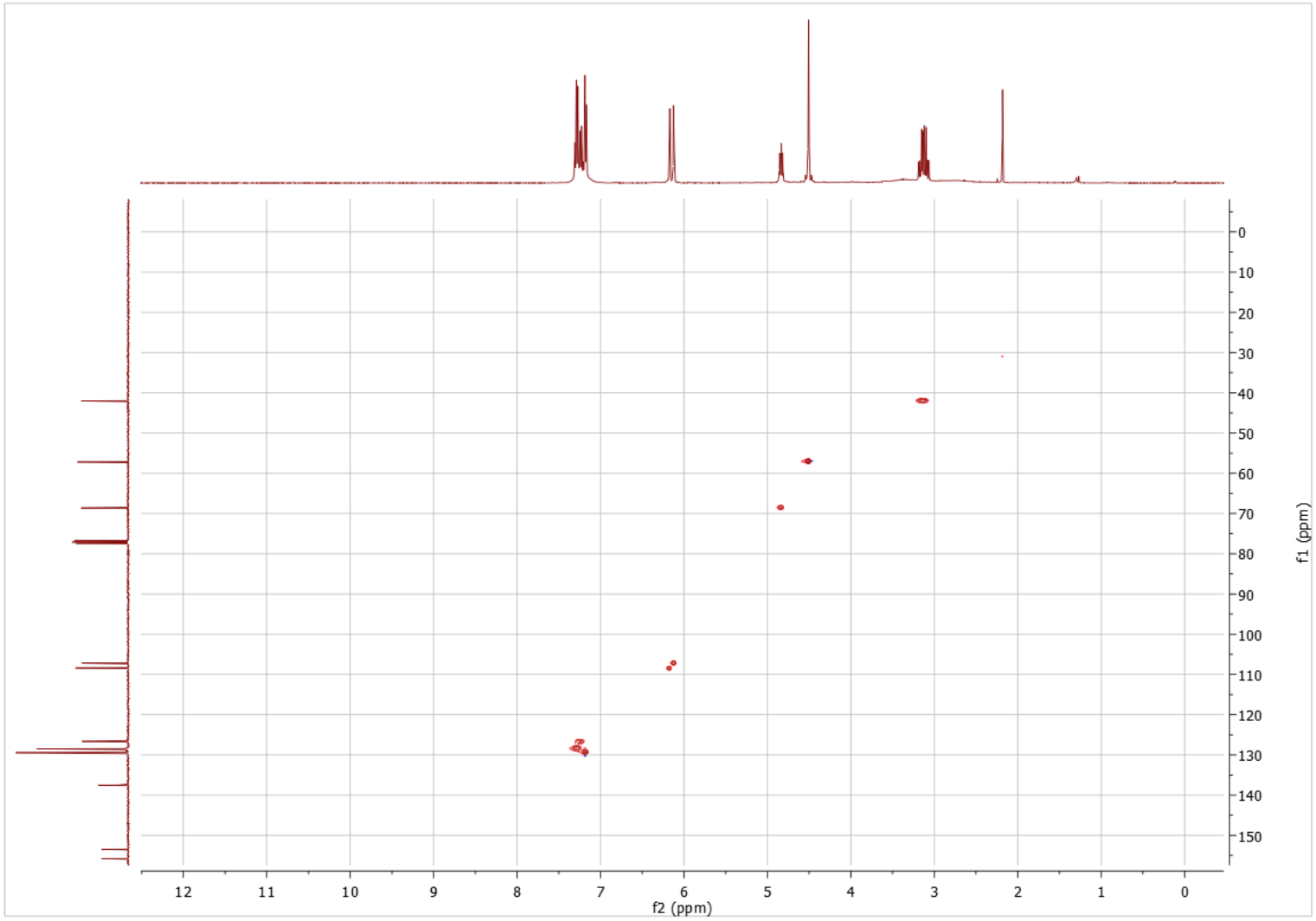

A25. ^{1}H-^{13}C- HSQC ($CDCl_3$) spectrum of Compound **1h**.

A26. FTIR spectrum of Compound **1h**.

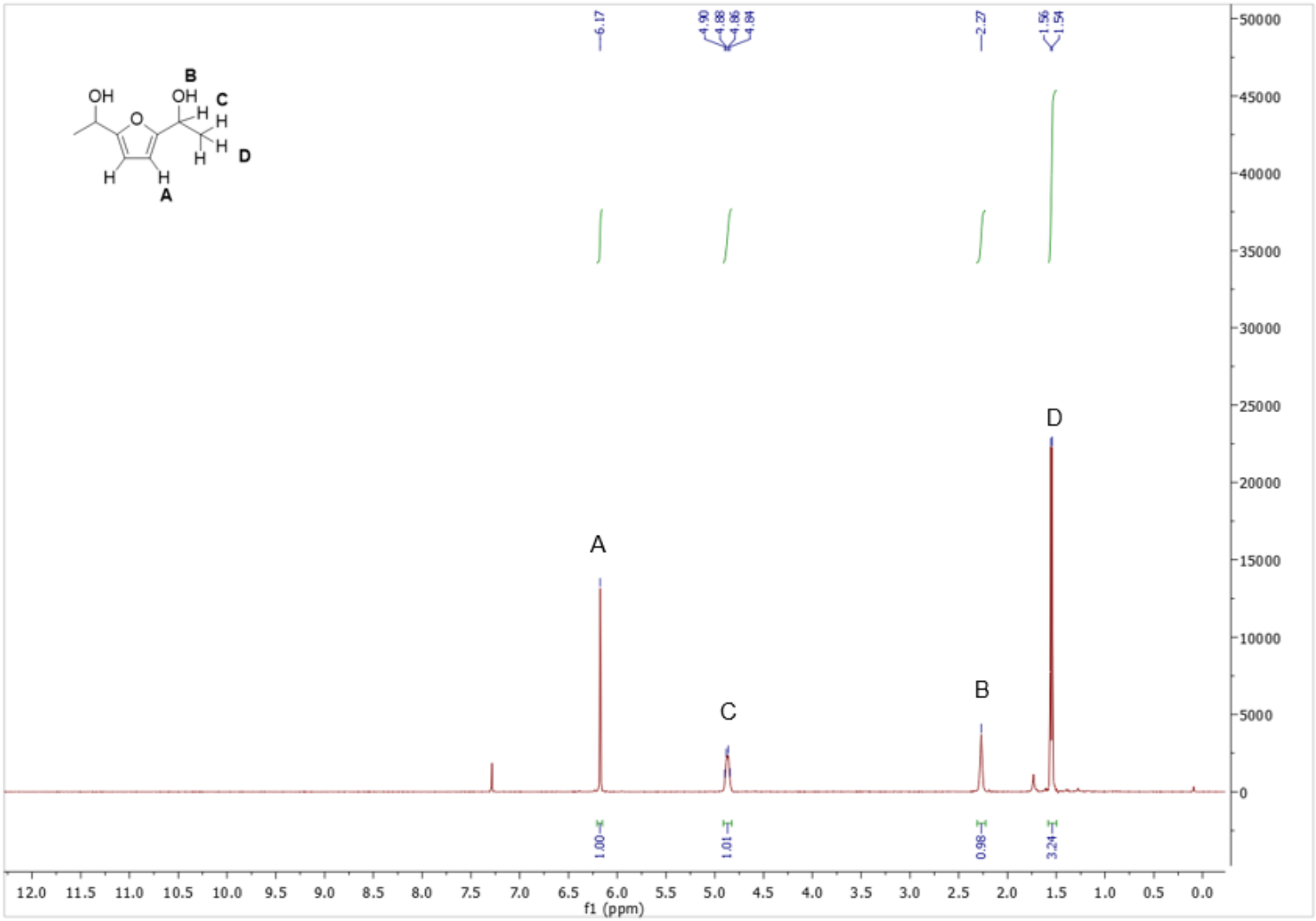

A27. ^{1}H NMR ($CDCl_3$) spectrum of Compound **2a**.

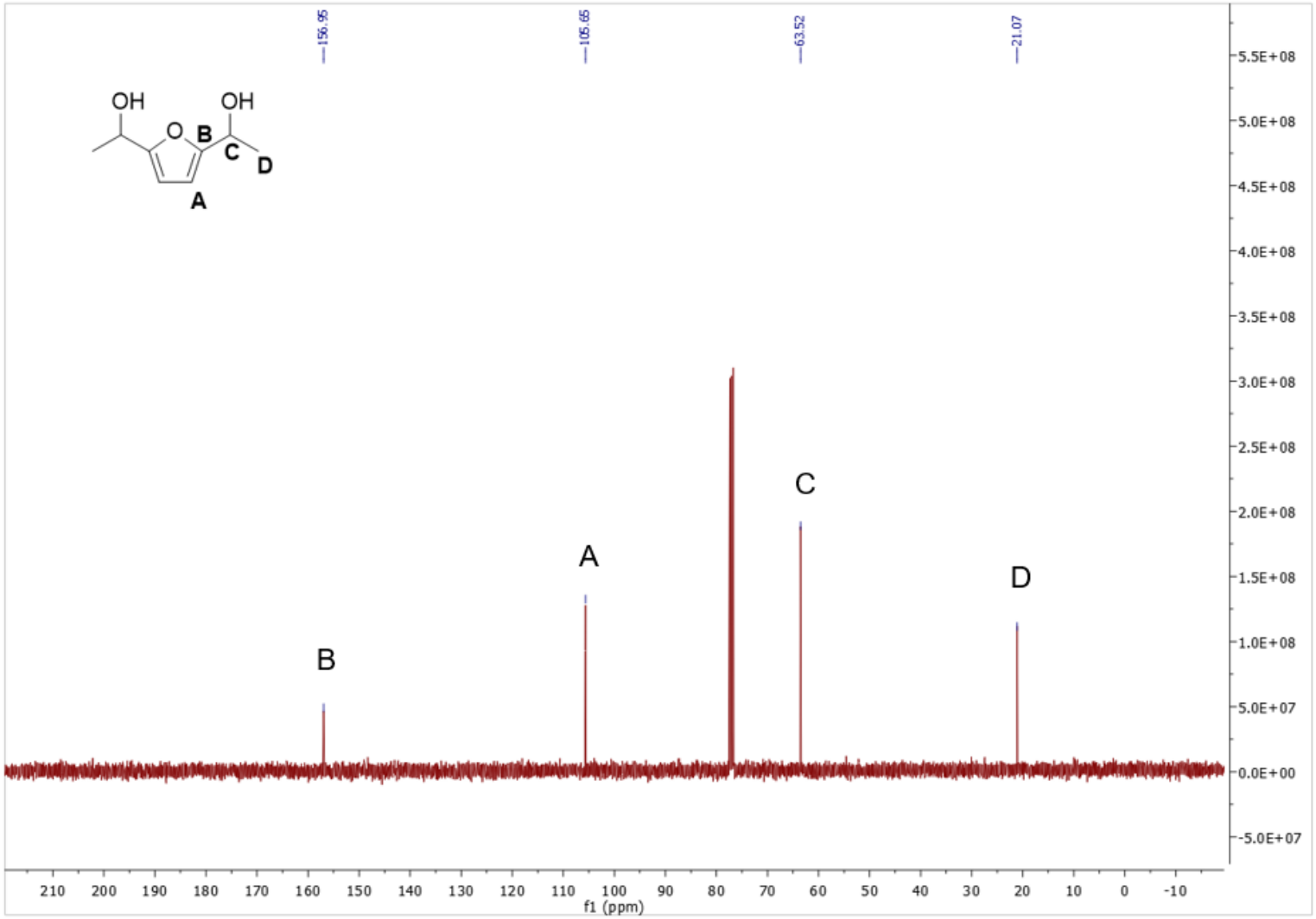

A28. ^{13}C NMR ($CDCl_3$) spectrum of Compound **2a**.

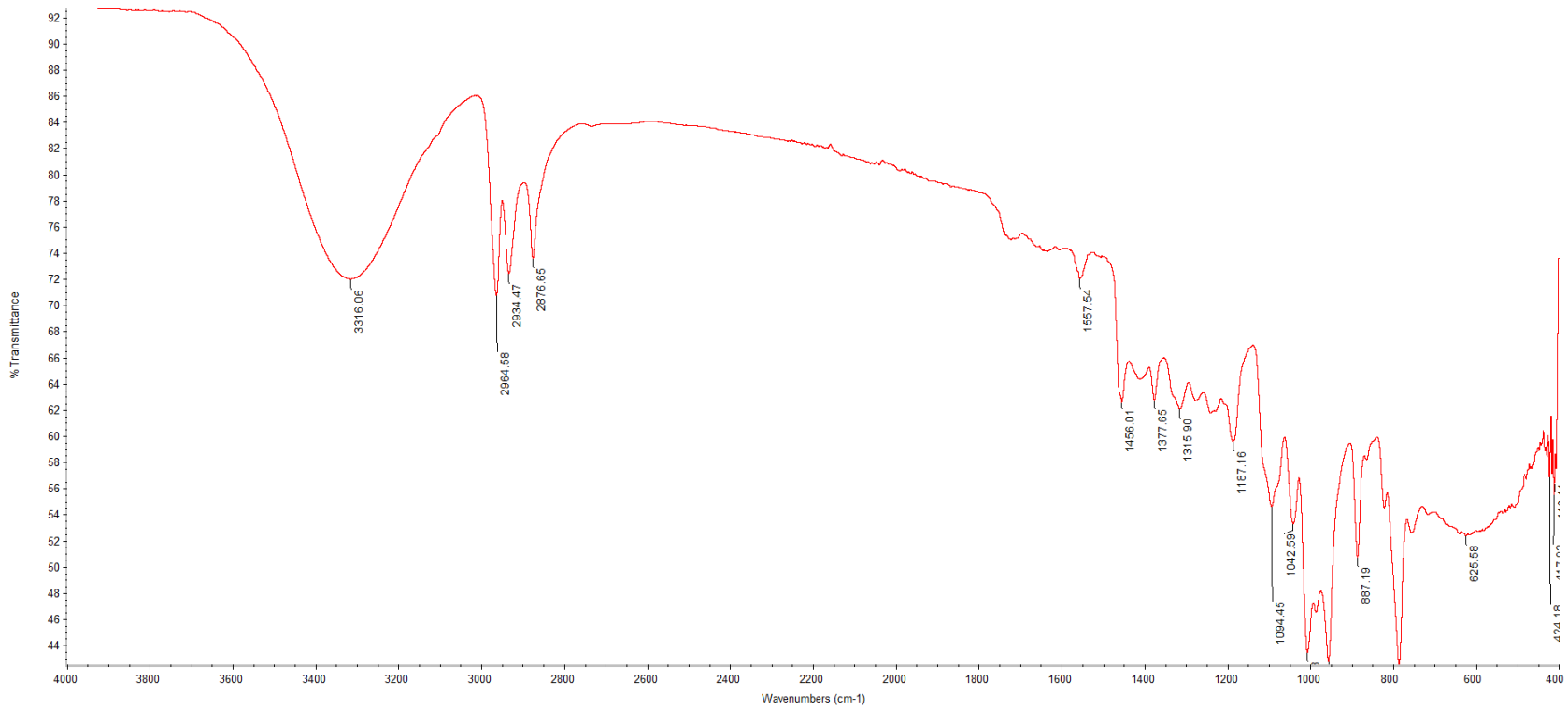

A29. FTIR spectrum of Compound **2a**.

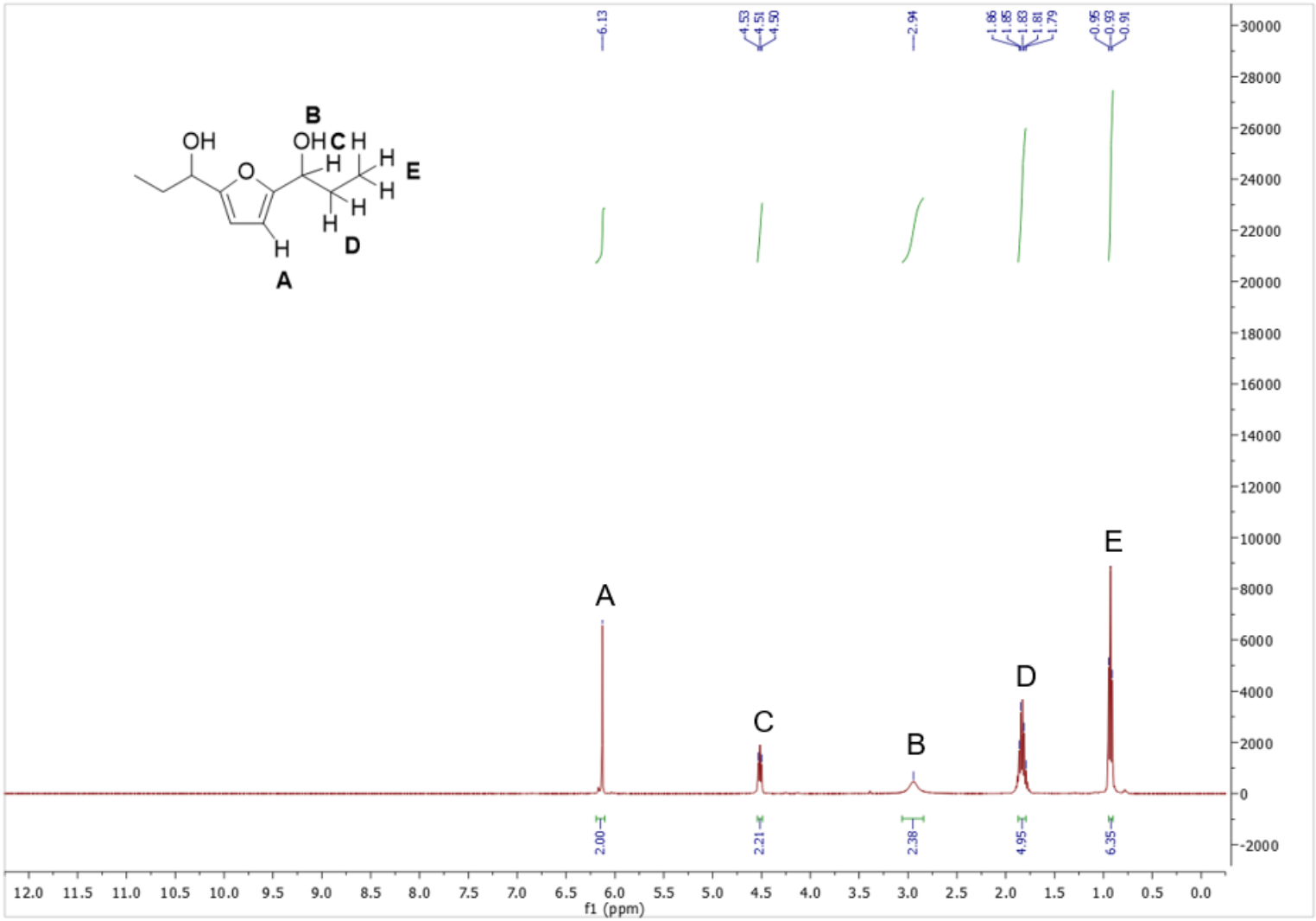

A30. ^{1}H NMR ($CDCl_3$) spectrum of Compound **2b**.

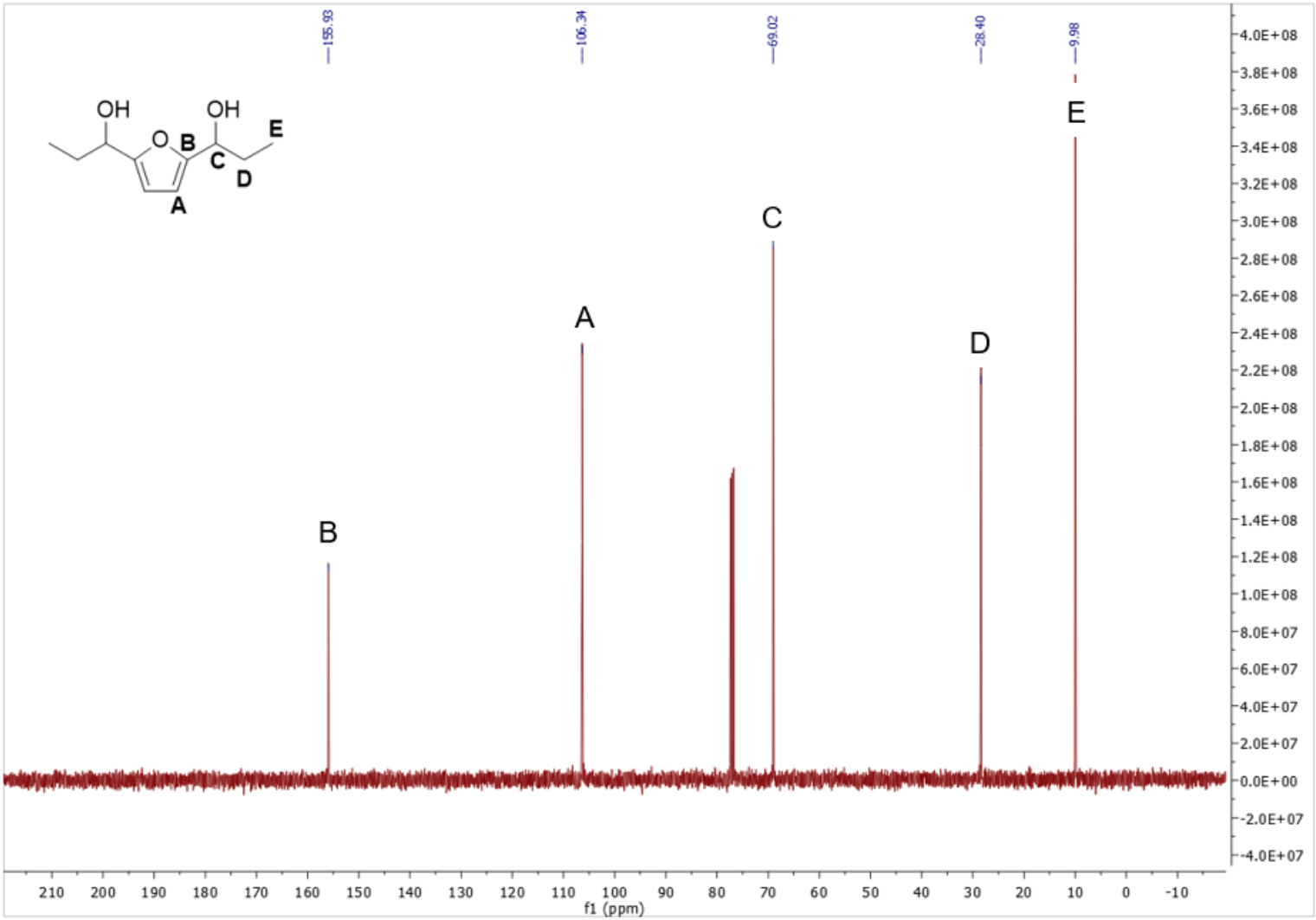

A31. ^{13}C NMR ($CDCl_3$) spectrum of Compound **2b**.

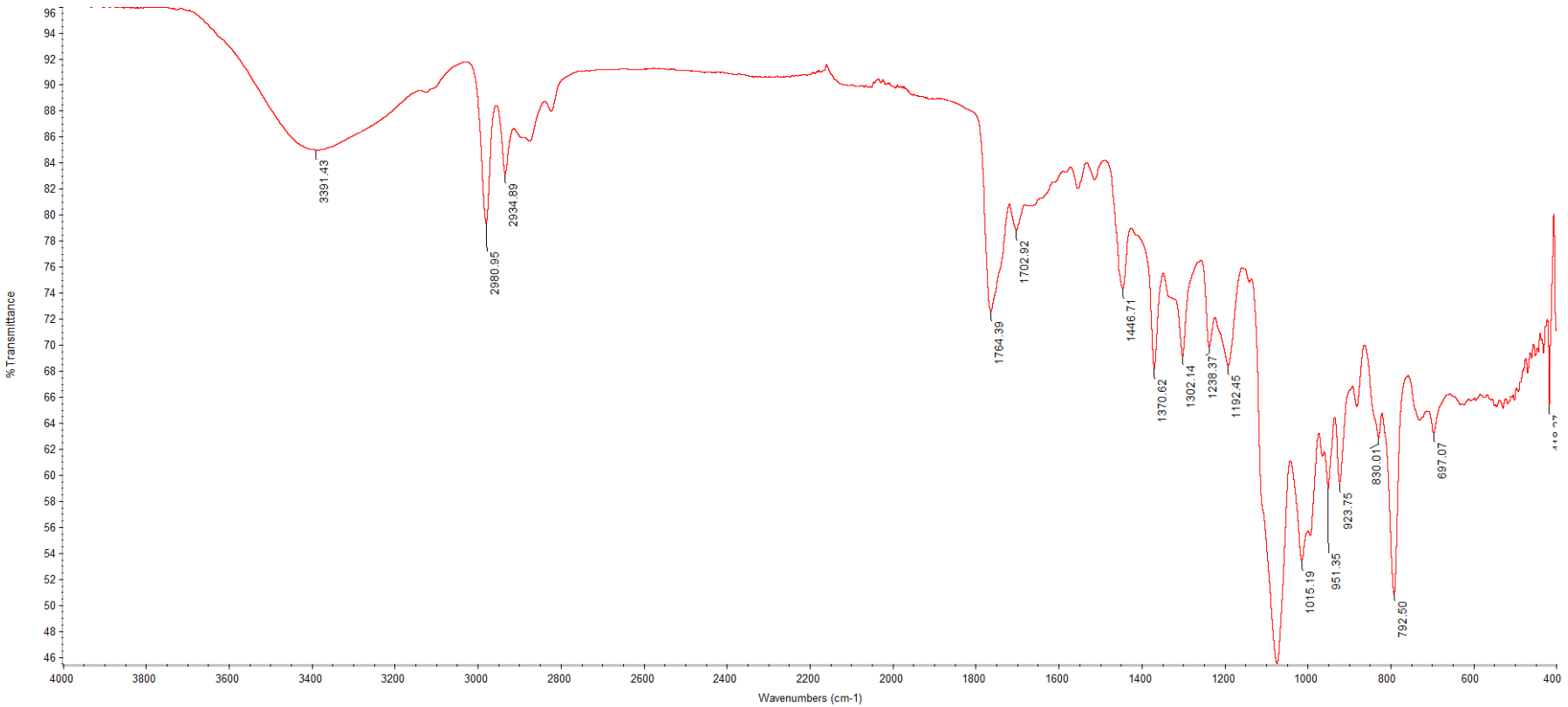

A32. FTIR spectrum of Compound **2b**.

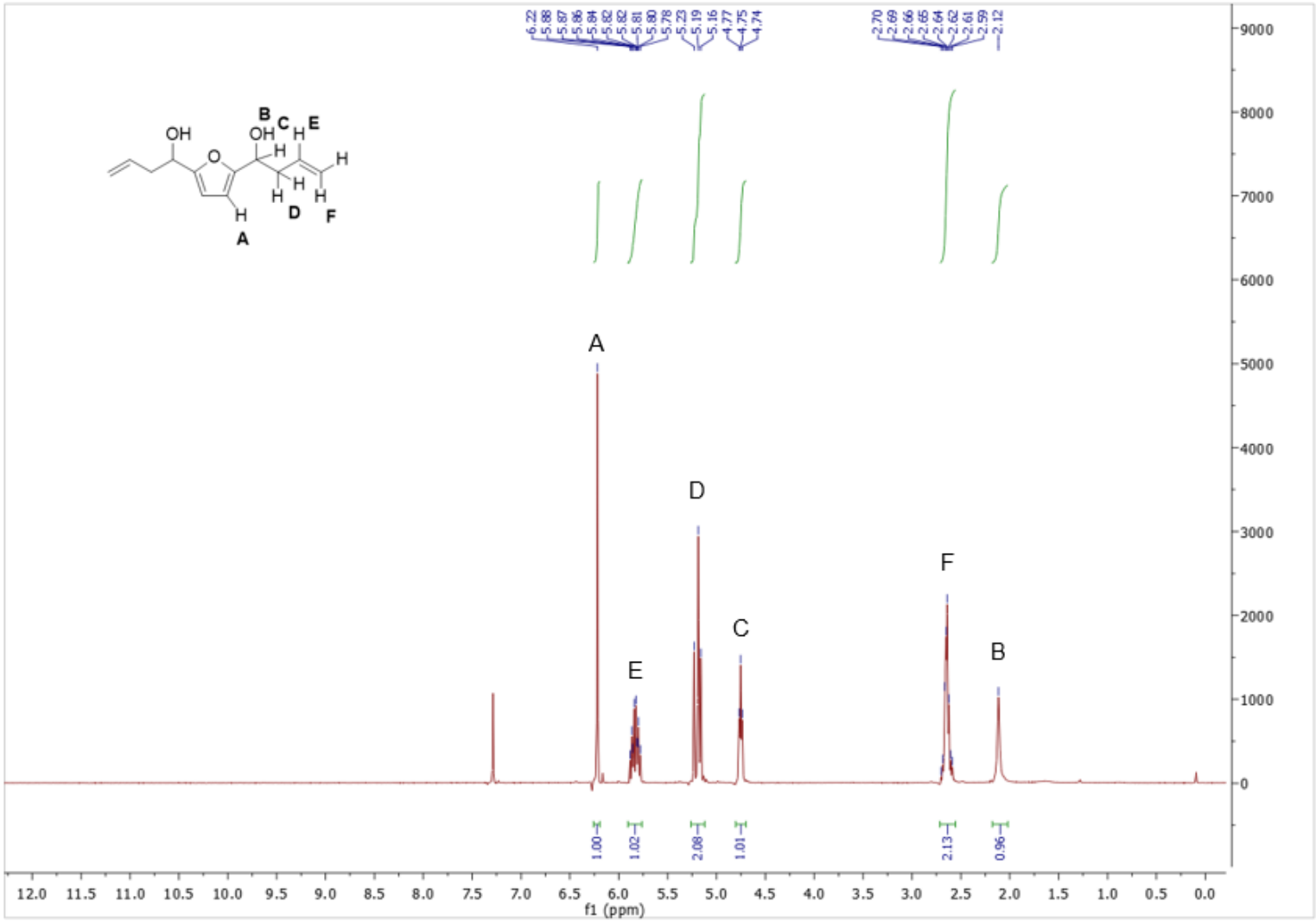

A33. ^{1}H NMR ($CDCl_3$) spectrum of Compound **2c**.

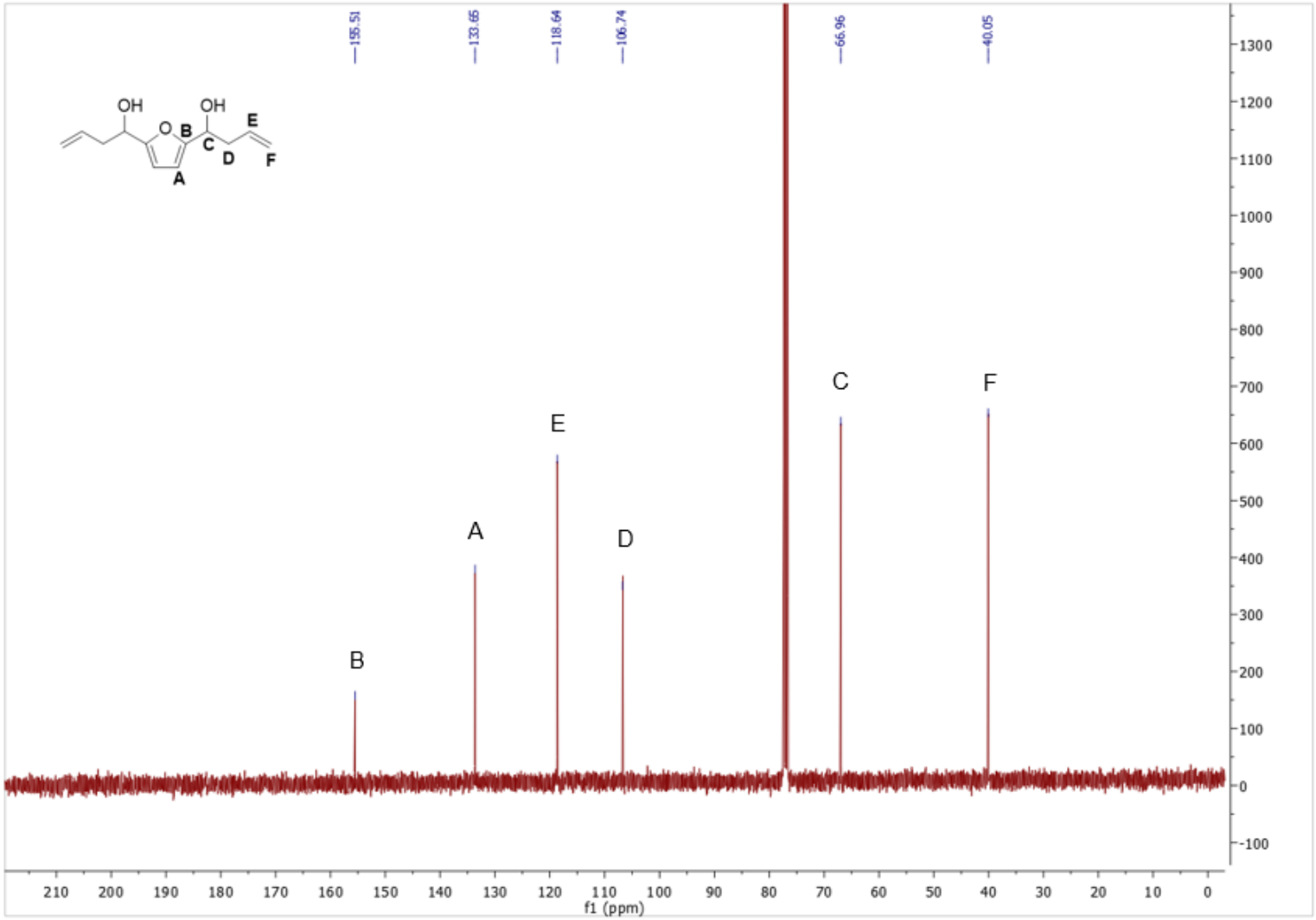

A34. ^{13}C NMR ($CDCl_3$) spectrum of Compound **2c**.

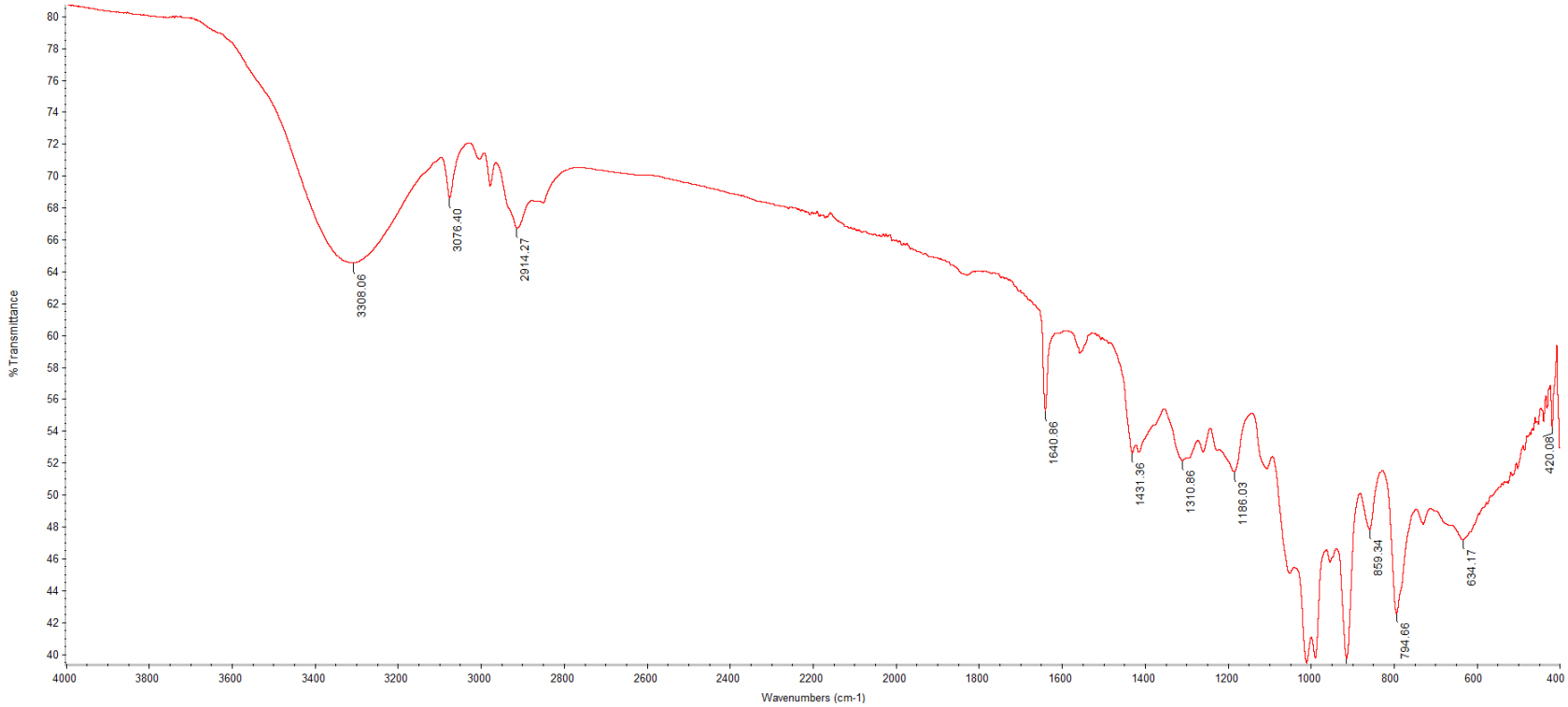

A35. FTIR spectrum of Compound **2c**.

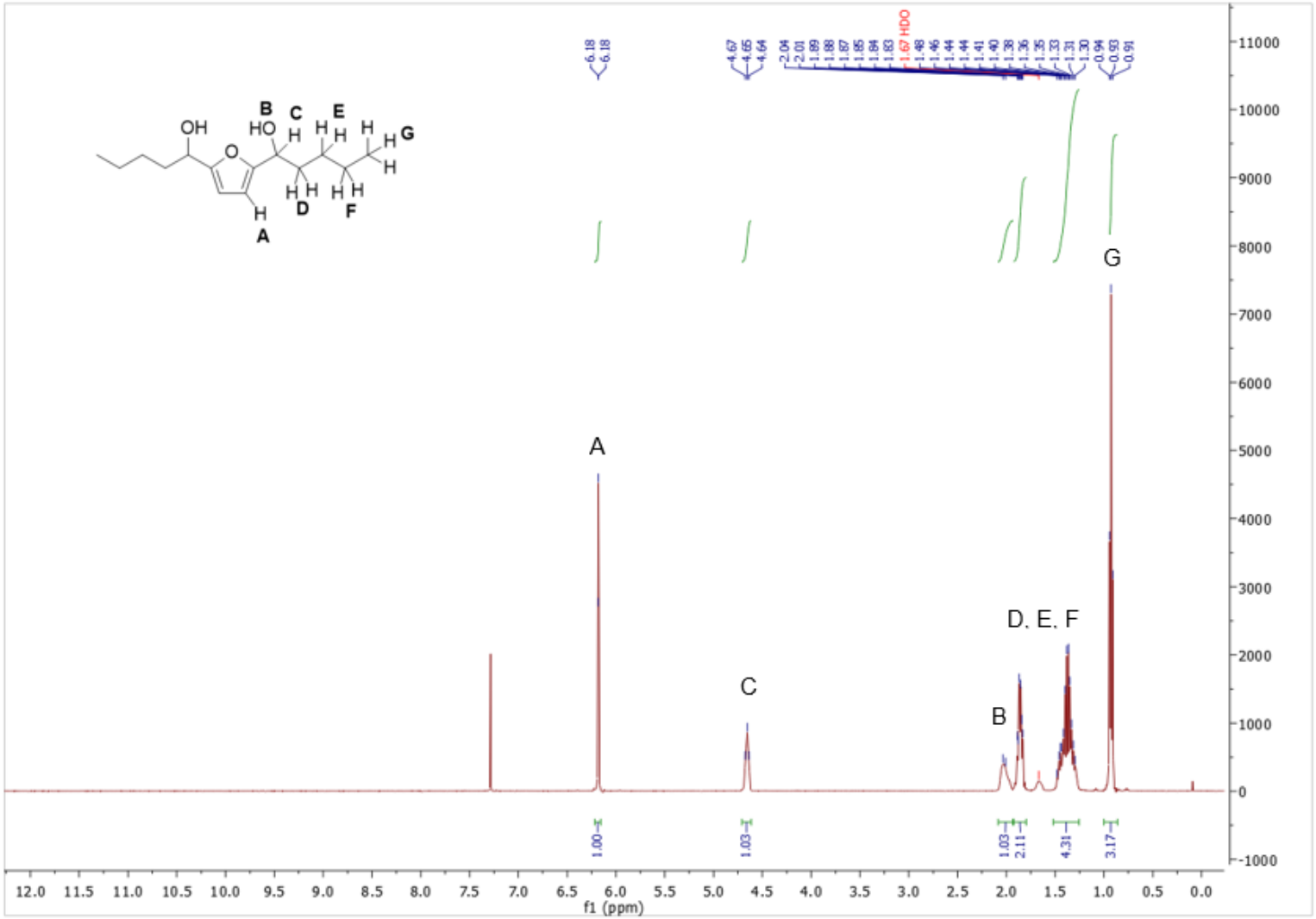

A36. ^{1}H NMR ($CDCl_3$) spectrum of Compound **2d**.

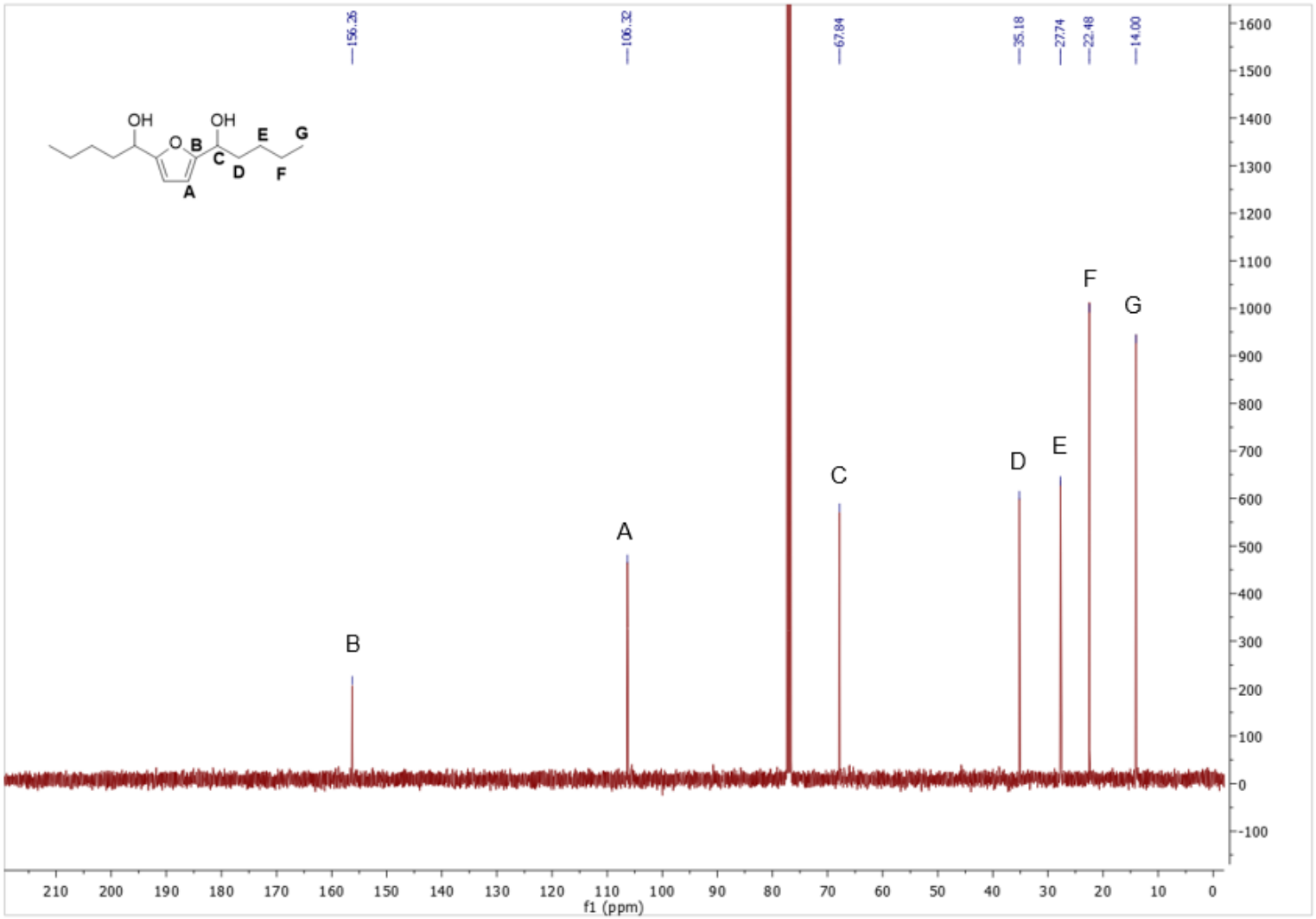

A37. ^{13}C NMR ($CDCl_3$) spectrum of Compound **2d**.

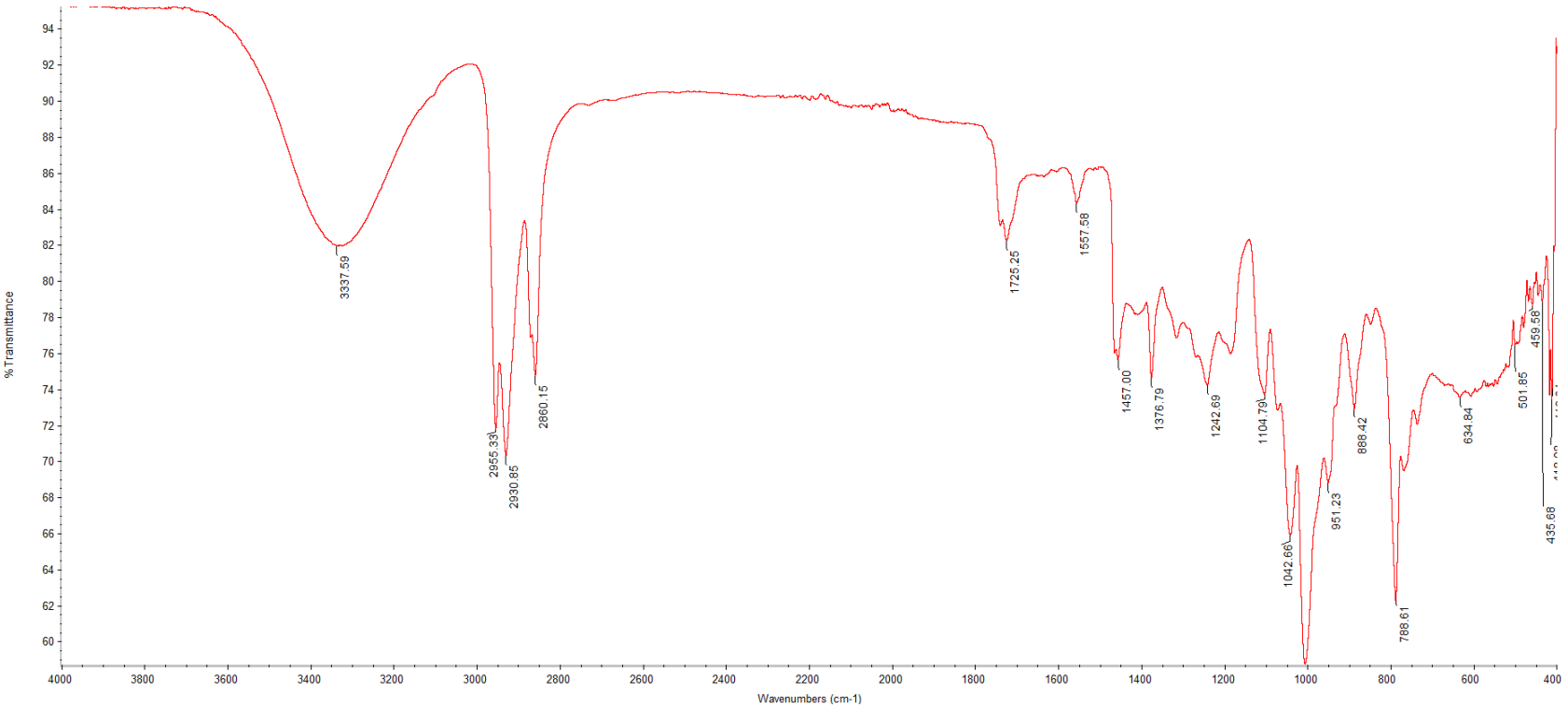

A38. FTIR spectrum of Compound **2d**.

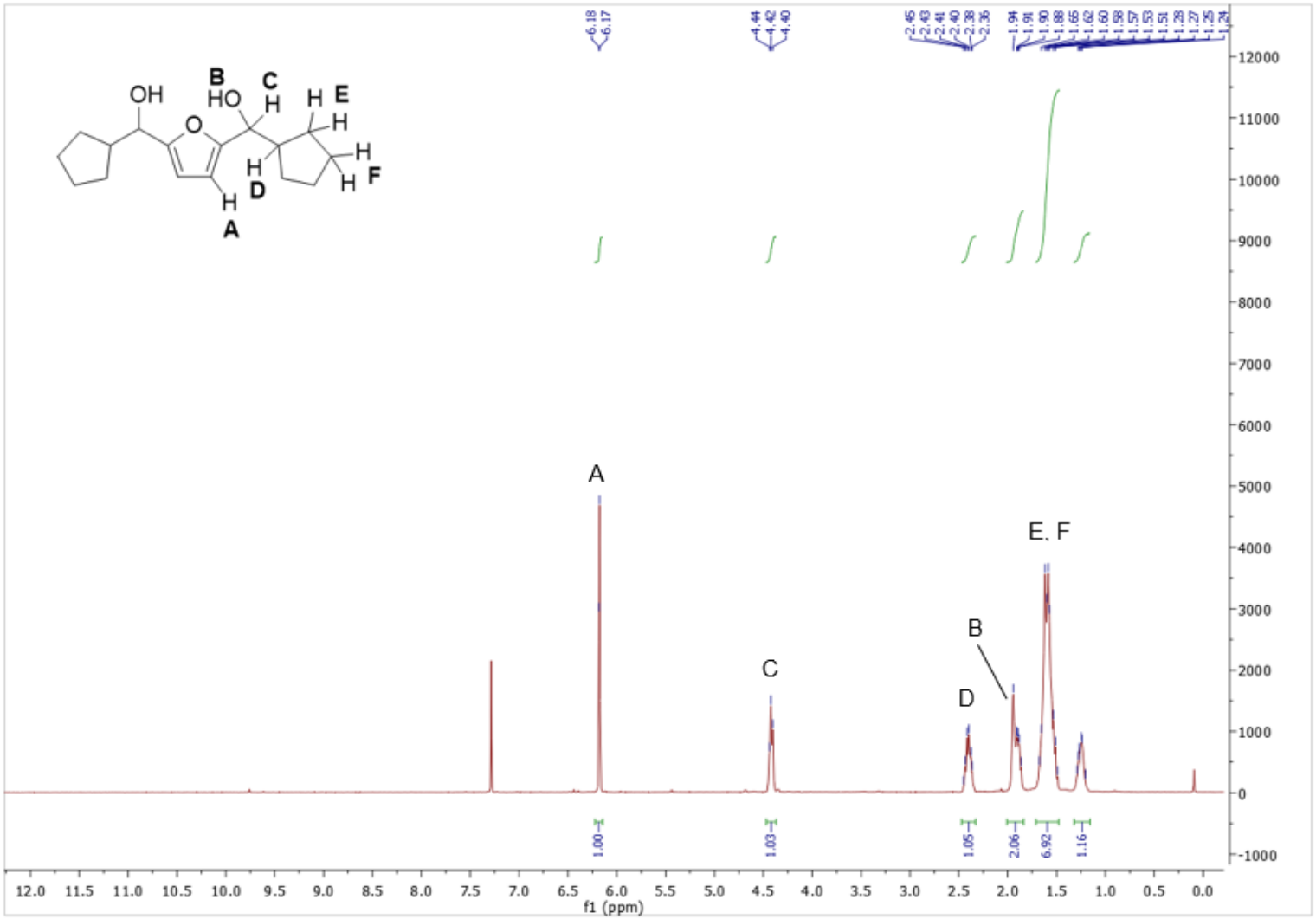

A39. ^{1}H NMR ($CDCl_3$) spectrum of Compound **2e**.

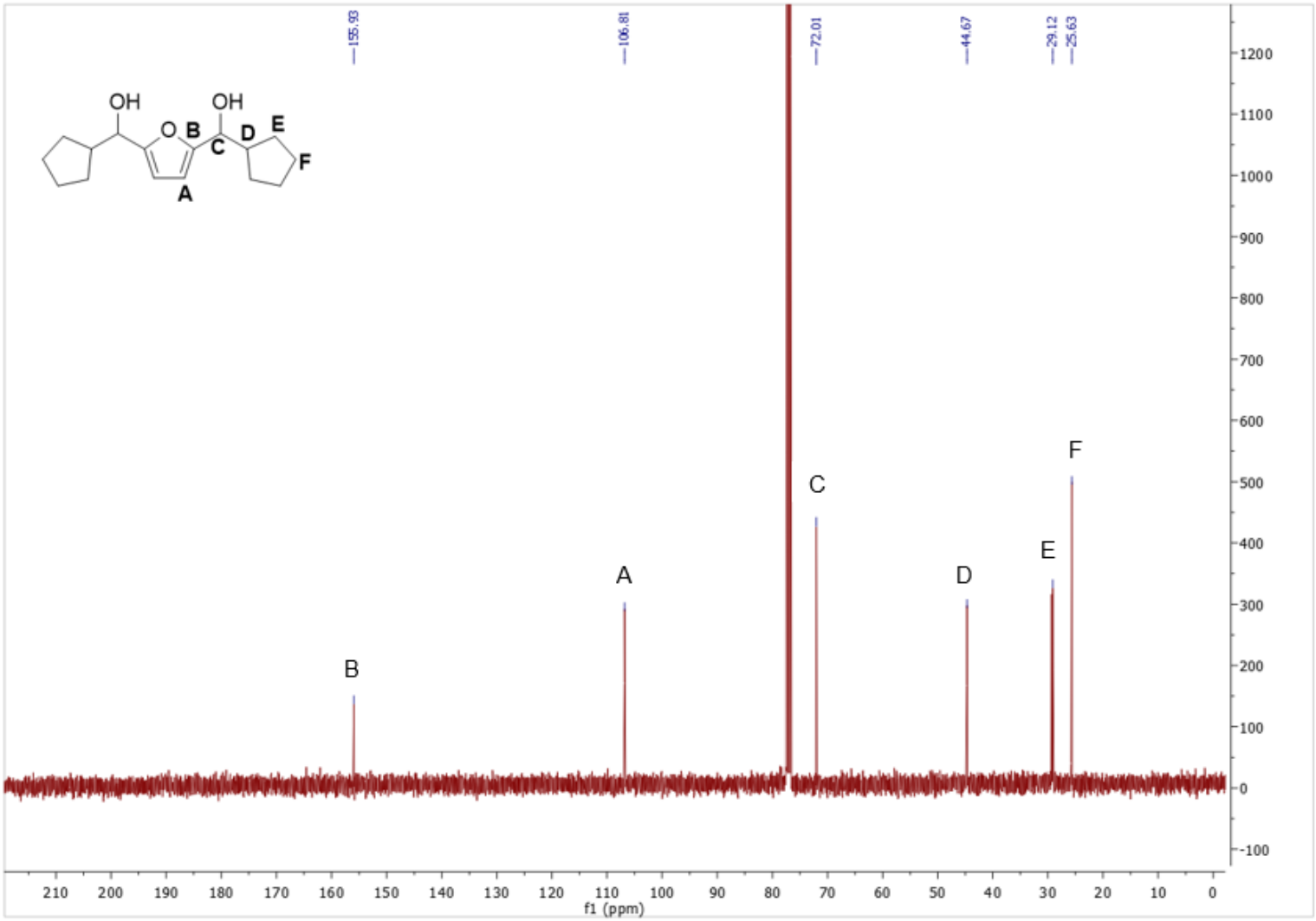

A40. ^{13}C NMR ($CDCl_3$) spectrum of Compound **2e**.

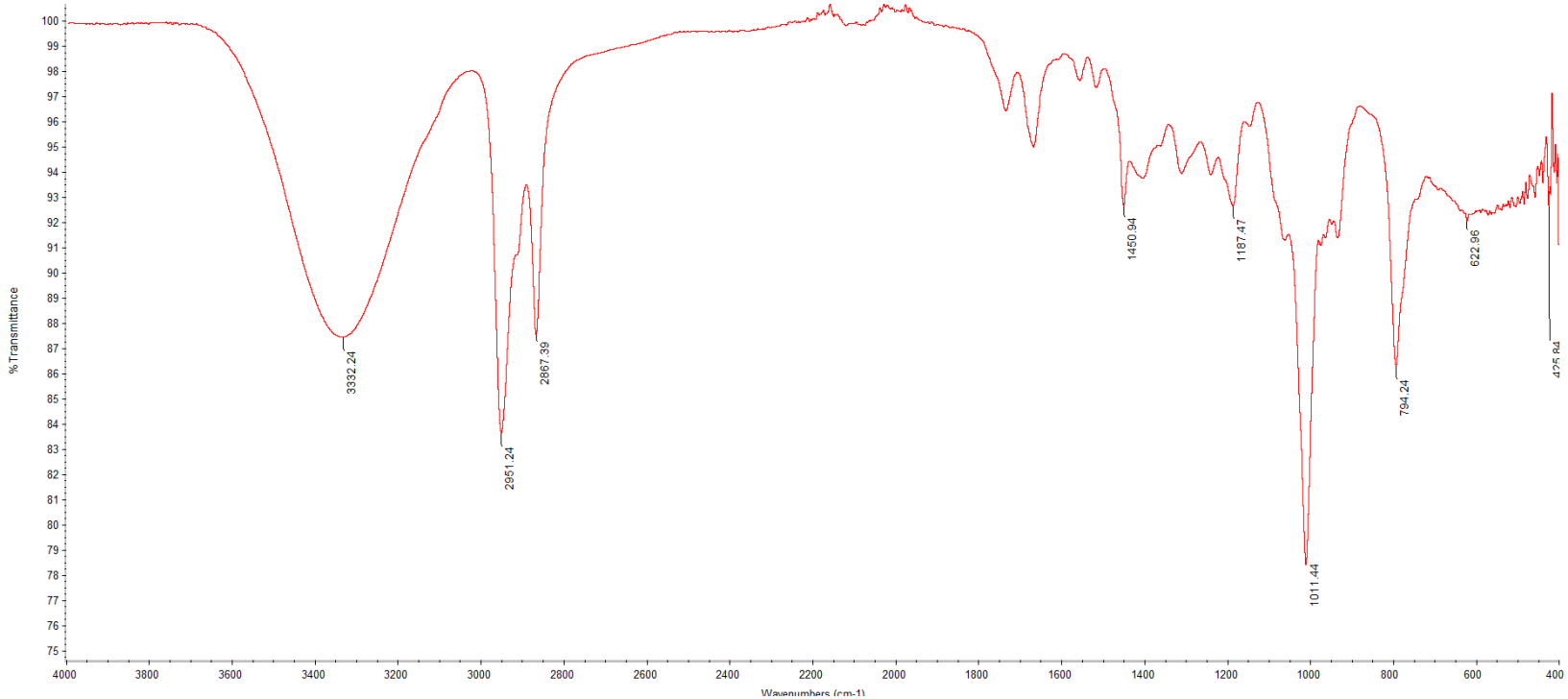

A41. FTIR spectrum of Compound **2e**.

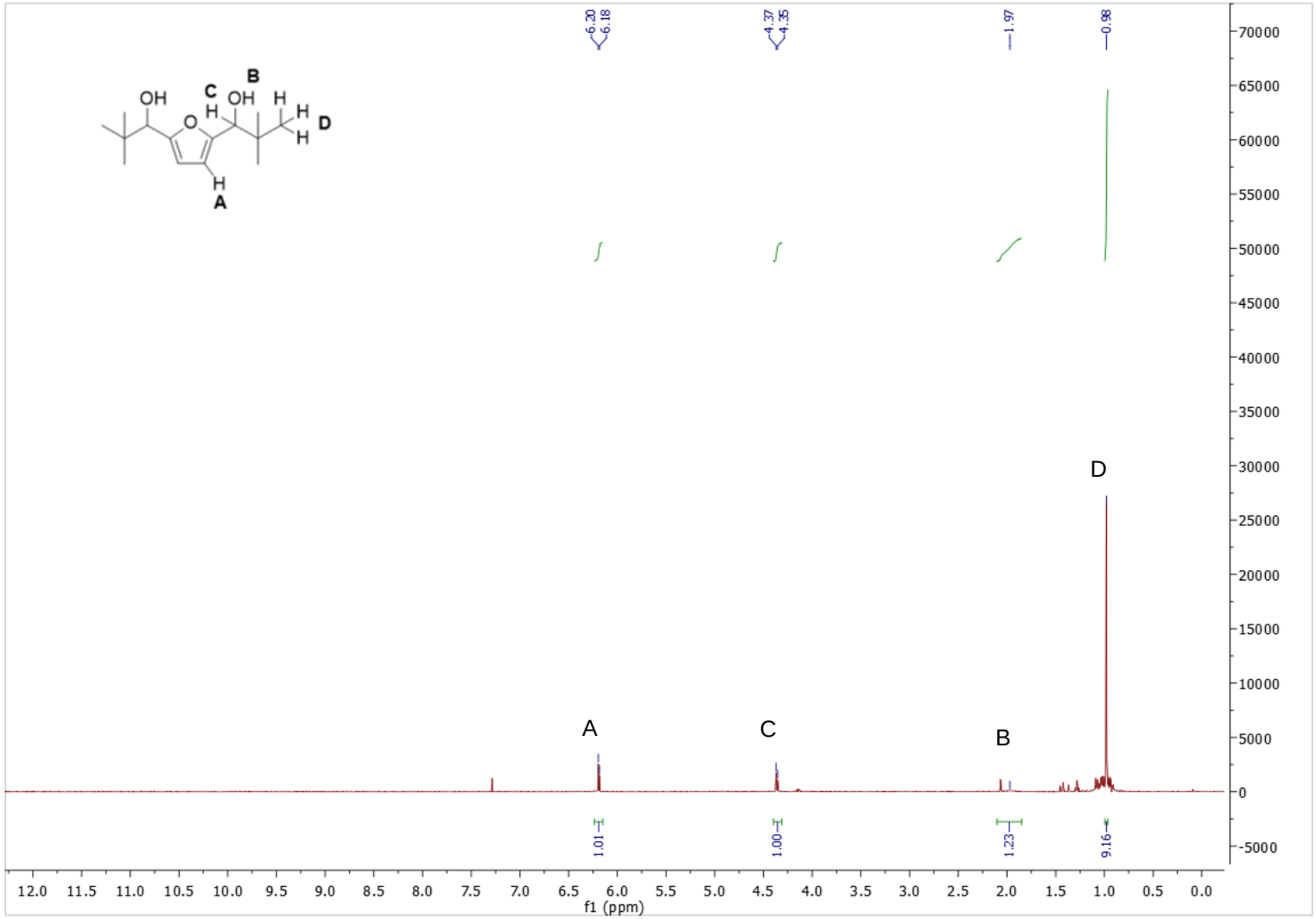

A42. ^{1}H NMR ($CDCl_3$) spectrum of Compound **2f**. Crude NMR, key peaks highlighted.

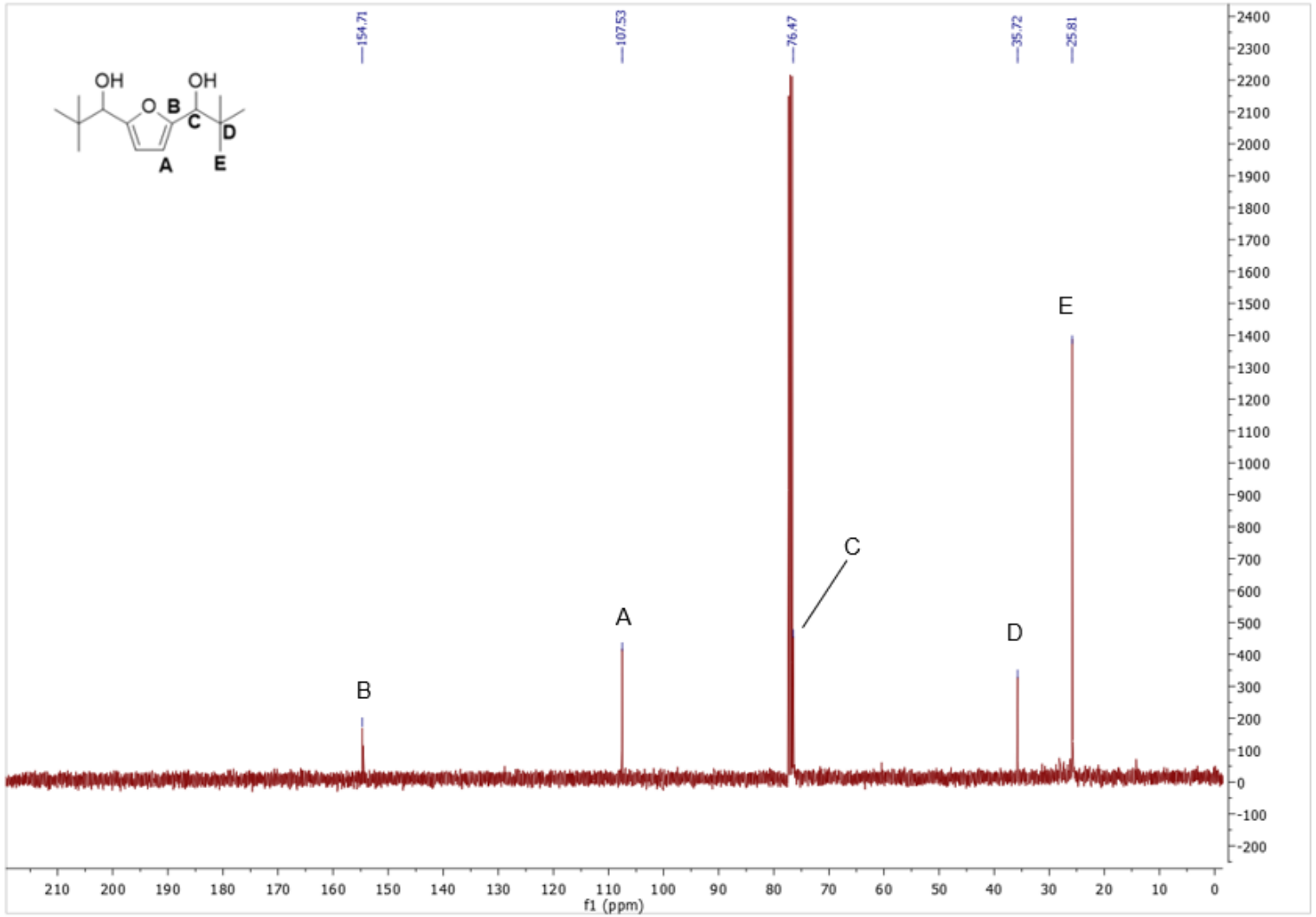

A43. ^{13}C NMR ($CDCl_3$) spectrum of Compound **2f**.

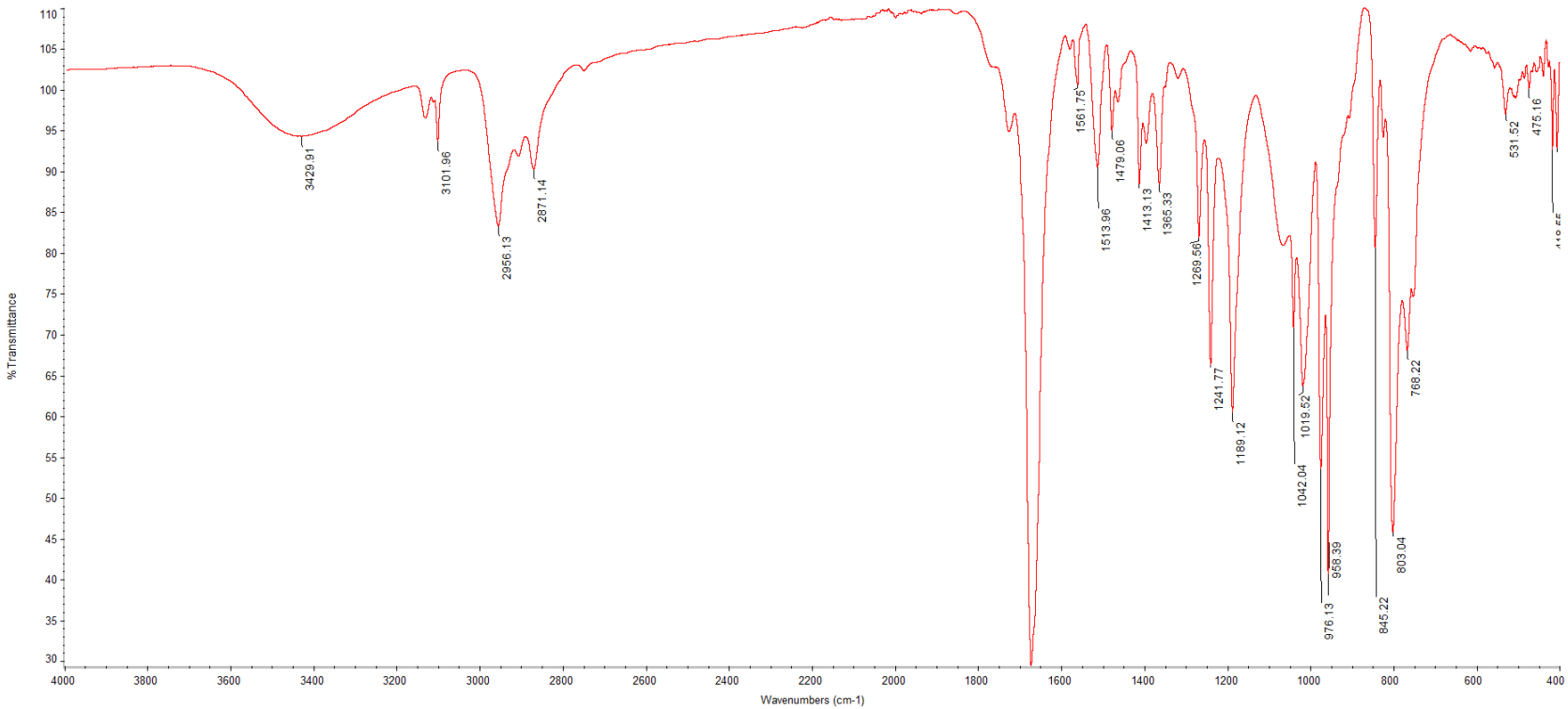

A44. FTIR spectrum of Compound **2f**.

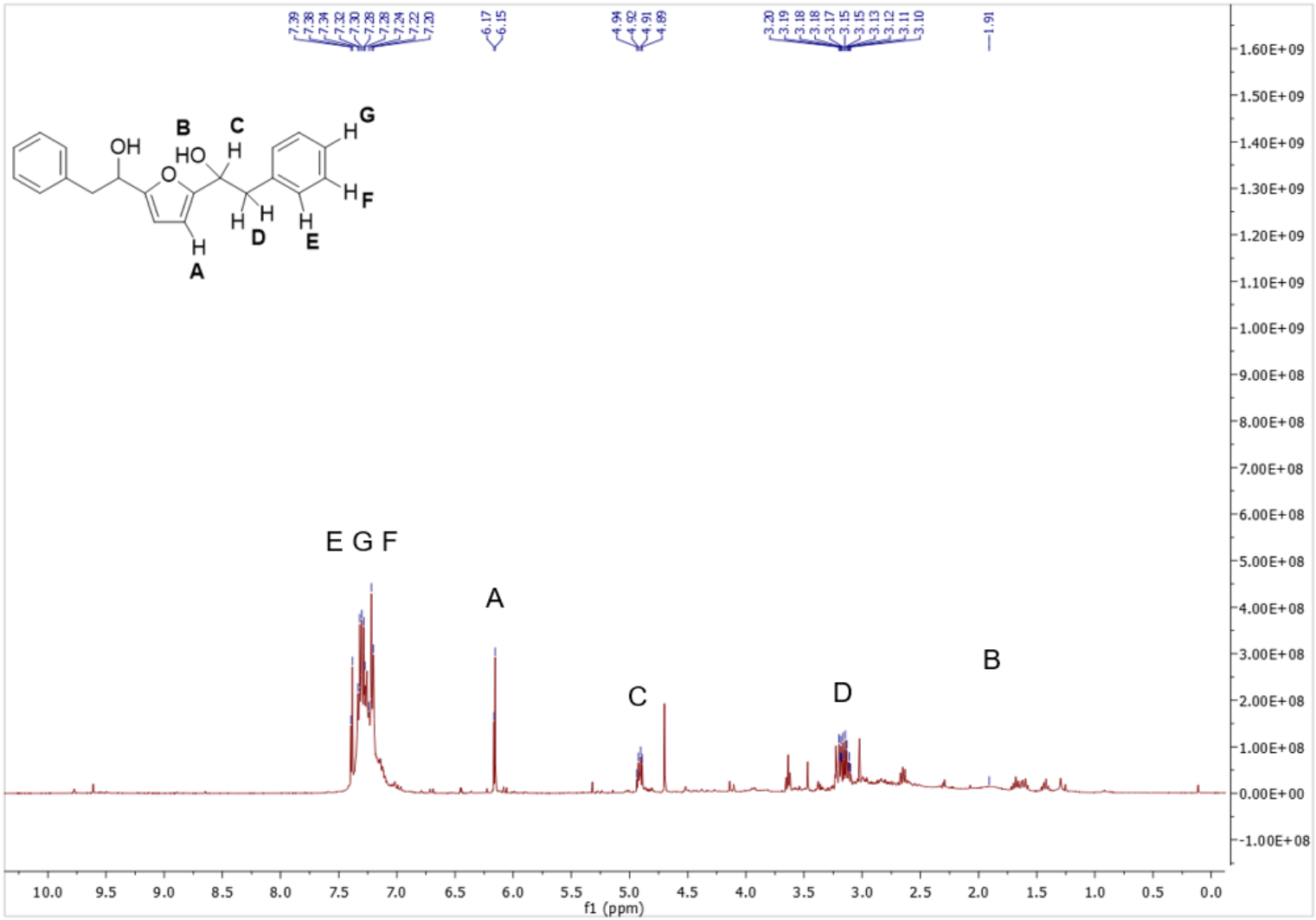

A45. ^{1}H NMR ($CDCl_3$) spectrum of Compound **2g**. Crude NMR, Key peaks highlighted. Compound degrades once concentrated.

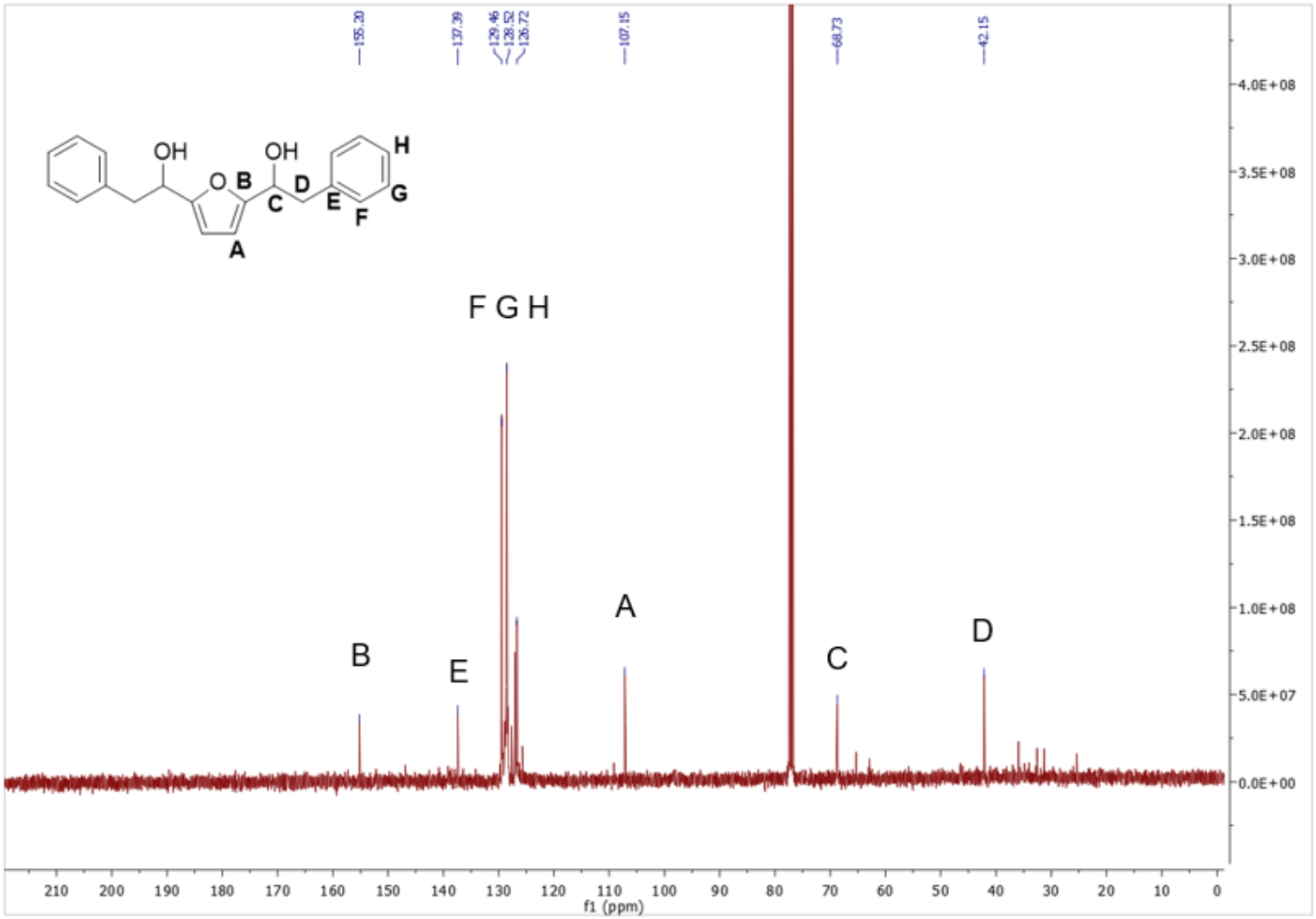

A46. ^{13}C NMR ($CDCl_3$) spectrum of Compound 2g. Crude NMR. Key peaks highlighted. Compound degrades once concentrated.

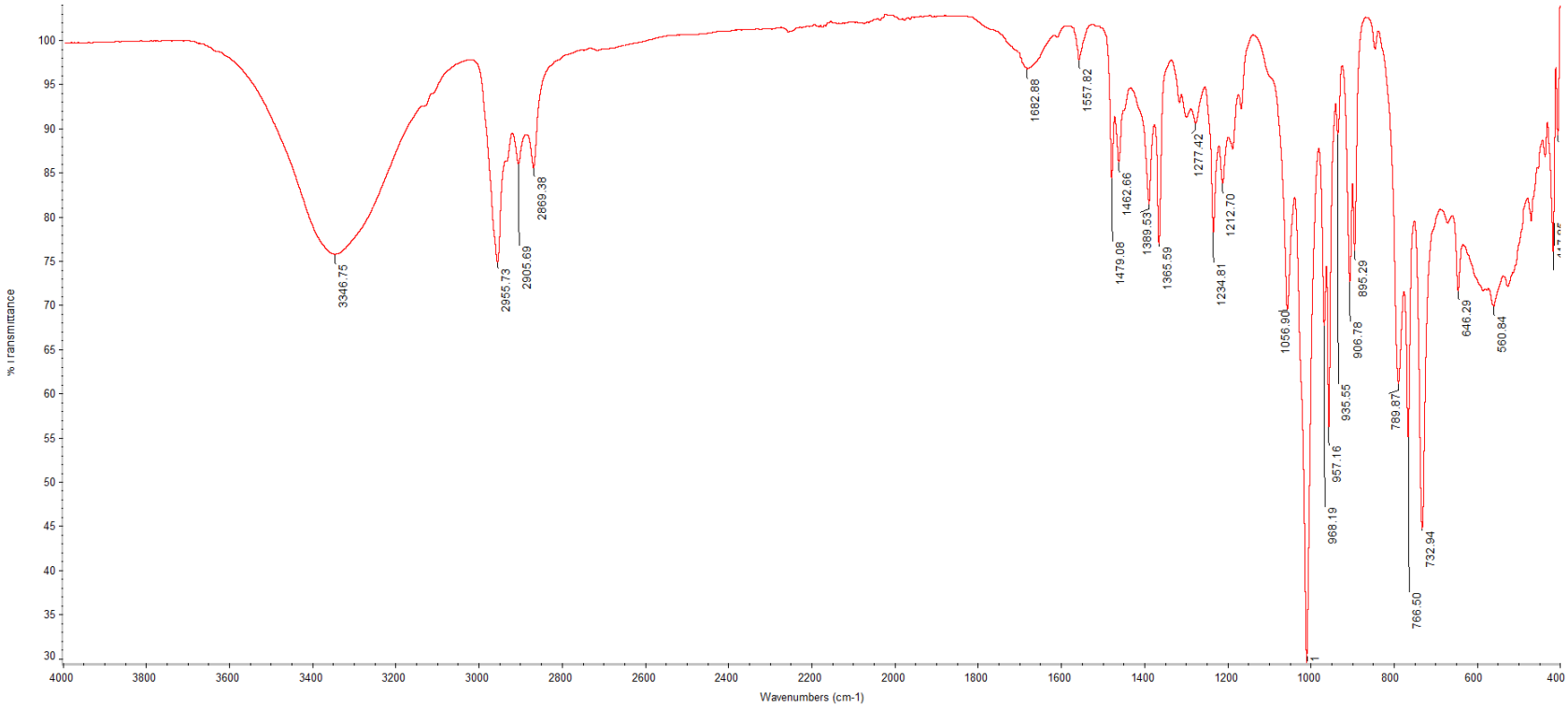

A47. FTIR spectrum of Compound **2g**.

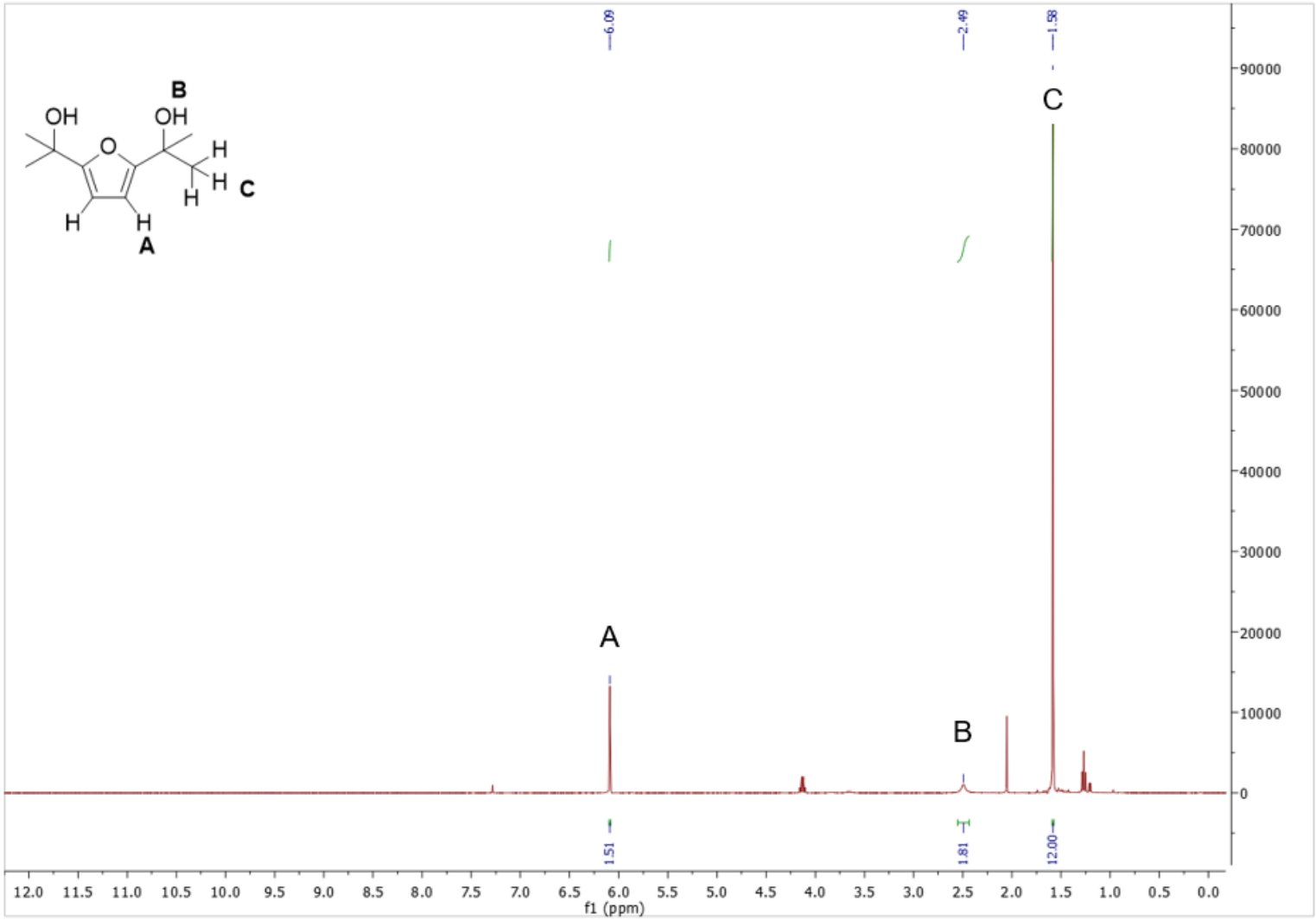

A48. ^{1}H NMR ($CDCl_3$) spectrum of Compound **3**. Minor ethyl acetate impurity; compound degrades if completely dried.

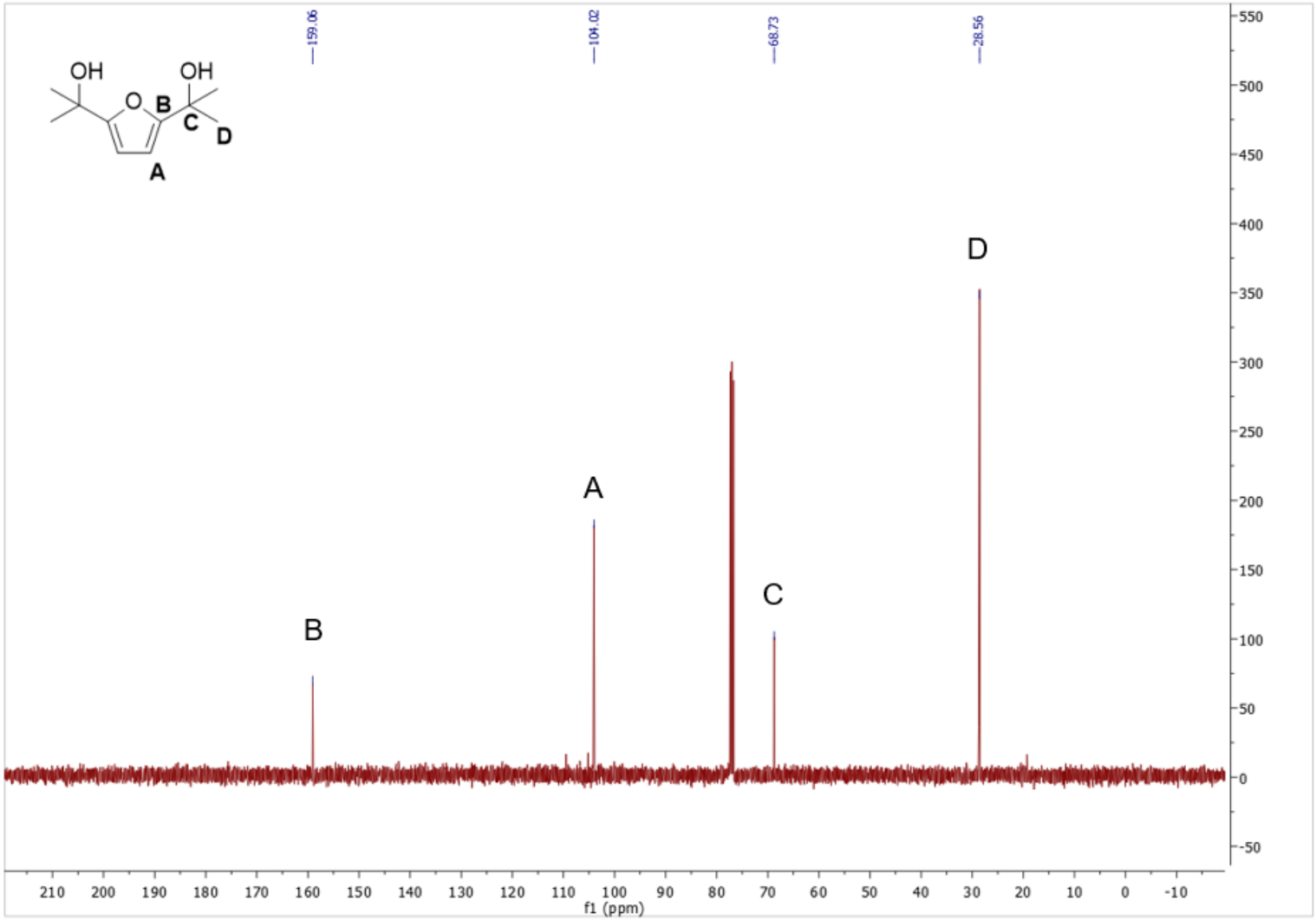

A49. ^{13}C NMR ($CDCl_3$) spectrum of Compound **3**.

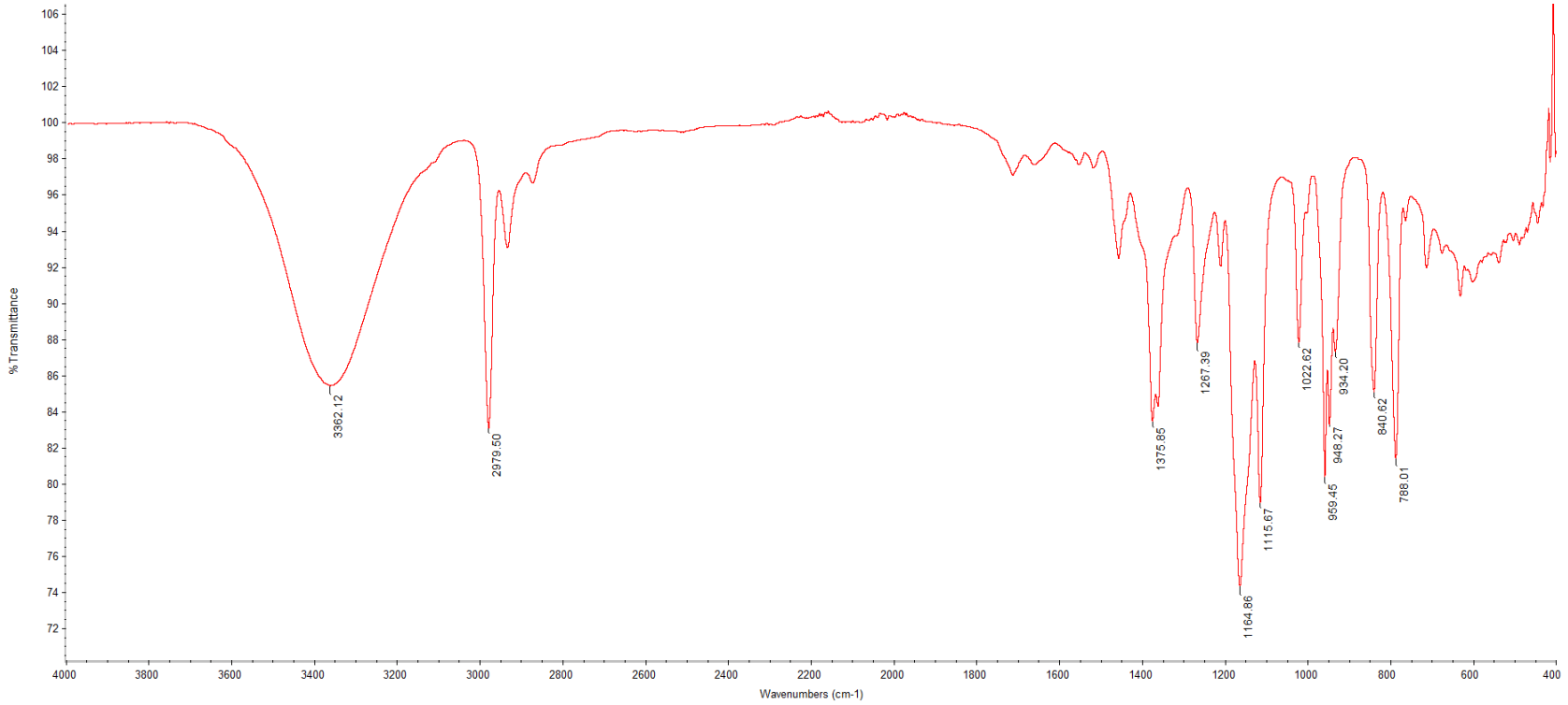

A50. FTIR spectrum of Compound **3**.

APPENDIX B: SPECTRA FROM CHAPTER 3

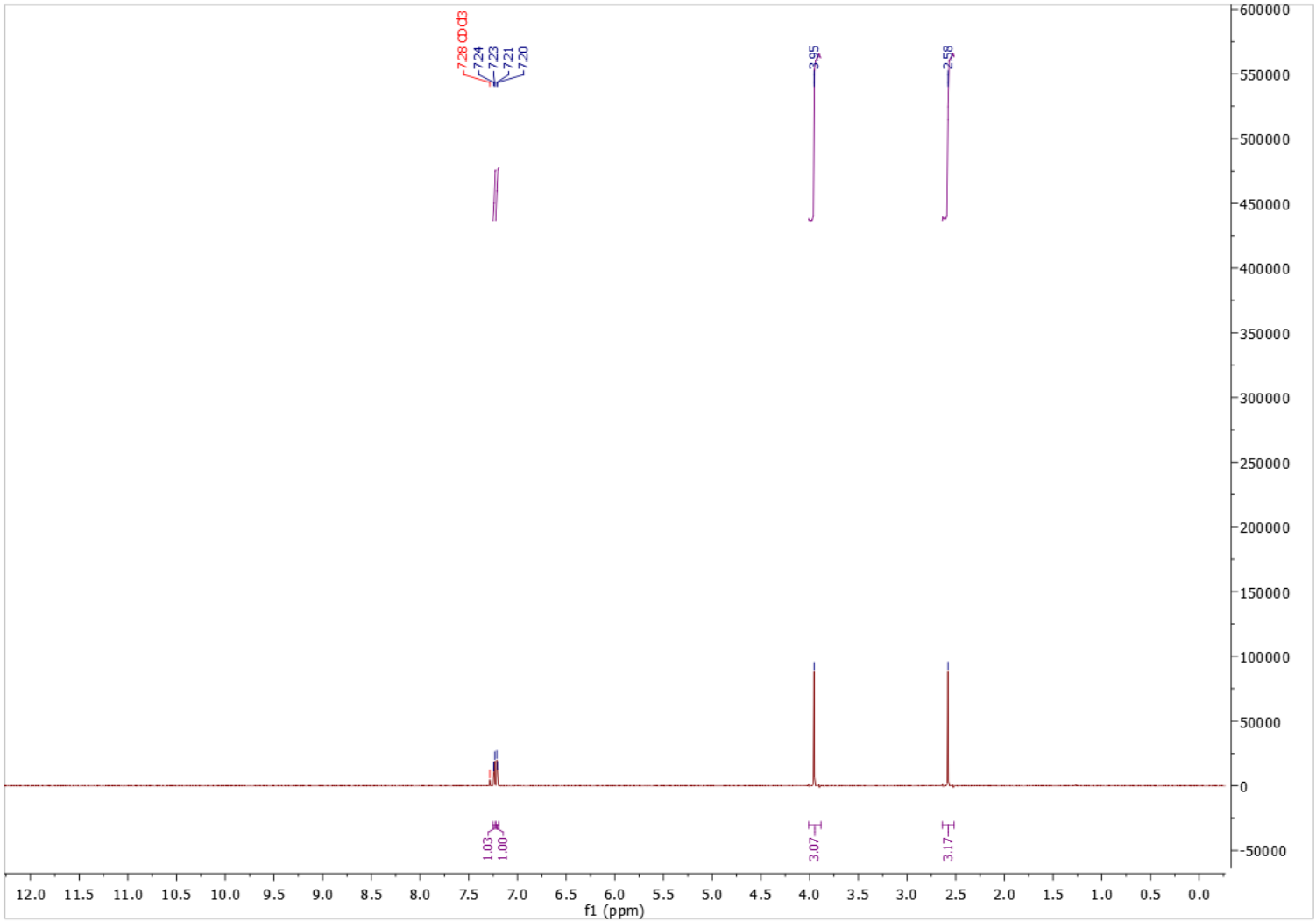

B1. ^{1}H NMR ($CDCl_3$) spectrum of **5-acetyl-2-methylfuroate**.

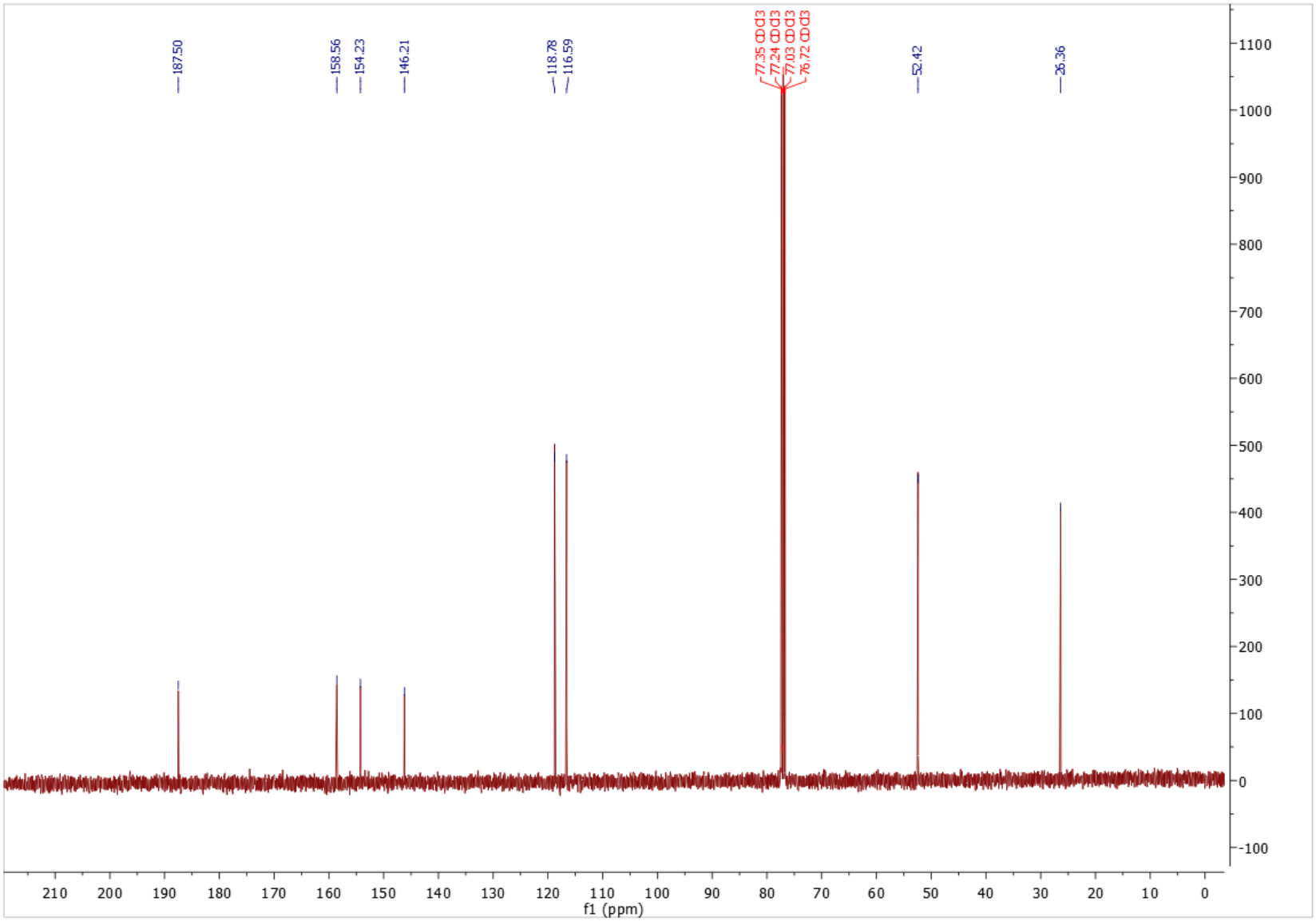

B2. ^{13}C NMR ($CDCl_3$) spectrum of **5-acetyl-2-methylfuroate**.

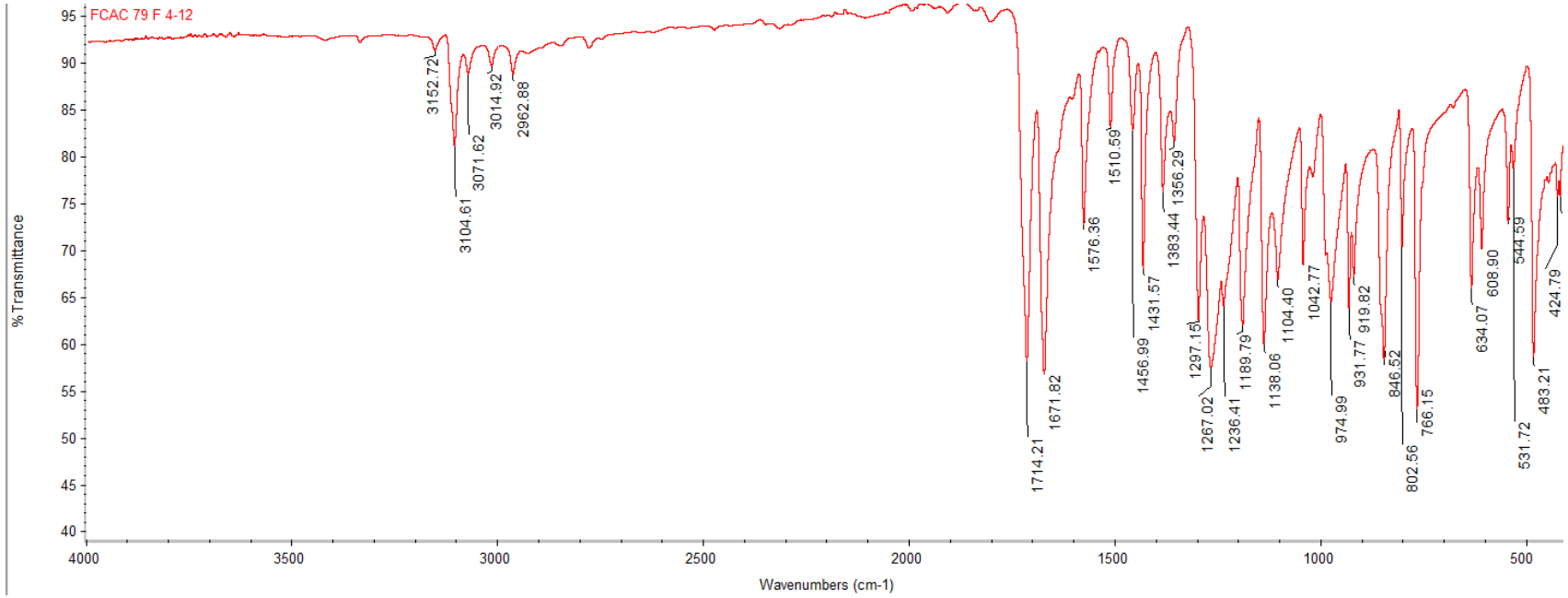

B3. FTIR spectrum of **5-acetyl-2-methylfuroate**.

APPENDIX C: SPECTRA FROM CHAPTER 4

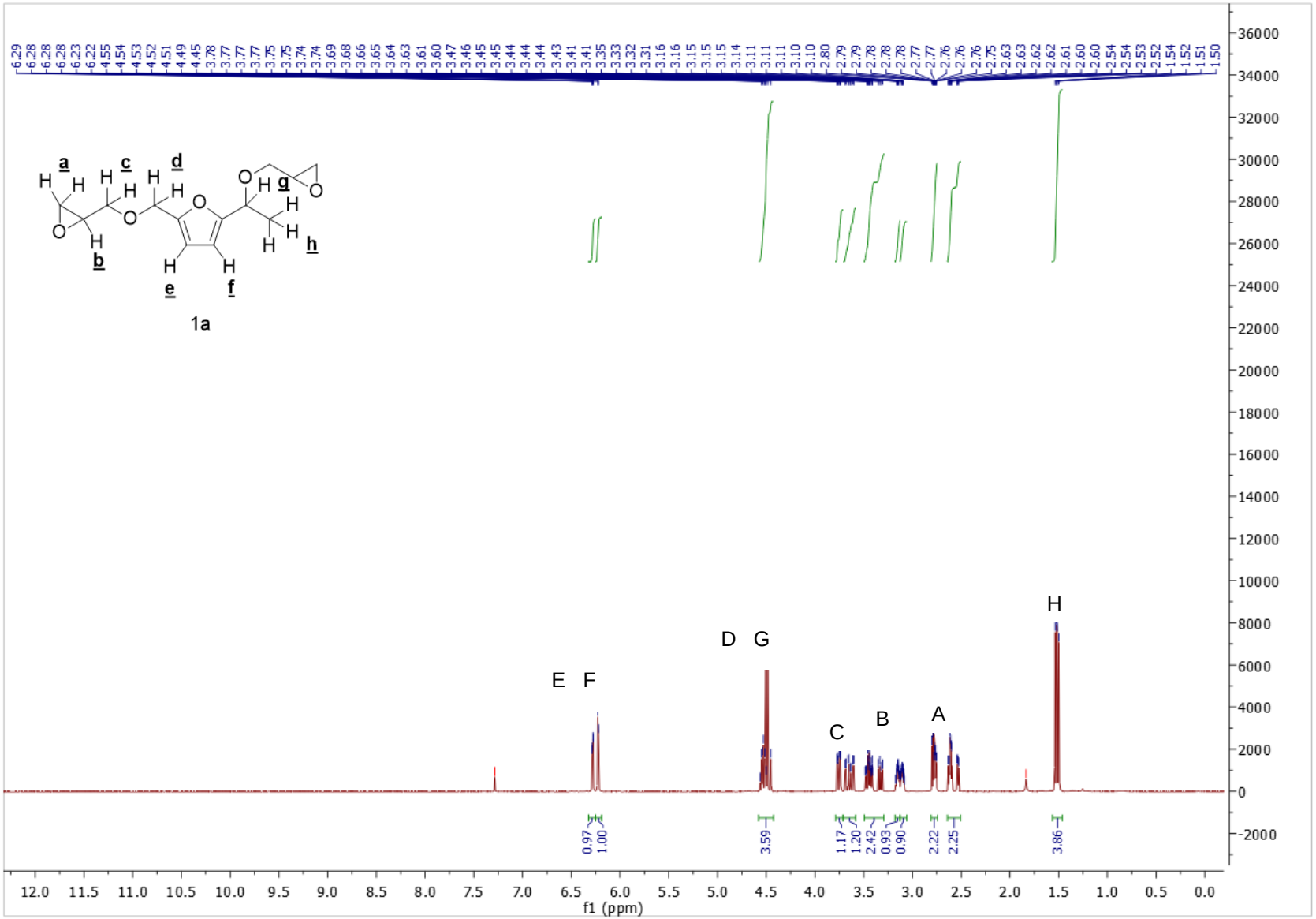

C1. ^{1}H NMR ($CDCl_3$) spectrum of Compound **4a**.

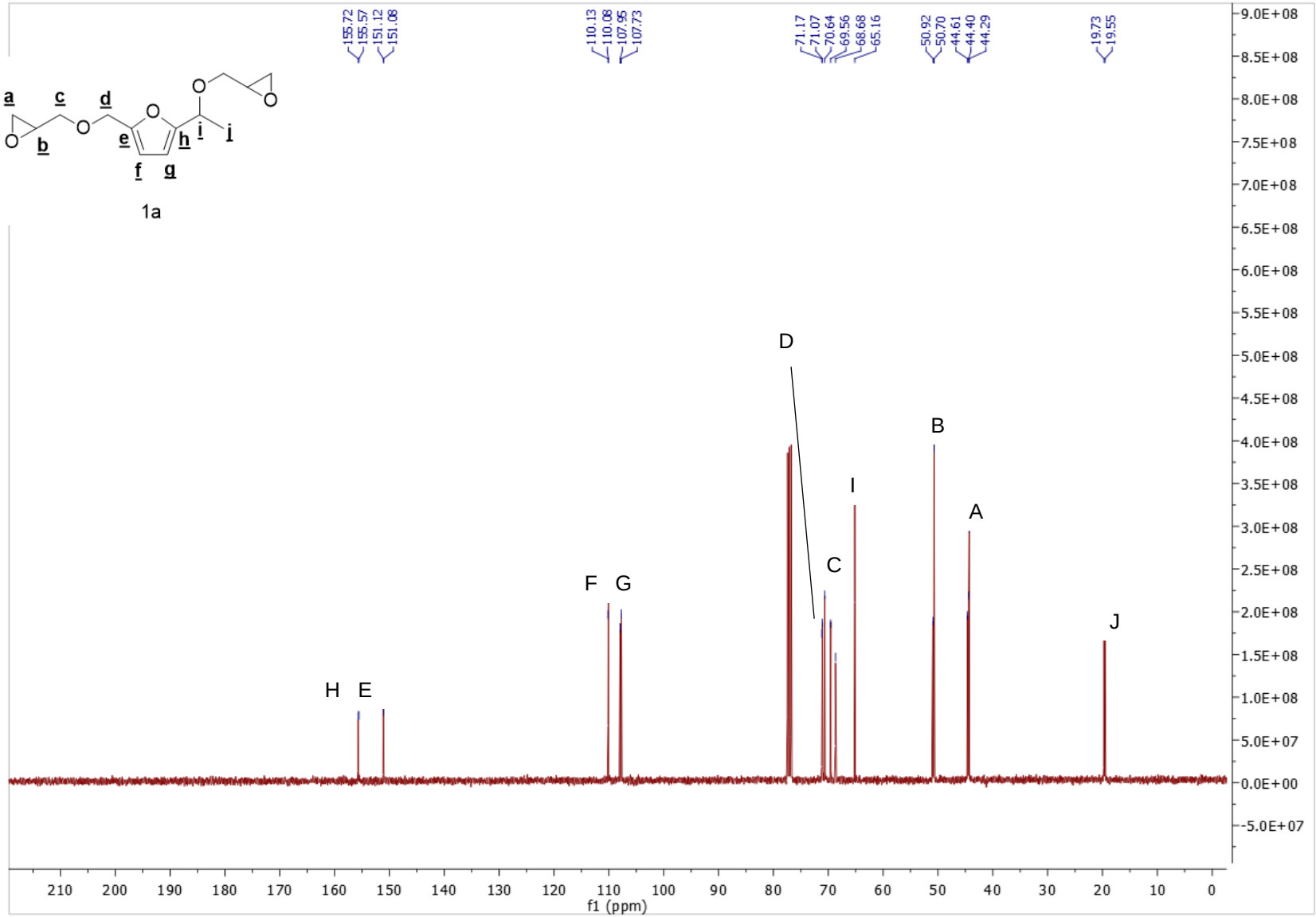

C2. ^{13}C NMR ($CDCl_3$) spectrum of Compound **4a**.

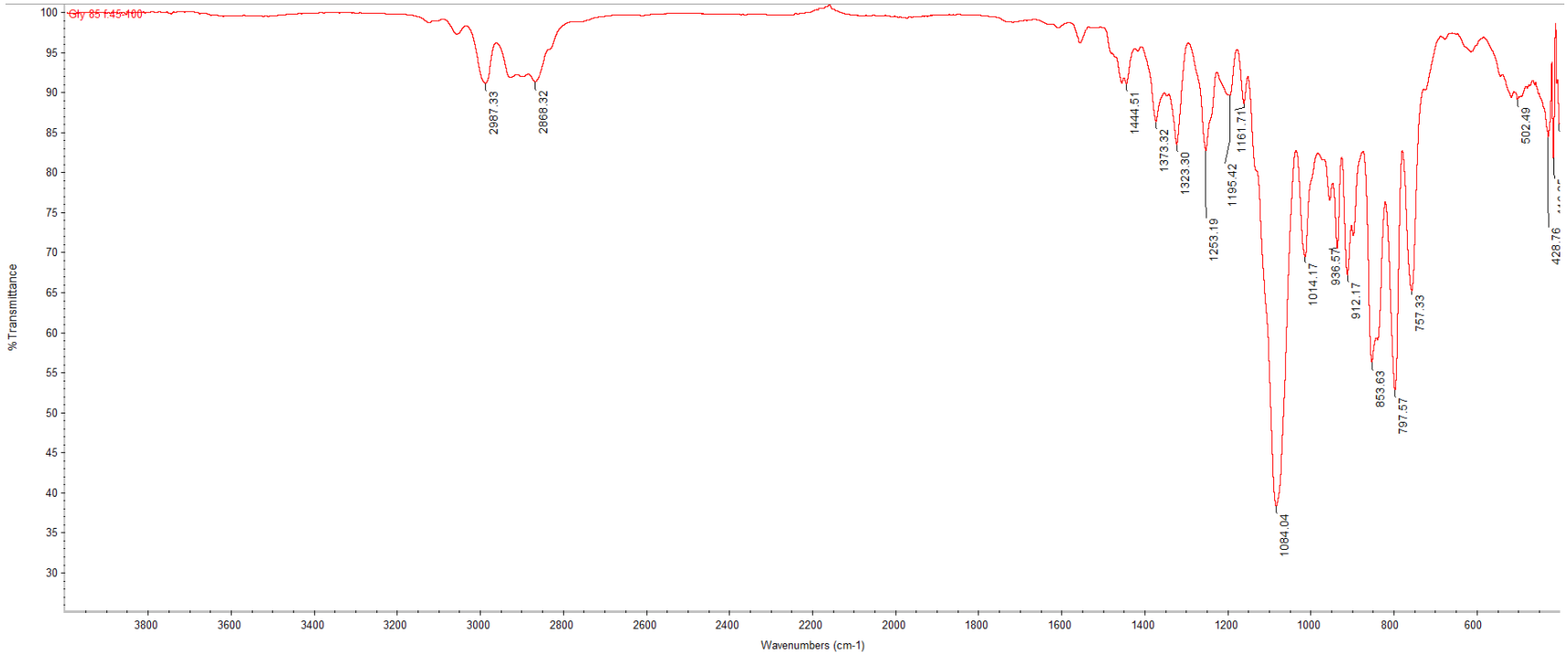

C3. FT-IR spectrum of Compound **4a**.

C4. HRMS (ESI, Na+) spectrum of compound **4a**.

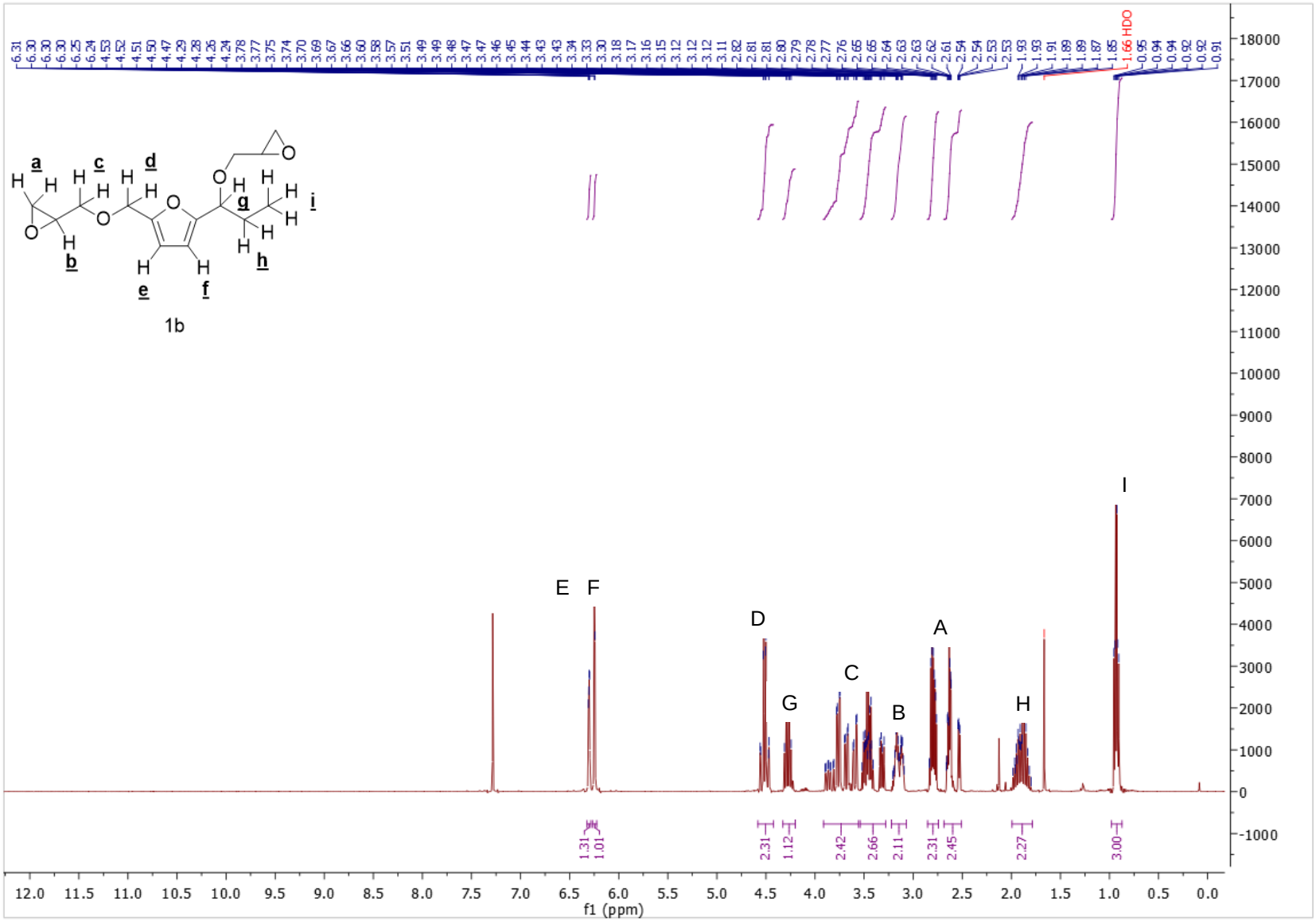

C5. ^{1}H NMR ($CDCl_3$) spectrum of Compound **4b**.

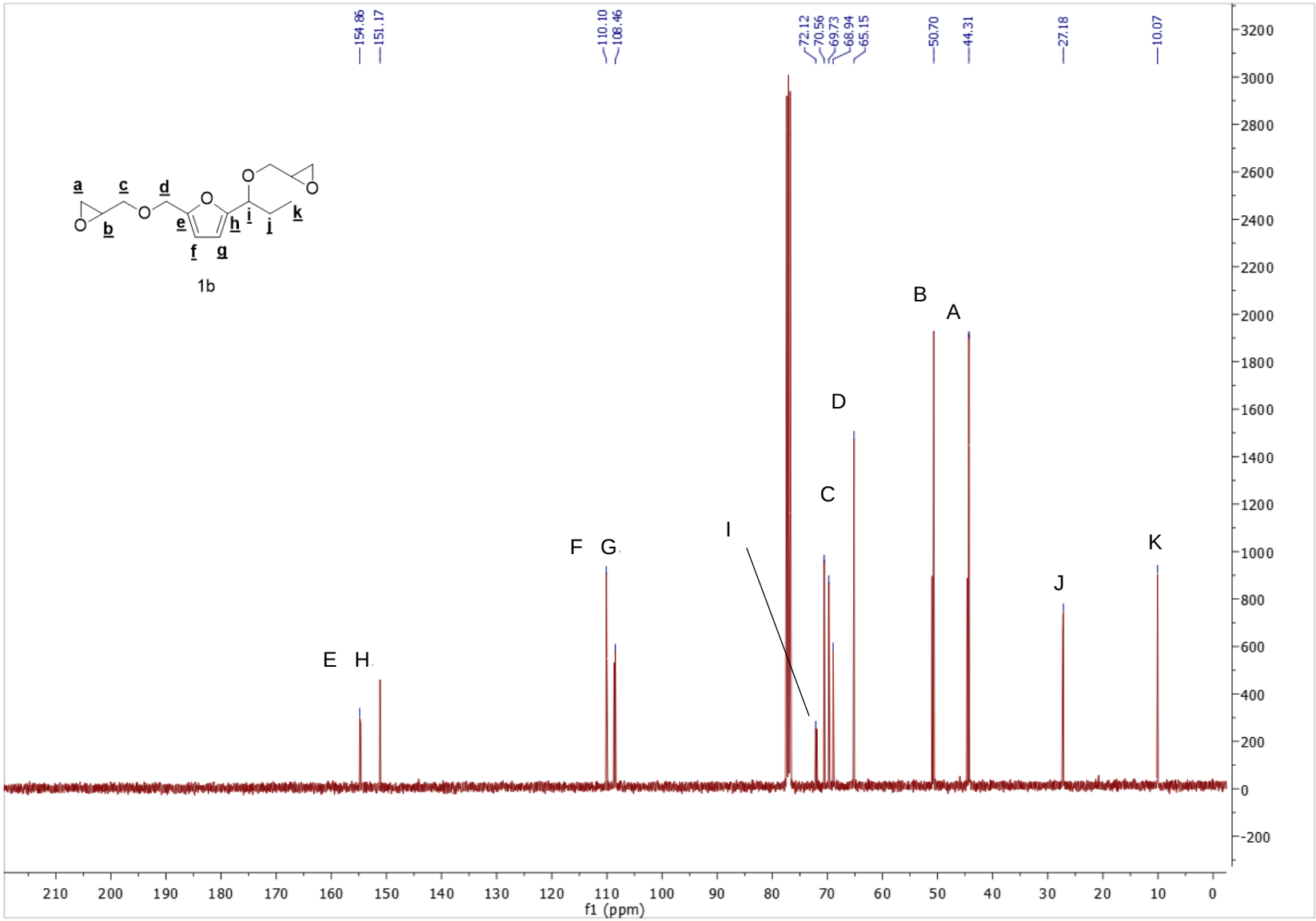

C6. ^{13} C NMR ($CDCl_3$) spectrum of Compound **4b**.

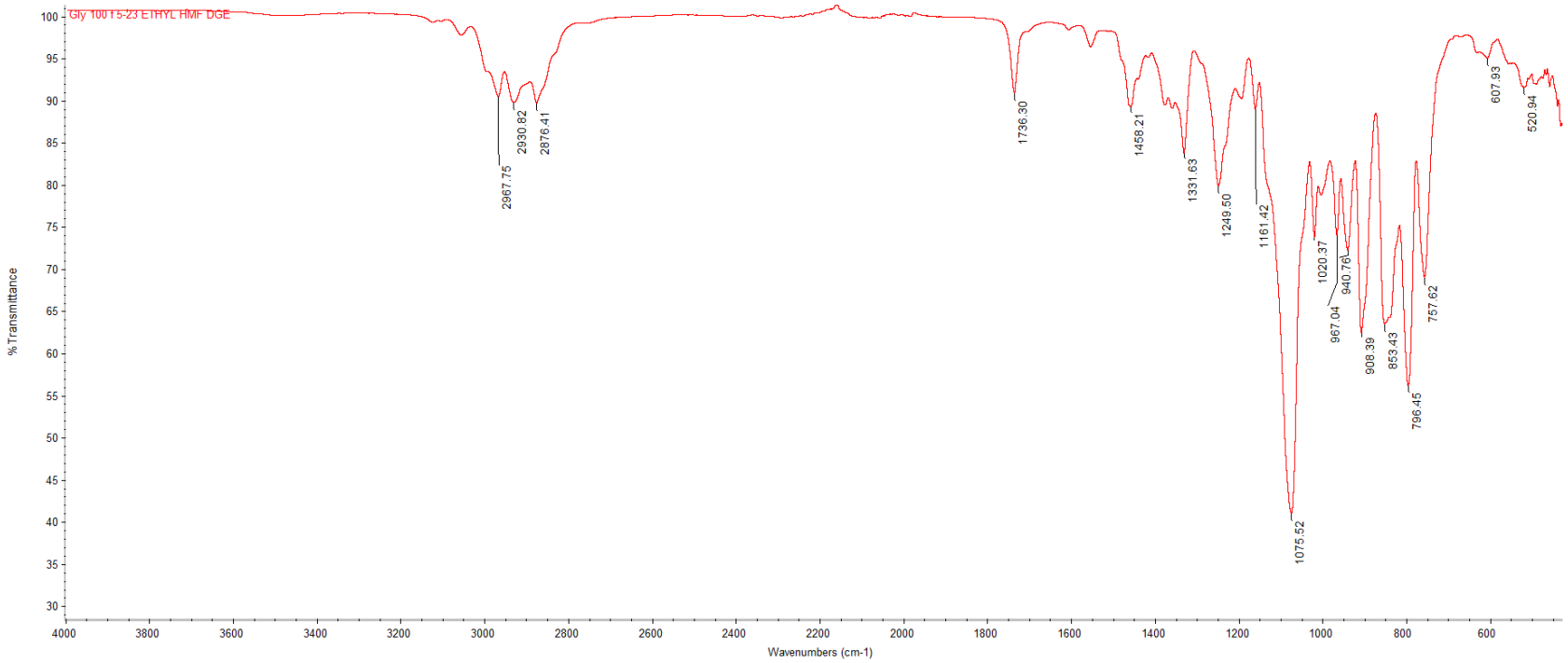

C7. FT-IR spectrum of Compound **4b**.

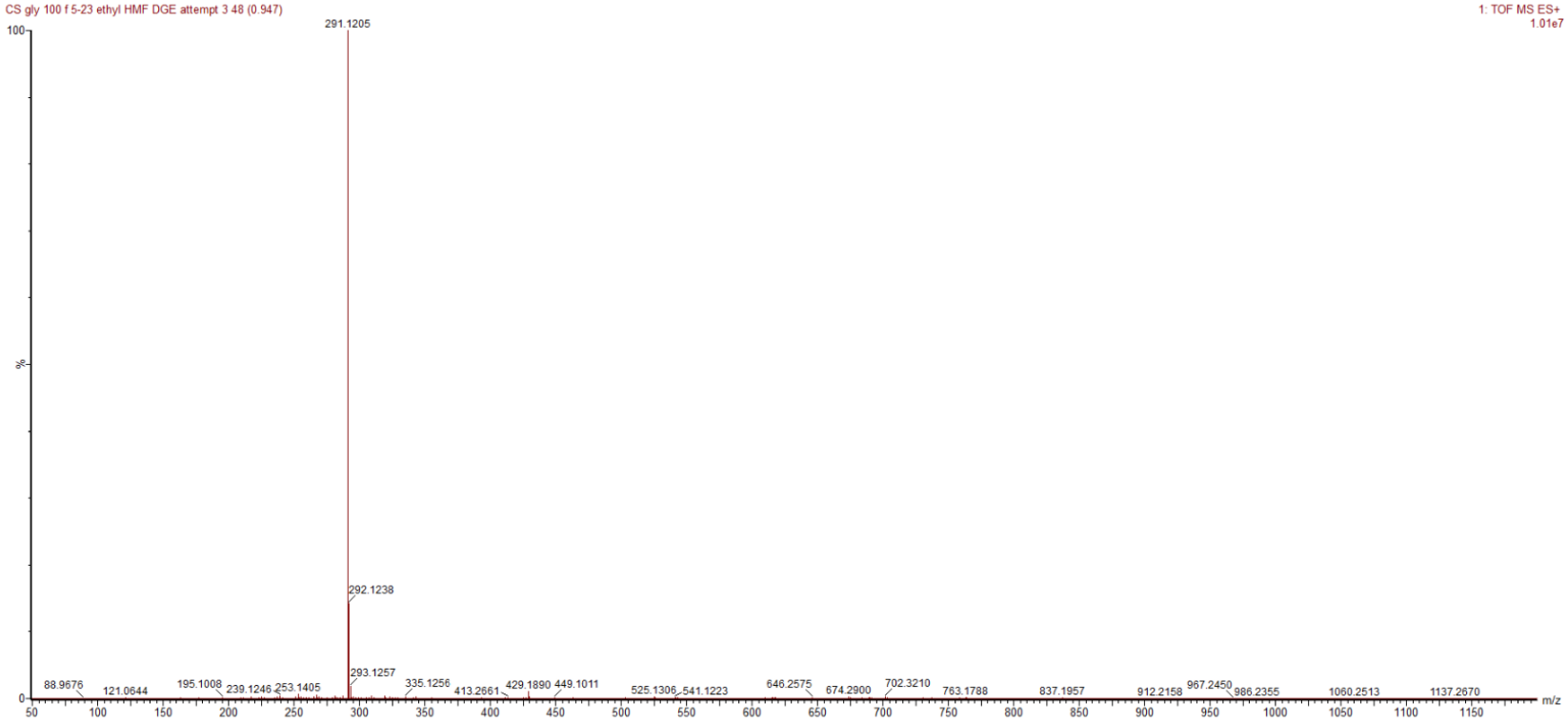

C8. HRMS (ESI, Na+) spectrum of compound **4b**.

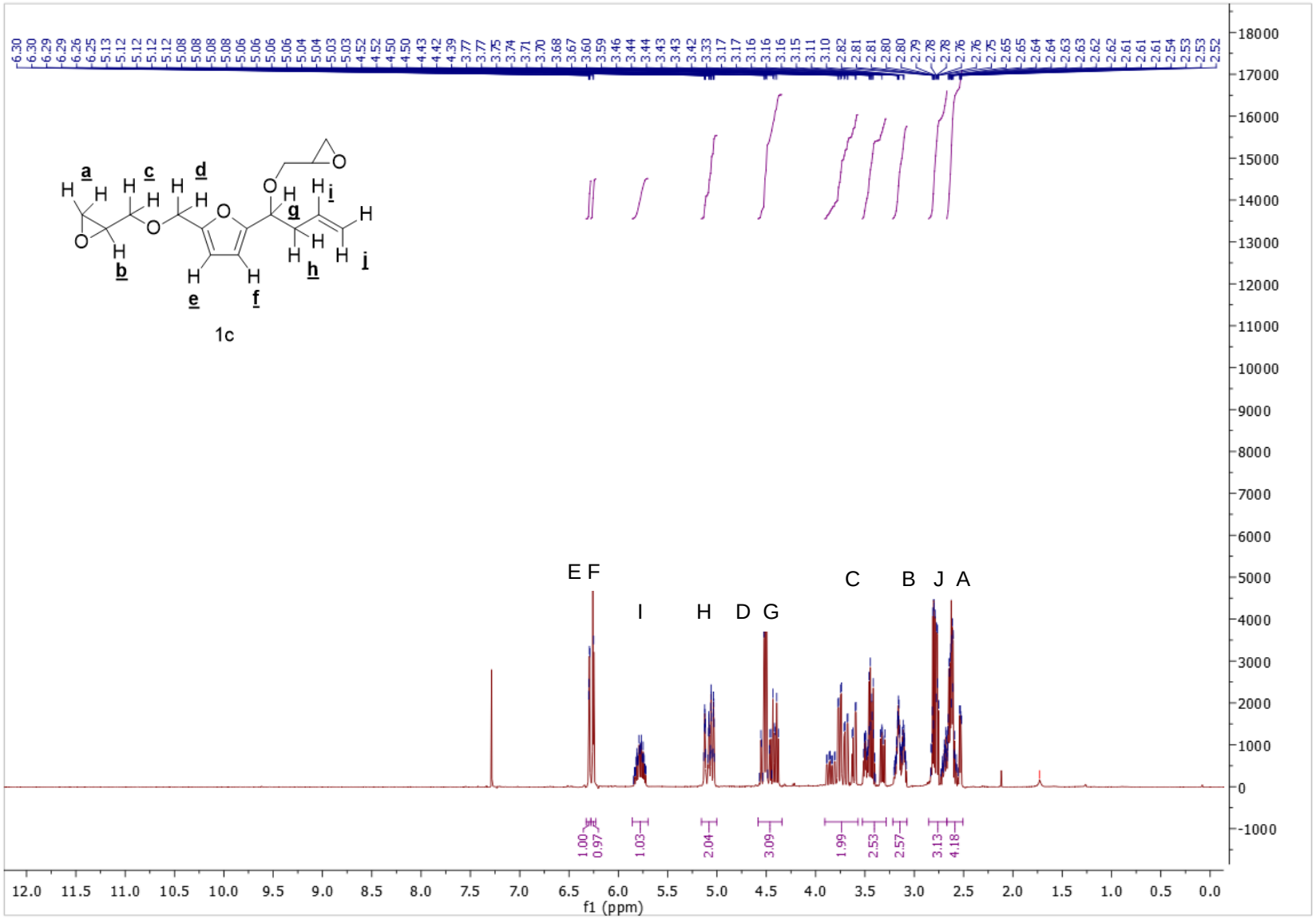

C9. ^{1}H NMR ($CDCl_3$) spectrum of Compound **4c**.

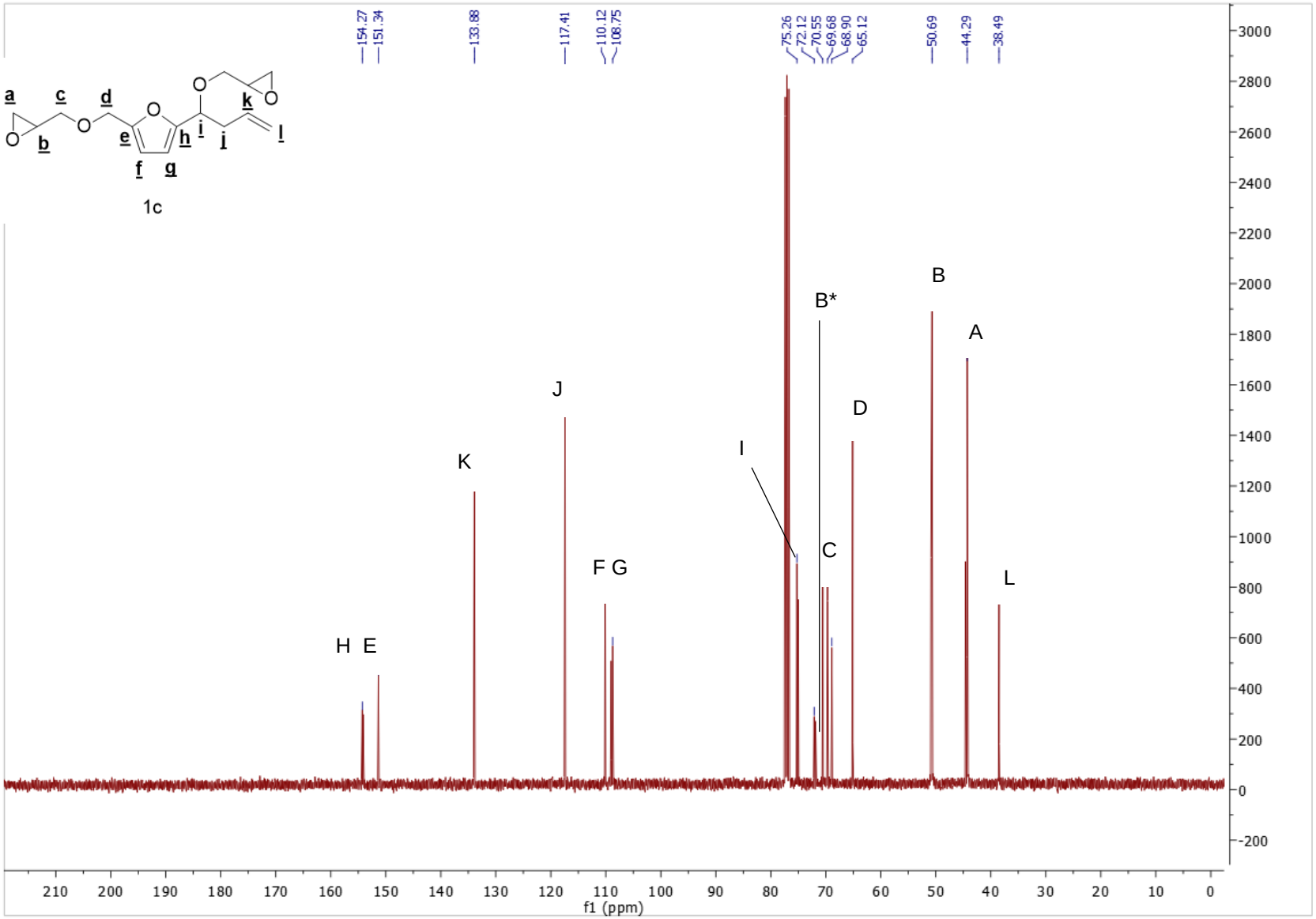

C10. ^{13}C NMR ($CDCl_3$) spectrum of Compound **4c**.

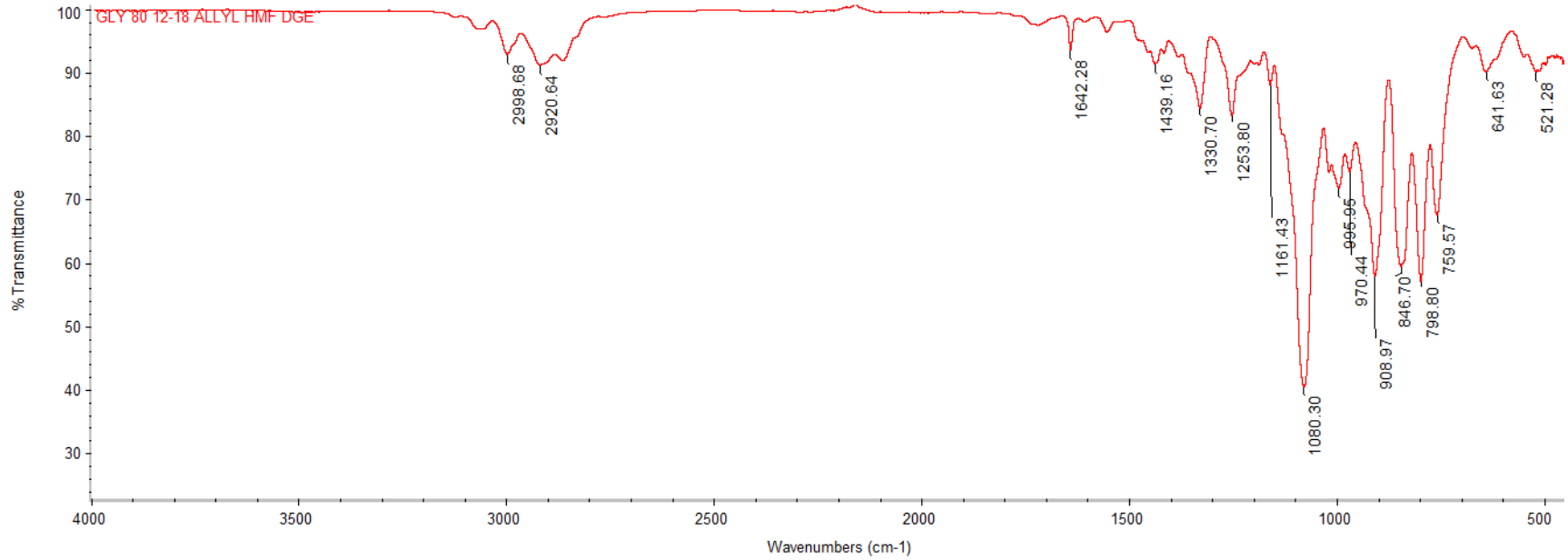

C11. FT-IR spectrum of Compound **4c**.

C12. HRMS (ESI, Na+) spectrum of compound **4c**.

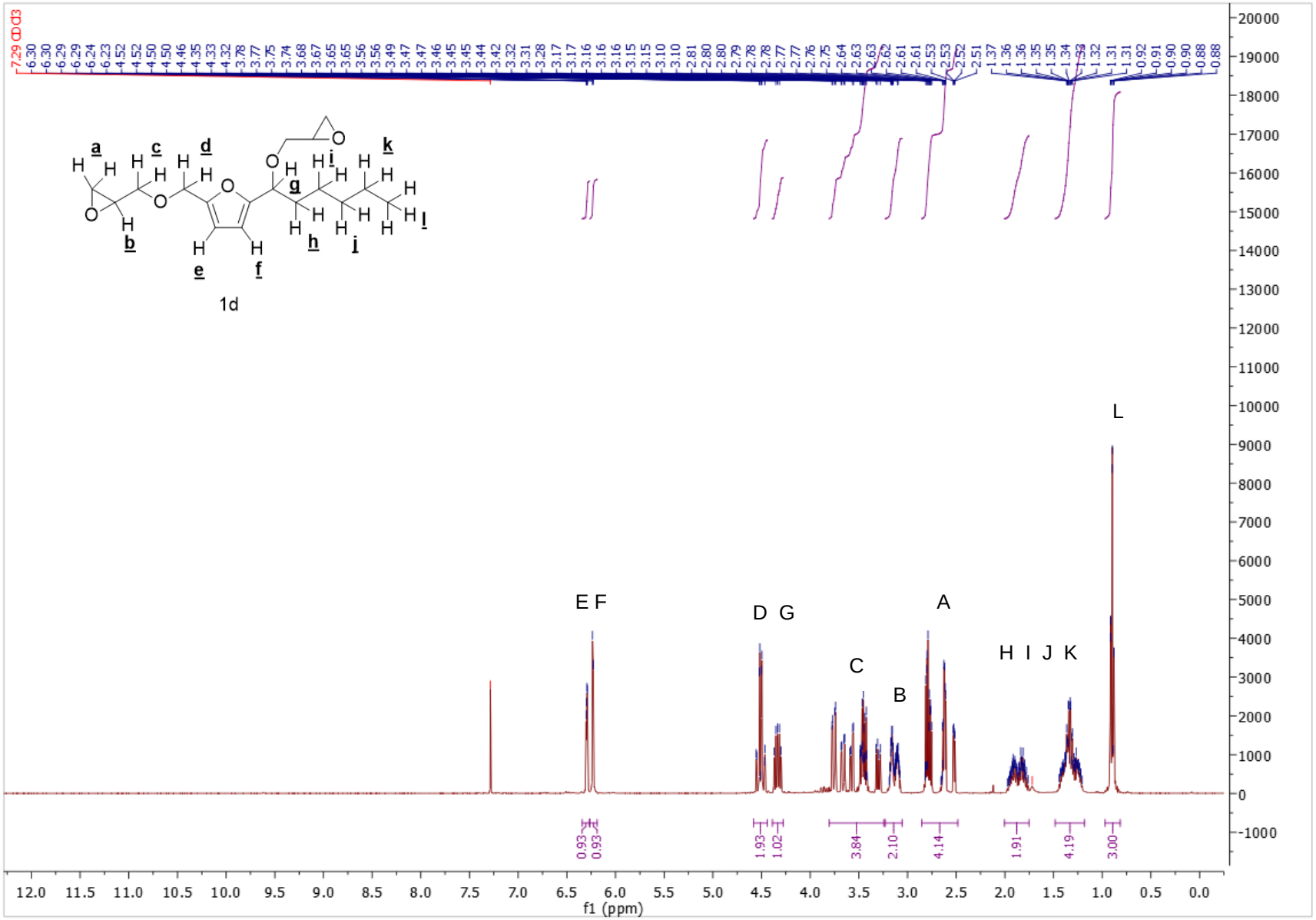

C13. ^{1}H NMR ($CDCl_3$) spectrum of Compound **4d**.

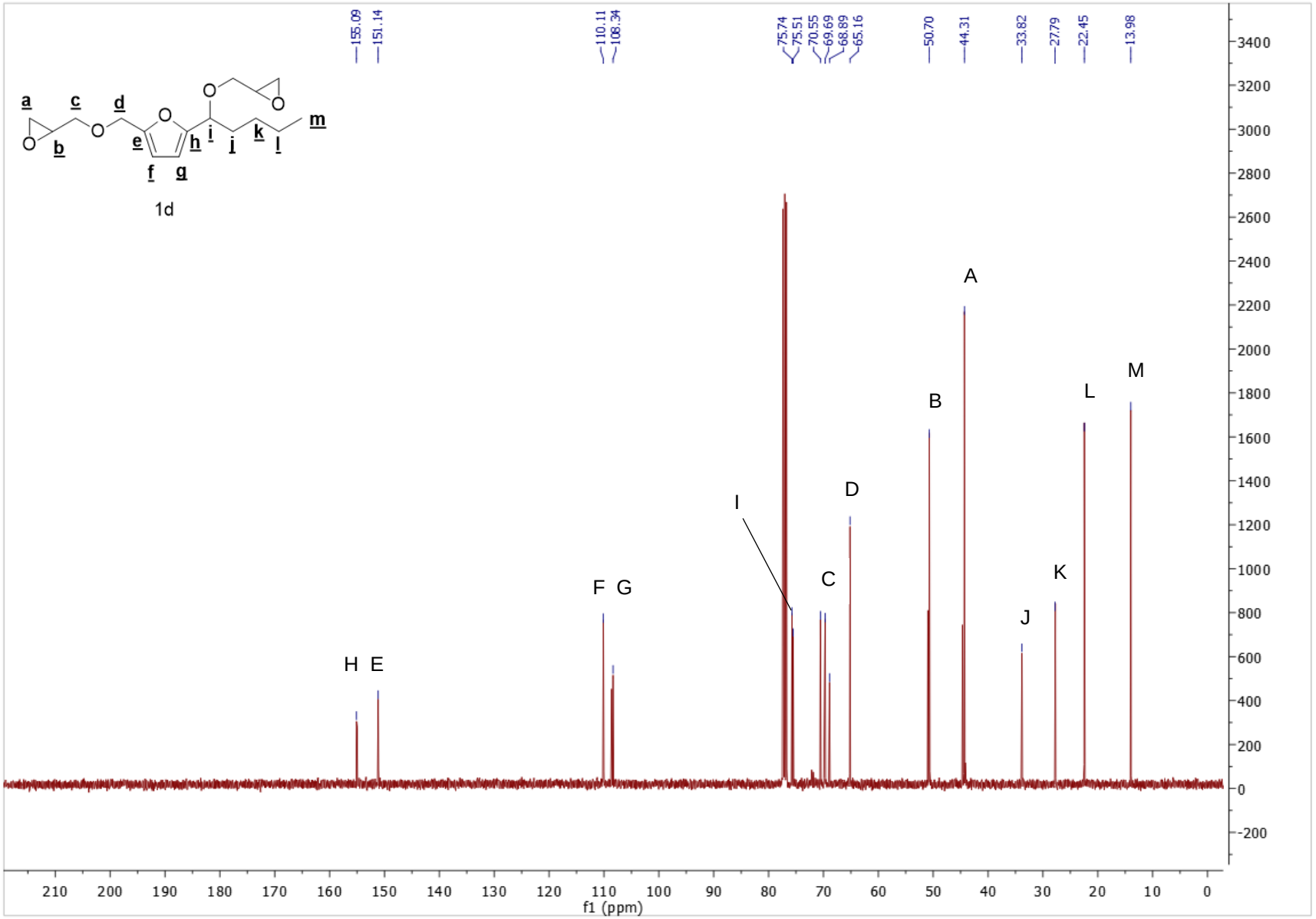

C14. ^{13}C NMR ($CDCl_3$) spectrum of Compound **4d**.

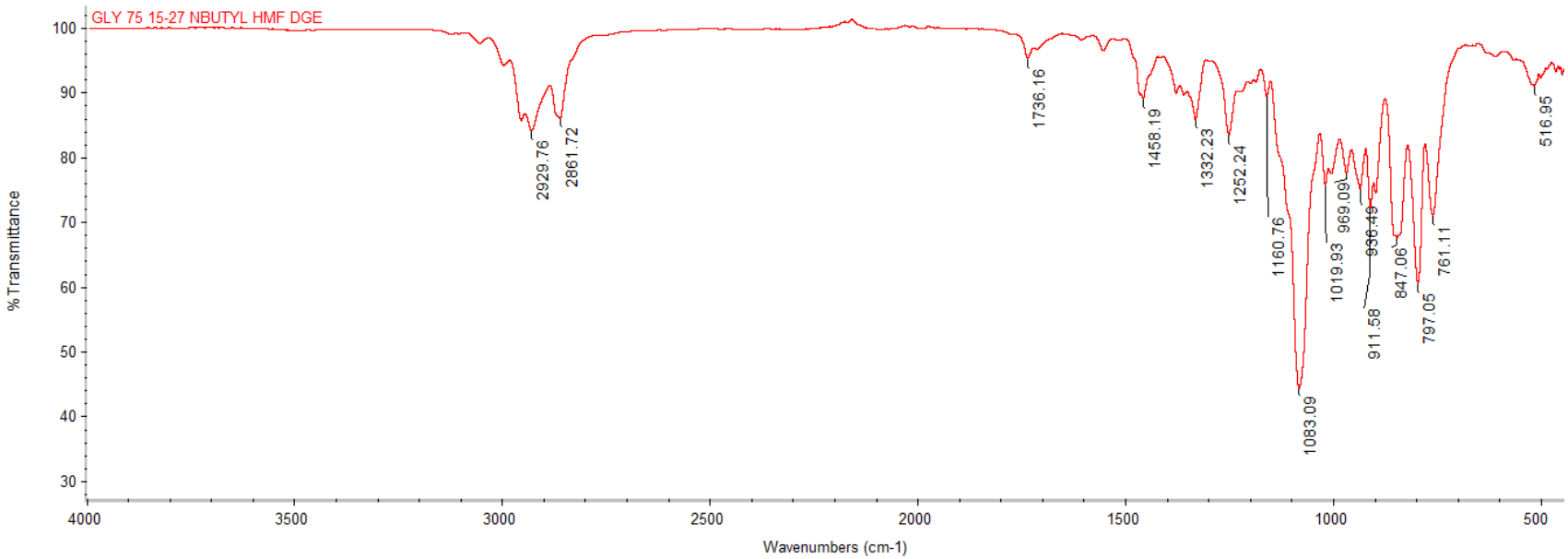

C15. FT-IR spectrum of Compound **4d**.

C16. HRMS (ESI, Na+) spectrum of compound **4d**.

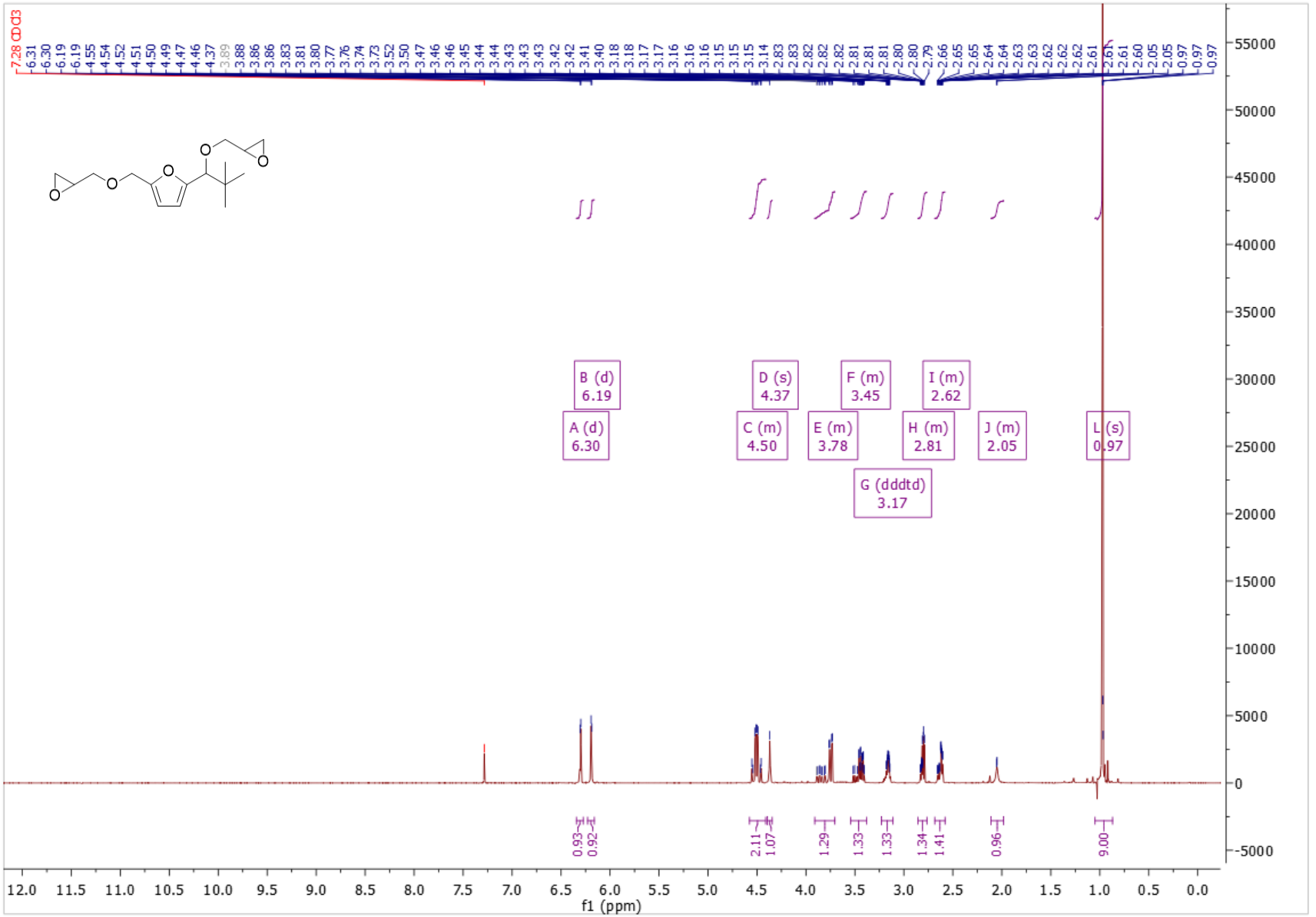

C17. ^{1}H NMR ($CDCl_3$) spectrum of Compound **4e**. *contains monoglycidyl ether impurity.

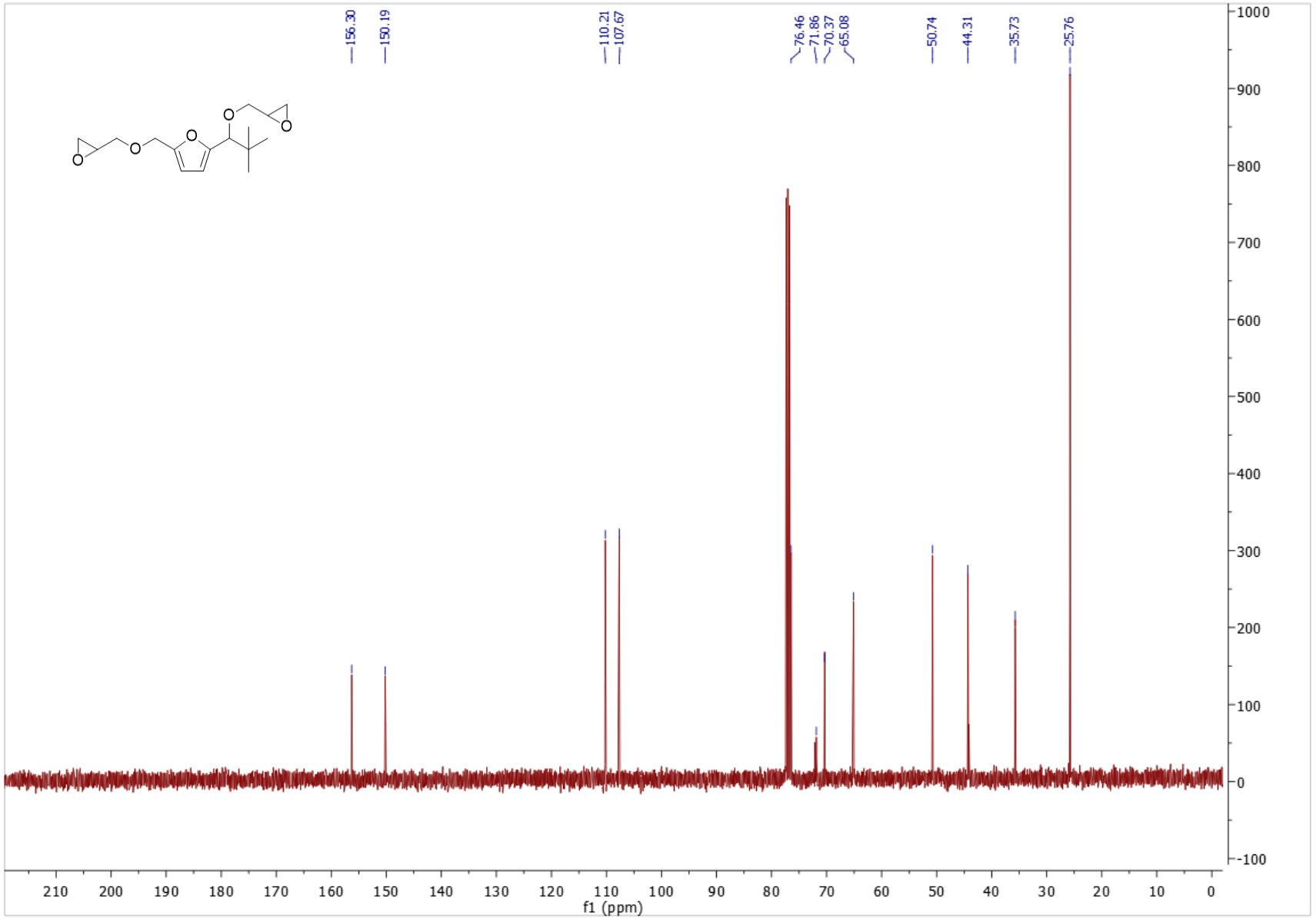

C18. ^{13}C NMR ($CDCl_3$) spectrum of Compound **4e**.

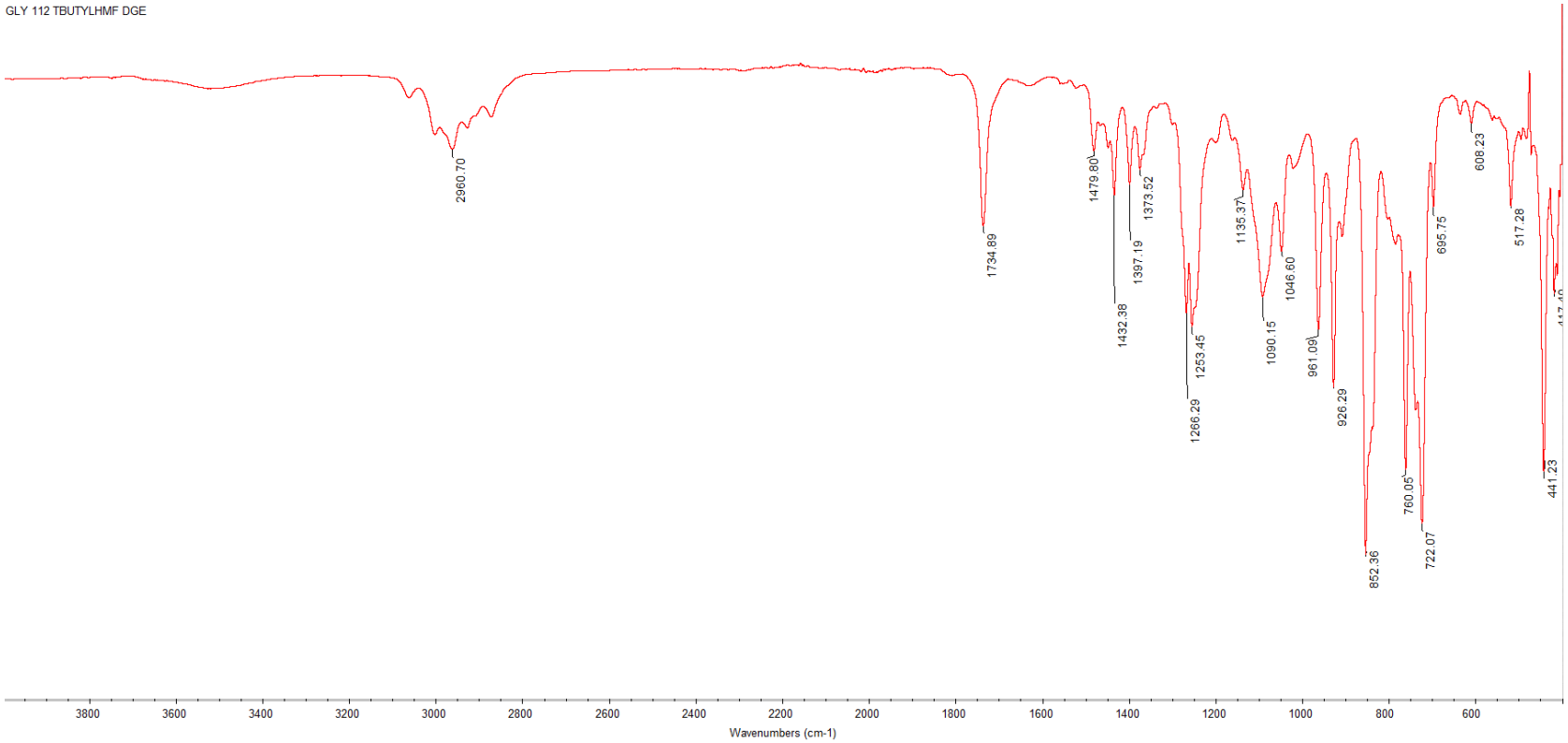

C19. FT-IR spectrum of Compound **4e**. *contains monoglycidyl ether impurity.

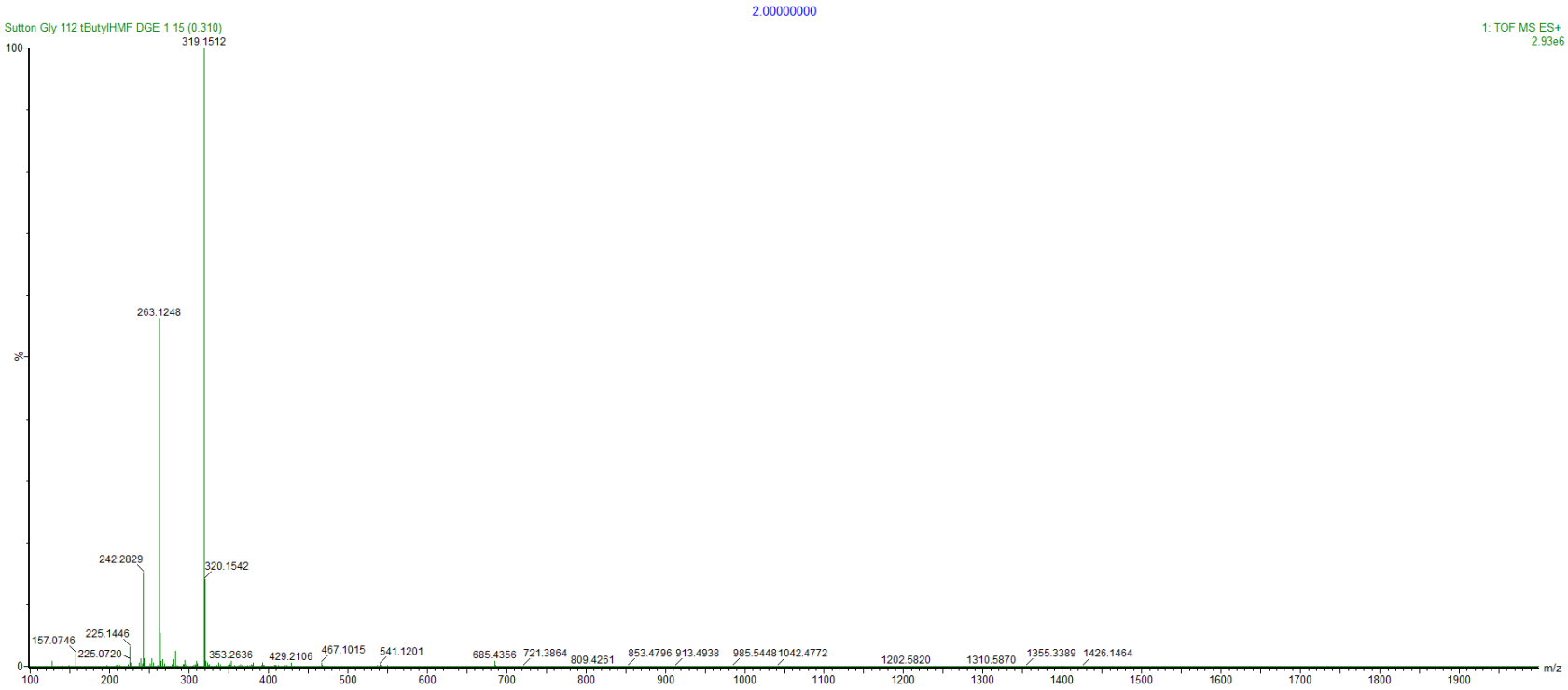

C20. HRMS (ESI, Na+) spectrum of compound **4e**.

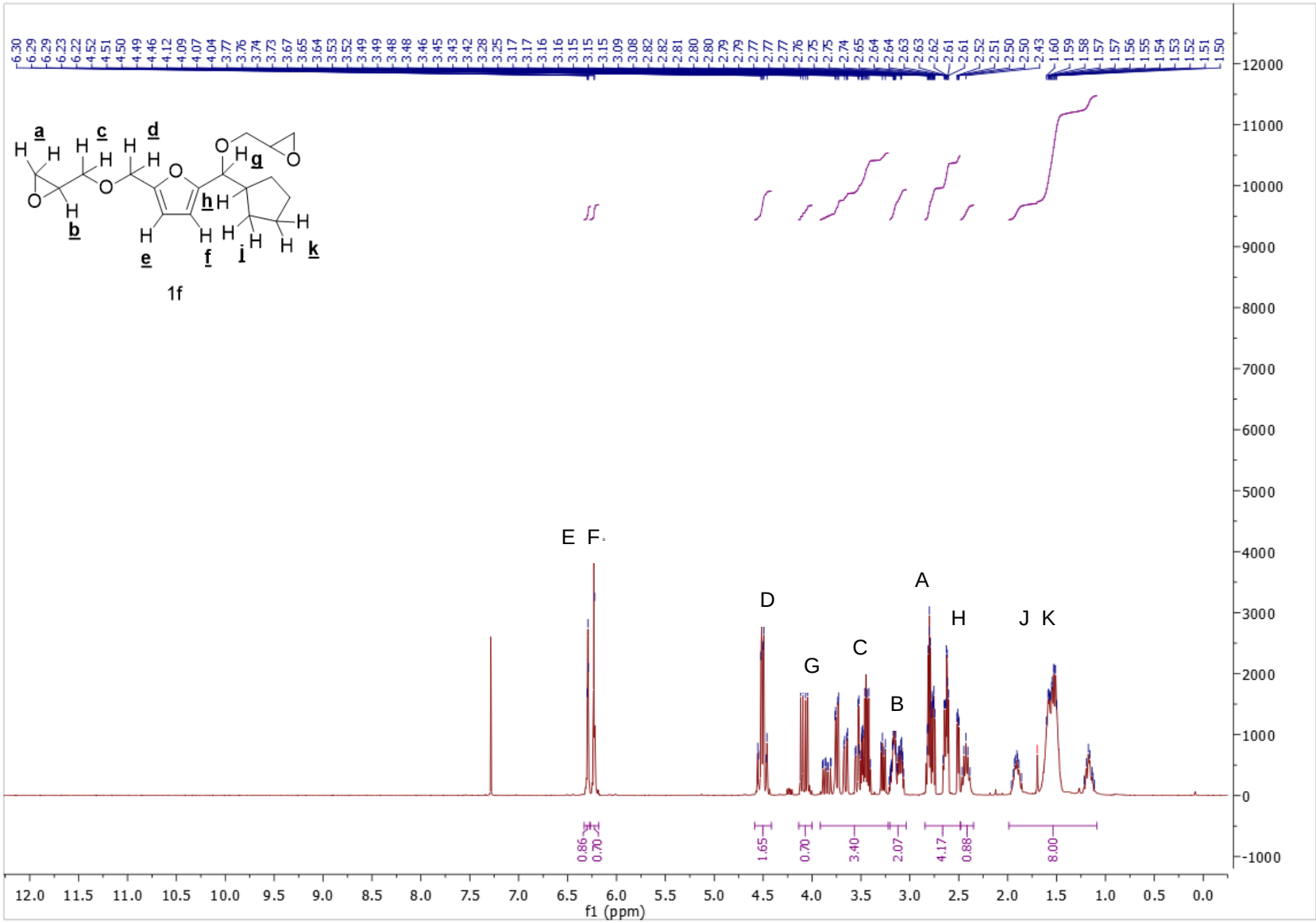

C21. ^{1}H NMR ($CDCl_3$) spectrum of Compound **4f**.

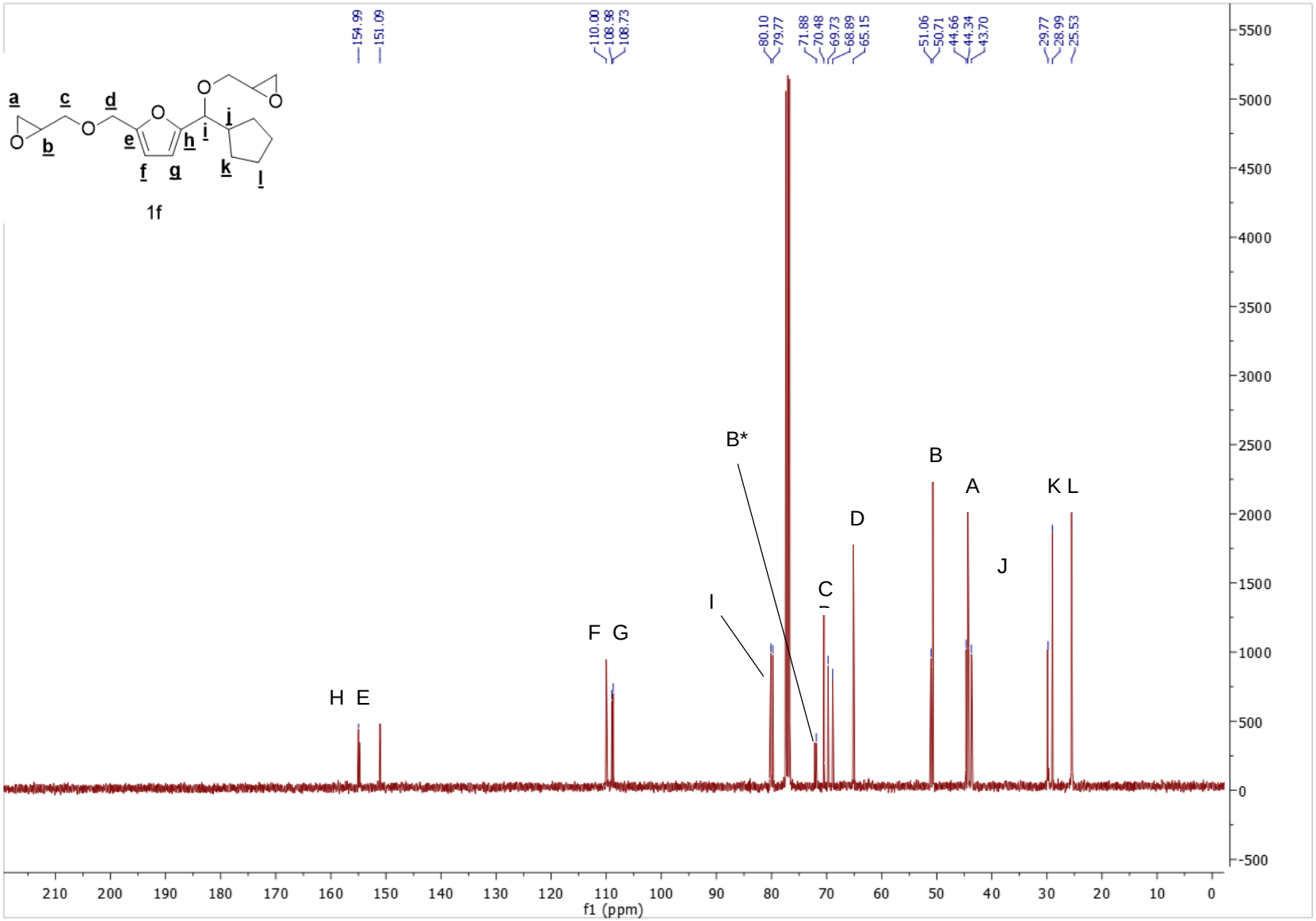

C22. ^{13}C NMR ($CDCl_3$) spectrum of Compound **4f**.

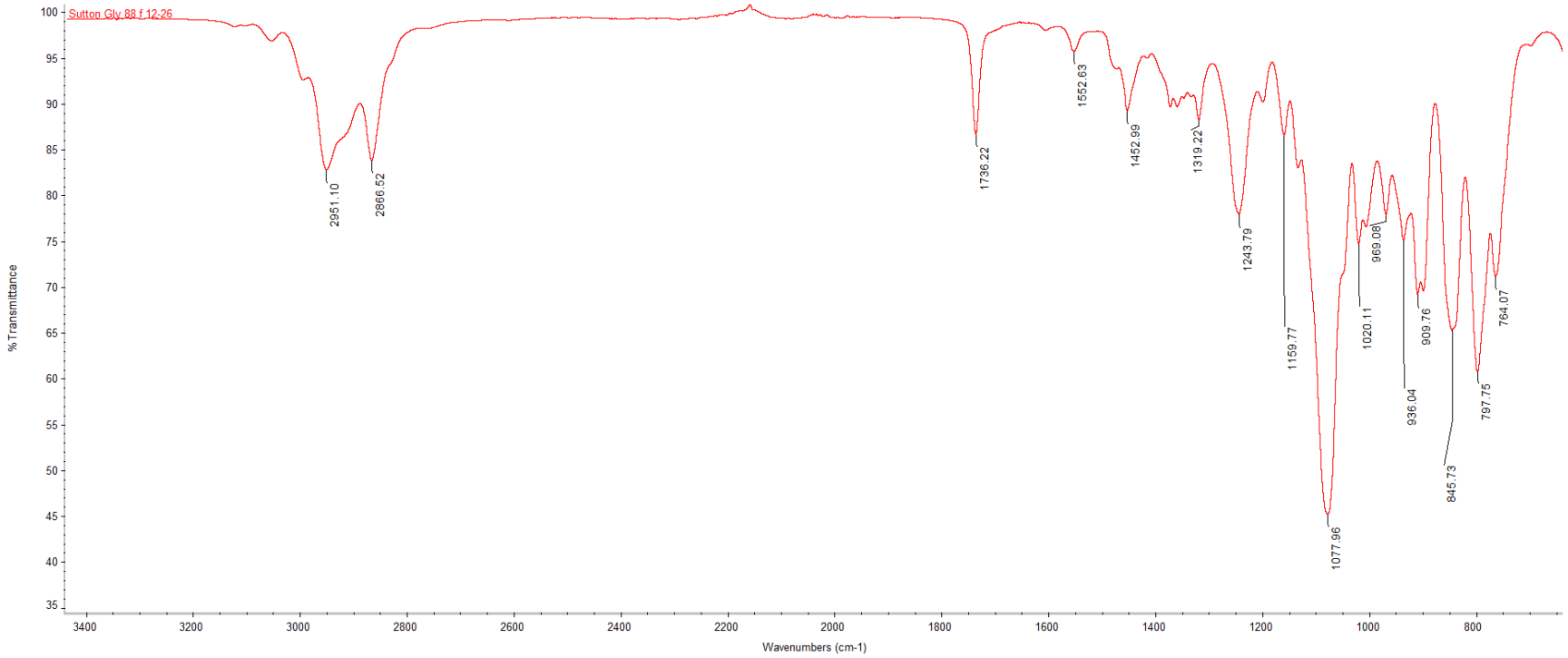

C23. FT-IR spectrum of Compound **4f**.

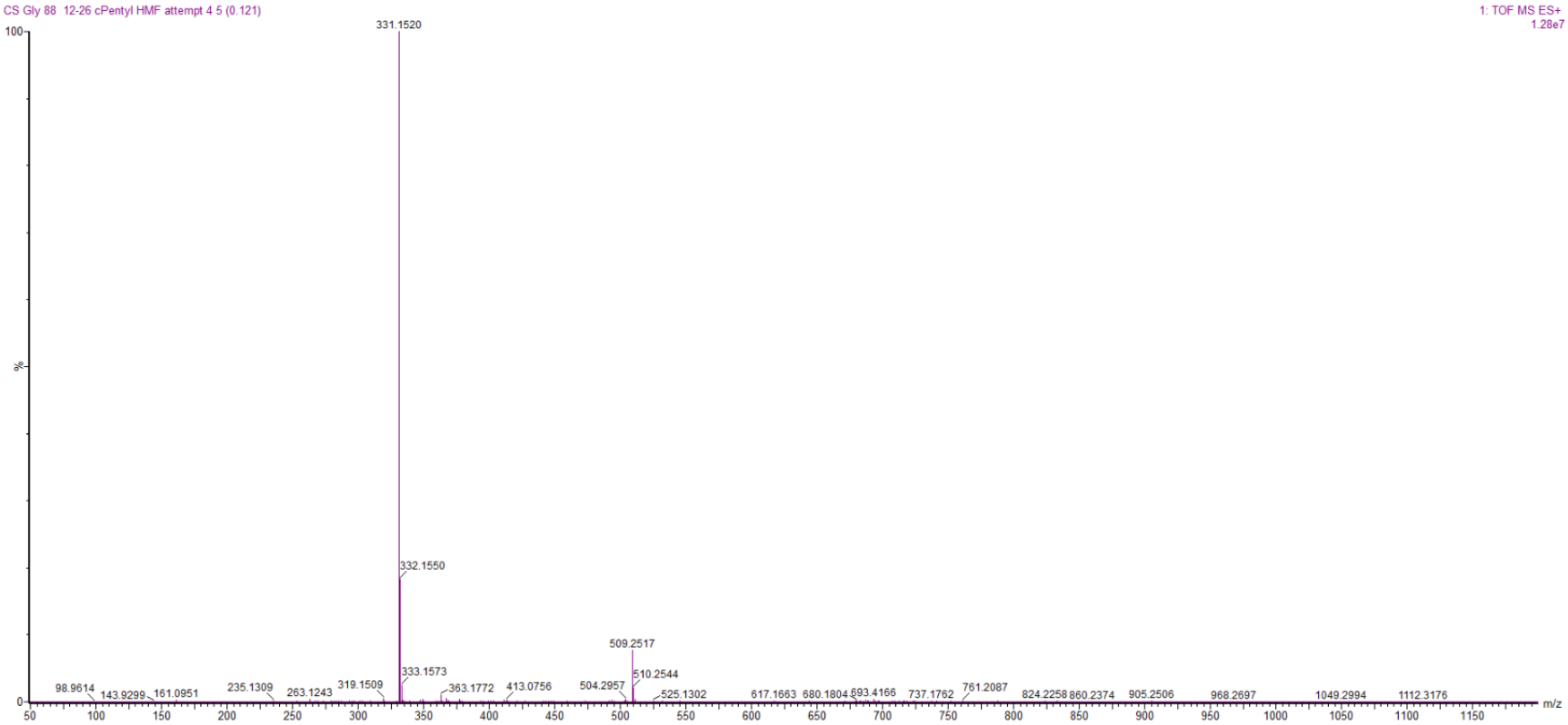

C24. HRMS (ESI, Na+) spectrum of compound **4f**.

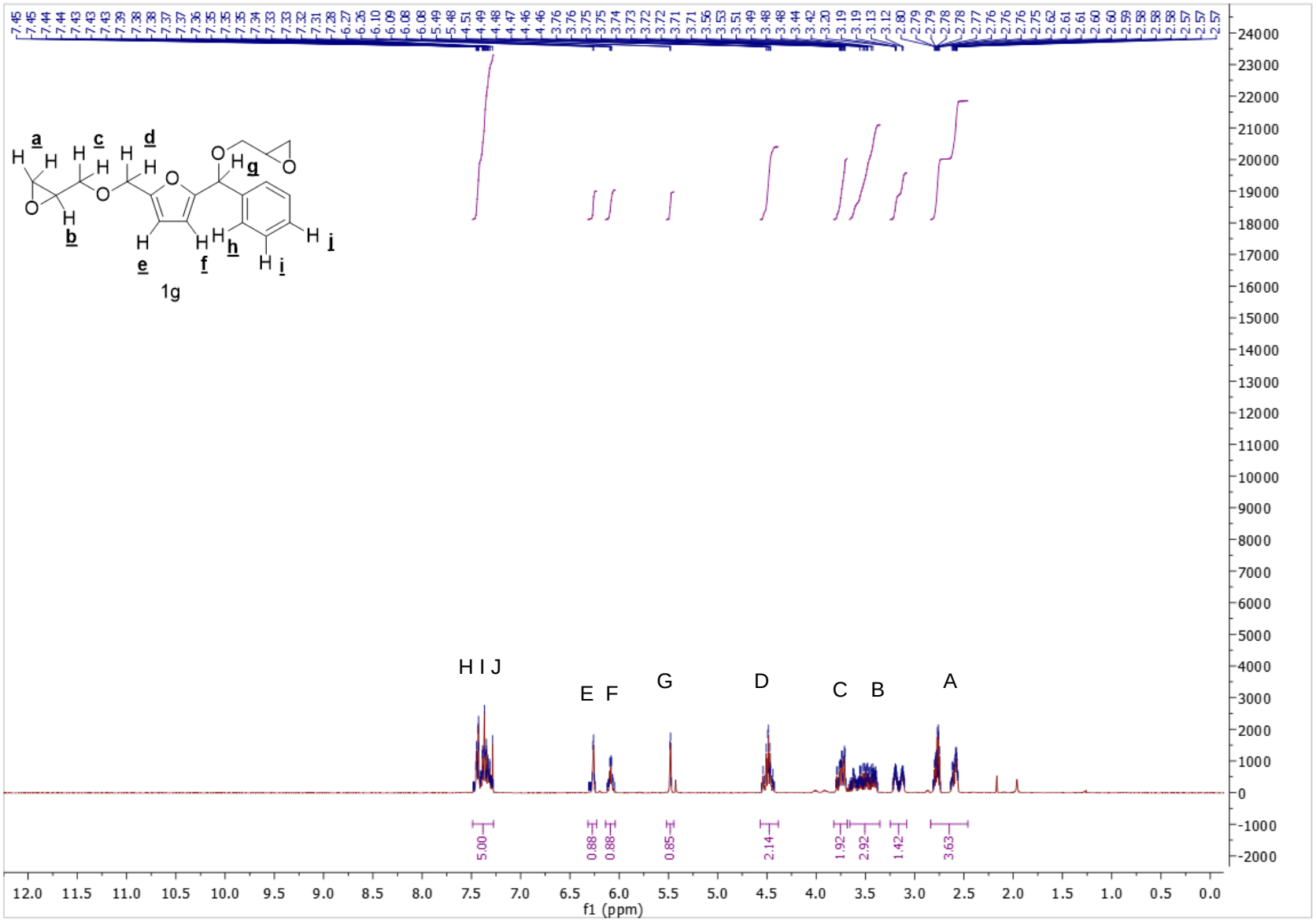

C25. ^{1}H NMR ($CDCl_3$) spectrum of Compound **4g**.

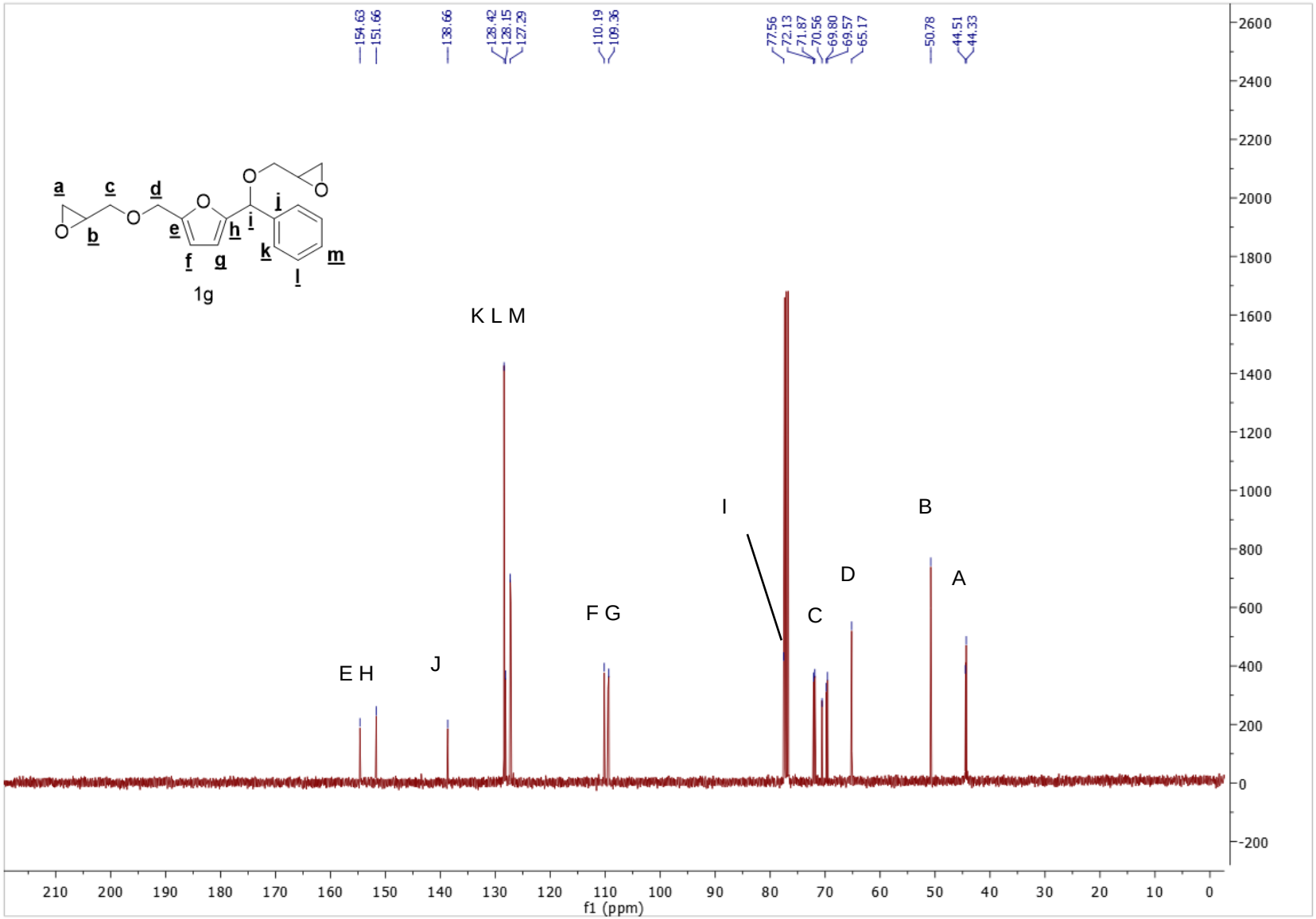

C26. ^{13}C NMR ($CDCl_3$) spectrum of Compound **4g**.

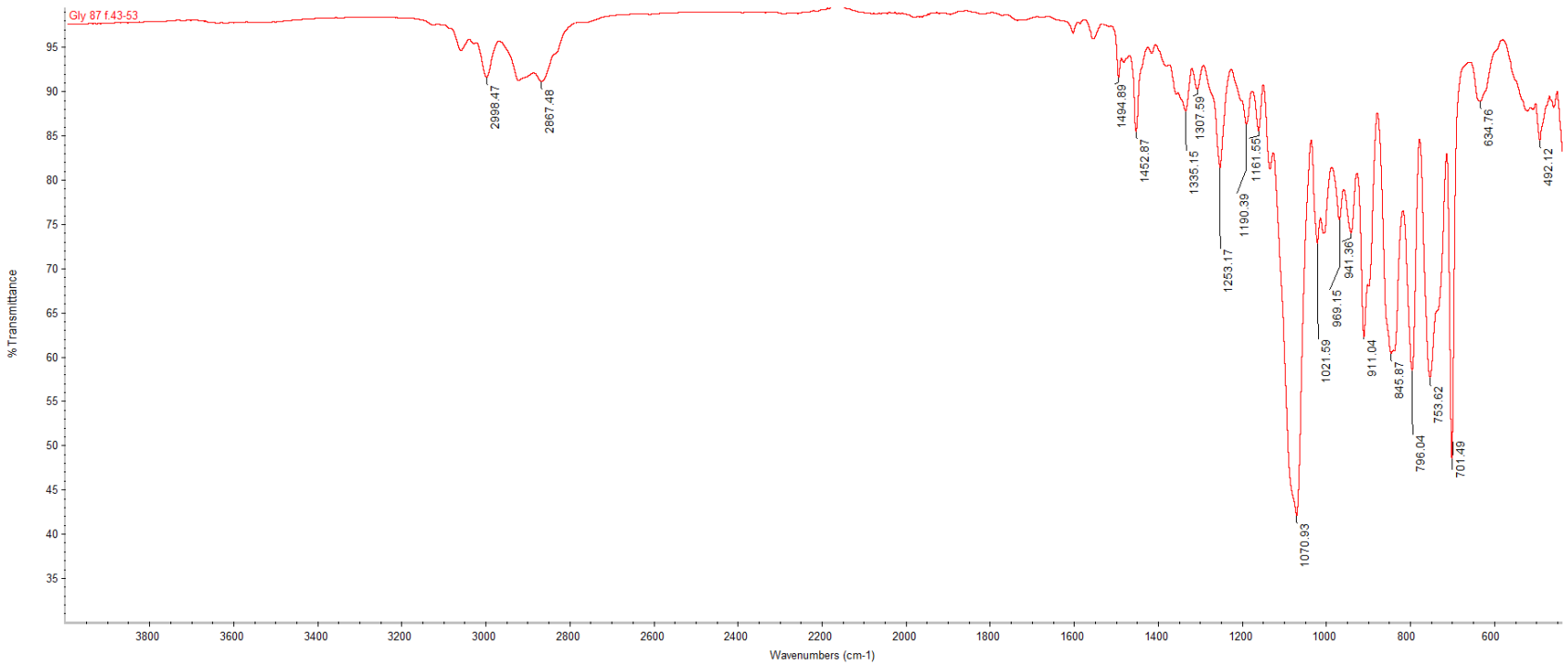

C27. FT-IR spectrum of Compound **4g**.

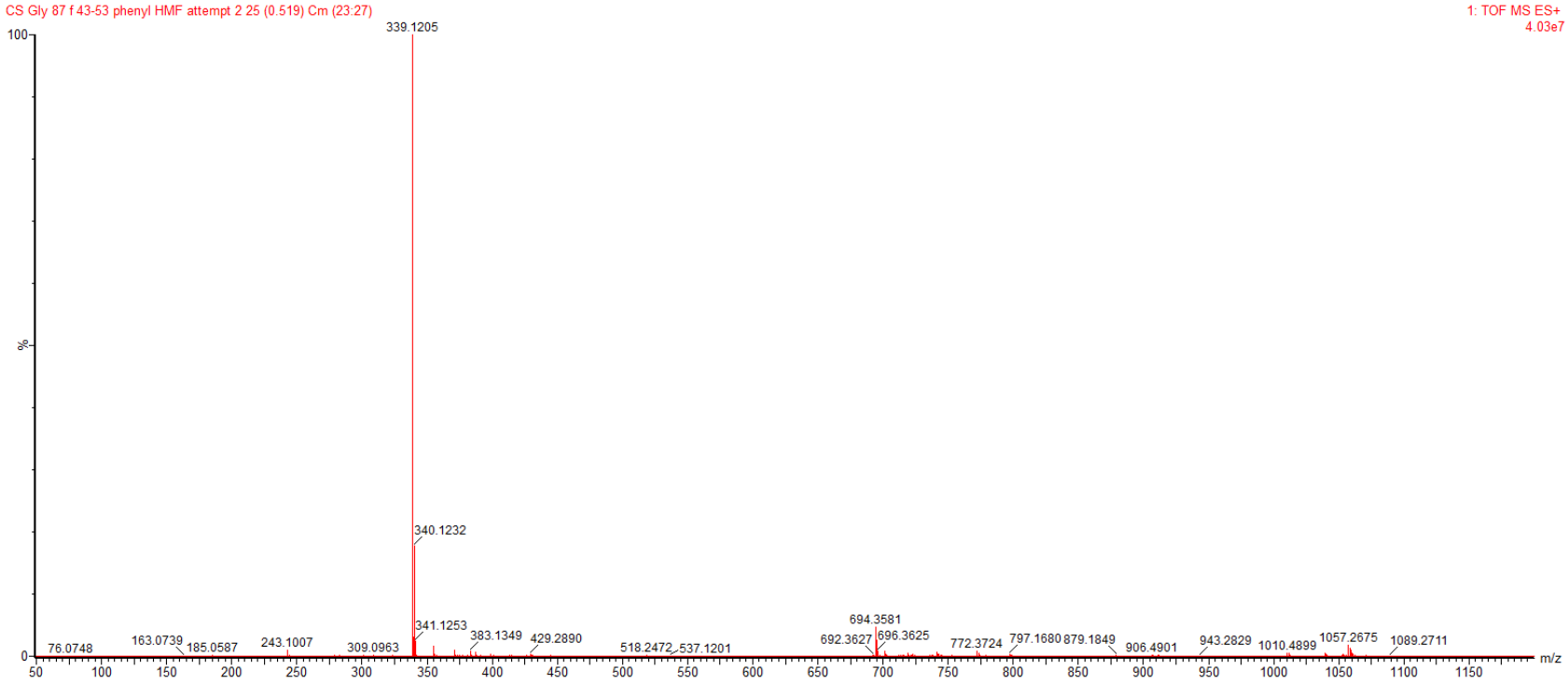

C28. HRMS (ESI, Na+) spectrum of compound **4g**.

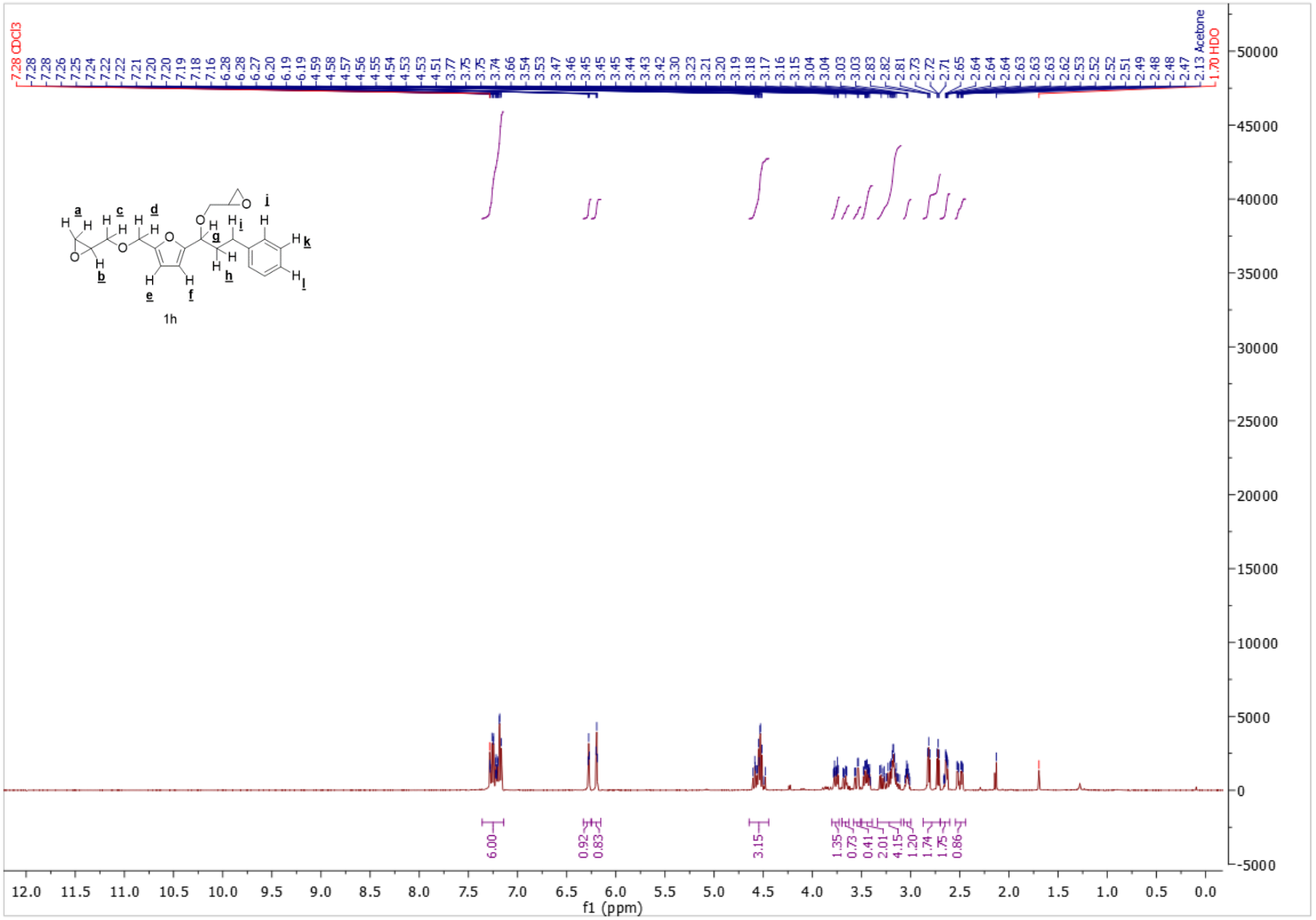

C29. ^{1}H NMR ($CDCl_3$) spectrum of Compound **4h**.

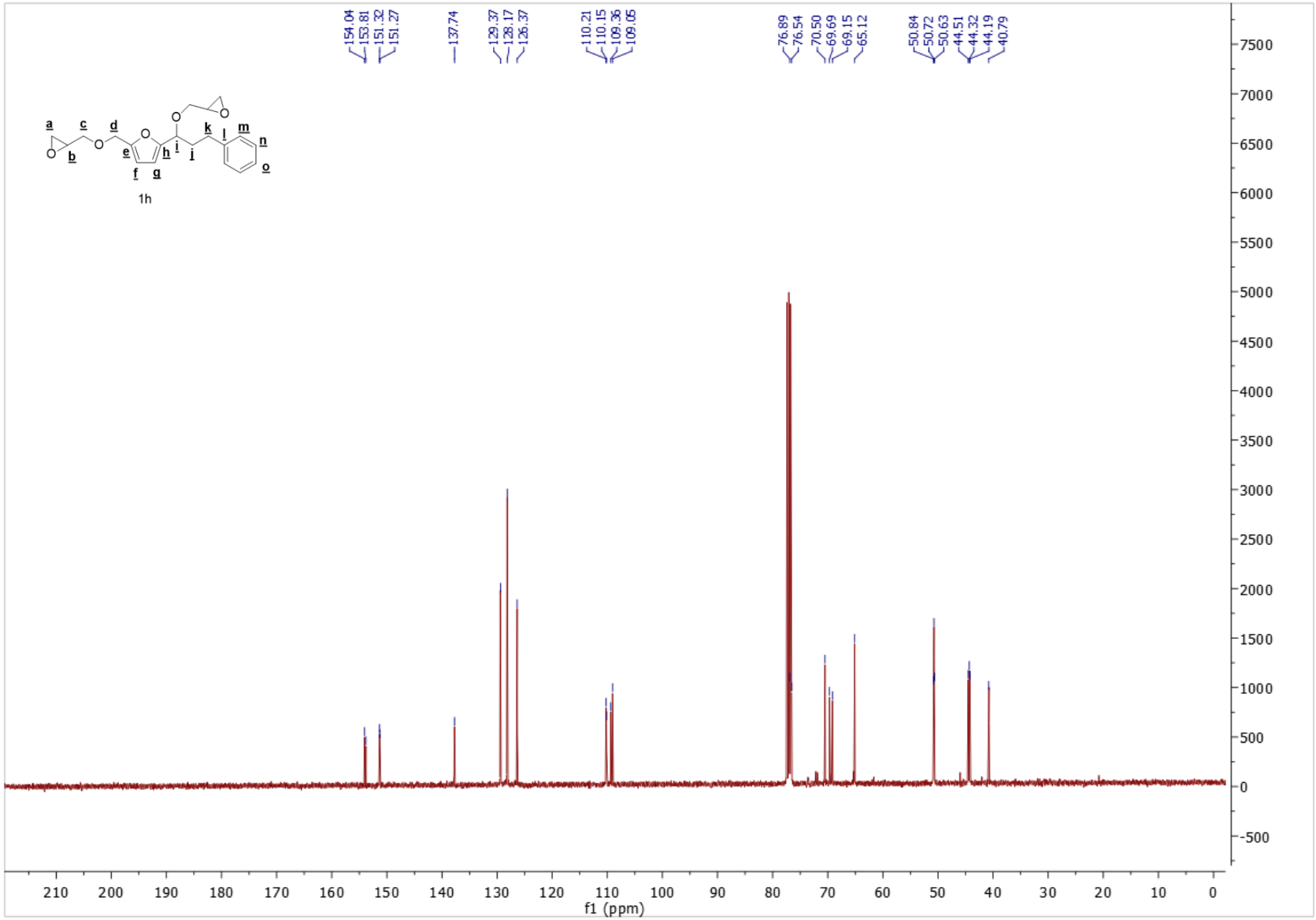

C30. ^{13}C NMR ($CDCl_3$) spectrum of Compound **4h**.

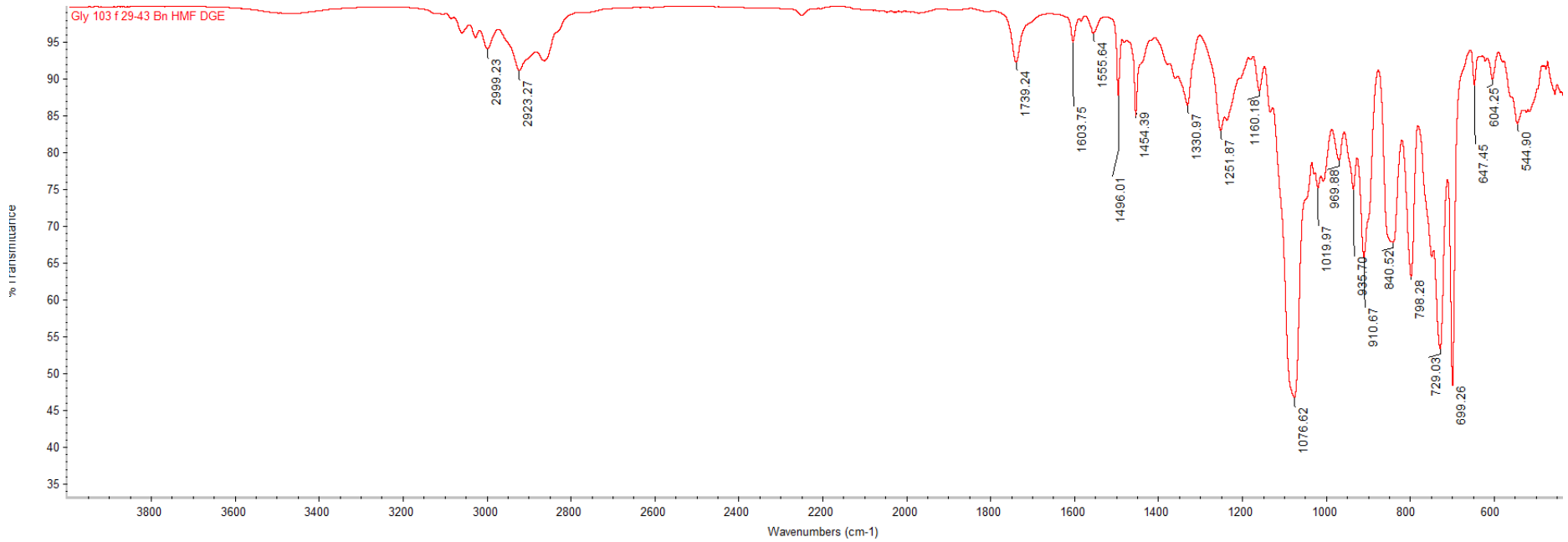

C31. FT-IR spectrum of Compound **4h**.

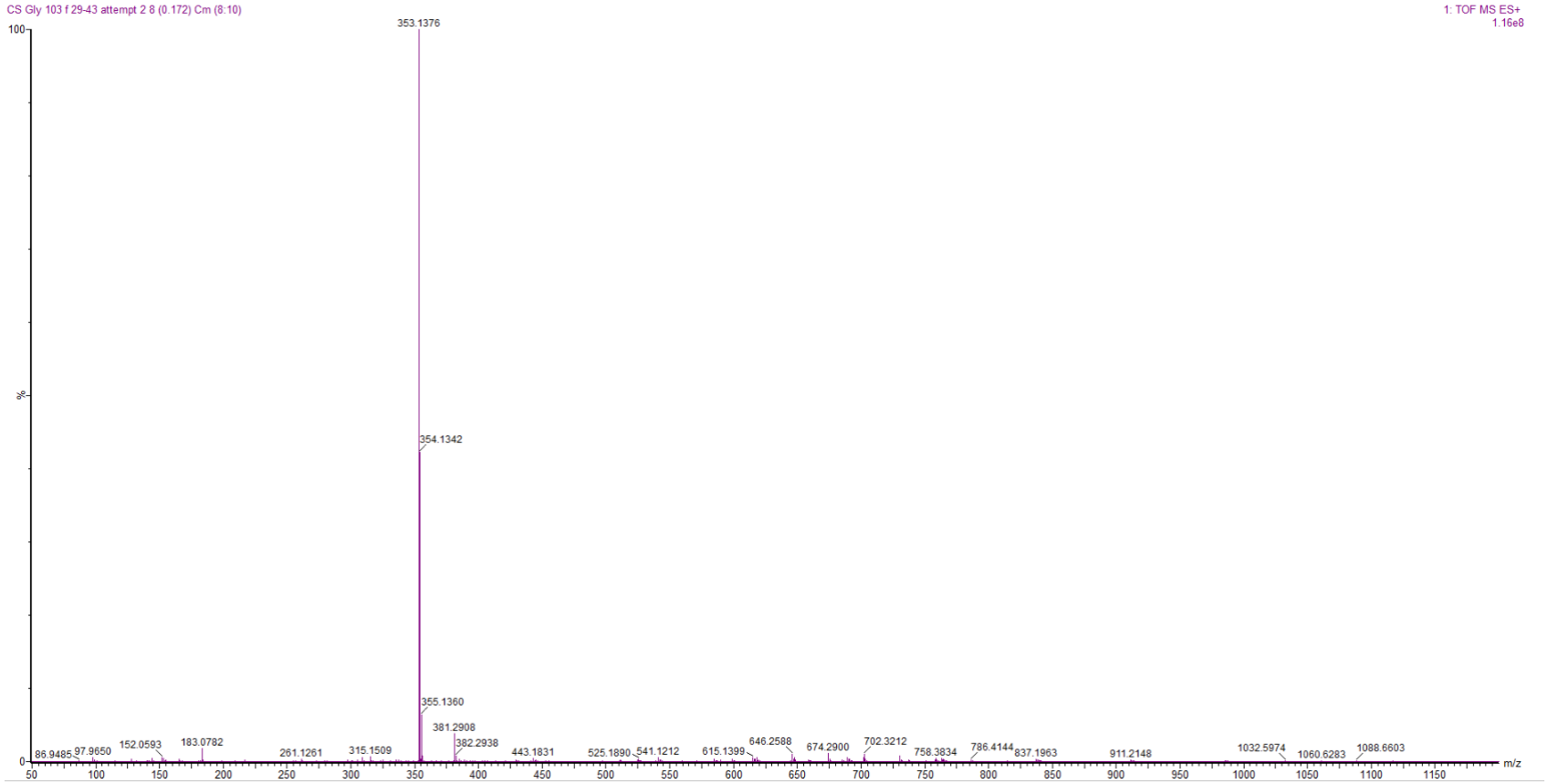

C32. HRMS (ESI, Na+) spectrum of compound **4h**.

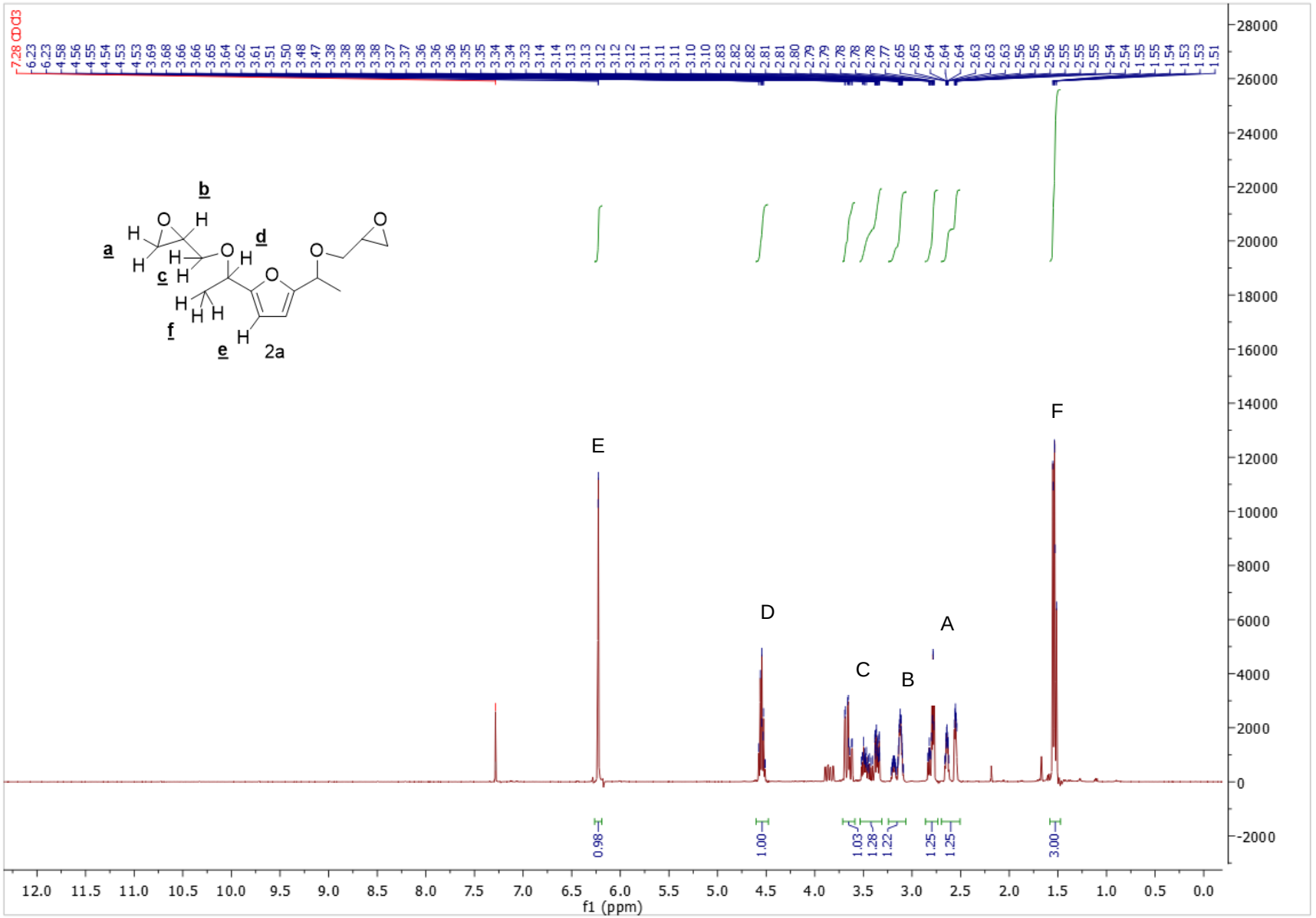

C33. ^{1}H NMR ($CDCl_3$) spectrum of Compound **5a**.

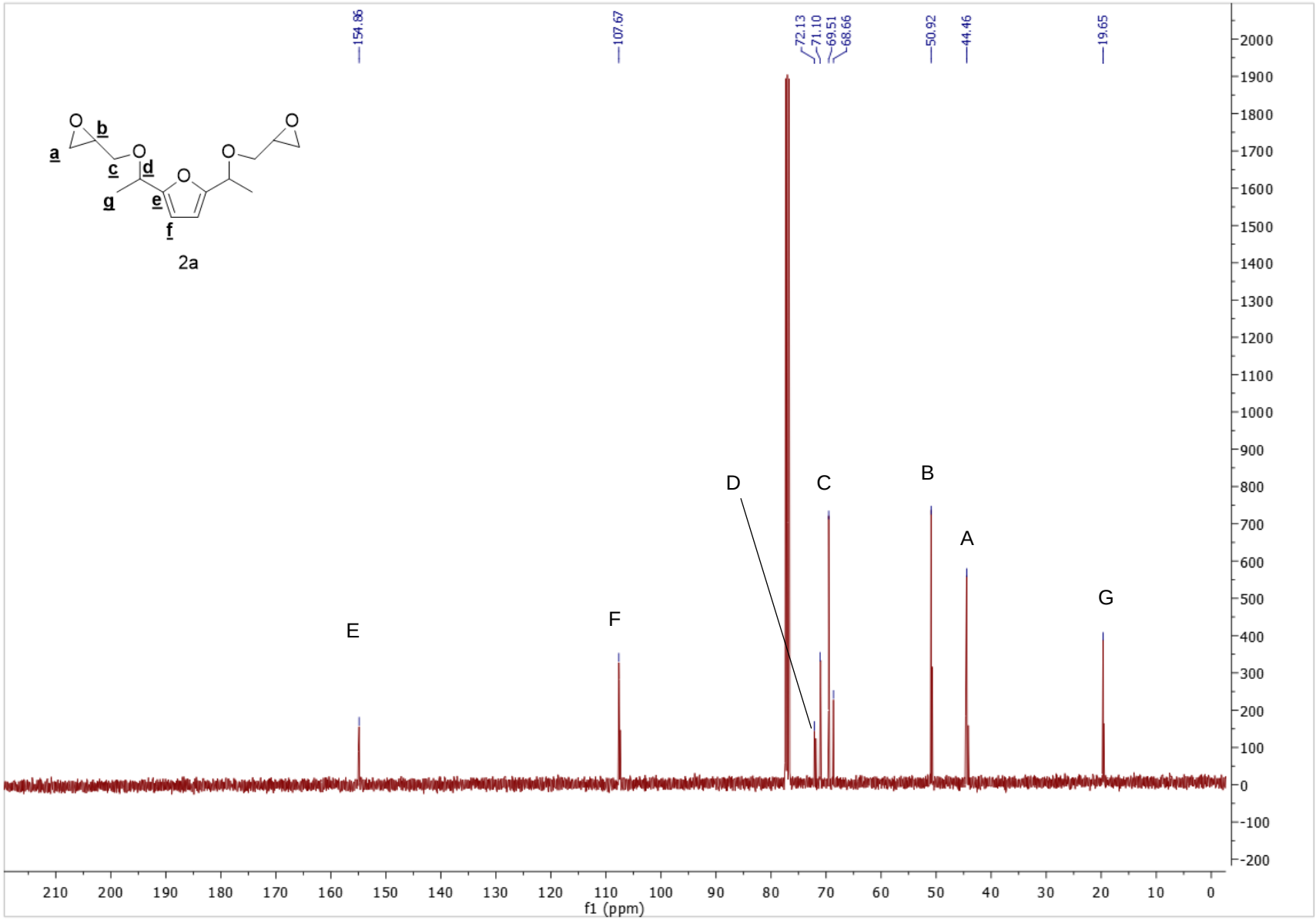

C34. ^{13}C NMR ($CDCl_3$) spectrum of Compound **5a**.

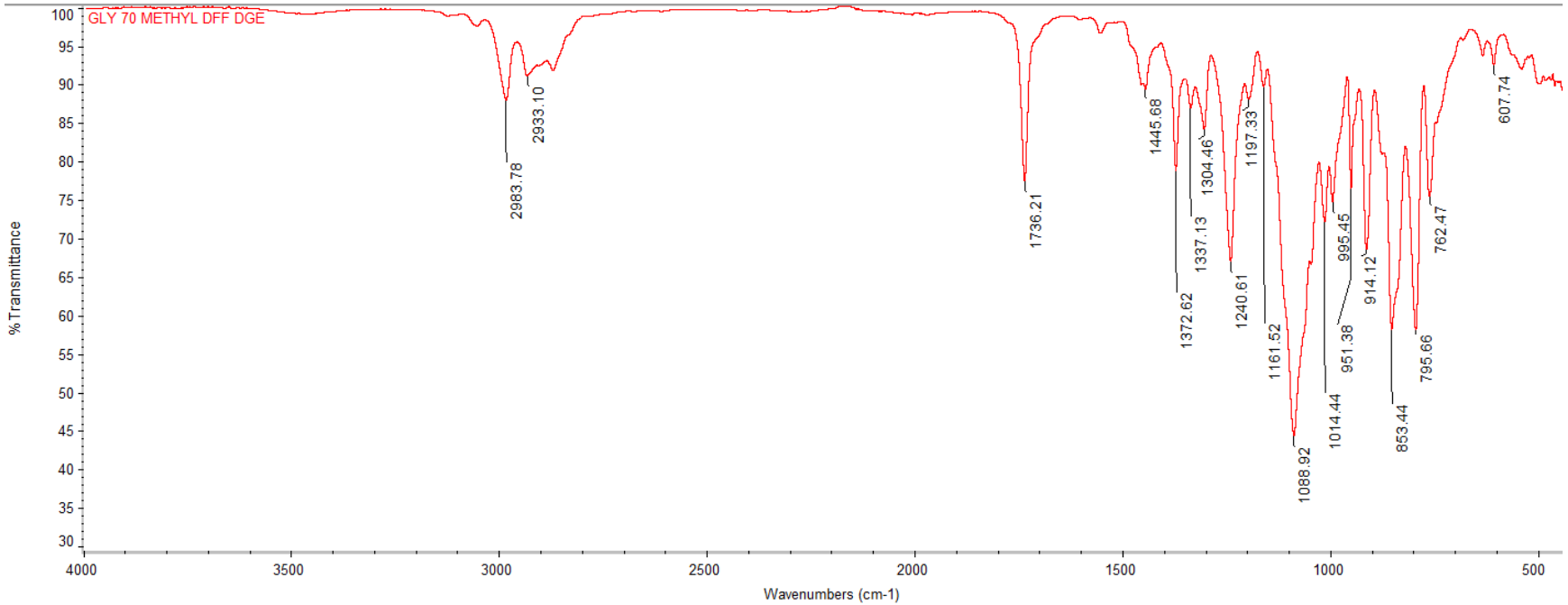

C35. FT-IR spectrum of Compound **5a**.

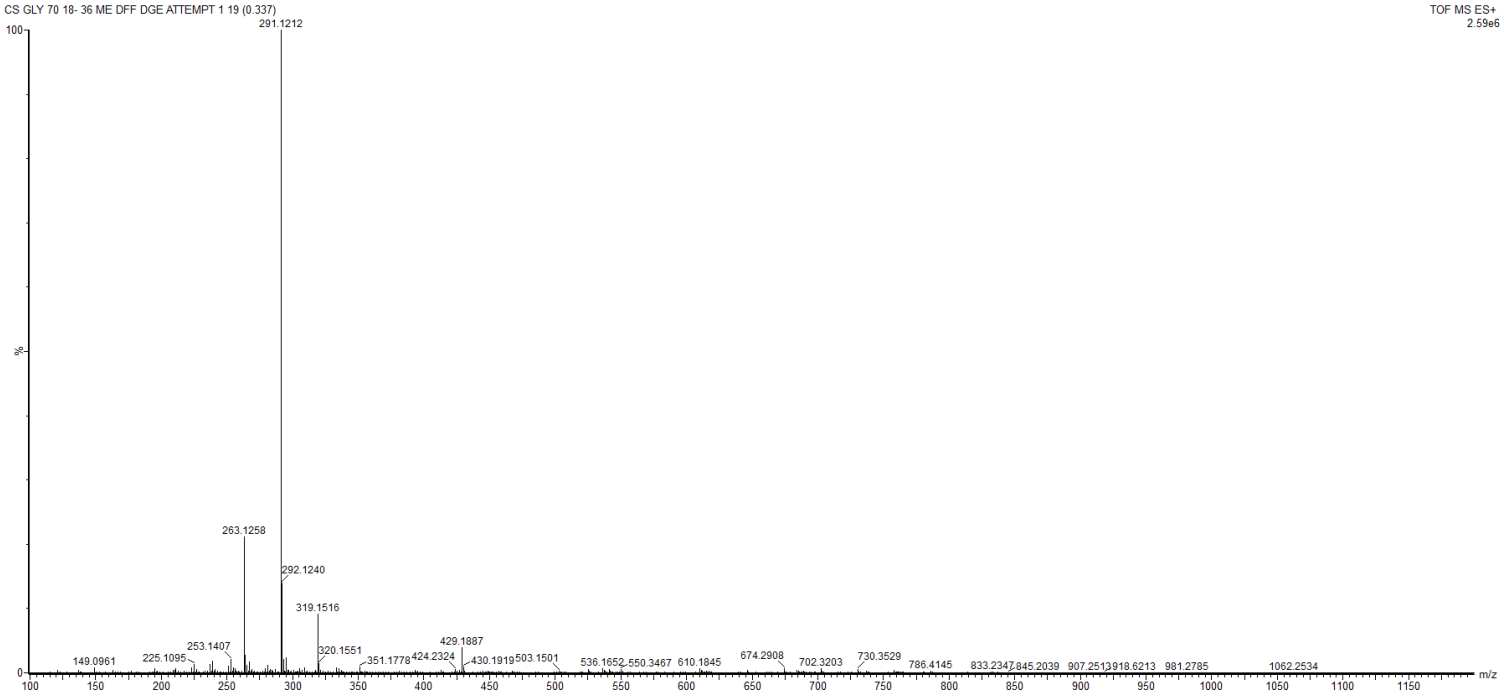

C36. HRMS (ESI, Na+) spectrum of compound **5a**.

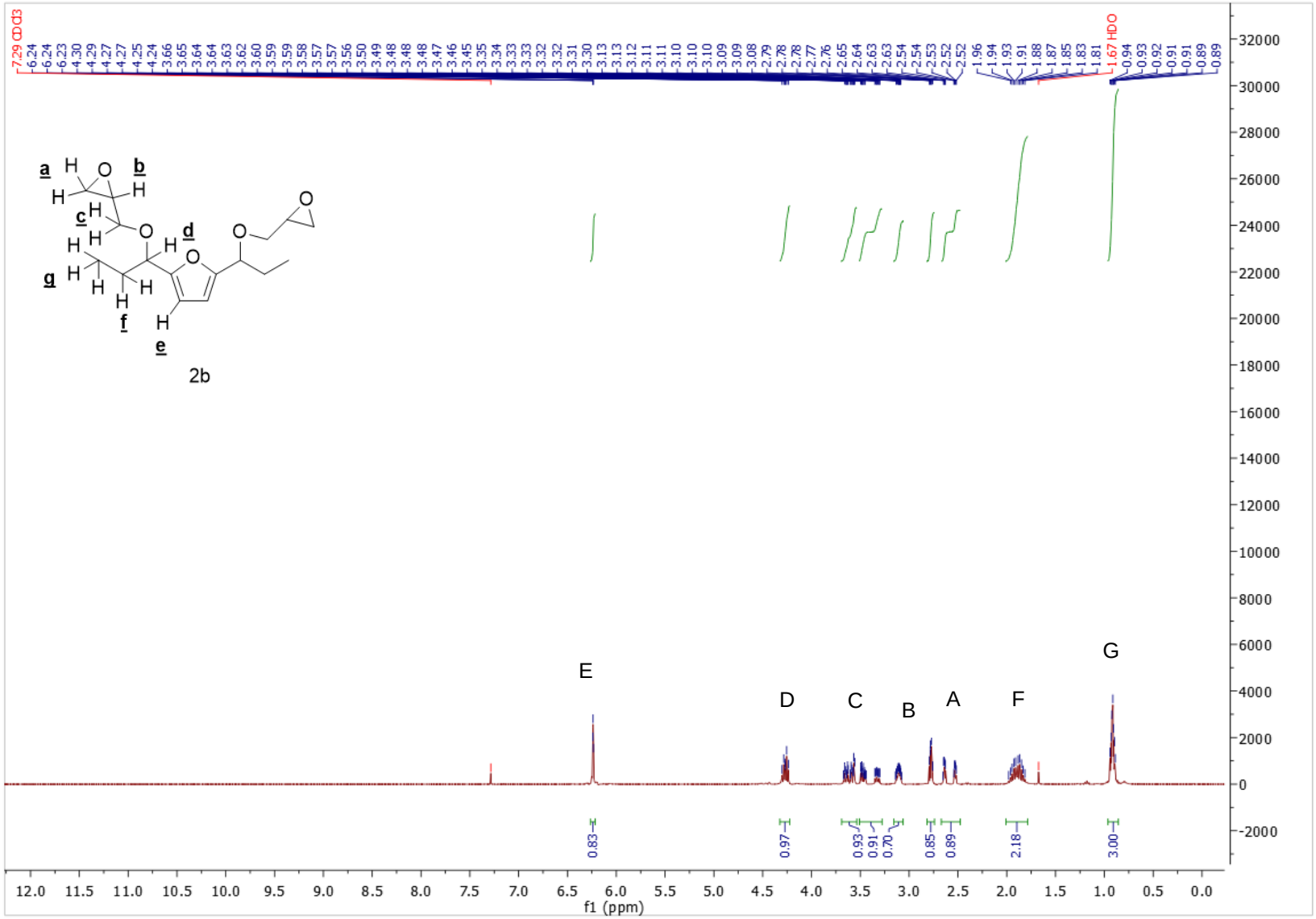

C37. ^{1}H NMR ($CDCl_3$) spectrum of Compound **5b**.

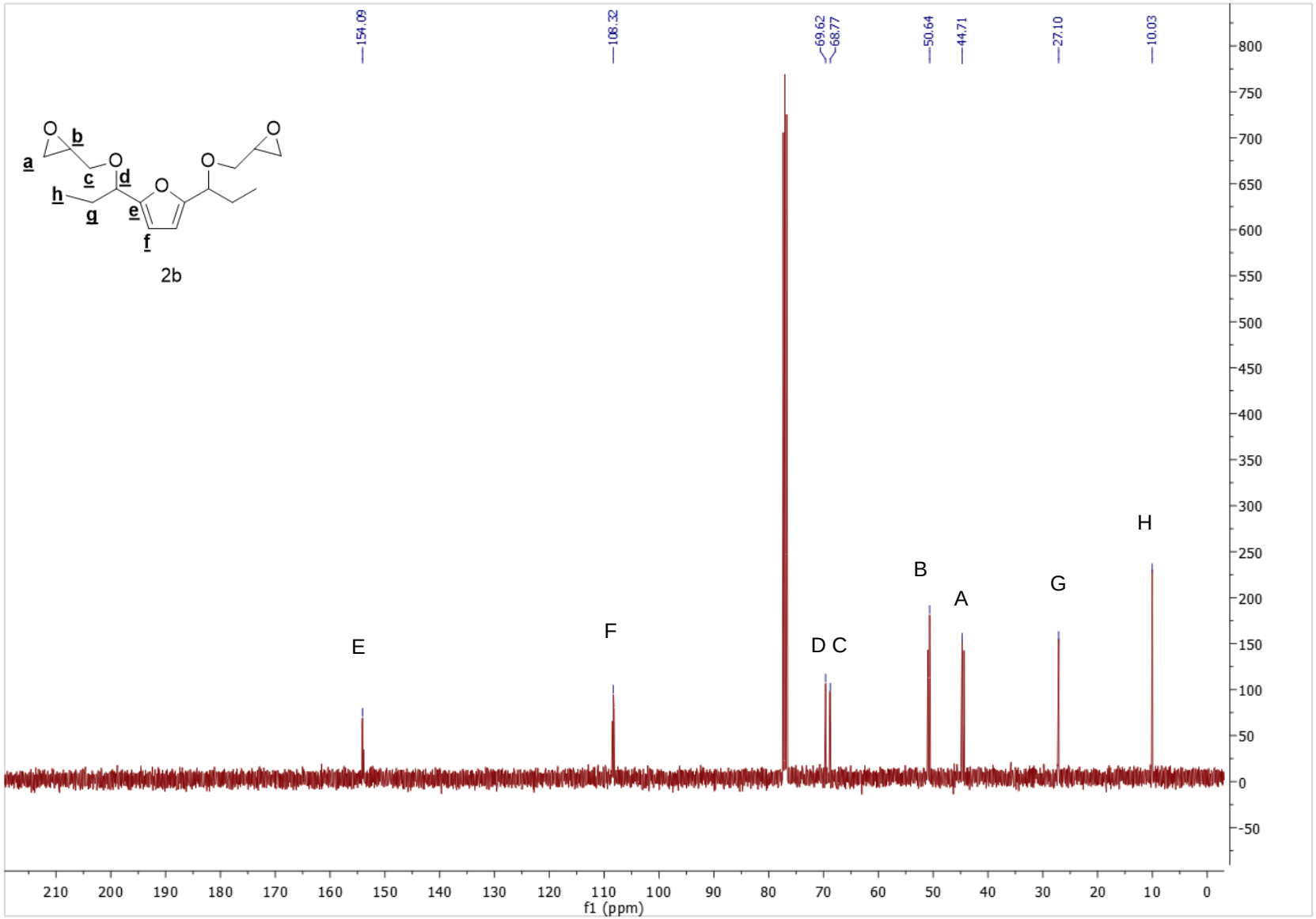

C38. ^{13}C NMR ($CDCl_3$) spectrum of Compound **5b**.

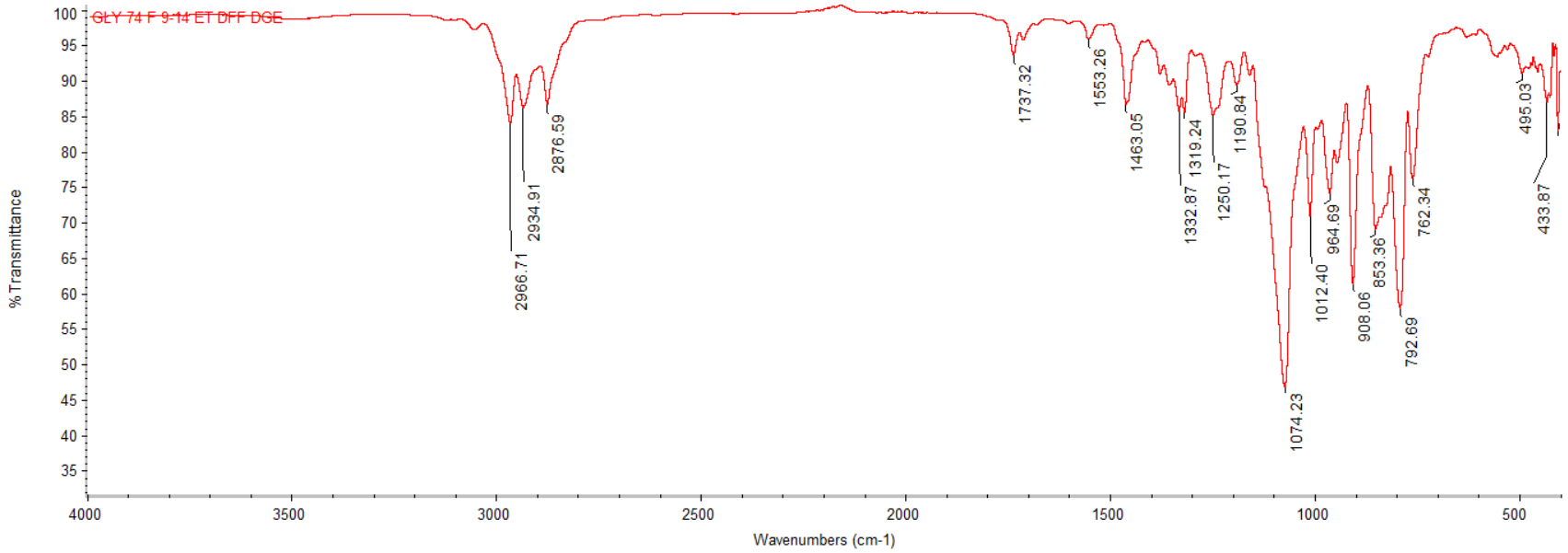

C39. FT-IR spectrum of Compound **5b**.

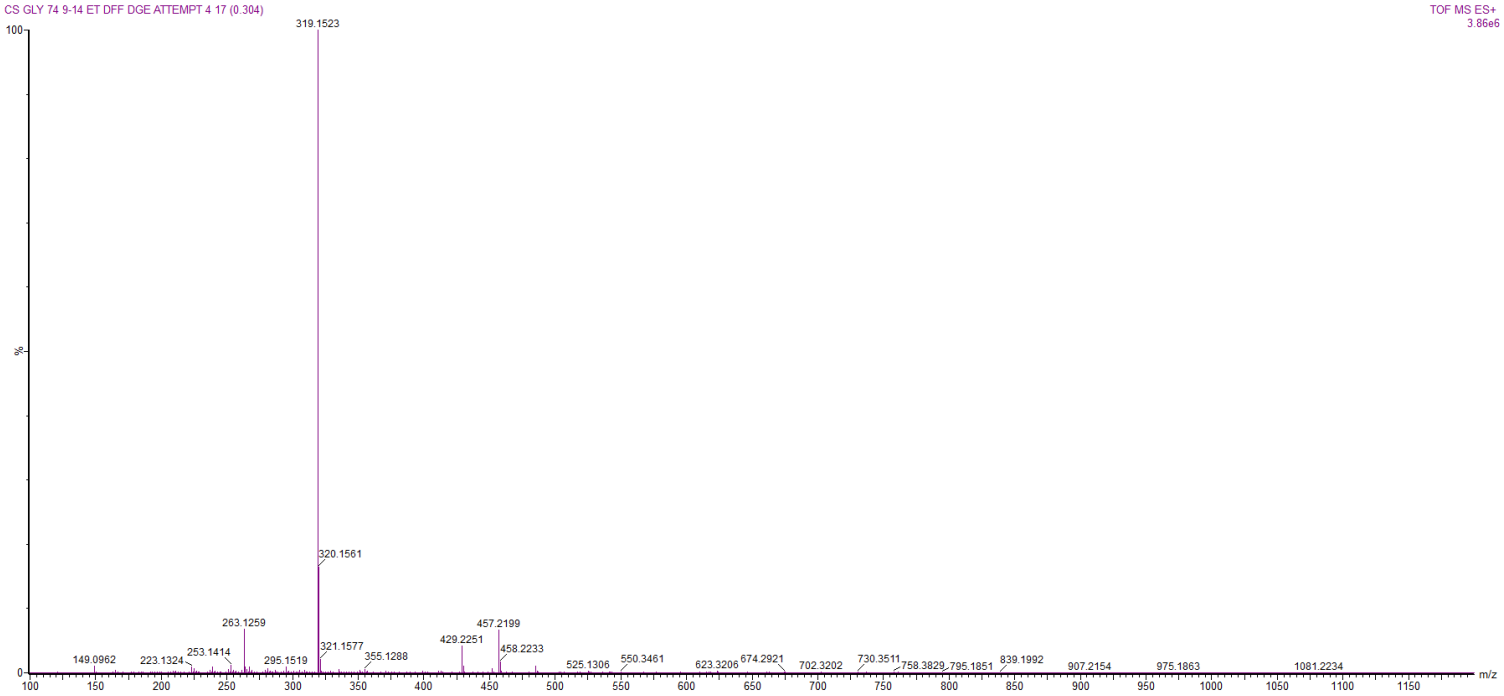

C40. HRMS (ESI, Na+) spectrum of compound **5b**.

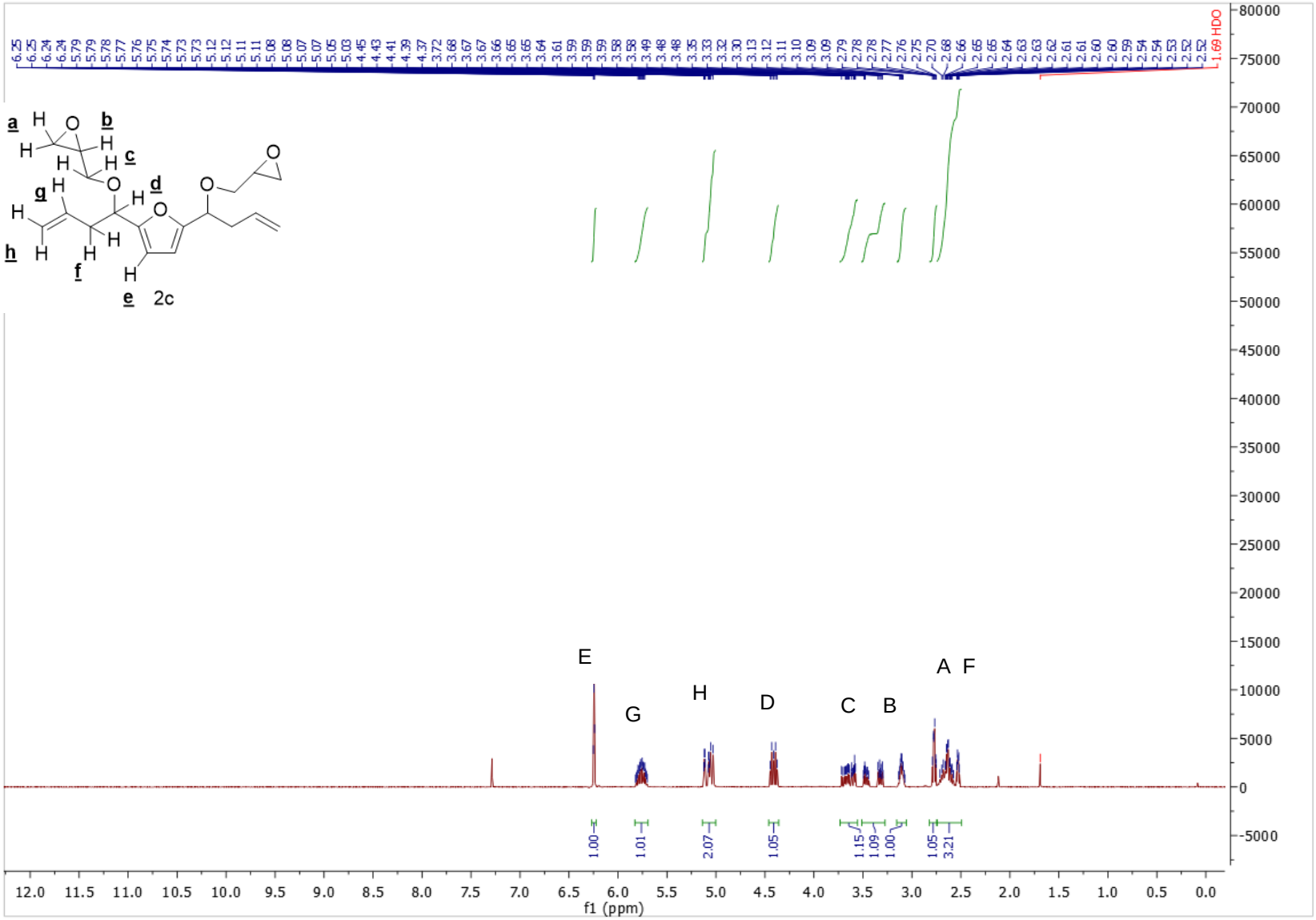

C41. ^{1}H NMR ($CDCl_3$) spectrum of Compound **5c**.

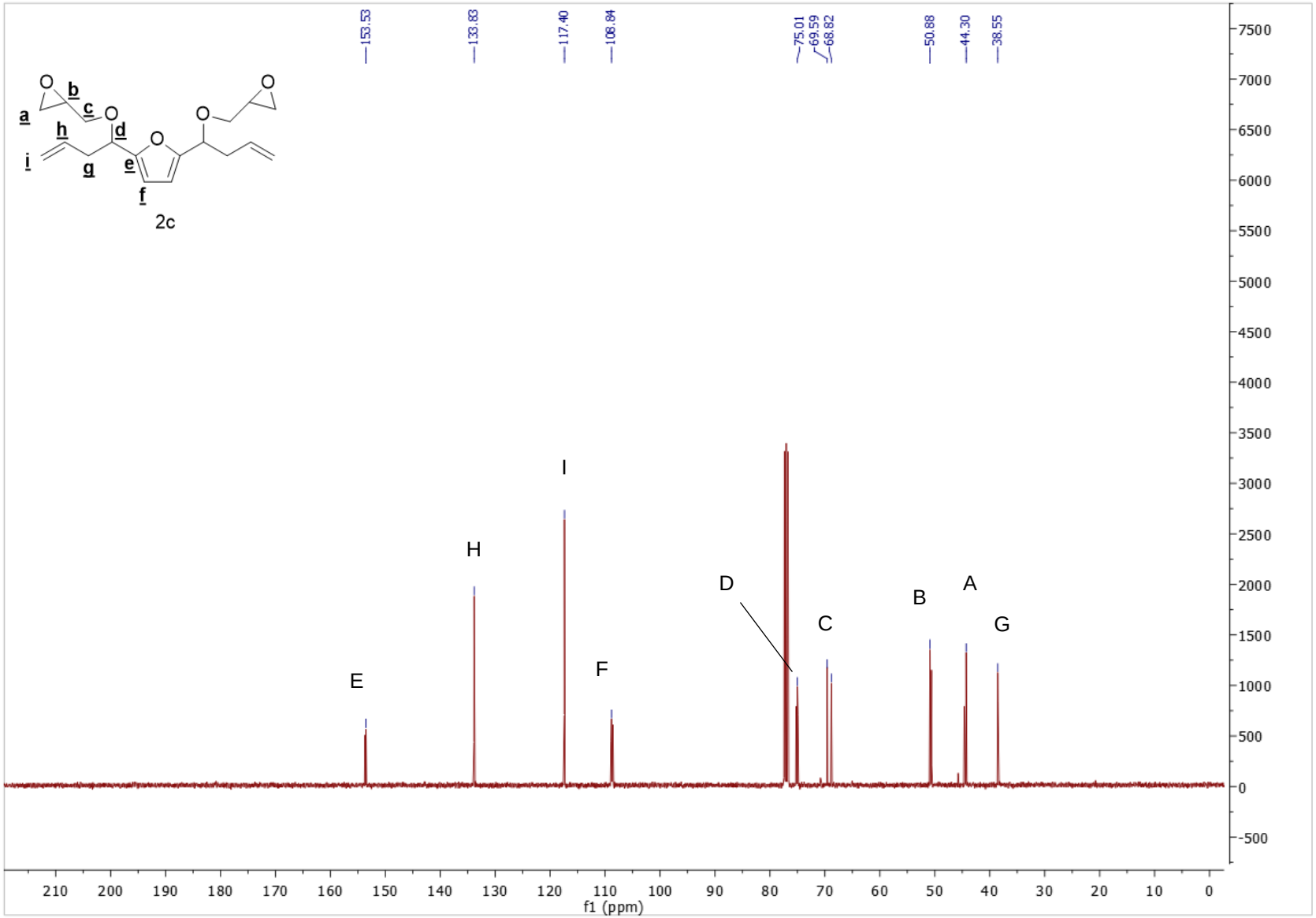

C42. ^{13}C NMR ($CDCl_3$) spectrum of Compound **5c**.

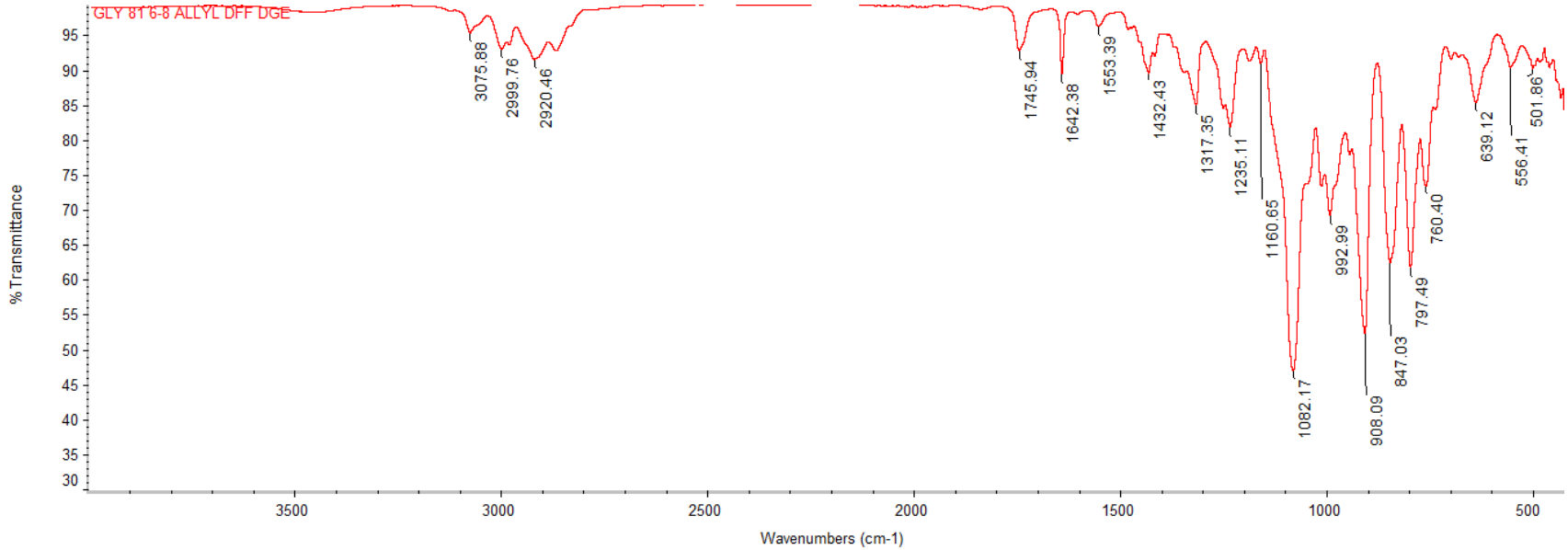

C43. FT-IR spectrum of Compound **5c**.

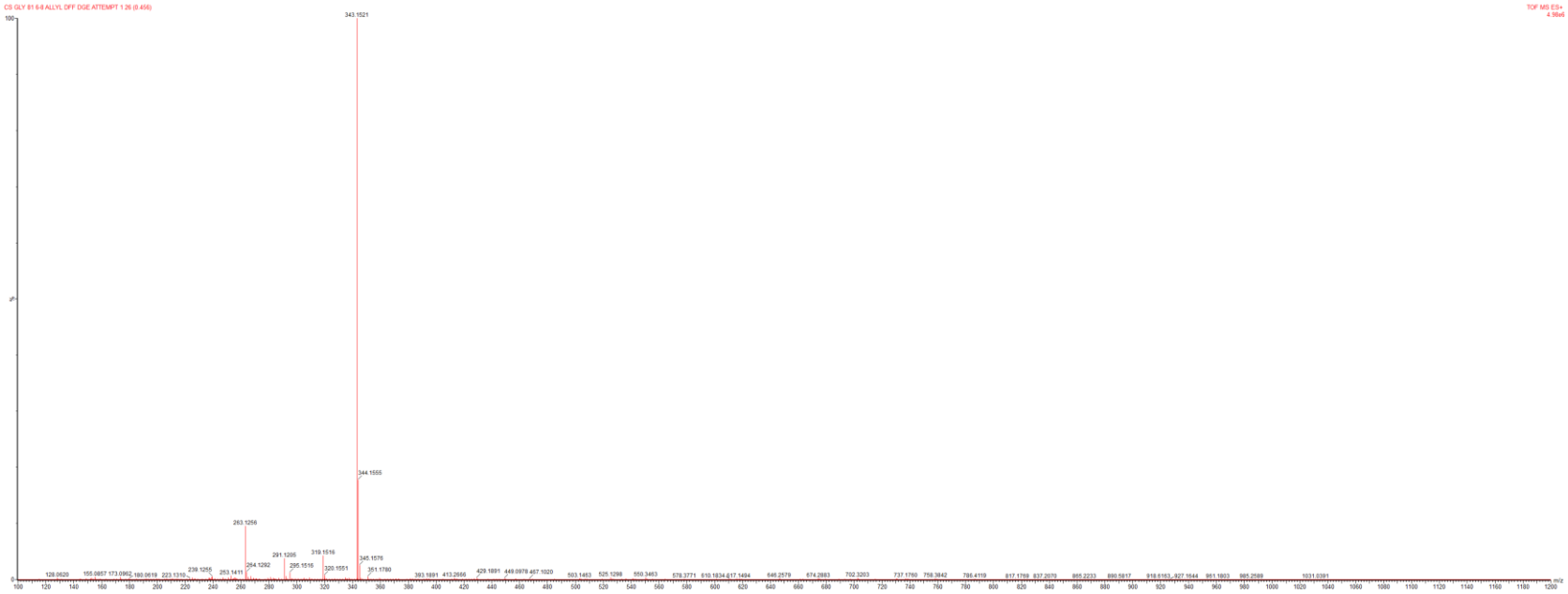

C44. HRMS (ESI, Na+) spectrum of compound **5c**.

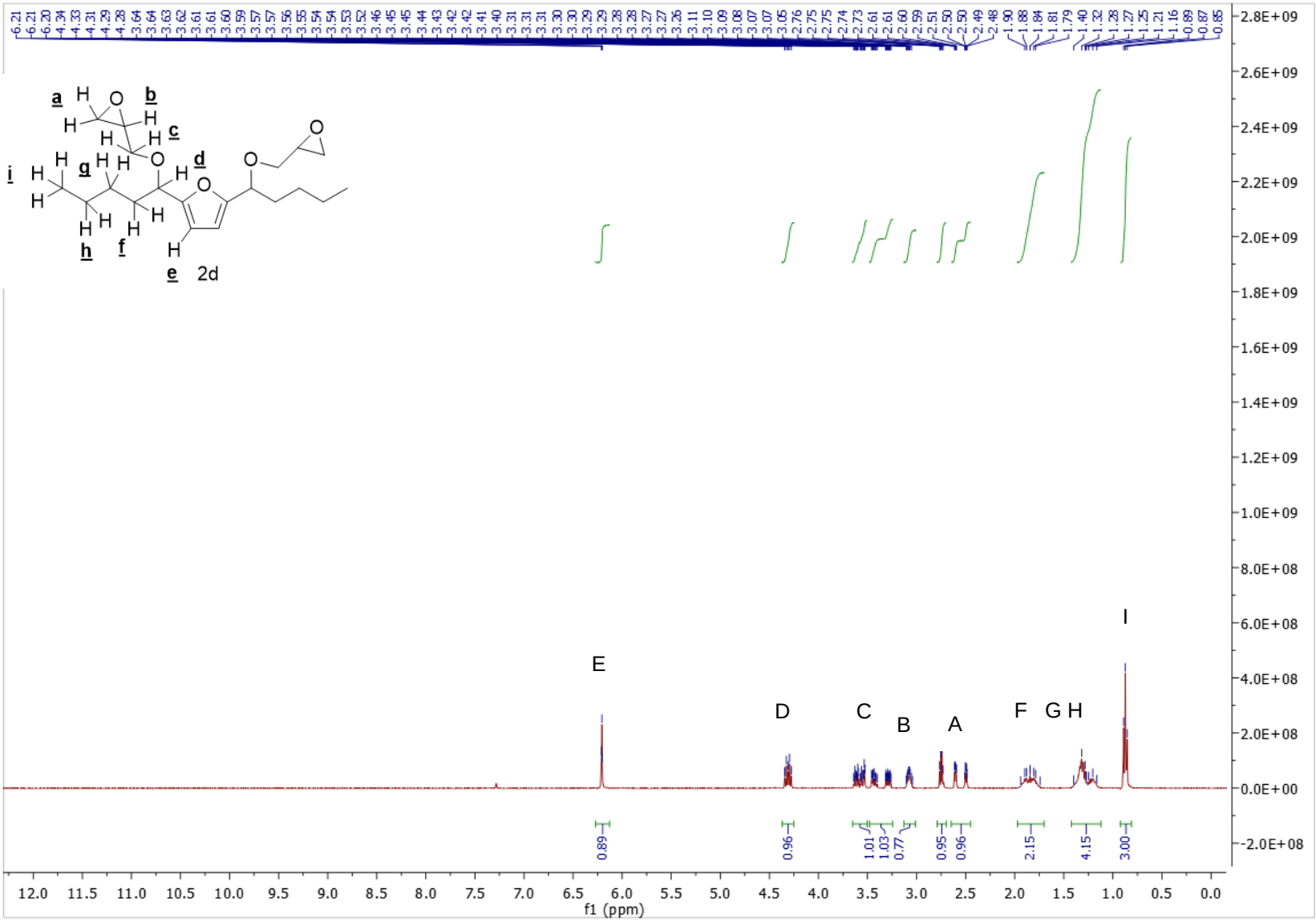

C45. ^{1}H NMR ($CDCl_3$) spectrum of Compound **5d**.

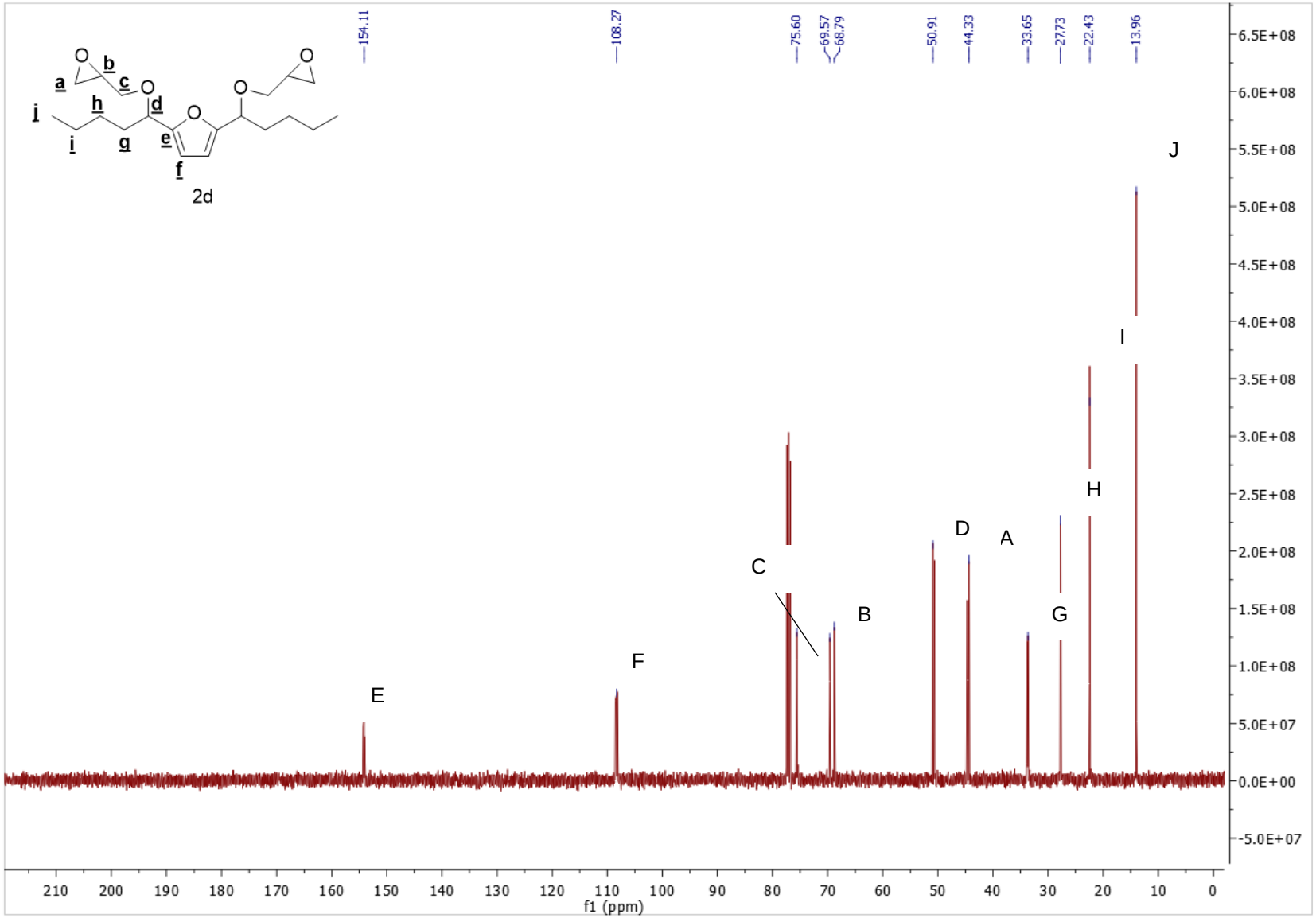

C46. ^{13}C NMR ($CDCl_3$) spectrum of Compound **5d**.

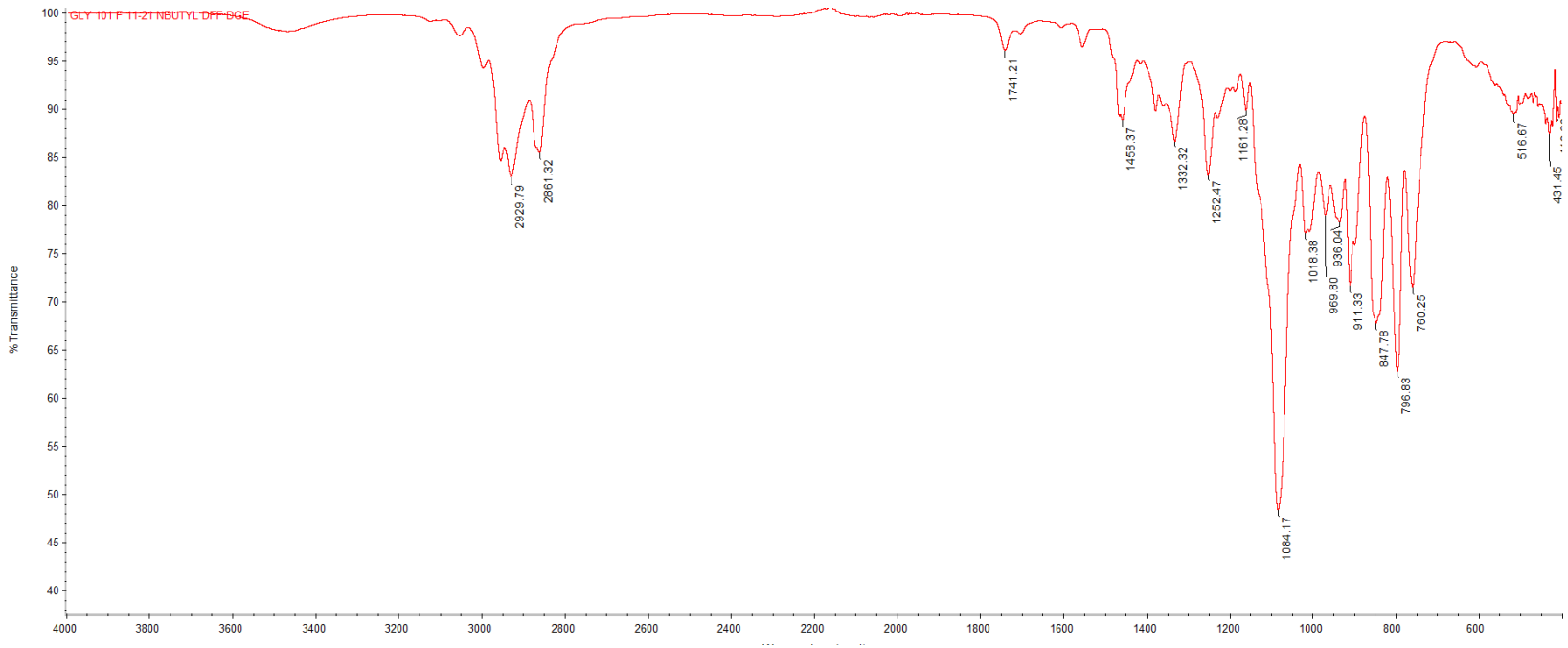

C47. FT-IR spectrum of Compound **5d**.

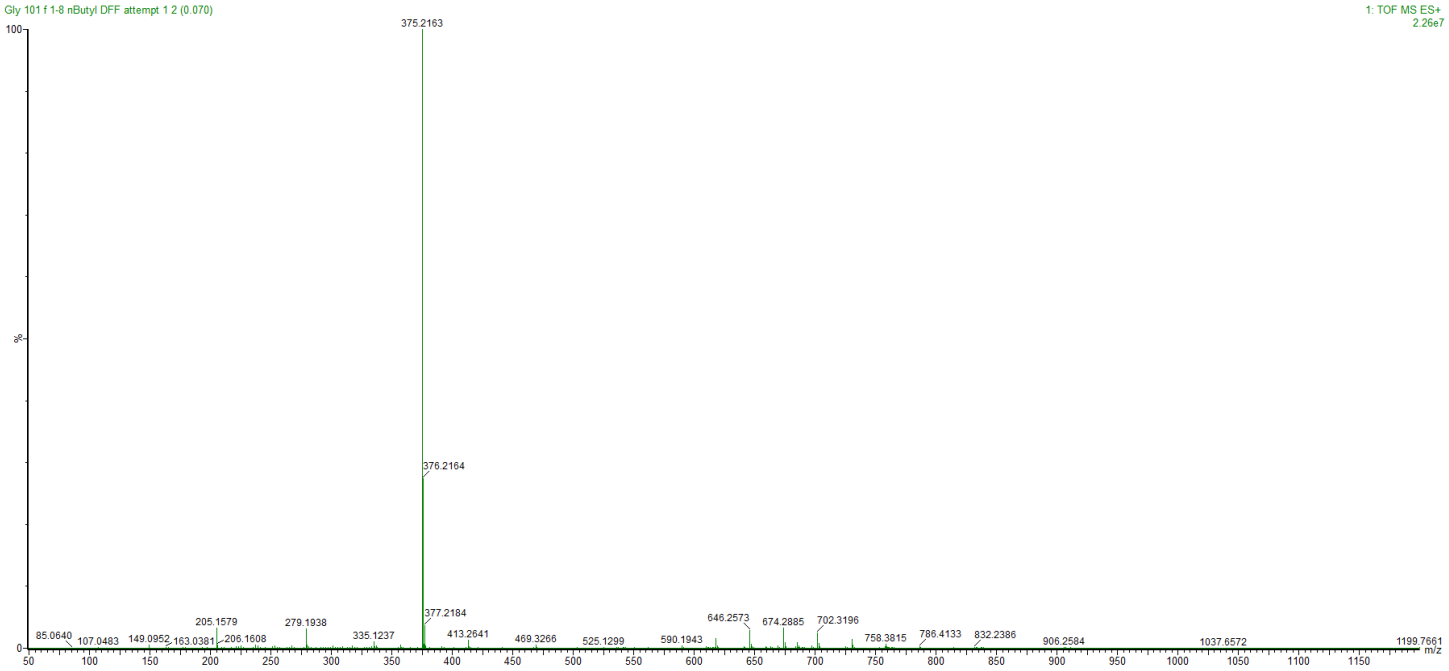

C48. HRMS (ESI, Na+) spectrum of compound **5d**.

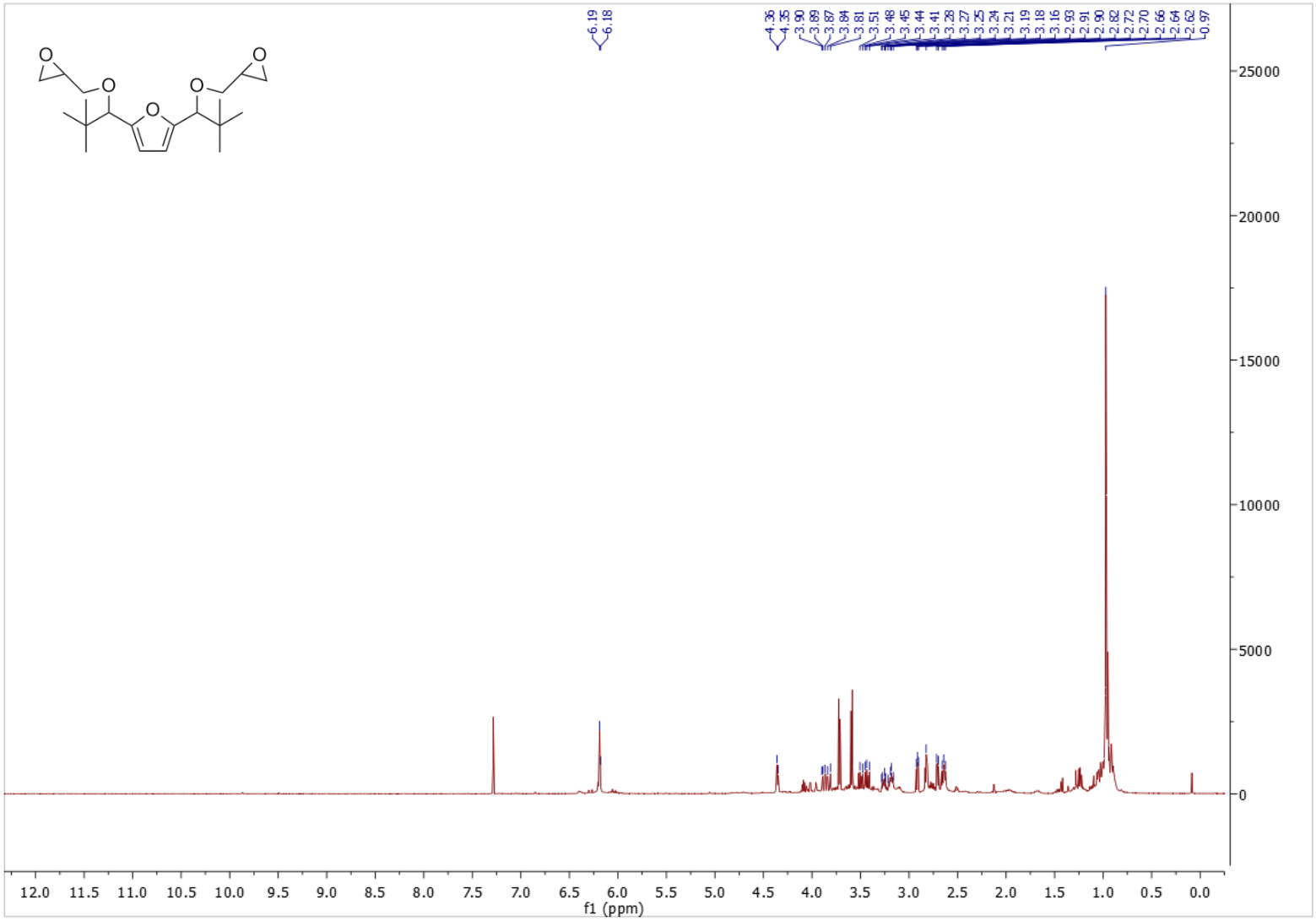

C49. ^{1}H NMR ($CDCl_3$) spectrum of crude Compound **5e**.

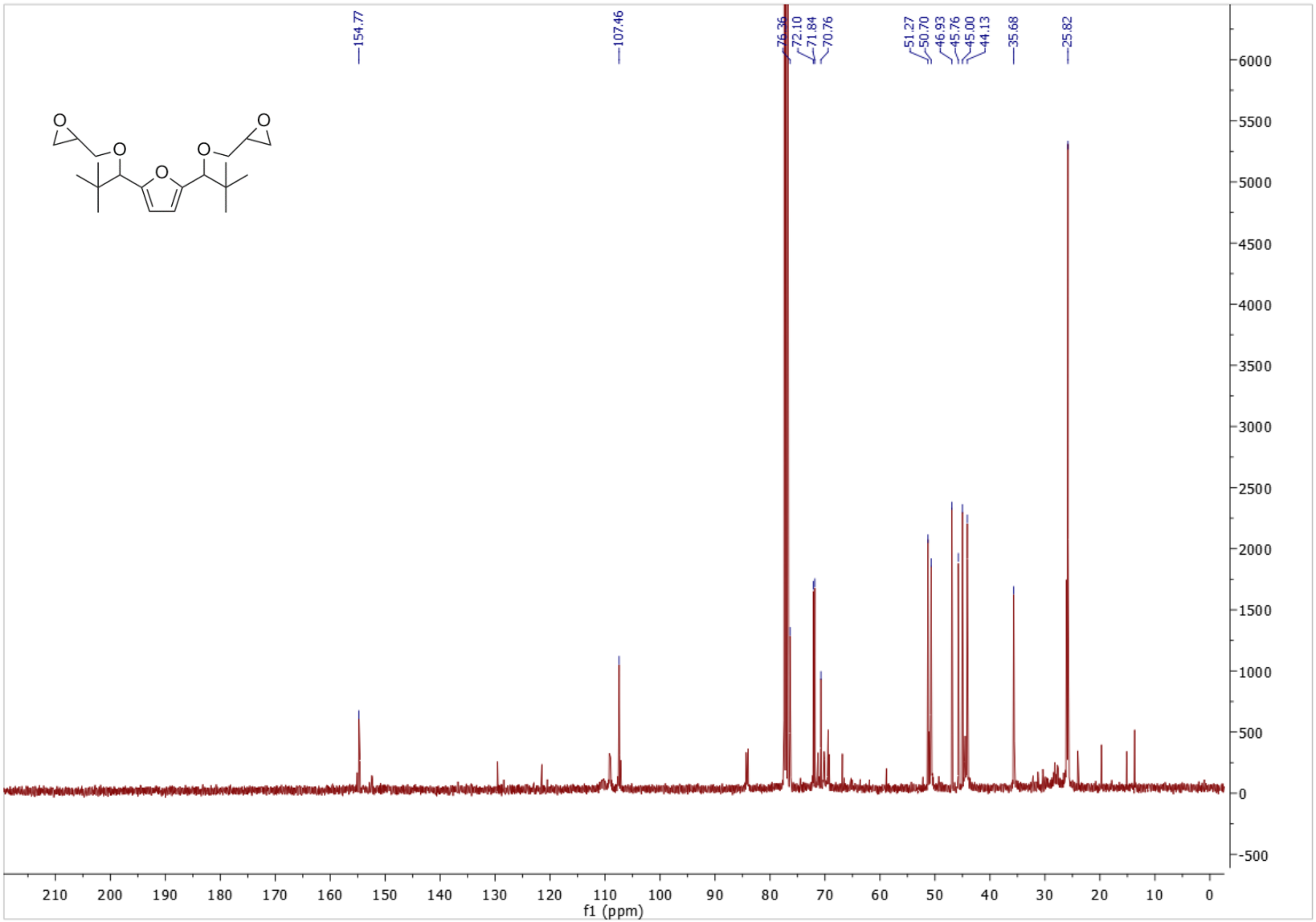

C50. ^{13}C NMR ($CDCl_3$) spectrum of crude Compound **5e**.

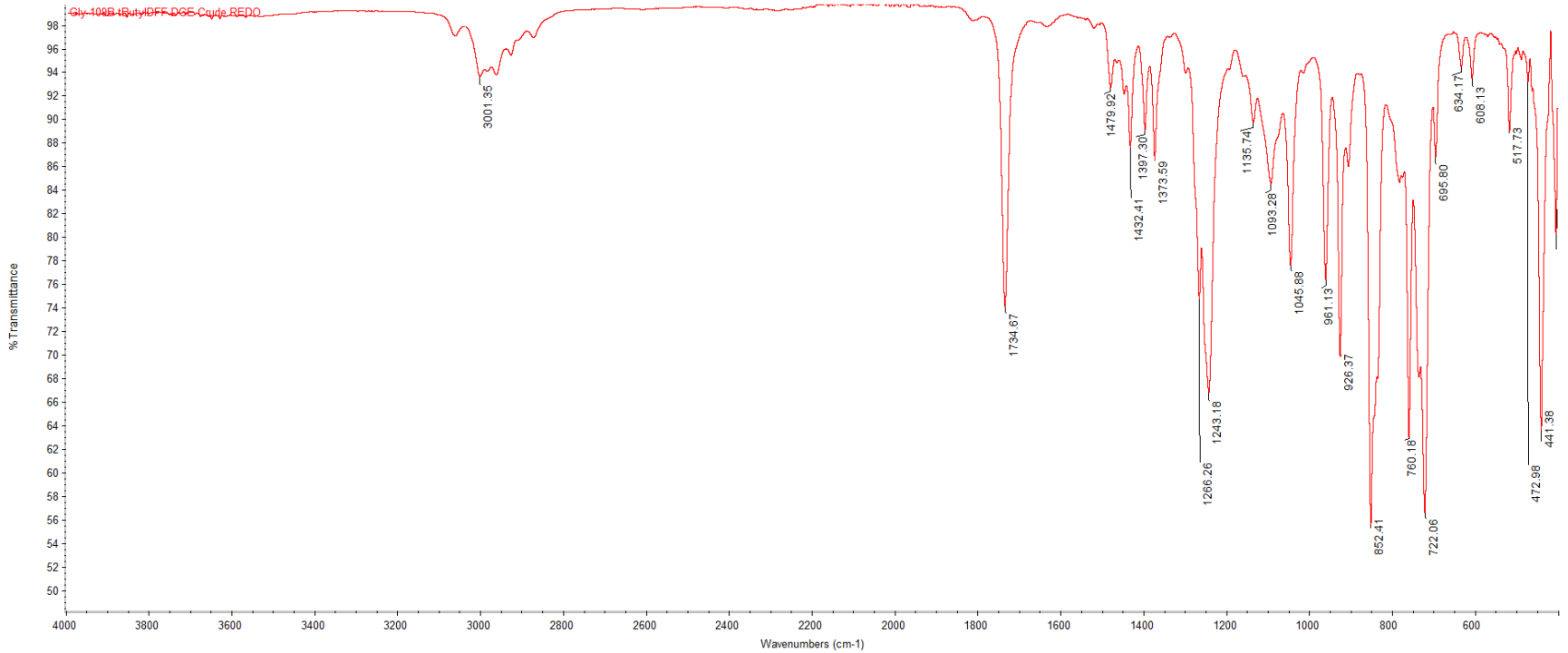

C51. FT-IR spectrum of crude Compound **5e**.

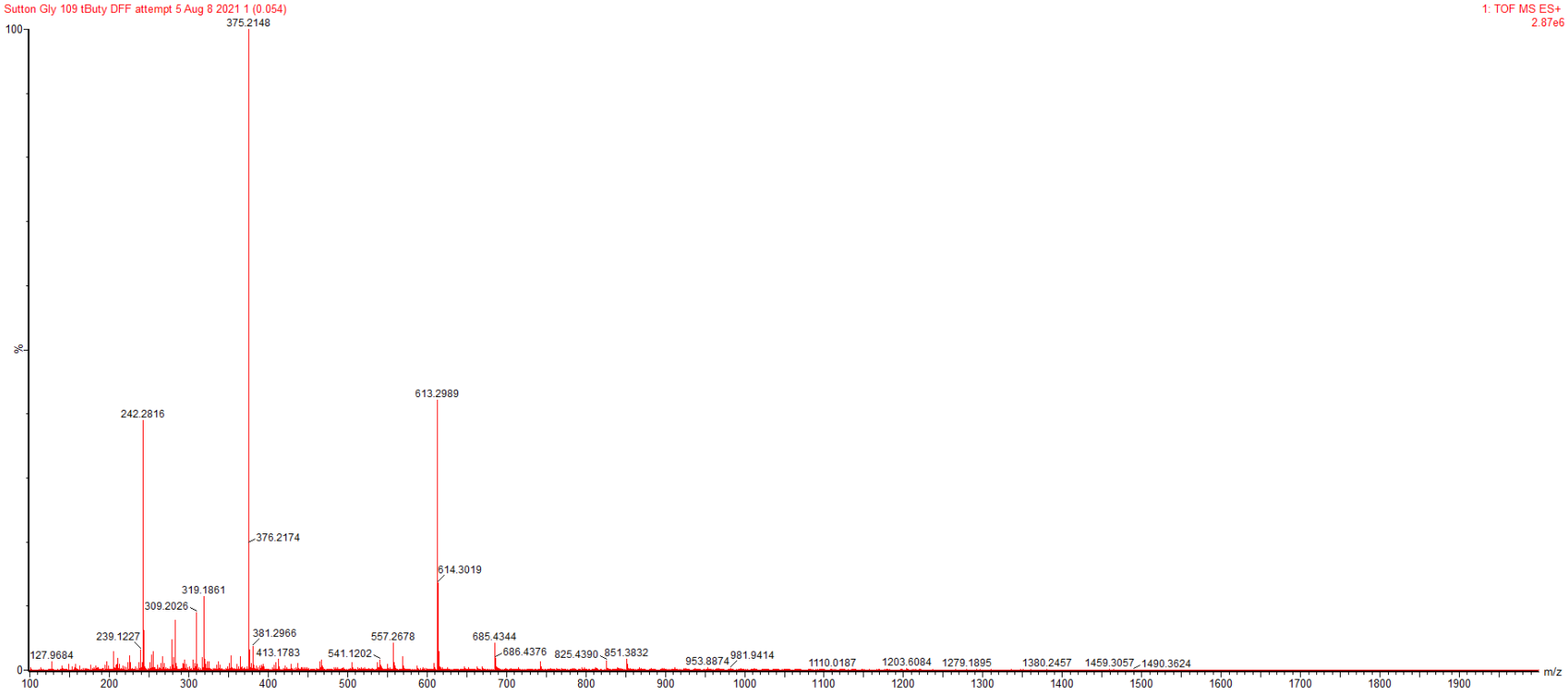

C52. HRMS (ESI, Na+) spectrum of crude Compound **5e**.

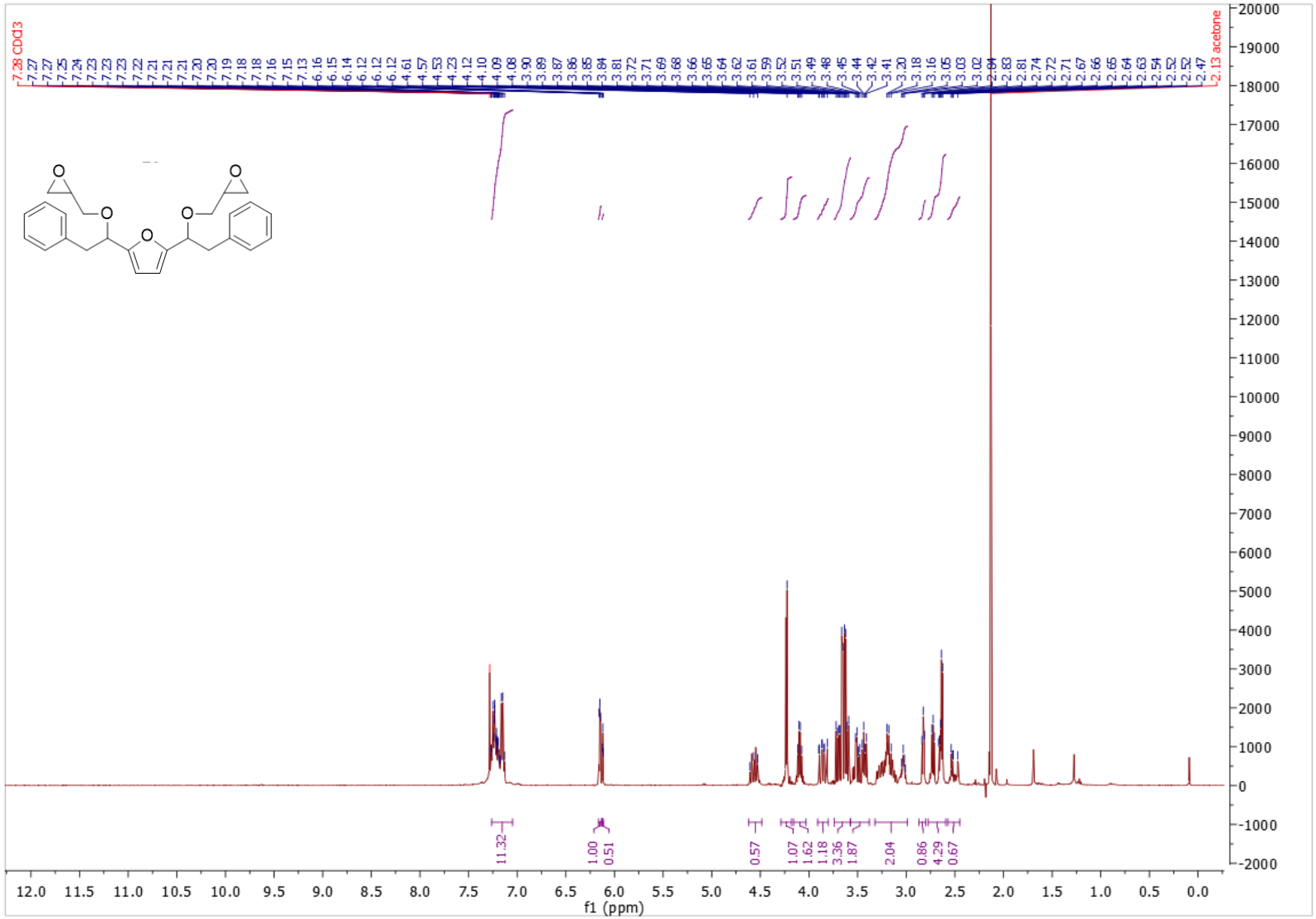

C53. ^{1}H NMR ($CDCl_3$) spectrum of Compound **5g**.

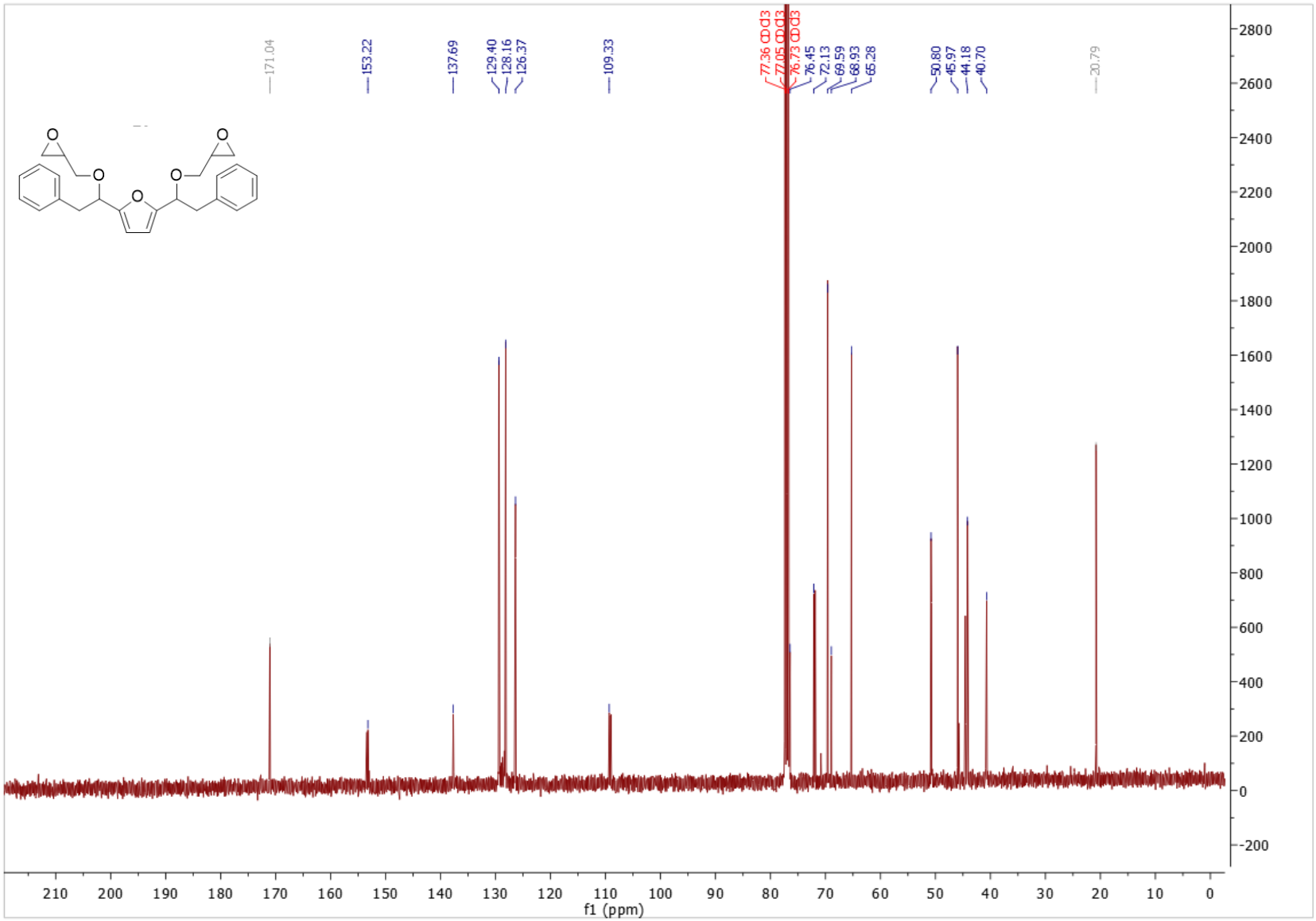

C54. ^{13}C NMR ($CDCl_3$) spectrum of Compound **5g**.

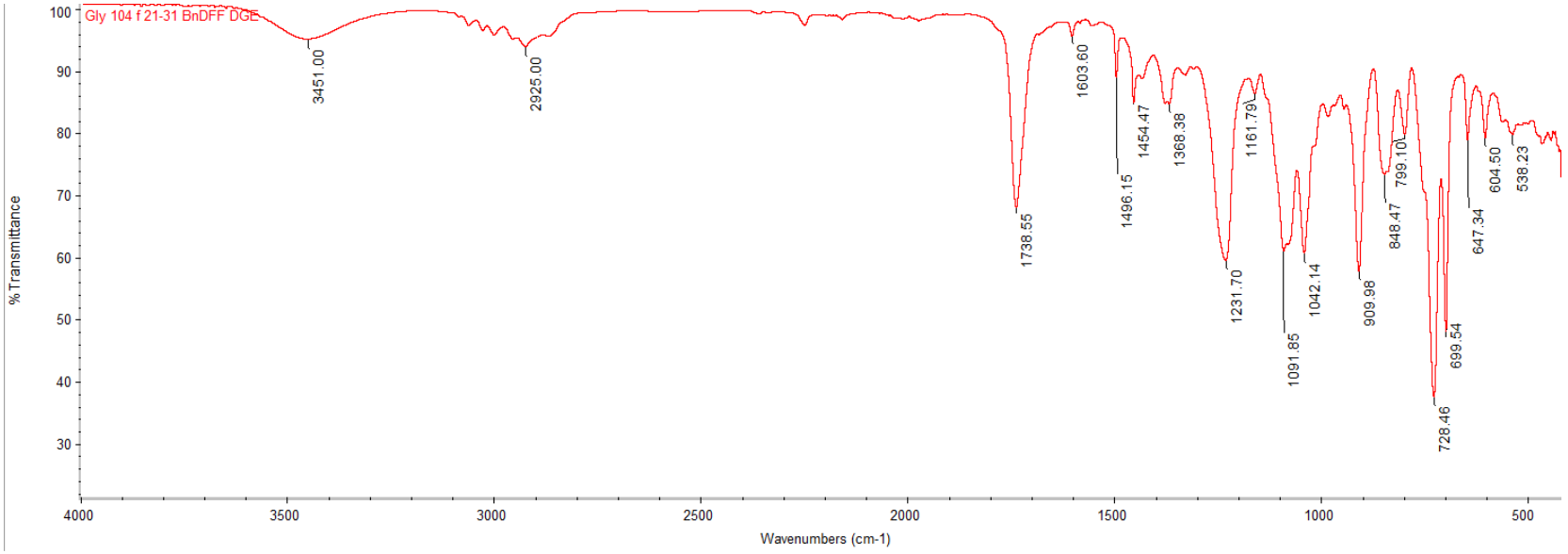

C55. FT-IR spectrum of Compound **5g**.

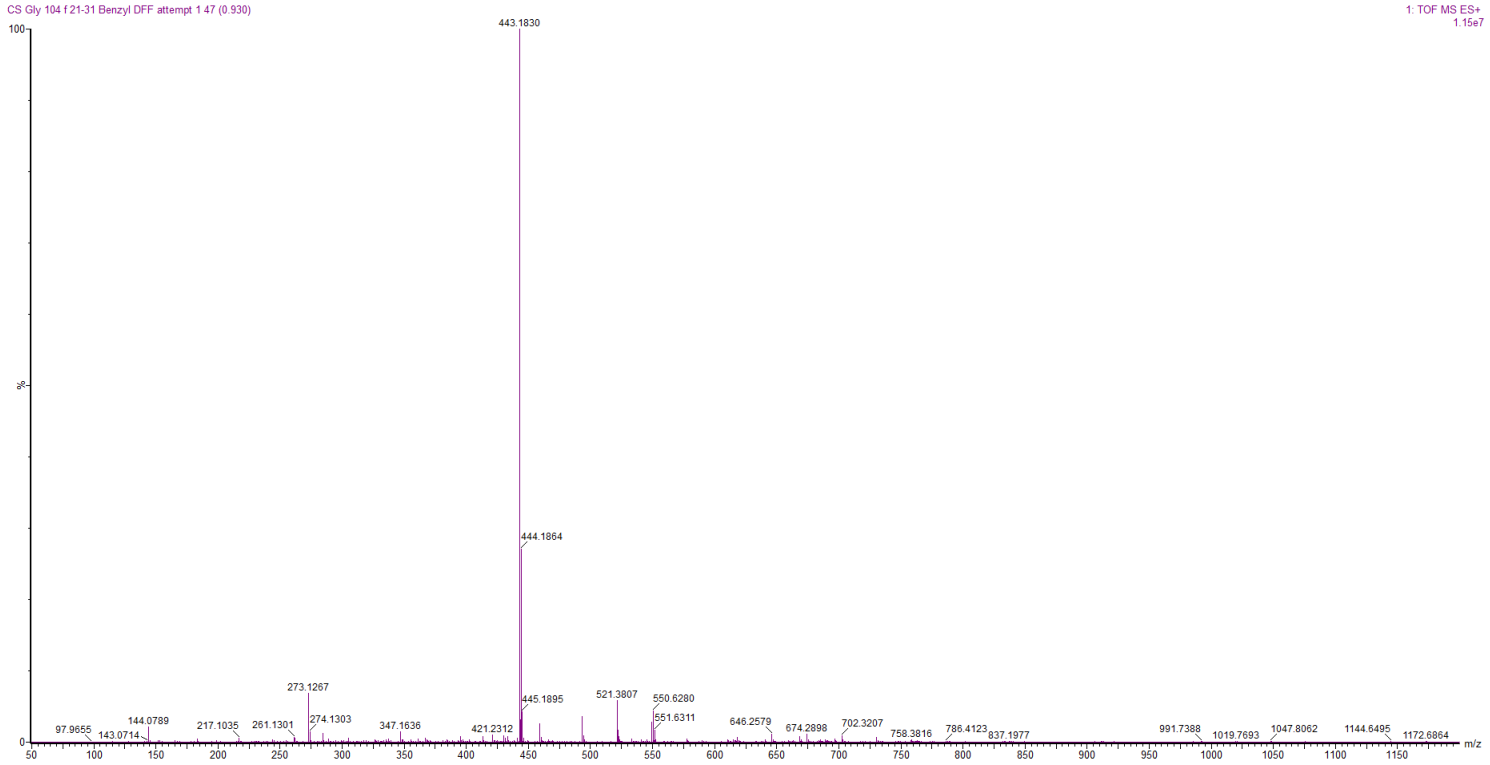

C56. HRMS (ESI, Na+) spectrum of compound **5g**.